U.PORTO
FACULDADE DE DESPORTO
UNIVERSIDADE DO PORTO

ASSESSMENT OF BIOMECHANICAL INTERNAL DYNAMICS AND MECHANICAL LOADS EXERTED IN LOWER LIMB DURING HIGHLY DEMANDING HUMAN MOVEMENTS

Filipa Manuel Alves Machado de Sousa

Porto, 2006

U.PORTO
FACULDADE DE DESPORTO
UNIVERSIDADE DO PORTO

ASSESSMENT OF BIOMECHANICAL INTERNAL DYNAMICS AND MECHANICAL LOADS EXERTED IN LOWER LIMB DURING HIGHLY DEMANDING HUMAN MOVEMENTS

Academic dissertation submitted with the purpose of obtaining a PhD degree in Sports Sciences, under the law 216/92 from October 13.

Supervisor: Professor Doctor João Paulo Vilas-Boas Soares Campos

Filipa Manuel Alves Machado de Sousa

Porto, 2006

Sousa, Filipa M. A. M. (2006). Assessment of Biomechanical Internal Dynamics and Mechanical Loads Exerted in Lower Limb during Highly Demanding Human Movements. Doctoral Thesis in Sport Sciences according to the law 216/92 from October 13.

Key Words: Mechanical Internal Loads, Inverse Dynamics, *In Vivo* Direct Measurements.

To my Parents

and Grandmother

To Maria

Acknowledgements

I would like to express my sincere thanks and gratitude to all that, for some reason were involved in this project.

To Professor João Paulo Vilas-Boas, my supervisor, for his scientific orientation and guidance during all this years. Thank you for the enormous support and friendship and all the international opportunities concede.

To Professor Paavo Komi for giving me the opportunity to fulfil a dream, and for your scientific and professional guidance during this work. For providing me a warm and comfortable stay during the long Winter cold dark days, as well as, the long Spring and sunny days in Jyväskylä.

To Professor João Abrantes, from the Lisbon Technical University, for the unconditional support, and kindness during all this years of friendship. For his help in providing me the opportunity to work in his laboratory from the Faculty of Human Movements in Lisbon.

To Professor Alberto Carlos Amadio, from the Physical Education School, from the University of São Paulo, Brazil, my co-supervisor, for his help and guidance in my first biomechanics "experiences".

To Professor Antônio Carlos Guimarães for being an example of academic excellence, support and friendship. Thank you for the opportunities conceded. We all miss you…

To Professor Jefferson Loss, from the Federal University of Rio Grande do Sul, Brazil, for your unconditional help, support, and friendship, despite of being physically so far away. Thank you for the essential contribution in this work and for firstly introducing me in the inverse dynamics solutions.

To Professor Bento and Professor Marques for the constant incentive and support during all my academic education.

To Professor José Alberto Duarte, for all the facilities and assistance in the assessment of some biochemical parameters related with the toxicity of the optical fibre in humans. Thank you for the opportunity for sharing your knowledge and scientific competence.

To Professor José Maia, for all your kindness and constant care during all this years of friendship.

A special thanks to João Carvalho, from the Department of Physics, Faculty of Engineering, University of Porto, for all the dedication and friendship during this long, long path. I would like to express my sincere gratitude, for the arduous task of sharing with me this extenuating work. Thanks João for everything! … even for the tension and the end-less hours waiting for you…

To Professor Leandro Machado, my colleague from the laboratory and office for the collaboration and support during the preparation of the inverse dynamics routines, and the reviewing of the manuscript.

To Orlando Fernandes, from the Laboratory of Biomechanics, Faculty of Human Movements, Lisbon Technical University, for his constant support during the dancers evaluation and for all this years of unconditional friendship and dedication.

To my friends Filipe Conceição, Joana Carvalho, António Lima, André Seabra, António Ascensão, Zé Magalhães, Ana Luisa, Luisa Estriga, Cristina Claro, Denise Soares, Pedro Gonçalves, and all the other colleagues from the Faculty of Sports, for the constant support and motivation, during this difficult process.

To Maria Luisa Carle, production director from the National Ballet Company of Portugal and to the distinguished dancers, Frederico Gameiro, João Pinto and Margarida Pimenta, for their precious help and the graceful moments offered during the jumps evaluation.

To all my dearest family, for all the support and motivation, during all this years. A special thanks to my mother-in-law, for the difficult path of taking my place of mother, while I'm away from Maria.

To my lovely and adorable Parents, Sister, and Grandmother, and to my little "*tree musketeers*", Zé, Manel and João. Thank you for the unconditional dedication during the good and the not so good moments. I am so proud of all of you. Thank you for your love and the wonderful family that we are.

To Pedro and little Maria, for being the reason of my life.

Abstract

The evaluation and quantification of the mechanical loads imposed to the human system is extremely important for the understanding of mechanical stress of biomaterials, and injuries. It can be used to assist and prepare adjusted training programmes in daily life activities, in recreational activities, in physical and sports activities, such as in high level sports performances as well as in classical dance, in which the body structures are especially submitted to extreme efforts and stressful conditions. Our major research question was the assessment of the mechanical loads and internal dynamics exerted in the lower limb, during the performance of highly demanding human movements. The purposes of the present study were:

a) to develop an appropriate methodology to estimate the internal dynamics and mechanical loads exerted in the lower limb, during highly demanding physical movements with strong technical limitations and kinematical restriction: jumps in classical ballet.

a1) from the external dynamics of the subject, solve the classical movement equations and obtain the forces and intersegmentar moments. This is the classical domain of Inverse Dynamics.

a2) from the intersegmentar moments obtained in the previous step, and the musculoskeleton geometry, obtain the muscular forces using one of several methodologies: pure inverse decomposition with an *Ad Hoc* merit function; combine a muscle model in a forward/inverse dynamics approach with an *Ad Hoc* merit function; combine an electromyography (EMG) driven muscle model in a Forward/Inverse Dynamics approach.

b) directly measure the behaviour of the two compartments (contractile and elastic components), of the muscle-tendon complex of the synergistic pair of muscles, medial gastrocnemius and soleus, during different intensity drop jumps (stretch-shortening cycle movements). It was measured the fascicle length of both muscles with ultrasonography, in order o examine the contribution of the contractile and the elastic components to the potentiation of the muscle-tendon complex.

In general, two main findings should be stressed out from this study:

a) the complex interaction of muscles performing a simple task (landing), includes the role of the synergists, antagonists and bi-articular/energy transfer muscles;

b) each muscle undergoes a complex interaction with the tendon tissue to with it is connected, storing and recovering some energy, and make the overall movement a little more efficient.

Through the analysis of the magnitude of the peak values from articular force estimated, it is possible to observe the injury potential that the anatomical structures are exposed to. The evaluation of movement in terms of moments and power, allows a better and new comprehension about the individual strategies for movement performance, occasionally allowing a technical intervention, helping in the improvement of performance. The knowledge of intra articular forces, particularly in this activity but also in many others, is an important tool for the understanding of the risks of injury associated to repetitive efforts, and its eventual prevention. The recorded data from live executions confirm the existence of important pre-activation and co-contractions. These will need to be taken into account in any muscle decomposition/inverse dynamics approach. In general, the studies of our thesis contribute to the knowledge of: the nature and attenuation of the imposed loads to the human locomotor system; the mechanism of energy transfer and conservation, and to the potentiation of movement's efficiency.

Resumo

A avaliação e quantificação das cargas mecânicas impostas sobre o sistema locomotor humano é uma tarefa que se reveste de extrema importância, nomeadamente para o conhecimento do *stress* mecânico a que estão sujeitos os biomateriais e dos possíveis mecanismos de lesão que podem ser desencadeados. Além disso, pode também ser útil para preparar ajustados programas de treino, quer seja em actividades físicas básicas diárias, como em actividades de recreação, ou actividades físicas e desportivas, tais como nos desportos de alto nível de rendimento, ou na dança clássica, nas quais as estruturas anatómicas estão particularmente submetidas a esforços mecânicos extremos. O tema central da nossa pesquisa foi a determinação das cargas mecânicas e da dinâmica interna exercida sobre membro inferior, durante a execução de movimentos de elevada exigência atlética. Os objectivos da presente dissertação foram:

a) desenvolver uma metodologia apropriada para estimar a dinâmica interna e as cargas mecânicas exercidas sobre o membro inferior, durante a execução de movimentos de elevada exigência atlética, com fortes limitações técnicas e restrições cinemáticas: os saltos na dança clássica.

a1) através da dinâmica externa do sujeito, resolver as equações clássicas do movimento e obter as forças e momentos intersegmentares.

a2) através dos momentos intersegmentares obtidos no ponto anterior e da geometria do sistema músculo-tendinoso, obter as forças musculares, usando uma das seguintes metodologias: pura decomposição muscular inversa, utilizando uma função de mérito *Ad Hoc*; combinar um modelo muscular numa aproximação dinâmica Directa/Inversa, utilizando uma função de mérito *Ad Hoc*; combinar um modelo muscular electromiográfico numa aproximação dinâmica Directa/Inversa.

b) medir directamente o comportamento das duas componentes (contráctil e elástica) do complexo músculo-tendinoso do par de músculos sinergistas, *gastrocnemius* medial e *soleus*, durante a realização de *drop jumps* de diferentes intensidades (movimentos realizados em ciclos de alongamento-encurtamento). Foi medido, por ultrasonografia, o comprimento do fascículo de ambos os músculos, no sentido de examinar a contribuição das componentes, contráctil e elástica, para o mecanismo de potenciação do complexo músculo-tendinoso.

Os resultados obtidos permitem-nos concluir que:

a) a complexa interacção dos músculos que executam uma tarefa simples, como uma recepção ao solo (aterragem), deve incluir o papel dos músculos sinergistas, antagonistas e dos músculos bi-articulares, responsáveis pela transferência de energia;

b) cada músculo desenvolve uma complexa interacção com o tecido tendinoso ao qual está ligado, armazenando e devolvendo energia, e tornando o movimento em geral mais eficiente.

Através da análise da magnitude dos valores de pico de força articular estimados, é possível observar o potencial lesivo a que as estruturas anatómicas estão expostas. O conhecimento das forças intra-articulares, particularmente nesta actividade, mas também em muitas outras, é uma importante ferramenta utilizada para o entendimento dos riscos de lesão associados a esforços repetitivos, e a sua eventual prevenção. A avaliação do movimento em termos de momentos e potência, permite uma melhor e nova compreensão acerca das estratégias individuais utilizadas na realização do movimento, permitindo ocasionalmente uma intervenção técnica, no sentido de melhorar a realização do movimento. Concluindo, os estudos constituintes da presente dissertação, contribuem para o conhecimento: da natureza e dos fenómenos de atenuação das cargas impostas sobre o sistema locomotor; dos mecanismos de transferência e conservação de energia por parte dos músculos bi-articulares, e da potenciação da *performance* do movimento.

Résumé

L'évaluation et la quantification des charges mécaniques imposées sur le système de locomotion humain est une tâche d'extrême importance, surtout en ce qui concerne la connaissance du stress mécanique auquel sont soumis les biomatériels et des hypothétiques mécanismes de lésion qui peuvent être activés, étant utilisés pour réparer des programmes justes d' entraînement, soit dans des activités basiques quotidiennes, soit dans des activités de recréation, ou activités physiques et sportives, telles que dans les sports de haut niveau , ou dans la danse classique, où les structures anatomiques, ce sont particulièrement soumises à des efforts mécaniques extrêmes. Le thème central de notre recherche a été la détermination des charges mécaniques et la dynamique interne exercée sur le membre inférieur, pendant l'exécution de mouvements d'exigence maxime athlétique.
Les objectifs de la présente dissertation sont :
a) développer une méthodologie appropriée pour estimer la dynamique interne et les charges mécaniques exercées sur le membre inférieur, pendant l'exécution de mouvements d'exigence maxime athlétique, avec des fortes imitations techniques et des restrictions cinématiques : les sauts de la danse classique.

a) 1. a travers la dynamique externe du sujet, résoudre les équations classiques du mouvement et obtenir les forces et des moments inter segmentaires.

a) 2. a travers des moments inter segmentaires obtenus dans le point précédent et de la géométrie du système muscle-tendineux, obtenir les forces musculaires, en utilisant l'une des méthodologies suivantes : pure décomposition musculaire inverse, en utilisant une fonction de mérite Ad oc ; combiner un modèle musculaire dans une approche dynamique directe/inverse, utilisant une fonction de mérite Ad oc ; combiner un modèle musculaire dans une approche dynamique directe/inverse, en utilisant électromyographie de surface.
b) mesurer directement la performance des deux composés (contractile et élastique) du complexe muscle-tendineux du paire de muscles cinergistes, *gastrocnemius médial et soleus,* pendant la réalisation de *drop jumps* de différentes intensités. (des mouvements réalisés par des cycles de longuement-encourtment). La longueur du fascicule des deux muscles a été mesurée, par ultrasonographie, dont le but c'était d'examiner la contribution des components, contractile et élastique, pour le mécanisme de potentiation du complexe muscle-tendineux.
Les résultats obtenus permettent la suivante conclusion :
a)La complexe interaction des muscles qui développent une tâche simple, comme une réception au sol (atterrissage), insère le rôle des muscles cinergistes, antagonistes et des muscles bi-articulaires, responsables par la transférence d'énergie;
b) Chaque muscle développe une complexe interaction avec le tissu tendineux auquel il se lie, stockage et renvoyer l'énergie, en faisant le mouvement général plus efficient.
Par l'analyse de la magnitude des valeurs maximums de force articulaire estimée, il est possible observer le potentiel lesive auquel les structures anatomiques sont exposées. L'évaluation du mouvement en ce qui concerne des moments et la puissance, permet une meilleure et nouvelle compréhension des stratégies individuelles utilisées dans la réalisation du mouvement, permettant de temps en temps une intervention technique, pour améliorer la réalisation du mouvement. La connaissance des forces intra-articulaires, particulièrement pour cette activité, mais aussi pour des autres en général, c'est un important outil utilisé pour la compréhension des risques de lésion associés à des efforts répétés, et son éventuelle prévention. En conclusion, les études constituants de la présente dissertation, contribuent pour la connaissance de la nature et des phénomènes d'atténuation des charges imposées ; des mécanismes de transférence et de conservation d'énergie des muscles bi-articulaires, et de la potentiation de la performance du mouvement.

Table of Contents **page**

List of Abbreviations

AD	Analogic digital
aEMG	Averaged electromyographic signal
ANOVA	Analysis of variance
AT	Achilles tendon
BW	Body weight
CE	Contractile element
D	Distal
DH	Dropping height
DJ	Drop jump
[dt(land)]	Instant time of the landing phase
[dt(to)]	Instant time of the take-off phase
EMG	Electromiography
F	Force
F_{ext}	External force
F_z	Vertical component of the ground reaction force
[Fz(land)]	Maximum relative value of the ground reaction force on the landing
[Fz(to)]	Maximum relative value of the ground reaction force on the take-off
GRF	Ground reaction force
GTO	Golgi tendon organ
I	Moment of inertia
J	Joule
IEMG	Integrated form of electromyographic signal
M_{ext}	External moment
M	Moment of force
MG	Medial *gastrocnemius*
mJ	Milijoule
MPa	Mega Pascal
MRI	Magnetic resonance imaging
MTU	Muscle-tendon unit
N	Newton
NASA	National aeronautics and space administration
P	Proximal
PCSA	Physiological cross-sectional area
PE	Parallel elastic element

%MVC	Percentage of the maximum voluntary isometric contraction
[%mvc(land)]	Maximum EMG records on the landing phase
[%mvc(to)]	Maximum EMG records on the take-off phase
RMS	Root mean square
s	Second
SD	Standard deviation
SE	Elastic element
SLR	Short latency stretch reflex
SOL	Soleus
SRS	Short-range stiffness
SSC	Stretch-shortening cycle
T	Time
TT	Tendinous Tissue
2D	Two-dimensional
3D	Three-dimensional
ULS	Ultrasonography
μm	Micro
Veloc (land)	Relative muscular contraction velocity on the landing phase
Veloc (to)	Relative muscular contraction velocity on the take-off phase
VL	*Vastus lateralis*
Y	Young's modulus
yrs	Years

Index of Figures

Index of Tables

Index of Equations

Chapter 1
Introduction

1. Introduction

1.1. Definition and Importance of Internal Forces

The Biomechanics of human movement is a scientific discipline in a continuous process of establishment. According to Winter (1990), it can be defined as an interdiscipline which describes, analyses and assess the human movement. The biological system is studied using the knowledge and methods of physics, chemistry, mathematics, physiology, anatomy, and others. Strongly connected with the mechanics, the biomechanics examines the forces acting upon, and within, the biological structure, and the effects produced by such forces.

According to Nigg (1994) the external forces acting upon the biological system can be quantified using sophisticated measuring devices. Nevertheless, the determination of the internal forces remains a very difficult task, being a prominent area in the biomechanics of human movement, and one of its main topics of interest. Through the analysis of the internal forces, important considerations about the movement control and the mechanical loading imposed to the different structures of the locomotor system can be taken into account. The internal forces can be assessed using implanted measuring devices, or estimated from sophisticated mathematical model calculations.

Internal forces are closely related with movement's execution as well as with the mechanical loading imposed to the locomotor system. The locomotor system is composed by two important structures: the active elements and the passive elements. The muscles represent the active elements of the system, and are directly responsible by the internal force production. On the other hand, the tendon, ligament, bone and joints are the passive elements. They are submitted to internal forces produced by the muscles and his function is to transmit them.

Mechanical loading of a locomotor system is a prerequisite for morphological and functional adaptation of biomaterials. Biological structures need mechanical stimuli to maintain or increase their function capacity and morphological structure. The absence of loading will produce, in the unused biological structure, the loose of their structural strength and function. On the other hand, if stress and strain on bones, cartilage, tendon, ligaments and other tissues, increase to a certain extent and exceed the mechanical limits of the individual structures, micro and macro damages impair the material properties, and may lead to more

or less severe structural damages. The response to overloading results in either acute and chronic injuries and pain (Bruggemann, 2005).

The evaluation and quantification of the mechanical loads imposed to the human system is extremely important for the understanding of mechanical stress of biomaterials, and injuries, and can be used to assist and prepare adjusted training programmes in daily life activities, in recreational activities, in physical and sports activities, such as in high level sports performances as well as in classical dance, in which the body structures are especially submitted to extreme efforts and stressful conditions. The purpose is always to prevent injuries and overload mechanisms, and to control them.

It is implicitly assumed that exceeding loads applied to anatomical structures are highly harmful and potentially responsible for the appearance of serious injuries. A reduction of these exceeding loads can be extremely beneficial, and a good understanding of the mechanisms that determine injuries is essential to its prevention or to the applications on therapeutics.

1.2. Complex Research on Biomechanics

The structural and functional complexity of the human system determines serious methodological difficulties in measuring directly internal forces. In this way, using accurate biomechanical methods it is possible to estimate the variables of our interest. The human body is modelled as a set of rigid segments connected between them through articular joints, and the resultant movement is due to internal and external forces.

The development on biomechanics research always follows very closely the recent development of great scientific-technological research areas, such as cybernetics, robotics, electronics, etc, allowing, in one hand, the development of refined and sophisticated measurement instruments and, on the other hand, the development and validation of complex and sophisticated mechanical models, representing the behaviour of the biomechanical system.

The complexity of the biomechanics research requires, simultaneously, the combination of several measuring techniques: kinematics, anthropometry, kinetics and electromyography

(Baumann, 1995). Due to the high dependency of the biomechanics on experimental results, it's required a great accuracy in the measuring techniques. The importance of having refined measures and methods is essential to subsequently find the best human movements modelling approach.

1.3. Classical Ballet

Dance, nowadays, is technically more complex than in the past. Although the intuitive and sometimes instinctive methods used for gifted teachers are scientifically correct, in our time it has become almost impossible to develop a safe technique without a thorough understanding of the biomechanical laws, training principles and exercise physiology. Dancers are dancing faster and more brilliantly than ever before, and choreographers continue to break new ground, experimenting new ways of expressing emotion through movement.

In spite of the serene and calm appearance of the dancers, transmitted in the popular and famous paintings of Degas, in our days, the ballet training is one the most demanding and rigorous forms of physical activity. It involves both aesthetically and technically very demanding movements, which are usually presented using different or adverse criteria from those usually found and imposed in other physical activities. It's necessary to carry out a specific sequence of very technically demanding movements (such as on the arms, trunk and legs) in the smoothest possible way. Dancers use their musculature in a very unusual and intense way, especially concerning its excursion around the ankle joint. There is very little information available about the way dancers use their muscles to perform aesthetically beautiful movements with grace, achieving an illusion of effortlessness despite the intense physical demanding movements (Clippinger-Robertson et al., 1986; Ranney, 1988; Simpson and Kanter, 1997; Simpson and Pettit, 1997; Trepman et al., 1998; Trepman et al., 1994)

Therefore, is not a contradiction to include the various forms of dance and specifically the classical ballet in the area of sports science, once the major part of their movements are, physically and coordinative so (or more) demanding as the movements of the usual sportive disciplines.

Nevertheless, in classical ballet, against to the majority of sports competition, aesthetical aspects are the only criterion for the qualitative evaluation of the dance performance. The dancers move in a grand, noble manner. They appear to spend more time in the air than on the ground, seem to be momentarily suspended in the air like ignoring the law of gravity as they “float” through the air in long, slow leaps. How could this visual illusion be defined in scientific terms? How could the dancer create these dance illusions?

1.3.1 Ballet Jumps

In classical ballet, the jumps are one of the most important and usual elements that compose each training practice and each custom performance, being repeated constantly during the whole life of a dancer. In sport science, it is well demonstrated that the magnitude of forces produced during some jump performances can exceed largely the subject’s body mass (Amadio and Duarte, 1996). On the other hand, in dance, some studies confirm a relationship between the amplitude and the magnitude of articular forces during jumps, as well as recognize the potential damage consequences to the tissues involved in its dissipation (Simpson and Kanter, 1997; Simpson and Pettit, 1997).

Technically, the correct execution of a jump always involves the execution of a *plié* movement, in which a basic vigorous and harmonious bending movement of the knees is observed (a countermovement).

According to several authors (Clarkon and Skrinar, 1988; Trepman et al., 1998; Trepman et al., 1994), the *plié* is the most important, fundamental and basic element in classical ballet, representing the basis of the whole technical preparation, above which every movement happens, especially in powerful and sumptuous ballet jumps. The *plié* is an essential element both in the beginning of the jump movement, allowing an enhancement of the jump performance, as well as in the end of the jump, allowing easer and graceful landings and preventing injuries. The repetitive execution of the *plié* in training classes is used to improve strength, timing, alignment, trunk stability and coordination of joint movements.

The *plié* is one the first skills that should be teached to children in the beginning of a class. Usually, after the warm-up exercises, the *plié* is the first exercise in a ballet class. It can be taken to a *demi-plié* or a *grand-plié*. The *demi-plié* is a half bent of the knees (a knee

flexion) and should be done, in all positions but the second, as far down as possible without lifting the heels off the floor. The *grand-plié* is a deep bend of the knees, and the dancer bends all the way down until the thighs are almost horizontal to the ground and the buttocks almost reach the feet. In all positions except second, the heels release from the floor. Just like all the other movements in classical ballet, the *plié* is always done with the legs turned out.

Most of the dance movements begin and ends with a *plié*, being the first component of other movements. As the dancer turn or jump, the lower limb always change from being straight to bent at the knee or ankle level and the *plié* is repeated constantly. A correct dance movement requires the ability to *plié* with control, strength and stretch, so that the movement flows without stopping and appears to be seamless.

The forced lengthening of an active muscle before allowing it to shorten, leads to an enhanced response during shortening. This potentiation phenomenon during the shortening phase of a lengthening-shortening sequence of muscle actions, was earlier studied by several author's and is called stretch-shortening cycle (SSC) (Norman and Komi, 1979). In human movements the stretch-shortening cycle is a commonly used muscle action. In the same way as in the performance of the sportive jumps, ballet jumps follows the same potentiation mechanism of the SSC.

Although following a very specific technique and a standard terminology, there are no differences concerning the universality of the training principles between the classical ballet and the sports environment. The rules, strategies, principles, laws and concepts of the physics, chemistry, mathematics, physiology, anatomy, and others, are the same. The only thing that changes is the involvement of performance of the same biological system.

1.4. General Research Question

Our major general research question was the assessment of the mechanical loads and internal dynamics exerted in the lower limb, during the performance of highly demanding human movements.

1.5. Purposes

The purposes of the present study were:

a) to develop an appropriate methodology to estimate the internal dynamics and mechanical loads exerted in the lower limb, during highly demanding physical movements with strong technical limitations and kinematical restriction: jumps in classical ballet.

    a1) from the external dynamics of the subject, solve the classical movement equations and obtain the forces and intersegmentar moments. This is the classical domain of Inverse Dynamics.

    a2) from the intersegmentar moments obtained in the previous step, and the musculoskeleton geometry, obtain the muscular forces using one of several methodologies: pure inverse decomposition with an *ad hoc* merit function; combine a muscle model in a forward/inverse dynamics approach with an *ad hoc* merit function; combine an electromyography (EMG) driven muscle model in a Forward/Inverse Dynamics approach.

b) directly measure the behaviour of the two compartments (contractile and elastic components), of the muscle-tendon complex of the synergistic pair of muscles, medial gastrocnemius and soleus, during different intensity drop jumps (SSC movements).

    It will be measured the fascicle length of both muscles with ultrasonography, in order o examine the contribution of the contractile and the elastic components to the potentiation of the muscle-tendon complex.

1.6. Organization of the Thesis

The present study comprises eight chapters and one appendix.

Chapter 1 - Introduction

The present introduction includes the definition and the importance of the internal forces on biomechanics, the complexity of the biomechanics research, a general characterisation of movements in classical ballet, especially the ballet jumps, as well as the general research question of the thesis and purposes.

Chapter 2 – Review of Literature

This chapter presents a general review of literature about skeletal muscles, tendons, muscle-tendon unit, and stretch-shortening cycle movements, as well as biomechanical modelation, and methods to assess internal forces.

Chapter 3 – Force, Articular Moment and Mechanical Power in Elementary Ballet Jumps

The purpose of this first study was to access the internal dynamics of some balletic movements, e.g. the internal knee and ankle loads and their potential for injury, using the traditional inverse-dynamics approach.

Chapter 4- Biomechanical Analysis of Elementary Ballet Jumps: Integration of Force Plate Data and EMG Records

The purpose of this study was, using the EMG data, to access the importance of co-contractions in the ballet movements selected for the study.

Chapter 5- Data Processing and Filtering of Kinematical Signals

The aim of this study (technical note) was to present alternative filtering and smoothing schemes to process signals obtained from kinematics, in order to increase the accuracy of the inverse dynamic approach in the calculations of intra articular moments and forces. We test the applicability of these new approximants, comparing both usual and alternative filtering and smoothing techniques.

Chapter 6- Estimation of muscle forces and joint moments using a forward-inverse dynamics model

The assessment of biomechanical loading and a better understanding of how the body transmit and attenuate the impact forces through the muscles, bones and joint tissues is an extremely important topic of interest for exercise prescription and injury prevention. The main purposes of this study were: 1) to calculate the joint reaction forces and moments of forces in ankle, knee, and hip joints, during very demanding ballet jumps, using the inverse dynamics approach, and 2) to present an electromyographic (EMG) driven forward-inverse dynamics model to estimate muscle forces and joint moments.

Chapter 7- Intensity and Muscle Specific Fascicle Behavior During Human Drop Jumps

The main purposes of this study were: directly measure (with ultrasonography) the behaviour of the two compartments (contractile and elastic components), of the muscle-tendon complex of the synergistic pair of muscles, medial gastrocnemius and soleus, during high intensity drop jumps (SSC movements), and examine the contribution of the contractile and the elastic components to the potentiation of the muscle-tendon complex.

Chapter 8- Conclusions

In this chapter we present the main findings of these studies and the some considerations about the future research.

Appendix I

In appendix I we present in more detail a little review about the mathematical filters, used in chapter 5, for data processing and filtering the kinematical signals used to in the inverse dynamics approach.

1.7. References:

Amadio, A. C. and Duarte, M. (1996). Fundamentos biomecanicos para a analise do movimento. EEF-USP, Laboratório de Biomecânica, Sao Paulo.

Baumann, W. (1995). Procedimento para determinar as forças internas na biomecânica do ser humano - aspectos da carga e sobrecarga nas extremidades inferiores. In: Klavdianos, A. C. D., Fonseca, J. C. P. (eds) VI Congresso Brasileiro de Biomecânica. Sociedade Brasileira de Biomecânica, Brasília

Bruggemann, G. P. (2005). Mechanical loading of biological structures and tissue response. In: Rodrigues, H., Cerrolaza, M., Doblaré, M., Ambrósio, J., Viceconti, M. (eds) ICCB 2005 - II International Conference on Computational Bioengineering, Lisboa, pp. 25-26.

Clarkon, P. M. and Skrinar, M. (1988). Science of Dance Training. Human Kinetics, Champaign.

Clippinger-Robertson, K. S.; Hutton, R. S.; Miller, D. I. and Nichols, T. R. (1986). Mechanical and Anatomical Factors Relating to the Incidence and Etiology of Patellofemoral Pain in Dancers. In: Shell, C. G. (ed) The Dancer as Athlete - The 1984 Olympic Scientific Congress Proceedings. Human Kinetics Publishers, Champaing, Illinois, pp. 53-72.

Nigg, B. M. (1994). Definition of Biomechanics. In: Nigg, B. M., Herzog, W. (eds) Biomechanics of the Musculo-Skeletal System. John Wiley & Sons, Chichester, p. 2.

Norman, R. W. and Komi, P. V. (1979). Electromechanical delay in skeletal muscle under normal movement conditions. Acta Physiol Scand 106: 241-248.

Ranney, D. (1988). Biomechanics in Dance. In: Clarkson, P. M., Skrinar, M. (eds) Science of Dance Training. Human Kinetics, Champaign, pp. 125-144.

Simpson, K. J. and Kanter, L. (1997). Jump distance of dance landings influencing internal joint forces: I. Axial forces. Med Sci Sports Exerc 29: 916-927.

Simpson, K. J. and Pettit, M. (1997). Jump distance of dance landings influencing internal joint forces: II. Shear forces. Med Sci Sports Exerc 29: 928-936.

Trepman, E.; Gellman, R. E.; Micheli, L. J. and De Luca, C. J. (1998). Electromyographic analysis of grand-plie in ballet and modern dancers. Med Sci Sports Exerc 30: 1708-1720.

Trepman, E.; Gellman, R. E.; Solomon, R.; Murthy, K. R.; Micheli, L. J. and De Luca, C. J. (1994). Electromyographic analysis of standing posture and demi-plie in ballet and modern dancers. Med Sci Sports Exerc 26: 771-782.

Winter, D. A. (1990). Biomechanics and motor control of human movement. Jonh Willey & Sons, New York.

Chapter 2
Review of the Literature

2. Review of the Literature

2.1. Skeletal Muscles

Skeletal muscles represent the most abundant tissues of the human body. They comprise approximately 40% (Loocke et al., 2004) of the total body weight and are organized into hundreds of separate organs, the body muscles, each of which is composed of fascicles containing bundles of fibres, themselves composed of parallel and/or in series bundles of myofibrils. The myofibrils consist of series of contractile units, the sarcomeres, composed by the contractile proteins, the actin and myosin myofilaments (Huxley, 2000a; Huxley and Hanson, 1954; Lieber and Friden, 2000).

Skeletal muscles are responsible for the relative motion of the bones and provide strength and protection to the skeleton by distributing loads and absorbing shocks.

2.1.1. Mechanical Contraction in Skeletal Muscles

In striated skeletal muscles, muscle contraction result from the sliding movement between thick filaments, especially composed by myosin, and thin filaments specially composed by actin, within the sarcomere. This is achieved by the cyclic action of the cross-bridges composed of the heads of myosin molecules projecting from the thick filament, which attach to the thin filament, exert force for a period of time and detach in the end (Herzog, 2000b; Huxley, 2000b). Therefore, the development of force depends on these cross-bridge attach-detach cycles. As much as the number of cycles occurring at the same time the greater will be the force production, i.e., force varies with the amount of overlap between thick and thin filaments within a sarcomere (Gordon et al., 1966). Subsequently, the force is transmitted to tendons through a serial and parallel way (Huijing, 1999; Young et al., 2000).

2.1.2. Skeletal Muscles Architecture

According to Huijing (1992) and Lieber and Friden (2000; 2001) the skeletal muscle architecture, i.e., the arrangement of muscles fibres within and between muscles is a structural property of whole muscles that determine their function.

Muscle fibres are usually represented in bundles, projected from an origin, on a proximal tendon plate, to an insertion, distally. According to Hijikata (1993), each fascicle comprises

muscle fibres arranged in parallel and/or in series. Although it was proposed previously in the literature that different muscles produce different amounts of force, due to their different fibre sizes, presently it is known that fibre size between muscles varies not much. Then, architectural differences between muscles are considered the best predictor of force generation, i.e., the force produced in muscle is highly dependent on its architecture.

Voluntary movements are imposed by the joint moment requirements. Moments about joints, in turn, are caused almost exclusively by muscular forces, although ligaments, bony contact and other soft tissues forces may contribute to the joint moment. The shortening of muscle fibres produces movement in the tendons and induces changes in joint angles. Therefore, the muscle architecture has a considerable effect on the force-producing capacity of the muscle (Huijing, 1992). Understand the movement control requires the knowledge of how a single muscle's force is produced and controlled, and how the muscles crossing a given joint interact with each other during a given movement.

Morphologically skeletal muscles can be classified in two great types: muscles with fibres arranged in parallel to the muscle's force generation axis (fibres placed side by side) and pennate muscles, in which the fibres are inserted into tendons at a certain angle (pennation angle) relative to the force generation axis. However, the major part of the muscles is composed of fibres that are inserted at several angles relative to the axis of force generation (multipennate muscles) (Kawakami et al., 1993; Lieber and Friden, 2001).

The advantage of the pennation arrangement of some muscles is his greater physiological cross-sectional area (PCSA). The physiological cross-sectional area of a muscle is a measure of the number of sarcomeres in parallel with the angle of pull of the muscle. In pennate muscles the physiological cross-sectional area is:

$$PCSA = \frac{V \cos\theta}{l \times d} \tag{2.1}$$

where V is the muscle volume

d is the density of muscle

l is the length of muscle fibres

and $\cos\theta$ is the pennation angle (angle between the long axis of the muscle and the fibre-angle).

Pennate muscles contain more muscle fibres than parallel fibre muscles, however, each fibre is shorter. The force produced in pennate muscles will be greater that in the paralleled muscles, as PSCA and maximal force are considered to varying proportionately (Fukunaga et al., 1996b; Maganaris et al., 2001; Narici et al., 1992). Due to its short fibres, pennate muscles shorten under contraction less than those parallel fibre muscles.

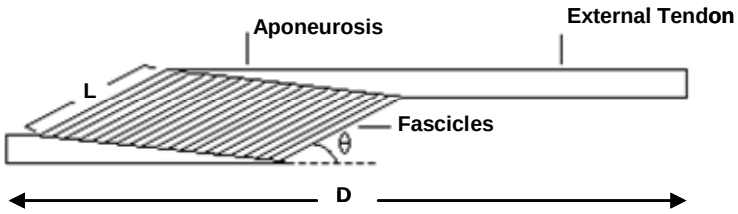

Figure 2.1 Diagram of a muscle with fibres of uniform length and its tendons.

For a typical muscle with fibres of uniform length (Figure 2.1), the force exerted by every muscle fibre is routed through the same total length of the tendon (D – L cos θ). The pennation angle of mammalian muscles with different design has been measured at resting length, and generally varies between 0º and 30º (Alexander, 2000). Thus, as the cos θ varies between 0.87 (cos 30º) and 1.00 (cos 0º), close enough to 1, so we can estimate the effective length of the tendon, for most practical purposes, as D – L.

According to Yamaguchi et al. (1990) the overall length D of the human *gastrocnemius* is about 450 mm and the muscle fibres are around 50 mm long, so the effective length of the Achilles tendon is about 400 mm (Figure 2.1).

However, experimental studies of muscle fibre lengths suggest that, especially in the parallel arrangement, the muscle fibres do not extend to the entire fascicle length and even less to the entire muscle length (Ounjian et al., 1991; Young et al., 2000). According to the authors, among long parallel fibred muscles arrangement, we can found the presence of fibres with intrafascicular terminations that provide both lateral and serial connection of muscle fibres and are able to transmit the tension to neighboring fibres and to the muscle tendon (Monti et al., 1999).

2.1.3. Bi-articular Muscles

Some muscles and their tendons can span more than one joint. Bi-articular muscles are most common (*rectus femoris*, hamstrings, *gastrocnemius*, etc). A bi-articular muscle, which crosses two joints, can either accelerate both joints in the same direction as the direction of moment which it produces, or it can negatively accelerate one of the joints in the opposite direction to the direction of the moment which it produces at that joint.

The existence of muscles that span two joints can provide a number of advantages to the musculoskeletal system. Bi-articular muscles appear to perform unique actions which could not be performed by a set of two mono-articular muscles (van Ingen Schenau et al., 1987). It has been argued that these two types of muscles (mono and bi-articular) perform different functions. The mono-articular muscles are especially concerned with the generation of positive work, whereas the bi-articular muscles, control the distribution of net joint moments and joint power over the joints (Bobbert and van Ingen Schenau, 1988; Gielen et al., 1990; Jacobs et al., 1993; Jacobs and van Ingen Schenau, 1992). According to Gielen et al. (1990), if the biological limbs would be supplied only with mono-articular muscles, the movement would be rather inefficient, since, for a great number of movements, the mono-articular muscle would dissipate a large part of the work delivered by other muscles. With bi-articular muscles the negative work in a joint can be avoided, making the movement coordination more efficient. Nevertheless, in explosive movements, it was demonstrated that the key to success rely in the efficient physiologic and biomechanical cooperation between mono and bi-articular muscles (Gregoire et al., 1984).

2.1.3.1. Energy Transfer between Segments

The understanding of the way how energy transfer is processed along articular joints is influenced by the knowledge of the physical relationship established between ground reaction forces, its intensity, direction and point of application, and the dynamic parameters of body segments (position, velocity, acceleration and inertial characteristics). This relationship is mediated by the muscles, i.e. the force producers, and its action is controlled by the nervous system. The effects of the muscle mechanical production are varied and dependent on the interaction of the skeletal-muscle with the different structures of the nervous system and the environment.

According to Bobbert and van Ingen Schenau (1988), movements coordination is a function of the nervous system and depends on the timing, amplitude and frequency of muscle activation. The coordinated action of the nervous system comprises not only the regulation of the movement itself but also the stiffness of the neuromuscular system, especially important in movement control.

Bi-articular muscles, like *gastrocnemius*, plays a crucial role in the transformation of rotational movements in the joints into translational movements of the body's centre of gravity, and in the optimal use of the energy produced by the muscle groups located proximally, distributing the net joint moments and joint power over the joints (Jacobs et al., 1996; van Ingen Schenau, 1989; van Ingen Schenau et al., 1987; van Ingen Schenau et al., 1990). The transportation of mechanical energy between joints, has been widely discussed (Bobbert et al., 1986a; Bobbert and van Ingen Schenau, 1988; Jacobs et al., 1996; van Ingen Schenau et al., 1985; van Ingen Schenau et al., 1990). According to the authors, during vertical jumps, the transfer of mechanical energy from proximal to distal joints of the lower extremities occurs due to the unique action of the bi-articular muscles.

According to Stefanyshyn and Nigg (1998), the mechanical energy produced by muscles enables the movement of the body during athletic activities. The maximal performance of an athlete's ability is largely dependent on the mechanical energy generated, absorbed or transferred. Therefore it's understood provide further insights into athletic performances.

In human jumping, the *gastrocnemius* muscle is used to transport energy from knee-joint, produced by knee extensors, to the ankle joint (Gregoire et al., 1984). A considerable amount of positive work around the ankle (40%) is delivered by the *gastrocnemius*, indicating that high positive work output is an important function for human *gastrocnemius* in jumping (Bobbert et al., 1986a; Ettema et al., 1990a).

In a study of Prilutsky and Zatsiorsky (1994), the authors estimate the amount of mechanical energy transferred by the bi-articular muscles between leg joints, during vertical jumps and jogging, in human healthy subjects. It was shown that during the landing phases of jumping and shock-absorbing phase during running, the transfer of mechanical energy was from distal to proximal joints (18.6 ± 4.2 J). On the other hand, during the push-off phases of squat jumps and running, the transfer of mechanical energy was from proximal to

distal joints (178.6 ± 45.7 J). The author's suggest that the bi-articular muscles compensate the deficiency in work production of the distal mono-articular muscles, distributing the mechanical energy between segments and joints. During the push-off phase, the muscles of proximal joints transfer, to the distal joints, a part of the generated mechanical energy. During the landing phase, the muscles from proximal joints help the distal muscles to dissipate the mechanical energy of the body, allowing more efficient performance movements. In the same way, the long tendons of the lower extremities bi-articular muscles help the small volume distal muscles to dissipate the mechanical energy of the body.

2.1.3.2. Estimation of Energy Transfer

The intersegmentar energy transfer enable by the bi-articular muscles can be estimated according to different, but non contradictory concepts. In both estimations, first, is necessary to calculate the force produced individually by each muscle involved.

According to Bobbert et al. (1986a) and Jacobs et al. (1996), the first concept consist in the determination of the mechanical power originated in the proximal joint of the bi-articular muscle. For example, in the case of the *gastrocnemius* muscle, the power transmitted through the proximal joint (knee) to the distal joint (ankle) is equal to the product of the moment of force generated by the muscle in the knee, by the angular velocity of the same joint, the knee:

$$P_{Trans(k-a)}(t) = F_{Gas}(t) \times b_{Gas}(t) \times \varpi_{knee}(t), \qquad (2.2)$$

where, $P_{Trans(k-a)}(t)$, is the mechanical power transfer by the *gastrocnemius* muscle from the knee to the ankle,

$F_{Gas}(t)$, is the force produced by the *gastrocnemius* muscle,

$b_{Gas}(t)$, is the moment arm of the *gastrocnemius* muscle related to the knee,

and the $\varpi_{knee}(t)$, is the angular velocity of the knee.

According to Prilutsky and Zatsiorsky (1994) and Prilutsky et al. (1996), the second concept to estimate the intersegmentar energy transfer consist in the determination of the difference between the power originated by the net joint moments and the sum of the power originated by the muscles that cross that joint.

$$P(t) = P_a(t) - \sum_{i=1}^{n} Pm_i(t), \quad (2.3)$$

where,

$P(t)$, is the mechanical power transferred by the bi-articular muscles

$P_a(t)$, is the power developed by the joint moment

$\sum_{i=1}^{n} Pm_i(t)$, is the sum of powers developed by all the muscles serving each joint

$Pm_i(t) = Fm_i \times V_{oi_i}$, is the muscular power, i.e., the product of force originated by the muscle *i*, and the velocity by which the origin and insertion of the *i* muscle come near or drift apart from each other.

If we just have mono-articular muscles in our body, this different will be zero. Due of the bi-articular muscles, muscular and articular powers are different. According to the authors, the difference between moments allows the estimation of the rate at which energy is transferred to that own joint or, by the contrary, estimate the rate at which energy is transferred from that joint to another neighbouring joint. The parameter $P(t)$, not only allows knowing the value of the power produced by muscles, but also the rate and direction at which energy flows. The time integral of power $P(t)$ gives the amount of energy transferred. In fact, if the total power produced by muscles that cross a joint and the power of moment at the joint have the same sign, and $P(t)$ were positive, in this case the mechanical power is transferred to that own joint, i.e., an extra amount of mechanical energy comes to the joint. By the contrary, if $P(t)$ were negative, i.e., the power of moment at the joint is smaller than the total power of muscles serving a given joint, the energy is transferred from this joint to the adjacent joints.

2.2. Tendons

2.2.1. Functional Anatomy of Tendons

Tendons are fibrous cords which attach the muscle to the bone being integral part of the muscle-tendon complex. Tendons are usually submitted to highly tension loads, nevertheless they are extremely resistant and capable to return to its initial position after being actively stretched. The major functions of tendons are: transference of forces

between muscle and bone, and, storage and recovery of elastic energy (Alexander and Bennet-Clark, 1977; Cavagna, 1977; Enoka, 2002; O'Brien, 1992).

Tendons include not only the external fibrous bundles (external tendon) that connects the muscle to the bone, but also the *aponeurosis* (internal tendon) into which the muscle fibres insert. The whitish aspect of tendons is due to its lower blood supply. Its composition is about 30% of collagen and 2% of elastin, inlaid in an extracellular matrix also containing 68% of water (O'Brien, 1992).

2.2.2. Physical Properties

2.2.2.1. Stress-Strain Curve

A typical stress-strain curve for tendon is illustrated in Figure 2.2. Stress and strain characterize the intrinsic force capacity and extensibility of the tendon. When a tendon is submitted to a load, an elastic response is observed and it's possible to distinguish three distinct regions: a) toe region, b) linear region and c) failure region.

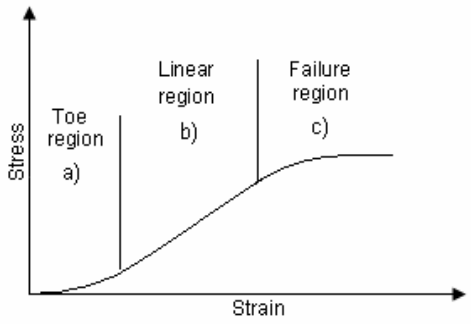

Figure 2.2 A typical stress-strain curve for a tendon (not scaled), where it's possible to observe the three regions: a) toe region, b) linear region and c) failure region (based on Nigg and Herzog, 1994).

Due to the straightening of crimped collagen fibrils and elasticity of elastin, the initial part of the stress-strain curve has considerable strain deformation with little accompanying resistive stress - the toe region. This region lies within approximately 3% of the strain. Afterwards this portion is followed by a linear region, where the fibrils are oriented themselves in the direction of the force, and the stiffness is basically the same of the collagen fibrils. This reversible region usually defines the elasticity of the tendon and extends to about 4-5% of the strain, with stress values of about 5 to 30 MPa (Rack and Westbury, 1974). Loadings beyond this linear region cause permanent deformation. The

collagen bundles are breaking and the tissue then ruptures. This ultimate region of the tendon is about 8-10% of the strain (Nigg and Herzog, 1994).

Another important aspect of tendon behaviour is viscoelasticity. Tendons exhibit a nonlinear and viscoelastic behaviour. Viscoelasticity indicates that the mechanical behaviour of the material is time dependent. Thus, the relationship between stress and strain is not constant, but depends on the time of displacement or load.

The slope of the elastic region (linear region) of the stress-strain relation is defined as the Young's modulus (Y) being defined as the ratio between stress (σ) and strain (ε) and represents the normalized stiffness of the tissue:

$$Y = \frac{\sigma}{\varepsilon} \tag{2.4}$$

According to Bennet et al. (1986), the elastic modulus for mammalian tendon varies from 0.8 to 2 GPa, with an average value of 1.5 GPa. This variability can probably be attributed to different methodological procedures used during measurements.

One other phenomenon characteristic of a viscoelastic material is hysteresis or energy dissipation. This means that if a viscoelastic material is loaded and unloaded, the unloading curve will not follow the loading curve. The difference between the two curves represents the amount of energy that is dissipated or lost during loading. The energy expended during a tension deformation is not completely recovered when the deforming force is removed (Figure 2.3).

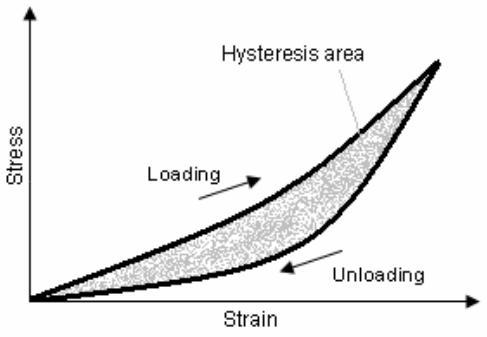

Figure 2.3 A schematic stress-strain curve for a tendon loading and unloading. The shaded area is the hysteresis area. The difference between the two curves, loading and unloading represents the energy lost or dissipated during loading (based on Nigg and Herzog, 1994).

Because of the low hysteresis of tendons, they are capable of storing and releasing considerable amounts of elastic strain energy. When a muscle is activated and the muscle-tendon-unit is stretched, the energy associated with the deformation of the tendon is almost completely recovered when the force is removed. Some author's showed that hysteresis of several vertebrate tendons varies from 6-11% (Ker, 1981; Ker et al., 2000).

2.2.3. Elastic Properties of Tendons

Although some elastic energy can be stored and recovered within the myosin cross-bridges, most elastic strain energy is stored and recovered within the collagen of *aponeurosis* and tendons of the muscle-tendon-unit (Alexander and Bennet-Clark, 1977).

According to Hof et al. (1983) and Bobbert (2001) some of the most intriguing design aspects of the human musculoskeletal system are the distal muscle-tendon-unit and specially those of the plantar flexors muscles, where the muscle fibres themselves are only 6 to 7 cm long, while the distance from origin to insertion is 40 to 50 cm. In this way, a large part of the muscle length is spanned by purely elastic structures and is of general consensus that tendinous tissue does not simply transfer forces to the skeleton.

Tendons seem inextensible when handled, but they are appreciably stretched when submitted to considerable forces. Although being a low deformation tissue, tendons are not inextensible and as already appreciated, they are highly non-linear in their biomechanical behaviour. These non-linear spring-like characteristics allows an interesting mechanical interaction between muscle and tendon (Lieber et al., 2000).

Tendons have an important energy-saving role in locomotion (Alexander, 1988), acting like springs, storing elastic energy when the active muscle is stretched as the foot is set down, and returning this energy in elastic recoil as the foot is lifted (van Ingen Schenau and Cavanagh, 1990). Nevertheless, according to Roberts (2002), tendons not only store and return elastic energy, but also act to reduce the corresponding muscle's fibre shortening velocity to allow the fibres to operate at a more favourable contractile state. The reduction in fibre velocity will increase the contraction efficiency and reduce the corresponding metabolic cost.

Isolated tendon properties have been determined in detail biomechanically by several authors (Ker et al., 1998; Loren and Lieber, 1995; Rack and Westbury, 1984). Nevertheless, Griffiths (1991) experimentally showed muscle shortening during tendon lengthening, indicating that is not appropriate to consider either muscle and tendon properties in isolated studies when trying to understand their physiological and biomechanical roles.

2.2.3.1. Compliance in Tendons

During a muscle contraction, tendons are stretched in agreement with their compliance and this is higher at low tensions and diminishes as the applied tension increases (Griffiths, 1991). Tendon compliance also varies greatly between different muscles due to the great range that exists in tendon thickness and length, and also due to the differences that exist in the material properties correlated with function and age (Nakagawa et al., 1996; Rack and Westbury, 1984).

A compliant tendon enables the storing energy during stretch and the release of this energy during recoil (Alexander, 1983).

According to Griffiths (1991) and Roberts (2002) the compliance of the tendon has a substantial influence on the function of the whole muscle, and this property can be illustrated with a simple experiment. When a stretch is applied to a contracted muscle (isometric contraction), the entire muscle-tendon unit is held at a constant length while the muscle is stimulated to produce maximal force. In this case the muscle fibres actually shorten and all the stretch occurs in the tendon. Because the muscle-tendon unit length is held constant, the shortening of the muscle fascicles is possible only with the stretch of the series elastic component external to the muscle fascicles, i.e. the tendon.

The changes in length that muscles undergo due to the action of the contractile component is affected by both tendon as well as the other components of series elasticity (cross-bridges, actin filaments and to a lesser degree in the myosin filaments).

In a study of Bobbert (2001), the author show that the series elastic element compliance of the triceps surae has a considerable effect on the maximum height achieved during the squat jump. The same effect was previously presented by Pandy (1990). In tasks such as

the explosive leg extension movements, long compliant tendons, as in the plantar flexors group, allow a considerable maximization of the performance.

2.2.3.2. Energy Dissipation

Another important property of tendon that should be taken into account in the studies of human movement is energy dissipation. It can be defined as the energy lost as a fraction of the work done stretching the tendon and, according to Alexander (2000), the percentage of energy recovery is about 88 to 95% for tendons.

It is important for the efficiency of tendon function that its energy dissipation should be low. Tendons would work less well as energy-saving springs, if less energy is returned in their elastic recoil and more dissipated as heat.

The exact knowledge of length-tension characteristics of human tendons under physiological conditions is crucial to understand the interaction between muscle fibres and tendons, in human movements.

2.2.3.3. Tendons Stiffness

According to Proske and Morgan (1987), stiffness seems to be the most important property of tendons that should be taken into account. The stiffness of an ideal spring is the inverse of its compliance and usually defined as:

$$k = dF / dx, \tag{2.5}$$

i.e., the derivative of the force in order to the displacement of equilibrium position (deformation). When a force F compresses or stretches a spring, the work achieved by the force F is stored as strain energy in the deformed structure. The amount of energy (E) stored in an ideal spring of stiffness k is equal to the work done (W) by the stretching force. It can be determined by integration of equation:

$$\Delta E = W = \int F * dx = \int k * x * dx = \frac{1}{2} k * x^2 \tag{2.6}$$

Nevertheless the stiffness characteristics of the living tissues are variable, non-linear, and subject to damping (Shorten, 1987).

According to Ito *e*t al*.* (1998), Ker (1981), Loren and Lieber (1995), Rack and Westbury (1984), the tendon stiffness increased with increasing tendon force. The tendon will be stretched more easily when the force is small and becomes less compliant with increment of force.

2.2.4. Achilles Tendon

The Achilles tendon (AT) spans two joints and connects the calcaneus to the *gastrocnemius* and *soleus* muscles, comprising the largest and strongest muscle complex in the calf. Because of their anatomic position, the AT and its muscles are the ones that in many activities are the first structures to take up the impact loads. They are therefore also accessible to either chronic or acute injuries.

The *gastrocnemius* and *soleus* muscles, via the Achilles tendon, function as the major plantar flexors of the ankle joint. In walking as well as in running and jumping activities, this musculotendinous complex provides the primary propulsive force for locomotion. Whereas the *gastrocnemius* muscle functions primarily as a plantar flexor at the ankle, the *soleus* muscle has a postural role as well, preventing the body from falling forward during standing. Contraction of this musculotendinous complex also functions to flex the knee and supinate the subtalar joint.

During locomotion movements, it is well know that AT is submitted to great loads. It has been suggested that the fracture stress (ultimate tensile stress) seems to be uniform for tendons and is about of 100 MPa (Alexander, 2000; Ker et al., 1988). By dividing the average tendon fracture stress of 100 MPa by the maximum tendon stress, a safety factor of 4 is estimated for the major part of the tendons (Ker et al., 1998; Maganaris and Paul, 1999). According to the authors, the most tendons in the human body are not normally at risk of fracture, unless a rapid tendon stretch is applied during eccentric muscle contractions. It is plausible that the AT approaches the safety limit if we consider the considerable large strain and stress that this tendon is submitted, especially during vigorous activities that involve eccentric muscle contractions.

In another way, it should be noted that there are considerable distinctions between tendon properties among subjects, as well as with animal data (Scott and Loeb, 1995). These differences reflect the substantial intersubject variation in AT loading during locomotion (Finni et al., 1998).

According to Magnusson *et al.* (2001), the greater tendon cross-sectional area, and thereby the lower stress for a given load, provided a greater safety factor against tendon fracture.
For example in two subjects with similar tendon forces, the stress was almost 50% lower in the subject with the larger tendon cross-sectional area (Magnusson et al., 2001).

Accordingly Ker *et al.* (2000) tendon ruptures occurs after 4.2h of cyclically loaded with maximum isometric force, indicating that the duration of loading may be important for the ability of tendon tissue to avoid overuse injuries.

Since the human *in vivo* triceps surae complex and AT is submitted to substantial forces during locomotion human movements, its mechanical properties are of considerable interest and relevance to the study of loading history.

2.2.4.1. Injuries in Achilles Tendon

Frequently submitted to considerable forces, the AT is usually associated with pathologies related to loading history (Kannus et al., 1997), including ruptures (Kannus and Jozsa, 1991). This vulnerability to injury is partly due to its limited blood supply and the combination of forces to which it is submitted. According to Soma and Mandelbaum (1994) and Jozsa et al. (1989), the most fragile area of the tendon with the poorest blood supply is approximately 2 to 6 cm above the insertion into the calcaneus. The blood supply diminishes with age, predisposing this area of the tendon to chronic inflammation and possible rupture (Mazzone and McCue, 2002). The peak of incidence to AT ruptures is usually about 30 to 40 years, and occurs very frequently during sports and other physical activities. The preventive care is of primordial importance. According to several authors (Ker, 1981) the tendon acts like a mechanical buffer to protect the muscle fibres from damage during an eccentric contraction (stretch). According to McCully and Faulkner (1986) the muscle fibres would be rapidly injured if tendons were not, at the same time, so strong

and compliant, allowing at the same time one of the most important role of tendon compliance: the storage and subsequent release of energy .

2.3. The Muscle-Tendon Unit (MTU)

The human movement is performed by the contraction of muscle fibres that are connected in series with tendons and all together compose the muscle-tendon unit (MTU).

The force from muscle contraction exerted by muscle fibres is transferred to the bone via tendons to produce joint movement. In this way the length change in muscle fibre is not necessarily the same as that of the muscle tendon complex (Cook and McDonagh, 1995; Griffiths, 1991; Ito et al., 1998; Roberts et al., 1997). During an isometric contraction apparently there's no change in muscle fibre length. However, due to elastic properties of tendon, we can see some shortening of muscle fibres and lengthening of tendon, even when the total length of the MTU is kept constant (Cook and McDonagh, 1995; Loren and Lieber, 1995). In this way, muscle fibres produce mechanical work and apparently there's no work done by the entire MTU.

According to a study from Ito and coworkers (1998) an increase in dorsiflexion isometric moment was accompanied by a shortening of fascicles and a lengthening of the tendon and *aponeurosis*. This can suggest that muscle fibres produce mechanical work that was absorbed by the tendon, even during isometric contractions. The magnitude of the internal shortening might be different between muscles, possibly due to architectural variations of the MTU.

Although the external tendon and *aponeurosis* are considered as the passive components of the MTU they cannot be understood purely as rigid links between the skeleton and muscles, particularly because of their non–linear properties. Tendons store and return elastic energy, as well as, reduce the muscle fiber shortening velocity, allowing the muscle to operate at a more favorable contractive state.

2.3.1. The Hill Muscle Model

The Hill model has been first presented in 1938 (Hill, 1938) and used by several authors to describe the muscle mechanics in natural movements. The model it's used to describe the behaviour of the MTU in terms of three functional distinct elements:

- two elements arranged in series: one elastic element (SE) and one contractile element (CE);
- one elastic element placed in parallel with the two others: the parallel elastic element (PE). (Figure 2.4)

The CE represents the force produced in the muscle by the cross-bridges and is described by the characteristic force-velocity and force-length relationships (Gordon et al., 1966; Hill, 1938).

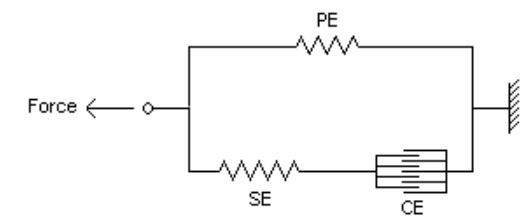

Figure 2.4 A Hill model of a single muscle fibre.

The SE is responsible for force transmission and is composed by two fractions: the active fraction localized in actin-myosin cross-bridges, and the passive fraction, mainly located in tendons (Huijing, 1992).

According to Hof et al. (1983), the PE, represents the mechanical properties of the resting muscle, acting in parallel with the part of the muscle that generates force - the contractile element. PE is constituted by connective tissue that surrounds the CE, through the muscle membranes: the epimysium which surrounds the whole muscle, the perimysium which surrounds the bundles of muscle fibres and the endomysium which surrounds each muscle fibre individually. Together these tissue sheaths, usually called as fascia, enclose the muscles or separate them into layers and finally connect them into external tendons.

Together, parallel and series elastic elements account for the passive tension properties of the whole muscle. The structures responsible for the parallel elasticity component include connective tissue binding muscles fibres and fascicles together, as well as intrafibrillar proteins like titin. Tendons are series elastic structures, but the series elasticity also resides within cross-bridges, actin filaments and to a lesser degree in myosin filaments.

2.3.2. Contractile Properties of the MTU

The basic contractile properties of the muscle, characterized by the force-length and force-velocity relations of the single fibre, are influenced by the way in which the fibres are organized in the muscle. An in-depth study of these relationships will permit a better understanding of the limitations and capabilities of the human movement.

When the muscle fibres are arranged in series it is improved the maximum shortening velocity of the muscle. In contrast, the maximum force that a muscle can exert is maximized by the parallel arrangement of the muscle fibre. When the muscle design includes a pennation angle, for the same volume of muscle, more fibres can be placed in parallel when the pennation angle is different from zero. As a result, the pennated arrangement can exert a greater maximum force, as already discussed.

According to Enoka (2002), the force exerted by a muscle is not solely dependent on the active process of the cross-bridges cycle and filament overlap. In addition, the connective tissue (that combines single fibres into whole muscle) and the cytoskeleton (involved in the alignment of the thick and thin filaments, alignment of the myofilaments and in the transmission of force from sarcomeres to skeleton), exert a passive tension/force. According to the author, the force exerted by a muscle is due to both the contractile and structural elements.

A specific part of the cytoskeleton provides connections that transmit the force generated by actin and myosin to intramuscular connective tissues and skeleton. Intermediate fibres are arranged longitudinally along and transversely across sarcomeres, between the myofibrils within a muscle fibre, and between muscle fibres. The intermediate fibres are probably responsible for the alignment of sarcomeres, the longitudinal and specially the lateral

transmission of force between sarcomeres, myofibrils and muscle fibres (Enoka, 2002; Maas et al., 2003; Monti et al., 1999; Young et al., 2000).

2.3.2.1. The Force-Length Curve

The force-length property of a muscle is defined as the maximal force that a muscle can exert as a function of its length. The length dependence comes predominantly from the overlap between the actin and myosin, so that the force developed by a sarcomere depends on the number of cross-bridges active at a given time and, therefore, the sarcomere length (Rassier et al., 1999). The classical experiments by Gordon et al. (1966) showed that the force-relation of isolated muscle fibres has approximately a bell-shaped pattern and provides a support to the sliding filament and cross-bridge theories of contraction suggested by Huxley (1957). As the muscle length increases from the resting length, the thin filaments are pulled apart from the thick filaments and there is less and less overlap between filaments, and less development of force. At the end, when there is no overlap, no active force is developed. As the muscle shortened to less than resting length, it's reached a point where the overlap of the cross bridges is maximal and an interference takes place. This results in a reduction of tension. Shortening the sarcomere still further will result in the collision of the ends of the myosin filaments with the Z band (Figure 2.5).

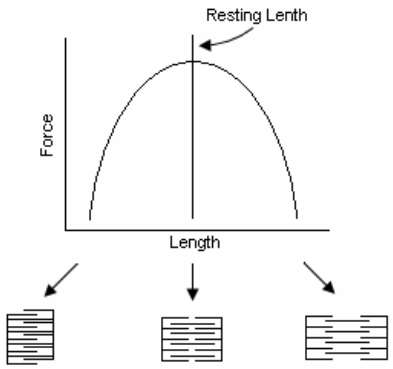

Figure 2.5 Force-Length curve of a single muscle fibre and the correspondent cross-bridge overlapping (based on Winter, 1990).

Gordon et al. (1966) were the first group of authors to describe the force-length properties of skeletal muscle sarcomeres. According to them, the peak active tension during the rapid rise of tension is constant across a sarcomere length and range from 2.0 to 2.2 µm. At

progressively longer sarcomere lengths, active tension decrease linearly, reaching zero at 3.6 µm (descending limb). When sarcomere length is < 2.0 µm, the developed tension is less than the peak value, decreasing linearly to a sarcomere length of ~1.7 µm and decreasing more steeply at even shorter sarcomere lengths (ascending limb).

When the length of the muscle increases or decreases beyond its resting length, the maximum force that the muscle can produce decreases following the form of the curve. The shape of the length-tension curve for the sarcomere determines the shape of the active length-tension curve of the whole MTU, and is due to the changes of the structure of the myofibrils at the sarcomere level (Figure 2.6). The length-tension curve of the whole muscle is enlarged by the presence of more passive elements, in particular the connective tissue that surrounds the contractile element. As the muscle length is changed, so is the sarcomere length. In addition the tendon and connective tissue is stretched, which behaves elastically, in the sense that the more it is stretched, the greater the passive tension is developed. When the muscle is at resting length or less, the parallel elastic component is in a slack state with no tension. As the muscle lengthens, the tension begins to build up, slowly at first instance and then more quickly, with a quite linear behaviour.

Following the figure below (Figure 2.6), the active force is the force produced by CE. The passive force results from the parallel elastic component, and depends on the amount of connective tissue. The total force developed is the sum of active and passive tension and represents the force transmitted through the tendon.

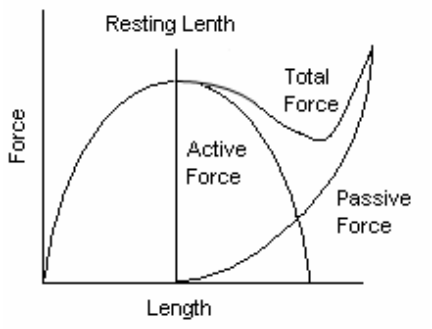

Figure 2.6 The global Force-Length curve of the MTU (based on Winter, 1990).

At shorter muscle lengths, all the force is due to the active components (cross-bridges activity) whereas at longer lengths, most of the muscle force is due to the passive

components. The passive force is the tension the muscle develops at lengths greater than its resting length, due to its elastic properties. It always present but the amount of active tension in the contractile element at any given length is under voluntary control.

When performing an isometric contraction, a certain muscle length is associated to each joint angle. The optimum joint angle, i.e. the joint angle corresponding to the optimum muscle length, determines the operating range in force-length relationship by the joint movement and tendon excursion. Therefore it's very complicated to measure the angle torque properties for intact human muscles due to difficulty in quantifying the force sharing between all muscles acting around the same joint. It's usually impossible to generate a voluntary contraction for a single agonist without activating the remaining agonists.

2.3.2.2. The Force-Velocity Curve

A hyperbolic curve that fits the relationship between force and velocity was been suggested by Hill, in 1938 (Hill, 1938). When a muscle is not loaded (F=0), it can contract at its maximal velocity. In a concentric regime, as the load on the muscle increase, the velocity of contraction decreases, until reaches a load at which the velocity drops to zero (isometric). At high speeds of contraction the muscle can only develop relatively little force and velocity is maximal when F=0, while at low speeds the muscle develops more force (Figure 2.7). This is due partly to the loss of tension as the cross-bridges in the contractile element break and reform in a shortened condition, and to the action developed by the viscosity of muscle fibres and connective tissue, which result in a resistance to the movement, in a proportional way to an increase in velocity (Winter, 1990).

Nevertheless, when the increasing of the velocity happens in an eccentric regime, the muscle is able to develop higher muscular tensions with an increasing velocity, but is less affected by changes in velocity in comparison to concentric actions (Komi, 1973).

According to Winter (1990), the reasons for this different behaviour in eccentric conditions are similar to those that account for the drop of tension during concentric contractions. First, within the contractile element it is clear that the force required to break the cross-bridges is greater than that required to hold it at isometric length. This force increases as the rate of breaking increases. Second, as well as in the shortening contractions the viscous friction it

is now very much present. Nevertheless, because of the direction of contraction is opposite, the force is now higher in order to surpass the internal friction.

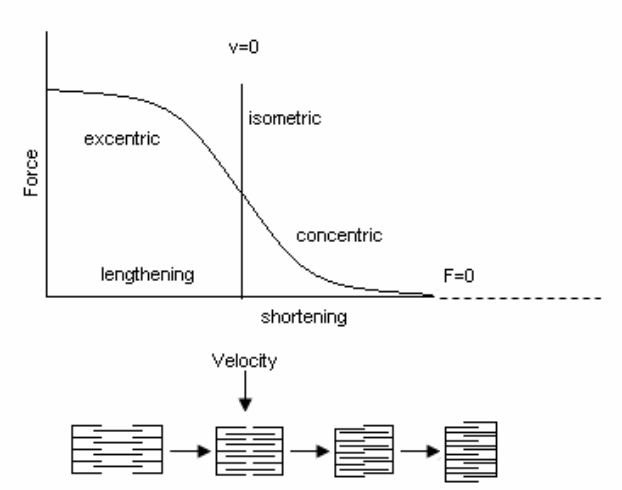

Figure 2.7 Force-Velocity curve of a muscle and the correspondent cross-bridge breaking and reforming (based on Winter, 1990).

2.3.3. Force Production

According to Stein et al. (2000), and Marsh et al. (1981), the force generated by a muscle depends on activation provided by nerve impulses, as well as on the properties of the muscle itself (force-length, and force-velocity relationships). These muscular factors include the mechanical properties of muscles, and the structural effects due to differences in muscle architecture.

The effects of the three factors are multiplicative, and the load against which the muscle is working affects the force as well as the length changes produced (Figure 2.8).

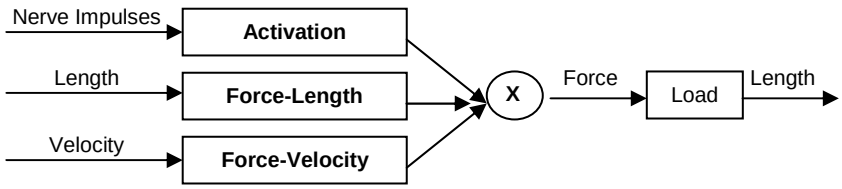

Figure 2.8 Factors affecting the force production (Adapted from Stein, 2000).

Nevertheless, these are only the primary factors determining muscular force production. According to several authors (Herzog, 2000a; Huijing, 2000; Joyce et al., 1969), several

other factors influence the muscular force production, like time history effects, and the involuntary inhibition of in vivo force production associated with reflex pathway. The interaction between the primary and these secondary factors is fundamental and affects the muscular force production.

2.3.3.1 Activation

The activation commands to a muscle are relayed via the α-motoneurons. A muscle is organized in terms of motor units (the motoneuron and all the muscle fibres innerved by the neuron). So the activation of a motor unit will cause force production in all fibres contained on it and the magnitude of muscle force will depend on the number of motor units activated, the frequency of stimulation, and the size of the activated motor units (Herzog, 2000a).

2.3.3.2. Force-length and Force-velocity

As already mentioned, the force-length and force-velocity relationships depends on the degree of coincidence between the actin and myosin filaments within the myofibrils, i.e., the contractile properties of muscle fibres, as well as, in the organization of fibres in the muscle, and the arrangement of the muscle around the joint.

2.3.3.3. History Dependence

Previous shortening or lengthening has an effect on muscle's force generating capacity (Joyce et al., 1969). The previous shortening leads to a deficit in isometric force, i.e., actively shortening a muscle causes a temporary loss of part of its contractile strength capacity. This basic mechanism of force depression is mainly attributed to inhomogeneities in the sarcomeres lengths along the fibre (Edman et al., 1993; Herzog and Leonard, 1997). On the other hand, an active stretch increases isometric force generating capacity (Edman et al., 1978; Herzog and Leonard, 2002). This enhancement was attributed to altered cross-bridges function, and also to sarcomere inhomogeneities (Edman, 1999; Edman et al., 1993; Herzog and Leonard, 2002; Morgan, 1990).

2.3.3.4. Reflexes

A reflex is a response to a specific sensory stimulus. Two features of the sensory stimulus are particularly important in shaping the reflex response. First, the precise location of the stimulus determines in a fixed way the particular muscle that contract to produce the reflex response. Second the strength of the stimulus determines the amplitude of the response.

When an appropriate stimulus is applied to the receptor ending, an impulse is initiated, which passes along the afferent process to the spinal cord where it synapses with a connecting neuron. Finally, a motoneuron is excited, and the nerve impulse is conducted down the efferent fibre to a muscle.

Reflex responses arising from muscular afferents, particularly from muscle spindles and Golgi tendon organs contributes significantly to muscle activation and affect the force production. These muscular and tendinous receptors are especially important in the neural control of force production.

2.3.3.4.1. Stretch Reflex

When a muscle experiences a brief, unexpected increase in length, his response is known as the stretch reflex (Sinkjaer, 1997). According to Enoka (2002), the two main functions of muscle are: generate power and react to perturbations. So, the muscle needs to react appropriately and the stretch reflex helps the muscle achieve this capability.

2.3.3.4.2. Muscle Spindles

The muscles spindles are the primary proprioceptors in the muscle. They are fusiform shapes and lie in parallel with the skeletal muscle fibres. When the muscle is stretched, so are the muscle spindles. The muscle spindles contain specialized elements that are especially sensitive to muscle length changes, and velocity length changes. In response to muscle stretch, action potentials are generated in the muscle spindles afferents neurons (group Ia and II), and propagated centrally to the spinal cord with the stretch information, which will trigger the stretch reflex. The reflex therefore tends to counteract the stretch, enhancing the spring- like properties of the muscles (Enoka, 2002).

2.3.3.4.3. Golgi Tendon Organs

The Golgi Tendon Organs (GTO) is another proprioceptor that comes into play during stretching and is located exclusively at the *aponeurosis* or muscle-tendon junctions. In contrast to the muscle spindle, the tendon organ is a relatively simple sensory receptor. It includes a single afferent (Ib) and no efferent connections (Enoka, 2002). Through the Ib sensitive fibres, the GTO are constantly sending information's about the intensity of the muscular contraction, being especially sensitivity to changes in muscular force (monitoring tension developed in muscle). When a muscle and its connective tissue attachments are stretched (passively or actively), the strands of collagen excite the Ib afferent neurons, and a inhibitory reflex is initiated, in order to avoid the development of excessive tensions during the muscular contraction, preventing damage in the muscular structures.

2.3.3.5. Force Transmission

The force that a muscle produces is transmitted from muscles to bone via several pathways:

(1) via the tendons (i.e. myotendinous force transmission),

(2) via intermuscular connective tissue to adjacent muscles (i.e. intermuscular myofascial force transmission),

(3) via other structures than muscles, i.e. the part that supports the nerves and blood vessels (i.e. extramuscular myofascial force transmission).

According to Maas et al. (2003), recent experiments have shown that in rat the position of a muscle relative to adjacent muscles, as well as the relative position to other surrounding tissues is an important co-determinant of isometric muscle force. During normal human movements, changes of muscle relative position occur and this relative position of a muscle determines the configuration of the surrounding connective tissues and, therefore, the fraction of force that is transmitted. According to the author, the connective tissue that surrounds muscle fibres (intra-, inter- and extramuscular connective tissue) plays an important role for force transmission from the contractile elements to bone.

2.3.4. Short-Range Stiffness

During a constant velocity shortening contraction, the force decline first rapidly and then more slowly. In contrast, during a constant velocity lengthening contraction the force increased at first rapidly and then more slowly. For a constant velocity contraction the slope of force indicates the stiffness of the muscle.

During the lengthening contraction (eccentric), stiffness is initially high (large change in force for a small change in length) and then decline. This high initial stiffness is referred as the short-range stiffness (SRS) (Rack and Westbury, 1974). According to Malamud et al. (1996) the SRS is greater in type I muscle fibres as compared to type II.

During an isometric contraction, if a muscle is forcibly lengthened, the attached cross-bridges are stretched and the average force exerted by each cross-bridges increases. This causes an increase in the SRS in the beginning of the lengthening contraction. Superimposing small stretches during a contraction, the stiffness of the fibres is greater in a lengthening contraction than in an isometric contraction. So, after the cross-bridges have been stretched by a certain amount, they detach and reattach quickly and generate a greater average force.

2.4. The Stretch-Shortening Cycle (SSC)

The forced lengthening of an active muscle before allowing it to shorten, leads to an enhanced response during shortening. This potentiation phenomenon during the shortening phase of a lengthening-shortening sequence of muscle actions, was earlier studied by several author's and is called stretch-shortening cycle (SSC) (Norman and Komi, 1979).

In SSC the eccentric action influences the performance of the subsequent concentric phase, and so, the final concentric action can be more powerful than that resulting from the concentric action alone. The advantage of the SSC is that a muscle can perform more positive work if it is actively stretched before being allowed to shorten (Cavagna et al., 1968). The result is that a greater quantity of work can be done during the shortening contraction, if previously the muscle simply performed a stretching.

When direct AT forces were measured during normal SSC activities in humans (Komi, 1990) or animal experiments (Gregor et al., 1988), it was observed that the mechanical performance of the skeletal muscles was considerably modified during the concentric part of the SSC and a clear enhancement of the performance was registered.

2.4.1. Neuromuscular basis of SSC

The performance potentiation in SSC is a complex phenomenon and can be attributed to elastic mechanisms or to the contractile machinery itself, or may result of varying neural activity with interaction of muscle and tendon compartments.

Considerable efforts have been undertaken to explain the mechanisms of performance enhancement in SSC and several experiments were performed in an attempt to clarify this question, both with isolated muscle preparations (Abbott et al., 1952; Cavagna et al., 1965; Chapman, 1985; Katz, 1939) and *in vivo* human studies (Asmussen and Bonde-Petersen, 1974; Cavagna et al., 1968; Finni et al., 2001a; Komi, 1973; Komi and Bosco, 1978; Monti et al., 1999; Walshe et al., 1998).

2.4.1.1. Storage and Release of Elastic Energy

The influence of the series elastic elements on the behaviour of the contractile machinery is of great importance for muscle functioning, especially during SSC, due to the great muscle force enhancement induced by stretch, and particularly with reference to the mechanism of storage and release of elastic energy.

According to some authors this phenomenon of performance enhancement is attributed to the possibility of reusing in the positive work phase of exercise, the elastic energy stored during the negative work phase in the series elastic elements and, to a lesser extent, in the parallel elastic elements, improving the mechanical efficiency of positive work.

A part of the mechanical work done on the muscle can be stored by the elastic components as elastic energy, and then transformed into external work during the subsequent shortening phase contraction (Cavagna et al., 1968; Ettema et al., 1990a). According to the

work-energy relation, an increase in the available energy will increase the amount of work that can be done later.

Muscle fibres not only transmit force to tendons but also interact with them because of the tendon compliance. When the muscle and tendon exert force, the external tendon and *aponeurosis* are stretched and store strain energy. A tendon is more compliant than active muscle fibres so, it will be responsible for a greatest proportion of energy stored. According to Alexander and Bennet-Clark (1977), the tendon elasticity may be much more important than muscle elasticity. The strain energy storage capacity of tendon is between 2000 and 9000 J/kg, around 5 to 10 times higher than that stored in the muscle. As a result, the capacity for elastic energy storage will be greatest in muscle groups with long compliant tendons, like the triceps surae muscle group (Biewener and Roberts, 2000; Hof, 1998). Several studies demonstrate the relative importance of tendon and non-tendon components of the series elasticity (Ettema et al., 1992; Ettema et al., 1990b). Evidences suggest that tendon elasticity predominates in many muscles. The limited range of extension of intrafibrillar compliant structures also translates into a very small capacity for energy storage within muscles compared with energy storage capacity of tendons. In muscles with short tendons and long fibres, the compliance of the non-tendinous component of the series elastic element may dominate the elastic behaviour of the muscle (Alexander and Bennet-Clark, 1977).

With the same amount of stretching force, a more compliant material will store more energy than a stiffer one (Shorten, 1987). The increased height of a jump is dependent on the elastic compliance of the tendon (Conceição, 2004).

2.4.1.2. Muscle Fibre Force Potentiation

Another mechanism of performance enhancement, the force potentiation (Enoka, 2002), suggest that the force from individual cross-bridges increases as a consequence of the preceding stretch. When a muscle is forcibly lengthened, the attached cross-bridges are stretched and the average force exerted by each cross-bridge increases. So, after the cross-bridges have been stretched by a certain amount they detach and reattach quickly and generate a greater average force (Bosco et al., 1981; Huxley and Simmons, 1971; Rack and Westbury, 1974). According to Edman (1996), a part of the force enhancement

during an eccentric action is due to an increased strain of the attached cross-bridges in combination with a slight increase in the number of attached bridges. The author suggest that there is evidences demonstrating that the cytoskeleton proteins, such as the titin and nebulin, form an important part of the elastic element that can be involved in the force enhancement during the eccentric stretch of the SSC. The titin protein appears to provide a connection between the thick filaments and the Z band, providing the alignment of the myofribils and the banding structure of skeletal muscles. It probably contributes significantly to the passive tension of muscle (Wang et al., 1979). The nebulin protein appears to regulate the length of the thin filaments and to influence the interaction between actin and myosin.

2.4.1.3. Stretch Reflex in SSC

Other factor contributing to force enhancement in the early stretch phases are the neuromuscular reflexes, e.g. the stretch reflex (Dietz et al., 1979; Gollhofer et al., 1992; Nicol and Komi, 1999; Voigt et al., 1998).

Before the contact phase with the ground the agonist muscles from that movement are preactivated, as a result of a pre-programmed process of the central nervous system (Dietz et al., 1979). This preactivation phenomenon, in allowing the connection of cross-bridges between the contractile proteins, will be responsible for the initial level of muscular stiffness. This will be the first factor that will allow the MTU to actively resist to the strong and quick stretch during the initial phase of the contact.

In conjunction with the series elastic element and contractile element interaction (elastic energy reuse), reflexes has been proposed to be the main mechanisms of stiffness regulation (Bosco et al., 1982a; Bosco et al., 1982b; Kilani et al., 1989; Komi and Gollhofer, 1997), specially during the eccentric part of SSC. Hoffer and Andreassen (1981) suggested that, when reflexes are intact, the muscle stiffness is greater, for the same operating force, than in an areflexive muscle. Stiffness regulation is very important in SSC exercises (Komi, 1984), and training has considerable influence for stiffness regulation so that the muscle can better sustain high impact loads and subsequently maintain good recoil characteristics (Komi, 1987).

During SSC exercises, when an active muscle is put under stretch, the activity from the muscle spindle and the GTO will determine which of these reflexes, facilitatory or inhibitory, will dominate and what will be the magnitude of the performance potentiation (Komi and Nicol, 2000; Walshe and Wilson, 1997).

Estimates of the relative contribution of stretch reflexes to overall muscle EMG during locomotion are in the range 25%–35% (Bennett et al., 1996; Yang et al., 1991).

2.4.1.4. Other Mechanisms

The role of all these mechanisms and the relative contribution of each mechanism to SSC, remains a controversial topic (Anderson and Pandy, 1993; Bobbert et al., 1996; Bobbert et al., 1986b; van Ingen Schenau et al., 1997) and other models and mechanisms have been proposed, such as the parallel elastic elements role (Wang et al., 1979), the sarcomeres instability (Herzog and Leonard, 2002; Morgan, 1990) and the Huxley inspired molecular charge transfer (Hatze, 1990).

According to Komi (1987) and Dietz et al. (1979) the performance potentiation in the SSC is attributed to several mechanisms such as the combined effects of restitution of elastic energy and stretch reflex potentiation of the muscle (neural potentiation). However, there's a difficulty in isolate, in normal SSC, the potentiation effects of pure elasticity from those of reflex influences, because any increase in reflex potentiation should lead to enhancement of elastic influences.

In human movements the performance enhancement during SSC has been observed in several movements (running, jumping, hopping, squatting, etc) by several authors (Asmussen and Bonde-Petersen, 1974; Cavagna, 1971; Cavagna et al., 1968; Finni et al., 2001a; Komi and Bosco, 1978; Walshe et al., 1998).

Komi and Bosco (1978) demonstrated very well the enhancement of performance following a muscle stretch, comparing vertical jumps performed with and without a preliminary countermovement. They found that healthy young men could jump 50mm higher in countermovement jumps than in squat jumps. Using a method that was first described by Asmussen and Bonde-Petersen (1974), they made extensive comparisons between vertical

jumps starting from a static position, jumps with a countermovement, and jumps done immediately following a drop to the ground from heights between 20 and 100 cm. Jumps heights were greater in the countermovement jumps and drop jumps than in jumps starting from static position. The countermovement jumps and drop jumps allow a forceful stretch of the elastic component of the leg extensor muscles before the concentric action of the jump and, therefore, strain energy may be stored in elastic components and recovered to enhance muscular performance during the concentric phase of the jump. In drop jumps, the jump height increases with increasing height of drop to an optimum height beyond which performance begins to decay. The author's measured the optimal drop height of about 62 cm in men, and 50 cm in women, but the capacity to tolerate and make use of the stretch varied between individuals.

According to Bosco et al. (1981) the enhancement of jumping performance is significantly correlated with speed of the pre-stretching movement and brevity of the delay between eccentric stretch and concentric contraction. Recently, Henchoz et al. (2006), confirmed that the transition time is determinant to the efficiency of the positive work in SSC exercises. The authors suggest that the positive work was highest without any transition time between the eccentric and concentric phases, i.e., between the end of the flexion and the beginning of the extension of the lower limbs in drop exercises with rebound conditions. The percentage of released elastic energy it will be maximum when the delay between the two phases is zero and progressively decrease until it reaches a minimal value for a certain transition time value.

2.5. Modelation

2.5.1. Biomechanical Modeling

The biomechanical modelling is a complex research process in a continuously development. Due to the complex nature of the biological system, the high number of variables related, and the difficulty to directly obtain quantification of those variables, modelling is an interesting and powerful solution.

According to Nigg (1994), a model is an attempt to represent the reality. An ingenious powerful scientific tool composed by several assumptions used to explain the observed phenomenon and increase the understanding of mechanics of movement. Results and

conclusions from a model can be used to increase knowledge and insight about reality, and can be used to estimate or predict variables of interest. A model is formulated by the laws of physics, and expressed by mathematical equations, allowing the quantification of the human movement.

According to Veloso and Abrantes (1991), the aim of a model is to extrapolate the date from an anterior known experience, into a new real factual date, with the purpose of increase the knowledge of the observed phenomenon. The new results can be compared with the anterior ones and confirm the validity of the suggested new model.

Biomechanical models come in a variety of forms. Conceptual, physical and mathematical models have all proved useful in biomechanics (Alexander, 2003; Koehl, 2003). According to the author's, conceptual models, have been used only occasionally to clarifying a point without having to be constructed physically or mathematically analysed. Physical models are designed to demonstrate that a proposed mechanism actually works, for example the folding mechanisms of insect wings (Alexander, 1983; Alexander, 2003; Alexander and Vernon, 1975) and may serve to check the results of a mathematical model. The author propose that physical models have been proved to be especially useful in biological hydrodynamics, where sometimes it is convenient to use models that differ substantially in size from the living natural system, allowing the achievement of some experiments that are not technically feasible with living organisms. As well as the mathematical models, the physical models yield quantitative results, and both modelling approaches involve simplifying assumptions, so that the predictions of the model can be tested by comparison with measurements on real organisms.

Mathematical models have been used more often than physical models. They can range from an extreme simplicity (some models of walking and running), to an extreme complexity, for example models that represent several body segments and muscles. Some of them are predictive, designed for example to calculate the effects of anatomical changes on jumping performance. Others try to find an optimum, for example the best possible technique for a high jump. A few ones have been used in optimization studies, which search for variables that are optimized according to observed patterns of a behaviour (Alexander, 2003).

2.5.1.1 Neuromusculoskeletal Models

According to Zahalak (1990), the skeletal muscles are the final effectors of a complex system, the neuro-musculoskeletal system, and the major responsible for the movement produced. The author suggests, that a satisfactory comprehension of movement is difficult to achieve without sophisticated model simulations. Usually, even for a simplest model, a very heavy computational effort is required, involving complex information about muscle activation, force and motion. At the same time, for the great amount of the parameters required, only a few one are accessible to direct experimental verification, such as limb positions, electromyograms and joint torques. The other parameters of interest such as individual muscles forces, neural activation, storage and reuse of energy, are usually predicted in the model.

In human movement analysis, for example, a high-speed camera system is used to record the changing positions and orientation of the body segments, a strain-gauge or a piezoelectric transducer is used to measure the magnitude and direction of the resultant external forces exerted on the ground, and, finally, surface or needle EMG electrodes are used to record the sequence and timing of muscle activity (Winter, 1990). Nevertheless, according to Pandy (2001) these data provide only a quantitative description of the kinematics and dynamics of the body movement, and do not explain how muscles work together to produce a coordinated movement. The understanding of muscle mechanism based on muscle modeling and simulation has risen a new understand of the functioning and interaction of the human neuromuscular and musculoskeletal system, the nature of load exerted by the muscles, failure mechanisms and potential causes of injury, in order to prepare strategies of intervention and reduce or prevent work-related musculoskeletal disorders.

Modeling a neuromusculoskeletal system starts with the choice of the model structure, i.e., the set of properties that are included in the model. Mathematically speaking, it is the set of equations connecting the input and output variables of the model. Although there still many problems need to be solved, neuromusculoskeletal modeling is a potential tool that can be expected to simulate and predict more realistically the behaviour of the human muscular system in workout and sports environments.

We can found, in the literature, a substantial number of remarkable published papers that historically represents the importance and the commitment of the authors concerning the development of biomechanical modelling (Brand et al., 1982; Braune et al., 1987; Crowninshield and Brand, 1981a; Elftman, 1939; Glitsch and Baumann, 1997; Hatze, 1977; Herzog, 1987; Pandy et al., 1990; Yamaguchi et al., 1990; Yeadon et al., 1990; Zajac, 1993).

Although variables as force development and power output of a few selected muscles have been experimentally evaluated during animal locomotion (Biewener et al., 1998), this type of study is very difficult in humans, for technical and ethical reasons (Finni et al., 2000; Fukashiro et al., 1995b). Even using experimental animals, it seems to be very difficult to determine muscle force and power output from several muscles simultaneously without affecting the nature of normal movements. In this regard, computer modeling and simulation is a useful tool for human and animal biomechanics. Presently, with the new computational resources available, a large-scale of models of the body can be used to produce realistic simulations of movement.

Three-dimensional computer modeling and simulation is a useful approach in the field of biomechanics. Using this approach, it is possible to evaluate the behaviour of individual muscles during various human movements. According to Nagano et al. (2005), for computer modeling and simulation to be a useful tool, it is better to develop a three-dimensional model instead of a two-dimensional musculoskeletal model, although a substantial portion of human movements can be assumed to be two-dimensional. For this reason, many researchers have used two-dimensional analysis in order to study jumping motions (Pandy and Zajac, 1991; Pandy et al., 1990; van Soest et al., 1993). However, human body musculature has three-dimensional characteristics that are hard to be reduced into two dimensions. Nagano et al. (2005) suggests that further valuable insights can be obtained through the research of the behaviour of human body using a three-dimensional musculoskeletal model as compared to using a two-dimensional model.

There are some subsystem models that are required to be simulated in a successfully neuromusculoskeletal model (Crago, 2000):

a. Body Segments

Modeling of multisegment movement is almost always based on the simplifying assumption that limb segments behave as rigid bodies connected by joints with fixed axes of rotation. Actually, more realistic models include flexible segments and joints with more than one degree of freedom. Each segment is characterized by the relative locations of successive joint centres of rotation, the mass, the location of the centre of mass, and the mass moment of inertia about each rotational degree of freedom.

b. Muscle

Usually muscle models are based on Hill model and include three elements. The contractile element that produces the active force, which is transmitted through the series elastic element, and the parallel elastic element, that produce force under passive conditions. The contractile element and the series elastic element is referred as the muscle-tendon unit, and force produced by the contractile element cannot be determined without taking into account the series elastic element. Muscle models based on the structure and chemistry of the Huxley model (Huxley, 1957), are an attractive alternative to the classical Hill model, for example the Zahalak model (Zahalak and Ma, 1990).

c. Joint Mechanics

The muscle and tendon paths relative to the joint centre of rotation determines the moment arm of the muscle, which in turn determines the relationship between force and moment, and the relationship between muscle length and joint angle.

d. Passive Viscoelastic Properties

The sources of passive viscoelastic joint moments include all moments that not contribute to active contraction of the muscle, segment inertias, or gravity; ligaments that restrict the movement in some directions; the joint capsule; blood vessels, nerves and fascia that cross joints, skin and joint surface friction.

e. Neural Components

The sensory receptors like muscle spindles and Golgi tendon organs are the major responsible for the augmenting of the muscle stiffness in the stretch reflex

(Matthews, 1981). The introduction of these structures in a model will facilitate the understanding of the central nervous system function.

According to Pandy (2001), modelling and simulation has risen to news insights in recent years. The approach can provide more quantitatively explanations of how the neuromuscular and musculoskeletal systems interact to produce human movements. Simulations of several ways of locomotion have provided considerable important insights about how the leg muscles work together to achieve a common goal during each task. The author suggest that movement simulations should include (*a*) a model of the skeleton, (*b*) a model of the muscle paths, (*c*) a model of musculotendon actuation, (*d*) a model of muscle excitation-contraction coupling, and (*e*) a model of the goal of the motor task.

(*a*) Modeling Skeletal Dynamics

When the skeleton is modeled (two or three dimensions), the relationship between the forces applied to the body and the resulting motion of the body segments can be expressed in the form:

$$M(\underline{q})\ddot{\underline{q}} + C(\underline{q})\dot{\underline{q}}^2 + \underline{G}(\underline{q}) + R(\underline{q})\underline{F}^{MT} + \underline{E}(\underline{q}, \dot{\underline{q}}) = 0 \qquad (2.7)$$

where $\underline{q}, \dot{\underline{q}}, \ddot{\underline{q}}$ are vectors of the generalized coordinates, velocities, and accelerations, respectively; $M(\underline{q})$ is the system mass matrix and $M(\underline{q})\ddot{\underline{q}}$ a vector of inertial forces and torques; $C(\underline{q})\dot{\underline{q}}^2$ is a vector of centrifugal and Coriolis forces and torques; $\underline{G}(\underline{q})$ is a vector of gravitational forces and torques; $R(\underline{q})$ is the matrix of muscle moment arms; $\underline{F}^{MT}$ is a vector of musculotendon forces and $R(\underline{q})\underline{F}^{MT}$ a vector of musculotendon torques; and $\underline{E}(\underline{q}, \dot{\underline{q}})$ is a vector of external forces and torques applied to the body by the environment.

(*b*) Modeling Muscle Paths

In a multijoint model of movement, it's necessary to know the way at which the muscle tendons insert on the bone. Two different methods are commonly used to model the paths of muscles in the body: the straight-line and centroid-line methods.

(*c*) Modeling Musculotendon Actuation

When muscles are included in a model of movement, their mechanical behaviour is usually described by a three-element Hill-type model (Winters, 1990). In the example presented by Pandy (2001), musculotendon dynamics is described by a single, nonlinear, differential equation that relates musculotendon force (F^{MT}), musculotendon length (L^{MT}), musculotendon shortening velocity (v^{MT}), and muscle activation (a^{m}) to the time rate of change in musculotendon force:

$$\dot{F}^{MT} = f(F^{MT}, L^{MT}, v^{MT}, a^{m}); 0 \le a^{m} \le 1 \qquad (2.8)$$

Given values of F^{MT}, L^{MT}, v^{MT} and a^{m} at one instant in time, Equation (2.8) can be integrated numerically to find musculotendon force at the next instant.

(*d*) Modeling Muscle Excitation-Contraction Coupling

The delay between muscle excitation and activation (the development of muscle force) is due mainly to the time taken for calcium pumped out of the sarcoplasmic reticulum, to travel down the T-tubule and joint to troponin (Ebashi and Endo, 1968). This delay is usually modeled as a first-order process (Pandy et al., 1990; Zajac, 1989), being u, the muscle excitation, i.e., the neural input, and a^{m} the muscle activation. Values of the constants range from 12–20 ms for rise time, τ_{rise}, and from 24–200 ms for relaxation time, τ_{fall} (Pandy et al., 1990; van Soest et al., 1993; Zajac, 1989).

$$\dot{a}^{m} = (1/\tau_{rise})(u^{2} - ua^{m}) + (1/\tau_{fall})(u - a^{m}); u = u(t); a^{m} = a^{m}(t) \qquad (2.9)$$

It is assumed in equation (2.9) that muscle activation depends only on a single variable u, although other models assume that a depends on two inputs, u_1 and u_2, representing the effects of recruitment and stimulation frequency (Happee, 1994; Hatze, 1978).

(*e*) Modeling the Motor Task

Modeling the goal or the cost function of a movement is not an easy proposal. Performance is determined by physiological and environmental constraints imposed by the movement task and especially these factors are very difficult to quantify and describe mathematically. Although the difficulties, modeling approach has been used together with dynamic optimization theory to simulate for example the human walking (Anderson and Pandy, 2001) or jumping (Anderson and Pandy, 1993; Pandy et al., 1990; van Soest et al., 1993).

2.6. Methods to Assess Internal Forces

The knowledge of forces imposed to the human body during movements, is of extreme importance in physical activity, coaching, physiotherapy, orthopaedics, diagnosis, rehabilitation, prosthesis, as well as in areas such as the motor control, robotics, biomechanics, etc.

The lower limb ankle, knee and hip joints are the most frequently structures in the human body liable to injuries. According to Amadio and Baumann (2000), it is of great importance the knowledge of the mechanical effort that an articular joint is submitted both in physical experiences, in rehabilitation, as well as in everyday life activities.

Although the intrinsic mechanisms responsible for different injuries is mostly unknown, it seems reasonable to assume that at least some of that are partly associated with the vigorous landing phase in running, jumping or hopping, immediately after the body contact with the ground. Assuming that forces produced during the landing phase are one of responsible factors in the etiology of the injury, it is extremely important a minutely mechanical analysis of this phase, including the estimation of forces and intersegmentar moments of force produced. Understand how muscles functions during movement - the timing of their contractions, the amount of force generated (or moment of force around a joint), the power and the resultant energetics produced in the contraction, - is of our special interest.

The knowledge of the forces and moments of force that act in the human body is a very important procedure to determine the causes and consequences of movement. There are

two possible approaches to determine internal forces: direct measurements and indirect measurements. In the direct determination, internal forces are quantified through force transducers implanted in the human body, and for this reason, a great experimental difficulty due to the extremely invasive process is reported. In the indirect determination of internal forces, indirect analytical procedures are used, and muscle forces are estimated using either inverse or forward dynamics techniques.

2.6.1. *In Vivo* Direct Measurements

It is from general consensus that it is very difficult to determine directly the *in vivo* loads transmitted by the muscles, ligaments and joint articular surfaces of human subjects (Komi, 1990). The measurement of muscle force in humans can be accomplished only with invasive techniques. Studies using direct recordings of tendomuscular forces provide novel and important insights into *in vivo* muscle function of a particular muscle, functional adaptation to variable conditions (Komi et al., 1992), sharing forces between muscles (Herzog et al., 1994b), role of elastic energy (Gregor et al., 1988) and neural control (Walmsley et al., 1978).

The *in vivo* tendon transducer method in humans, began with Komi and colleagues (Komi et al., 1984) using the implantable E-form transducer in the Achilles tendon, to record a slow walking motion, followed by the experiments with the buckle-type transducer (Komi et al., 1985), and finally the less invasive optic fibre technique (Komi et al., 1995).

2.6.1.1. Implantable transducers

The application of an *in vivo* measurement technique such as the implantation of a transducer in a human tendon, involves several stages of development and, as is often the case, imposing technological developments of measuring devices, which involves firstly, some previous experiments with animals (Komi et al., 1987).

2.6.1.1.1. The buckle transducer

Salmons (1969), was the first to introduce the design of the buckle type transducer for recording directly *in vivo* tendon forces in animals. Later, an E-form transducer was first

implanted around the Achilles tendon (Komi et al., 1984) on an human subject and kept in situ for 7 days before the measurements of a slow walking movement were obtained. This type of transducer however didn't satisfy the requirements of the pain-free and natural locomotion, and was replaced by the Salmon's original buckle type transducer (Salmons, 1969).

According to Komi and collaborator's (Komi, 1990; Komi et al., 1992; Komi et al., 1987), the buckle transducer consists of a main buckle frame, two strain gauges, and a centre bar placed across the frame. The frame and the centre bar are moulded from stainless steel. Different kinds of frame and cross-bar are available. The differences in frame size and in cross-bar bending ensure that a suitable transducer is available for almost any size of adult human Achilles tendon. To assist in the selection of the best possible transducer size, the ankle of the subject is first X-rayed (lateral view) before the surgery. The final selection is performed during the surgery. The tendon must match as closely as possible the interior width of the buckle frame to prevent possible sideway movements of the transducer. Possible damage in the structures of the tendon can occur if an excessive bending is induced, so the cross-bar is selected allowing just a slightly bending in the tendon. A quantitative criterion for select the correct sizing of the transducer and the cross-bar is used.

2.6.1.1.1.1. Implantation

During the surgery, the subject is in a prone position on the operating table. The transducer is implanted under local anaesthesia, which is injected around the calcaneal tendon. To provide normal proprioception during movements, the anaesthetic is not injected into the tendon or muscle tissue. It is necessary to make a incision of approximately 50 mm in length on the lateral side, just anterior to the tendon to avoid damage to small saphenous vein and the sural nerve. The correct sized cross-bar is then placed under the tendon into the slots of the frame. The cable containing the wires from the strain gauges is threaded under the skin and brought outside approximately 10 cm above the transducer. After the implant, the cut is sutured and carefully covered with sterile tapes. The cable of the transducer is now connected to an amplifying unit and immediately checked-up.

2.6.1.1.1.2. Calibration of the Transducer

The calibration of the transducers is performed immediately prior to the experiments. In contrast to animal experiments, in human subjects an indirect method was applied to calibrate the Achilles tendon transducer, and is not as simple procedure as is in animal experiments. The calibration was performed with the subject positioned in a prone position on a special calibration table where both static and dynamic loads can be applied. The operated foot is placed in a special shoe, which is fastened on to a freely rotation frame. The axis of foot (ankle joint) and lever was coincident. A pulley system with know weights was used to dorsiflex the foot. The direction of the pull was parallel to the Achilles tendon. Taking in to account the geometrical arrangements of the transducer, axis of rotation and pulley system, the exact values of Achilles tendon forces could be calculated. The dynamic response of the Achilles tendon could be calibrated by adding the spring system between the strain gauge and the weight of the dorsiflexing cable (Komi et al., 1987). According to Komi (1990), all this arrangement needs to be carefully and individually prepared to each subject. Even a small variation in the angle of pull of the tendon as well as in the common axis for foot and lever arm will introduce considerable errors in the absolute force levels.

2.6.1.1.2. Optic fibre technique

The emergence of the last presented less invasive optic fibre transducer (Komi et al., 1995), was introduced in order to overcome some of the disadvantages imposed by the buckle transducer. The great advantage of this less invasive technique over the buckle type transducer is that the insertion of the fibre is quicker and with almost no pain.

As in the case of the buckle transducer, the optic fibre technique was first applied in animal tendon (Komi et al., 1996), in spite of being already applied for measurement of foot pressure in different phases of cross-country skiing (Candau et al., 1993) and as a pressure transducer in sensitive skin application (Bocquet and Noel, 1987).

According to Komi et al. (1996), Arndt et al. (1998) and Finni et al. (2000; 1998) the use of the optic fibre as a transducer for tendomuscular forces measurements is based on light intensity modulation. When the fibre is compressed inside the tendon, a mechanical modification of the geometric properties of the plastic fibre is observed. A special optic fibre with a plastic covering buffer is carefully prepared at both ends for receiving and

transmitting light. The transmitter-receiver unit used in the optic fibre method contain a light emitting diode and a PIN photodiode receiver.

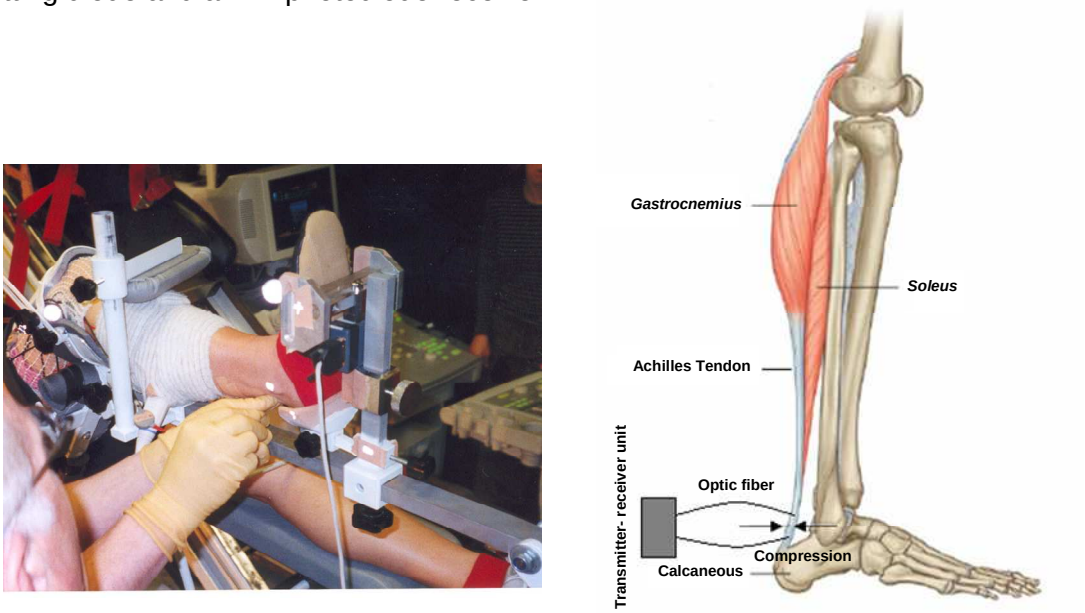

Figure 2.9 Demonstration of how the optic fibre is inserted through the Achilles tendon (left). After the needle insertion in the tendon, the sterile optic fibre is threaded through the needle. The needle is then removed and the optic fibre remains *in situ*. Both ends of the fibre are connected to the transmitter – receiver unit (right).

The plastic optical fibre consists in two layered cylinders (cladding and core) of polymers with small diameters. The light signal travels in the core and return to the unit for conversion into analogue signal. When the fibre is bent or compressed by external forces, the light is reduced linearly with pressure and the sensitivity depends on fibre index, fibre stiffness and/or bending radius characteristics (Bocquet and Noel, 1987) (Figure 2.9). The core (polymethymethachrylate) and cladding (fluorinated polymer) will be deformed and a certain amount of light is transferred through the core-cladding interface. In order to avoid the pure effect of bending, when the fibre is inserted through the tendon must have a loop large enough to exceed the so-called critical bending radius.

According to Butler et al. (1978) and Sidles et al. (1991), the tendomuscular loading has been shown to develop a tensile stress within the tendon fibres. During movements, when the tendon fibres are loaded by the compressive stress, is assumed to compress the optic fibre inside the tendon. The compressive stress ($T, N.m^{-2}$) is proportional to the tensile force (F) according to the following equation:

$$T = v * F * A^{-1} \quad (2.10)$$

where v and A are respectively the Poisson's ratio and the cross sectional area of the tendon.

It was reported by Komi et al. (1996) and Arndt et al. (1998), a linear relationship between the increasing loading of the tendon and the intensity of the light that passes through the optic fibre, even in maximal voluntary contractions (Finni et al., 1998).

2.6.1.1.2.1. Implantation

Before the insertion of the optic fibre, an anaesthetic cream containing lidocaine-procaine is placed over the skin surrounding the tendon and kept in place for at least one hour. In the case of the insertion of the Achilles tendon, the subject is lied in supine position on an ankle ergometer (Nicol et al., 1996) with the ankle angle at 90 degrees. A 19 gauge needle is passed through the Achilles tendon, 2-3 cm above the insertion of the tendon in the *calcaneous*. The needle is inserted perpendicular to the direction of the tendon. Aseptic conditions are ensured and a sterilised (ethylene oxide at 37º) optic fibre force transducer is then passed through the needle. The needle is removed and the fibre remains in situ. Both tips of the fibre are then carefully cleaned before being attached to the transmitter-receiver unit for the light intensity baseline correction. The system is ready for measurement.

2.6.1.1.2.2. Calibration of the transducer

The transducer is calibrated against the force level measured from a strain gauge in the lever arm of the ergometer. For the Achilles tendon optic fibre force transducer, the calibration is performed on the ankle ergometer (Nicol et al., 1996), where the subject perform an isometric plantar flexion at 10, 20, 30 and 40% of maximal voluntary contraction previously estimated. In each condition the subject maintains the predetermined force level for not much than 5 seconds. From the data recorded, the output of the optic fibre is know related to muscle force (*F*) that had been converted from the external force output (*F*') using the equation according to Figure 2.10 The optic fibre signal in volts is then converted into absolute force values according to the linear relationship obtained for each individual.

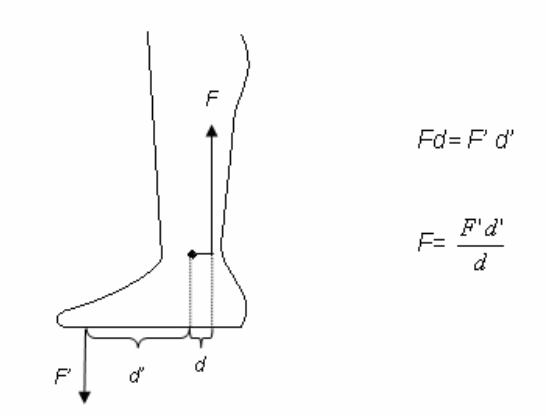

Figure 2.10 Measured forces and moment arms used in the calibration of the Achilles tendon forces. The optic fibre output is related to the muscle force (*F*) that has been converted from the external force output (*F'*) using the equation *Fd=F'd'*, where *d* = moment arm of the Achilles tendon force and *d'* is the moment arm of the foot.

2.6.1.1.2.3. Advantages

Although the optic fibre method may not be more accurate than the buckle transducer method, it has several unique advantages. First of all it is much less invasive and can be reapplied to the same tendon after a few days of rest. In addition, almost any tendon can be studied, provided that critical bending radius is not exceeded.

2.6.1.1.2.4. Methodological Considerations

During dynamic muscle work, the skin moves in relation to the tendon. According to several authors (Erdemir et al., 2003; Erdemir et al., 2002), during the Achilles tendon force measurements, it is possible that the skin movement during jumping may cause minor artifacts to the signal. According to Finni et al. (2000), the measured effect of the skin movement was calculated to be less than 2% of the peak forces recorded during locomotion, but probably increases during full ankle plantar flexion movements, due to the skin folded around the Achilles tendon. The problem is not presented in the patellar tendon.

Comparisons of the Achilles tendon force patterns measured with the optic fibre technique (Finni et al., 1998) and the buckle transducer in human walking (Komi, 1990), didn't provide any significant differences.

2.6.1.2. Critical Aspects of the Procedures

The buckle transducer method is naturally quite invasive, and in general receives a lot of criticism and objections by several ethical committees. Due to the relatively large size of the buckle transducer there are not many tendons in the human body, which can be selected for measurements. The Achilles tendon is, however, an ideal one due to large space between himself and the bony structures within the Karger triangle.

The method can only be used to demonstrate the loading characteristics of the entire muscle-tendon complex only. With exception for the animal experiments, the buckle transducer method cannot isolate the forces of the contractile and tendon tissues.

One of the great critiques that were presented against the direct measurement of internal forces is precisely the calibration process. In both cases (buckle and optic fibre transducers) of direct measurements, only the recording process is in fact accomplished in a direct way. The calibration process, as earlier expounded is achieved indirectly. Difficulties in the calibration procedure and problems in the application of the technique when long term and repeated implantation occur may be of interest and are a constant problem.

Nevertheless, in spite of the all possible criticisms there are many reasons to state that the *in vivo* direct tendon force measurement has considerable importance. This is the only method capable to evaluate individually the imposed loads by each muscle in an accurate and credible way. In spite of being an extremely invasive process and hardly applicable in sports environment, this method provide a highly accuracy in the obtained results, justifying, the commitment and devotion from some author's in the development of this methodologies.

There's no doubt that the method opened the way to better understanding the mechanisms of the neuromuscular function in complex movements. Its importance to all those interested in neuromuscular control of movement, muscle physiology, neurophysiology, motor control and/or musculoskeletal mechanics is unquestionable, besides to its clinical importance, that enable the true loading characteristics of the muscle tendon complex in almost any movements, including those that are expected to cause injury.

Next table present the different projects performed with the different type transducers.

Table 2.1 *In vivo* direct tendon force measurements (invasive) during human locomotion

Reference	Tendon	Transducer Type	Movement (s)
1) Komi et al. (1984)	Achilles	E-form	Slow walking
2) Komi et al. (1985)	Achilles	Buckle	Walking (1.2, 1.3, 1.6, 1.8 m/s) and Running (3-9 m/s)
3) Gregor et al. (1987)	Achilles	Buckle	Cycling
4) Komi, PV. (1990)	Achilles	Buckle	Walking (1.2-1.8 m/s), Running (3-9 m/s) and Jumping
5) Gregor et al. (1991)	Achilles	Buckle	Cycling
6) Komi et al. (1992)	Achilles	Buckle	Squat Jump, Counter movement Jump and Hopping
7) Fukashiro et al. (1993)	Achilles	Buckle	Squat Jump and Counter Movement Jump
8) Fukashiro et al. (1995)	Achilles	Buckle	Squat Jump, Counter movement Jump and Hopping
9) Nicol et al. (1995)	Achilles	Optic Fibre	Ankle dorsiflexion reflex
10) Gollhofer et al. (1995)	Achilles	Optic Fibre	Ankle dorsiflexion reflex and Isometric plantar flexion
11) Komi et al. (1995)	Patella	Optic Fibre	Isometric knee flexion
	Biceps Brachii		Isometric elbow flexion
12) Finni et al. (1998)	Achilles	Optic Fibre	Walking (1.1, 1.5, 1.8 m/s)
13) Arndt et al. (1998)	Achilles	Optic Fibre	Isometric plantar flexion
14) Nicol and Komi (1998)	Achilles	Optic Fibre	Passive dorsiflexion stretches
15) Finni et al. (2000)	Achilles, Patella	Optic Fibre	Submaximal Squat Jump and Counter Movement Jump
16) Finni et al. (2001) a	Achilles, Patella	Optic Fibre	Hopping
17) Finni et al. (2001) b	Patella	Optic Fibre	Submaximal Squat Jump, Counter Movement Jump and Drop Jump
18) Finni et al. (2001) c	Patella	Optic Fibre	Maximal knee extension (SSC), Counter Movement Jump and Rebound Jump
19) Finni and Komi (2002)	Patella	Optic Fibre	Submaximal Squat Jump and Drop Jump
20) Finni et al. (2003)	Patella	Optic Fibre	Knee extension (eccentric and concentric)
21) Kyrolainen et al. (2003)	Achilles	Buckle	Running (3-5 m/s) and Long Jump
22) Ishikawa et al. (2003)	Patella	Optic Fibre	Drop Jump and Squat Jump
23) Ishikawa et al. (2004)	Patella	Optic Fibre	Drop Jump
24) Ishikawa et al. (2005)	Achilles	Optic Fibre	Walking (1.4 m/s)
25) Ishikawa et al. (2006)	Achilles	Optic Fibre	Walking (1.4 m/s) and Jogging (2.7 m/s)

2.6.2. Indirect Determination of Internal Forces

2.6.2.1. Forward Dynamics

In the forward dynamics method, muscles activations are used as the inputs of the model to calculate the corresponding body motions (Figure 2.11). With the neural and/or electromyographic signals, together with force and torques previously obtained, it's possible to estimate the angular accelerations and finally the trajectories of the several body segments of the system. The technique involves numerical integration of forces and torques to produce the kinematic information. In forward dynamics, the real sequence of events in the human movement begins with the neural input, until the really accomplishment of segmental displacement. The body controls the movement sending the neural input to the muscles (electromyographic signal), and the muscular force is produced.

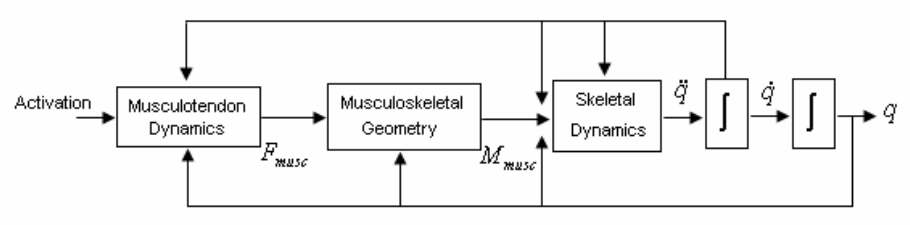

Figure 2.11 Forward dynamics method used to estimate muscle force.

These forces generate the net joint moments which are dependent on the articular geometry of the lever arms. The net joint moments causes the angular accelerations of the joints and are obtained by the equations of motion and the inverse matrix of inertia moments. With numerical integration, displacements of segments are finally obtained.

According to some author's (Pandy, 2001; Zajac, 1993), the forward dynamics is the most advisable method to study the muscular control of movement, how the muscular forces affect the movement and how the movement is produced. The main disadvantage of using forward dynamics is the need to accurately specify the initial conditions (activation).

2.6.2.2. Inverse Dynamics

In the inverse dynamics method, non-invasive measurements of body motion (position, velocity, and acceleration of each segment) and external forces are used as inputs in the model to calculate muscle forces (Crowninshield and Brand, 1981a; Glitsch and Baumann, 1997) (Figure 2.12). The method is based on the detailed description of the anthropometric and inertial characteristics of body segments, in the complete description of movement kinematics, and in the determination of external forces applied to the body. It allows the calculation of the joint reaction forces and net joint moments produced by the muscles around joints (Winter, 1990). The technique involves the derivative of position-time data to yield velocity and acceleration time data.

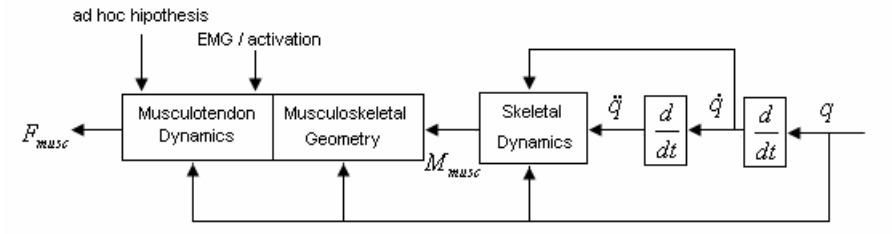

Figure 2.12 Inverse dynamics method used to estimate muscle force.

Taking into account the ground reaction forces, the moments of force in the contact position, the acceleration of the segments involved in the analysis and the equations of movement from classical mechanic analysis, namely the Newton-Euler equations (2.11 and 2.12), it is possible to estimate the forces involved in the movement through inverse dynamics, a powerful tool in gaining insight into the net summation of all muscle activity at each joint.

Newton (linear movement)

$$F = ma \quad \text{(force = mass * linear acceleration)} \qquad (2.11)$$

Euler (angular movement)

$$M = I\alpha \quad \text{(moment = moment of inertia * angular acceleration)} \qquad (2.12)$$

The principal disadvantage of using inverse dynamics is that errors embedded in the position-time data are greatly magnified by the time the data have been processed to yield acceleration (Hatze, 2000; Pandy, 2001).

2.6.2.2.1. The Free-Body Diagram

One of the main objectives of the biomechanical analysis is to understand how muscles function during movement: the timing of their contractions, the amount of force generated (or moment of force around a joint), the power and the resultant energetics produced in the contraction. Due to its complex nature, the human body is usually simplified as a system of rigid bodies connected by joints. A free rigid diagram of a rigid body consists of a drawing of the rigid bodies involved and a representation of all the external forces acting on the system. During the modelling process the representation and analysis of the human body as a free rigid body diagram is fundamental.

According to Winter (1990), the forces acting on the total body system are:

1. Gravitational forces: the force of gravity that acts downward through the centre of mass of each segment (equal to the magnitude of the mass times acceleration due to gravity, 9.8m/s^2).
2. Ground reaction or external forces: forces distributed over the contact area of the body, such as the ground reaction forces. These forces are usually measured by a transducer,

like a force plate, and in order to represent those forces as vectors, they must be considered acting at a point: the centre of pressure.

3. Muscle and ligament forces (internal): the muscle activity at a joint can be calculated in terms of net muscle moment. During a movement, if a cocontraction occurs at a given joint, this kind of analysis yields only the net effect of both agonist and antagonist muscles. Also the passive structures such as ligaments, at the extreme range of movement also play an important role. The moments generated by these tissues will be added or subtracted from those generated by the muscles (figure 2.13).

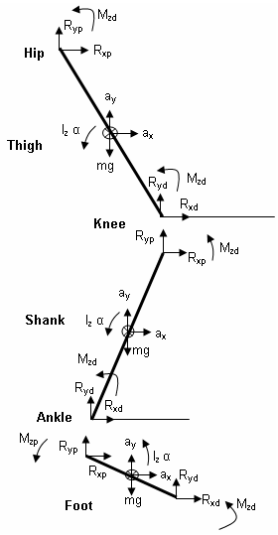

Figure 2.13 Complete free-body diagram of the tree body segments composing the lower limb, showing the reaction and gravitational forces, moments of forces, linear and angular accelerations.

The inverse dynamics approach provides the analyses of the segments one at a time, and calculates the reaction forces between segments. Each body segment acts independently under the influence of the reaction forces, the muscle moments and the forces due to gravity. The muscle forces acts at either proximal or distal ends. The calculations start at the ankle joint and continuing up to the hip joint.

Reducing the movement and considering it as occurring in only one plane, besides the kinematics, anthropometric data and ground reaction forces at the distal end of the distal segment, it is known:

$a_x, a_y =$ acceleration of the segment centre of mass

θ = angle of the segment in the plane of movement

α= angular acceleration of the segment in the plane of movement

R_{xd}, R_{yd} = reaction forces acting at the distal end of the segment

M_d = net muscle moment acting at the distal joint

It is Unknown:

R_{xp}, R_{yp} = reaction forces acting at the proximal joint

M_p = net muscle moment acting on the segment at the proximal joint

From Newton 2nd law:

$$\sum F_x = ma_x$$

$$R_{xp} + R_{xd} = ma_x$$

$$\sum F_y = ma_y$$

$$R_{yp} + R_{yd} - mg = ma_y \quad (2.13)$$

From Euler:

$$\sum M_z = I * \alpha \quad (2.14)$$

$$M_{zp} = I_z * \alpha - M_{zd} - R_{xp} * r_p * sen\theta + R_{yp} * r_p * \cos\theta + R_{xd} * r_d * sen\theta - R_{yd} * r_d * \cos\theta$$

where, r_p is the distance from the centre of mass of the segment to proximal joint and θ is the angle of the segment and the horizontal plane.

During this approach some body segment parameters are required to be known, such as the relative mass and mass moment of inertia (or radius of gyration) of each segment and the position of their centres of mass. These are determined mostly from cadaver studies and recently using new imaging technologies.

2.6.2.3. Inverse/Forward Dynamics

Comparing this two interesting tools, both of them are promising techniques that can be used to determine muscle force. Each one has different characteristics, nevertheless both provides accurate estimations and being remarkably similar in their predictions of muscle force.

If measurements of external forces and body motions are available, the inverse dynamics would be favored in calculations of muscle force, mainly because it is much less computationally expensive. Nevertheless, the effectiveness of the inverse dynamics technique is strongly dependent on the accuracy of the data recorded during a motion analysis experiment. Another problem is that moments and resultant joint reaction forces are net values. For example, if a subject activates is hamstrings, generating 25 N/m of flexion moment, and at the same time activates the quadriceps generating 20 N/m of extension moment, using an inverse dynamics approach, even if it is perfectly accurate, will estimate a net knee flexion moment of 5 N/m. This question is very important because the problem of cocontractions of muscles is very common, and should be taken in to account. Another important limitation is when we try to estimate muscle forces. Because of the multiple muscles (bi-articular muscles) spanning each joint, the transformation from joint moment to muscle forces yields a large number of possible solutions and cannot be readily determined. Finally the there is no current available models to examine muscle activation.

On the contrary, if however, the aim of our work is to find how changes in body structure affect function and performance of a motor task, then forward dynamic must be used because measurements of body motions and external forces are not available *a priori* in this instance. As well as inverse dynamics approach, the forward dynamics also have limitations. First, it requires estimations of muscle activation. It can be used EMG or a mathematical based optimization approach to estimate neural inputs. The EMG-driven models have been used recently to estimate moments about several joint. Second, the transformation from muscle activation to muscle force is difficult, and not yet completely understood, and most models are based in Hill-type classic model assumptions. Another difficulty is the determination of muscle-tendon moment arms and lines of action. Techniques to determine accurately these parameters are very difficult in human living subjects. Finally, estimations of joint moments are prone to errors due to the difficulty in obtain estimations of forces and finally verify if this forces are well predicted or not (validate the model).

An alternative perspective to bridge this gap between the two techniques involves the use of the knowledge from both inverse and forward techniques (Buchanan et al., 2005; Pandy, 2001). In the study of Buchanan et al. (2005), the authors used an EMG-driven forward dynamics model to estimate muscle forces and, from those, joint moments at the ankle joint. The joint moments were estimated using an inverse dynamics approach and the

parameters in the model were adjusted so that the joint moments from forward and inverse dynamics approaches were in close agreement, i.e., the parameters should be adjusted until the error between the two is minimized. Finally, the model was used to estimate muscle forces about the ankle joint, for new tasks (tasks that were not used to minimize the error).

One of the most significant challenges facing the modeling community today is finding new ways to more accurately describe structure of the musculoskeletal system (e.g. moment arms, muscle-fibre and tendon rest lengths, muscle cross-sectional areas, and muscle pennation angles). There is some evidence to suggest that musculoskeletal geometry (i.e. muscle paths) is the most critical element of the modeling process (Arnold et al., 2000; Buchanan et al., 2005).

The advantage of this hybrid approach is that the joint moments from the inverse dynamic solutions can be used to cross validate the forward dynamic modeling solutions.

2.6.2.4. Indeterminacy in Muscle Force Calculations

The human body locomotor system, represented by the rigid multibody system, allows the calculation of net joint moments of force, as well as the joint reaction forces. Nevertheless, estimating muscle forces is a major problem, even if we have good estimations of the moments of force produced at each joint (Winter, 1991). The number of muscle-tendon units that work together in agreement to produce the movement, always surpass the number of equations of movement and available constrains. In this so-called distribution problem, the number of unknowns exceeds the number of available equations describing the mechanics of the system (Crowninshield and Brand, 1981b). In this way, the system is indeterminate and in order to find a unique solution for the distribution problem, the number of system equations should be increased or the number of unknowns decreased. However, when increasing the number of equations, some non-trivial assumptions should be made, and when decreasing the number of unknowns, some important information about the behaviour of the system may get lost. In this way, and for many well supported physiological reasons, another solution was recently adopted, trying to understand the intrinsic problems of determining muscle forces: the mathematical optimization approach.

According to Collins (1995) in both forward and inverse dynamic approaches, a model of the musculature is necessary. Given the complexity of the musculature, the determination of the individual muscle forces remains an indeterminate problem, i.e. the number of load-transmitting elements at a joint exceeds the number of available equilibrium equations Consequently, a unique solution for the analytical determination of the forces in each structure cannot be obtained. There are an infinite number of different combinations of muscle, ligament and intra-articular contact forces that can be applied to maintain a particular posture or produce a given movement. This is due to the fact that a muscle never works alone, but is always involved in a coordination scheme with several complementary muscles. Furthermore, the tension in a muscle is not a constant parameter during motion, but varies according to the muscle length, velocity and activation parameters.

2.6.2.5. Optimization Techniques

It is generally impossible to calculate the forces of individual muscles unambiguously, from measurements of the accelerations of body parts and of the forces exerted on the environment. Optimization procedures are not only the way of solving this type of mathematical problems (distribution problem), but are also a good indicator of the physiology underlying the force-sharing among the internal structures such as the muscles.

An optimization technique usually assumes that loads are transmitted by joint structures according to some minimization criterion (optimal criterion). Criterions such as the minimal muscle force, minimal muscle stress, minimal energy expenditure or consumption, etc, are used to solve the general constrained problem. The usual approach for solving the indeterminate problem is to perform an optimization analysis of the variables in excess involved in the problem. This approach, however, is limited because the obtained values are not exactly identified from the problem, but rather estimated on the basis of a certain criterion.

The optimization approach assumes that at any instant of movement, the coordination of the involved muscles follows a rationale. An objective function is thus defined which quantifies the rationale involved. A set of constraints are defined and added, in order the results can be realistic and physiologically acceptable. The values of exerted forces can now be obtained.

The problem with optimization technique is that the principles by which muscles act at any instant in the human body are not readily apparent. It is reasonably accepted that the objective function used probably changes with the type of motion.

According to Nigg (1994), optimization problems, in general, are defined by: a) the cost function, b) the design variables, and c) the constraint functions.

a) The cost function is the function to be optimized and is defined as follows:
Minimize ϕ where:

$$\phi = \sum_{i=1}^{N} (F_i^m / M_{\max i})^3 \qquad \text{(Herzog, 1987)} \tag{2.15}$$

where:

N = total number of muscles considered

F_i^m = force magnitude of the ith-muscle

$M_{\max i}$ = variable maximal moment that the ith-muscle can produce as a function of its instantaneous contractile conditions

b) The design variables are the variables that are systematically changed until the cost functions are satisfied. The design variables must be contained in the cost function and for the distribution problem they are of the magnitudes of the individual muscle forces.

c) The constraint functions restrict the solution of the optimization approach to certain boundary conditions. In the distribution problems, typical inequality constrains are:

$$F_i^m \geq 0 \text{ for i=1, …, N} \tag{2.16}$$

and typically equality constraints are:

$$M_0 = \sum_{i=1}^{N} (r_{i/0} \times F_i^m) \tag{2.17}$$

which indicate that muscular forces must always be zero or positive and resultant joint moments, M_0, are assumed to be satisfied by the vector sum of all moments produced by the muscular forces.

Herzog and Leonard (1991), used a mathematical model to calculate how much force the three extensor muscles of cats, the *gastrocnemius*, the *plantaris* and the *soleus*, should contribute in walking and trotting strides, if the load were shared according to each of several optimization principles. They calculated what the forces would be if they were adjusted to minimize the total of the forces in the individual muscles, or the total of the stresses. They also calculated what the forces would be if the squares or cubes of these quantities were minimized. They compared these predictions with actual muscle forces, measured by means of transducers attached to the tendons of the three muscles. They found that none of the optimization criteria predicted the forces consistently well.

Happee (1994), introduced a new method for estimating muscular force and activation from experimental kinematical data. He combines conventional inverse dynamics with optimization utilizing a dynamic model. A solution for the load sharing problem is determined by the minimization of the weighted sum of squared muscle forces. The load sharing problem is solved with a dynamic constraint reflecting physiological muscle properties. This constraint takes into account the nonlinear dynamics of the contractile element and the series elastic element, active state and neural excitations dynamics.

Nevertheless, some authors highlighted that the solutions from optimization methods could be unsuitable, i.e., physiological unrealistic, specially because they fail in considering an indicator of muscle activity (Challis and Kerwin, 1993; Cholewicki and McGill, 1994; Cholewicki et al., 1995). A convincing alternative approach should associate optimization with electromyography signals, which provide the information on the level of muscle activity. Several studies have attempted to use electromyography signals as inputs of the system (Amarantini and Martin, 2004; Bogey et al., 2005; Buchanan et al., 2005; Koo and Mak, 2005; Lloyd and Besier, 2003; Manal and Buchanan, 2003).

2.6.2.6. Calibrate the Inverse Dynamics Solutions

One way to calibrate the inverse dynamics approach is to combine the *in vivo* direct measurements, with the results obtained from inverse dynamics to estimate the muscular loads. The process of fitting both approaches involves a previous step of optimization to obtain the individual activation parameters.

2.7. Other Evaluation Methods

2.7.1. Electromyography

2.7.1.1. Introduction

The study of the muscle function through the analysis of its electrical signal (electromyography) (Basmajian and De Luca, 1985), remained a support measuring device tool with limited applications, except if used simultaneously with other measuring methods (Clarys, 2000).

Recent advances in electromyographic registration technology and signal data processing are the major responsible for the increasing applications of EMG in areas such as neurology, neurophysiology, neurosurgery, biomechanics, bioengineering, orthopaedics, rehabilitation, ergonomics, sports sciences, etc..

Especially in sports sciences and ergonomics, EMG is often called kinesiological EMG, and is used for studying muscular function and coordination. According to Clarys (2000) the general aim of the EMG is to analyse the function and coordination of muscles in different movement and postures, in healthy as well as in disable subjects, in skilled actions as well as during training, in humans as well in animals, under laboratory conditions as well as during daily activities.

2.7.1.2. EMG/Force

Kinesiological EMG incorporates several research areas. Nevertheless, one of the most important burning issues in biomechanics is the relationship between EMG and the muscular force.

The notion that EMG can be related in some way to muscular force is very suggestive. Over the years, the neurophysiology and biomechanics of the muscular system have been investigated quite extensively in order to characterize the relationship between muscle activity and several dynamic and/or kinematic aspects of the movement behaviour.

An electromyogram is the expression of the dynamic involvement of specific muscles within a predetermined range of a movement. In the same way, the integrated version of that same pattern is the expression of its muscular intensity. However, intensity is not always related to force (Clarys, 2000)

Numerous efforts have been made to correlate the duration, magnitude and timing of muscle contraction with the amplitude, duration and maximum speed of limb motion. According to Basmajian and De Luca (1985) an increase in the firing rates of motor units, increase the force and the integrated form of the EMG (IEMG) as well as the recruitment of an increasing number of motor units increases the muscular force and the corresponding IEMG (Guimaraes et al., 1995; Guimaraes et al., 1994). In this way, according to the author's, there must be at least a qualitative relationship between the EMG signal and the corresponding force of a muscle.

The relationship between the EMG and the force output under static conditions has been extensively studied and can be considered as linear (Hof, 2003). Although the relationship varies from muscle to muscle, some general results have been obtained. For small muscles a nearly linear relationship between measured EMG and force has been obtained. For larger muscles the relationship is parabolic with the level of EMG activity increasing more rapidly than force (Basmajian and De Luca, 1985). The relationship between the EMG and force under dynamic conditions is less well defined (Rainoldi et al., 2000).

According to Herzog et al. (1994a) the difficulty in finding a relationship between the EMG signal and the corresponding values of force is, at least, partly due to the difficulties in measuring EMG and force from individual muscles, and the temporal delay between the two signals (electromechanical delay).

When measuring EMG signals (surface EMG) from a particular muscle, the skeletal muscles do not always stay in the same place during complex dynamic movements, as well

as the entire muscle belly may not be fully under the skin, but covered by parts of other muscles, tendons, or subcutaneous adipose tissue. In this way, the selection of muscles for EMG measurement requires careful considerations, because there are always the possibility that signals from adjacent muscles may also be recorded. The authors that use wire electrodes do not have necessarily this problem, although the use of this kind of technique is only almost exclusively used in laboratory applications.

In order to study the basic relationship between EMG and force, it's necessary not only to measure accurately the force of the muscle and the uncontaminated EMG, but specially to control precisely the activation to the muscle. It should be noted that currently there is no methods to measure muscle activation directly.

Manal and Buchanan (2003), presented a method to model the transformation between neural activation $[u(t)]$, and muscle activation $[a(t)]$. The process of transformation recorded EMGs to muscle activation is complex and involves several steps (Figure 2.14). First, the EMG is rectified, filtered and normalized to maximal values $[e(t)]$. Because EMG is a function of its previous values, the activation history of the muscle must be taken in to account. The output of process is the neural activation $[u(t)]$, and can be transformed to muscle activation $[a(t)]$, and then is used as an input to a Hill-type model to predict muscle force.

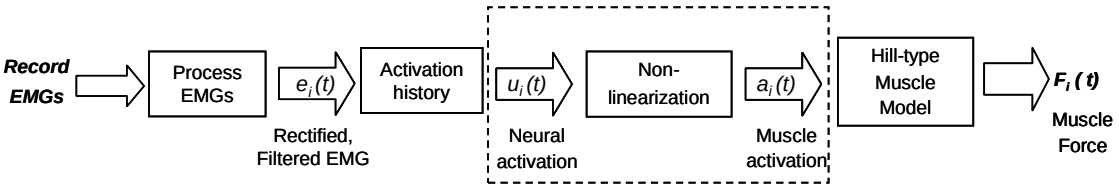

Figure 2.14 Schematic representation of the steps involved when estimating muscle force from EMG using a Hill-type model, according to Manal and Buchanan (2003).

In a study of Buchanan et al. (2005), the authors referred that after rectifying the EMG signals and low pass filtered to form an envelope, the signals are then normalized to a maximal voluntary contraction. However, according to the authors, the signal it is still lacking as a representation of muscle activation for tree reasons: (i) the signal is out of phase with muscle force (electromechanical delay), (ii) muscle activation is a function of its

recent history (Zajac, 1989). The transformation can be modeled as a second-order differential equation. This can be represented in a discretized form as:

$$u(t) = \alpha e(t-d) - \beta_1 u(t-1) - \beta_2 u(t-2) \tag{2.18}$$

where d is the electromechanical delay and α, β_1 and β_2 are the coefficients that define the second-order dynamics. This parameters map the normalized EMG values $[e(t)]$, to neural activation values $[u(t)]$. This filter should have unit gain so that neural activation does not exceed 1, meeting the following equation: $\alpha - \beta_1 - \beta_2 = 1$. Additionally, several constraints must be included if equations are to be stable (Buchanan et al., 2004), (iii) finally, the isometric EMG is not necessarily linearly related with muscle force. According to Manal and Buchanan (2003), based on Woods and Bigland-Ritchie (1983), for forces less than 30% of isometric force, this is a logarithmic relationship, and for higher force levels the relationship is linear.

2.7.1.3. Using EMG to Predict Force

Measuring the forces applied to a joint and estimating how these forces are partitioned by surrounding muscles and articular surfaces, is fundamental to understand the role of the muscles during human movements, and the possible mechanisms of injuries, in order to prevent it.

As already mentioned, the determination of individual muscle forces remains an indeterminate mathematical problem and to estimate the individual forces produced separately by each muscle, several studies have attempted to use electromyographic signals, in this context (Amarantini and Martin, 2004; Bogey et al., 2005; Buchanan et al., 2005; Koo and Mak, 2005; Lloyd and Besier, 2003; Lloyd and Buchanan, 1996; Manal and Buchanan, 2003; McGill, 1992).

Approximating muscle force from EMG signal is a challenging task. According to Bogey et al. (2005), the basic assumptions of the EMG-to-force processing are: 1) EMG signal is an adequate measure of muscle activation; 2) muscle length is determined; 3) muscle force, from muscle length and neural (EMG) activation, can be calculated using a force processing model of muscle contraction.

According to Koo and Mak (2005), if the EMG signals can be measured precisely and processed adequately to reflect the activation of each muscle crossing a joint, and if the activation can be modulated properly by anatomical and musculotendon models, it is possible to accurately estimate the individual muscle forces over a wide range of tasks and contraction models. Implicit to the EMG driven models is the EMG-to-activation processing, the musculotendon model, and the geometrical model of the joint, which entail a set of anatomical and physiological parameters (muscle rest length, tendon slack length, maximum isometric stress, shape factor of the EMG-force relationship, and electromechanical delay) that could affect the behaviour of the model. Because subjects are inherently different, to allow predictions across a number of different subjects, it is important to calibrate the model to an individual by adjusting subject-specific model parameters, with anatomical and physiological basis of muscle and EMG. According to Lloyd and Besier (2003), a non-linear least squares approach can be used with an appropriate set of calibration data to obtain model parameters that can be used in the musculoskeletal model to predict inverse dynamic joint moments. The model presented by the authors was cross validated across a wide range of tasks and better predicts the inverse dynamic joint moments than previous models.

According to Koo and Mak (2005), one of the limitations of the most of the EMG driven models reported in the literature, is that they tend to assume that once the model is calibrated, the same set of model parameters could still yield reasonable prediction in other tasks and testing configurations. On the other hand, the authors suggest that the estimation of muscle activation based on EMG signals seemed to be the major source of uncertainty with EMG driven models. Other factors such as the change of motor unit recruitment strategy of a muscle in accordance to the type of contraction that it performs, or if acts as agonist or antagonist, would also affect the linearity of the EMG-force relationship and hence affect the prediction accuracy of the model at different tasks.

According to Bogey et al. (2005), an EMG-to-force processing analysis can be used to estimate muscle moments and forces with a reasonable degree of accuracy. One important consideration that contributes for this assumption must be the accuracy of the inverse dynamics method in determining the joint moments. According to Wells (1981), the inaccuracy due to numerical differentiation and rigid body parameters are insignificant. Bogey et al. (2005) suggest that potential sources of error to the EMG-to-force processing

analysis are associated with the neural input (EMG). Factors like scaling of the EMG signal, mode of EMG signal acquisition, and the accuracy in representing the variable offset between the electrical signal of muscle and force development, must be taken in to account.

2.7.2. Imagiology

2.7.2.1. Introduction

Recent advances in imaging techniques such as the ultrasonography (ULS), made possible the observation of the dynamics of *in vivo* muscle and tendon tissues, clearly and not invasively, during movement in living humans (Fukunaga et al., 2000).

The first architectural data of skeletal muscles have been obtained mainly from cadaver specimens (An et al., 1981; Wickiewicz et al., 1984). According to Fukunaga and collaborators (1997b) it was showed that the architecture of active muscle fibres contracting differs considerably from those that occurs when movement is passively induced. Therefore the use of cadaver's data in the study of architecture and modeling of muscle function would result as an inaccurate or even as an erroneous method with inappropriate results.

2.7.2.2. Ultrasonography

Recent develops in ultrasonography have been made available to estimate directly and noninvasively skeletal muscle architecture, first during static movement conditions (Finni et al., 2003; Fukunaga et al., 1996a; Henriksson-Larsen et al., 1992; Kawakami et al., 1993), and recently during natural locomotion (Conceição, 2004; Finni and Komi, 2002; Fukunaga et al., 2001; Ishikawa et al., 2003; Ishikawa et al., 2005a; Kubo et al., 2000). With this technique, the instantaneous length changes in the fascicle and tendinous tissue can now be estimated during dynamic movements.

According to several author's, the accuracy, sensitivity and linearity of ultrasonography have been confirmed and allows the use of this technique as a valid method for the measurement of muscle architecture (fascicle length changes and pennation angles) (Fukunaga et al., 1997a; Fukunaga et al., 2000; Ishikawa et al., 2005a; Ishikawa et al., 2005b; Ito et al., 1998; Kawakami et al., 1993; Kawakami et al., 2000; Kawakami et al., 2002; Kurokawa et al., 2001), as well as for the determination of tendinous movement

during muscle contractions (Fukunaga et al., 1997a; Fukunaga et al., 1996a; Ito et al., 1998; Kawakami et al., 1993; Kawakami et al., 1998; Kawakami et al., 2000; Kubo et al., 1999; Muramatsu et al., 2001; Narici et al., 1996), tendon cross-sectional area (Ito et al., 1998), tendon excursion (Fukashiro et al., 1995a; Fukunaga et al., 1996a; Ito et al., 1998), and tendon stiffness (Fukashiro et al., 1995a). All this studies demonstrate the feasibility of using ultrasonography to quantify muscle and tendon architecture and deformation during loading, nevertheless these measurements are very sensitive to transducer orientation, and thus care must be taken to ensure a proper transducer alignment and placement (Hawkins, 2000).

In real-time ultrasonography, longitudinal sectional images over the midbelly of the muscles are obtained usually with the B-mode ultrasonic scanning on a linear-array probe (electronic transducer). The experimenter places the ultrasonic transducer in the longitudinal direction of the muscle and visually confirms the echoes from the *aponeurosis* and the fascicles of the selected muscle, so that the fascicle length can be measured. In the scanning images, muscle fascicles appear as dark lines lying between white striations of fat or connective tissue, running from the superficial to the deep *aponeurosis* (Figure 2.15). Fascicles can know be monitored directly through the ultrasonic echoes from interfascicle connective tissues and in order to confirm that the probe did not move during movement, a marker is usually placed between the skin and the ultrasonic probe (Fukunaga et al., 2000).

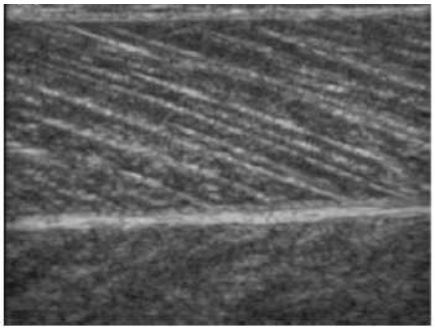

Figure 2.15. Example of a longitudinal ultrasonic image of the MG muscle of an healthy young male.

The angles at which fascicles arise from the *aponeurosis* can also be measured with a fairly reproducibility (Fukunaga et al., 1997a; Kawakami et al., 1993).

According to Komi and Ishikawa (2003), in association with direct *in vivo* measurements of tendon force, the measurement of fascicle length changes measured with the ultrasounds

technique, provides an increase in the understanding of muscle mechanics in human movement.

2.7.2.2.1. Methodological Considerations

The use of ultrasonography in dynamic movements requires an appropriate selection of the probe frequency according to the width of the muscle region selected. After the placement of the probe over the midbelly of the selected muscle the soundhead is slightly leaning on the muscle to find the best image, which should coincide with the plane of the muscle fascicle (Narici et al., 1996). The echoes reflected from *aponeurosis* and interspaces should be confirmed in order to avoid echoes of the reverberation artifacts and pitfalls of vascular origin. In many cases, however, in adult human superficial muscles, the probe length (60mm) does not cover the entire length of the fascicle. In this case appropriate approximations have been adapted for obtaining correct estimations of changes in the tensile structure lengths (Finni et al., 2001b; Muraoka et al., 2001).

Another methodological consideration is that sometimes the pennation angles may not be accurate vectors for predicting the effect of angulations of muscle fibres on force transfer to the tendon, because the *aponeurosis* lies at an angle to the line of action of the pennate muscle. According to Huijing (1992), this angle should be also considered in muscle models.

Real-time ultrasonography can be applied in dynamic movements, only in two dimensions. ULS is currently restricted to superficial muscles only.

2.7.2.3. Magnetic Resonance Imaging

Magnetic resonance imaging (MRI) is an imaging technique used primarily in medical settings to produce high quality images of the inside of the human body. Especially used to demonstrate pathological and physiological alterations of living tissues, MRI has also found many other novel applications outside of the medical fields, such as in biomechanics.

MRI requires specialized equipment and expertise people and allows evaluation of some body structures that may not be as visible with other imaging methods.

According to several authors, the MRI is widely considered to be the “gold standard” for the assessment of muscle morphometry, due to the high contrast between tissues of different molecular properties. The method has been validated through comparison with phantoms of known volume. (Esformes et al., 2002; Mitsiopoulos et al., 1998; Miyatani et al., 2000; Reeves et al., 2004). Like ULS, MRI allows the distinction between muscle and fat and does not involve exposure to ionising radiation. MRI uses radio frequency waves and a strong magnetic field, rather than x-rays, to provide remarkably clear and detailed pictures of internal organs and tissues.

In a study of Esformes et al. (2002), using MRI and ULS to estimate the muscle volume, *in vivo*, of the *tibialis* anterior (TA), and comparing the results of both imaging techniques, showed that MRI and ULS gave similar results (ULS: 133.2 $\pm$ 20 cm^3; RMI:131.8 $\pm$ 18 cm^3). Nevertheless, ULS method tends to underestimate muscle volumes smaller or larger than 120 cm^3. As most of the individual muscle volumes of the lower extremity, varies between 70 and 400 cm^3 (Fukunaga et al., 1992; Lieber et al., 1992), the data indicate that the ULS method introduce a measurement error of about 7%, and can only be used in superficial human muscles.

The MRI was systematically used in several studies to investigate the effects of ageing, amongst the individual constituents of muscles and viscoelastic properties of tendons in physical activity subjects (Maganaris et al., 2001; Morse et al., 2005; Narici et al., 2003; Reeves et al., 2003).

In a recent study of Morse et al. (2005) both MRI and ULS techniques were used simultaneously to study and compare the changes in muscle architecture of the *triceps surae* muscles in healthy physical activity young and elderly subjects and to discuss the functional implications of such changes due to age. The results showed that the total volume of the *triceps surae* muscle, as well as the pennation angle, were significantly smaller, in elderly than in young subjects. In elderly subjects, the fascicle length of the medial *gastrocnemius* was smaller than young subjects, nevertheless, no significant differences were found in the other muscles of the triceps surae group. The PCSA of the medial and lateral *gastrocnemius* muscles were found to be smaller in elderly than in young. No difference was observed in the *soleus* PCSA between the young and elderly subjects. In this way the relative PCSA composition of the *triceps surae* muscle group is maintained with

ageing and is scaled down harmonically with the decrease in muscle volume and fascicle length. The authors suggest that the relative contribution of the components of the *triceps surae* to the total force developed by this muscle group is maintained with ageing.

2.7.2.3.1. Methodological Considerations

The assessment to MRI for research purposes is often limited due to the large clinical demands and considerable costs. On account of being a difficult and expensive technique to implement, MRI is often used to validate (for comparison the results), the reproducibility of other techniques, such as the ULS.

2.8. References:

Abbott, B. C.; Bigland, B. and Ritchie, J. M. (1952). The physiological cost of negative work. J Physiol 117: 380-390.

Alexander, R. M. (1983). Animal Mechanics. Blackwell Scientific Publications, Oxford, UK.

Alexander, R. M. (1988). Elastic Mechanisms in Animal Movement. Cambridge University Press, Cambridge.

Alexander, R. M. (2000). Storage and Release of Elastic Energy in the Locomotor System and the Stretch-Shortening Cycle. In: nigg, B. M., Brian R., M., Mester, J. (eds) Biomechanics and Biology of Movement. Human -Kinetics, pp. 19-29.

Alexander, R. M. (2003). Modelling approaches in biomechanics. Philosophical Transactions of the Royal Society B: Biological Sciences 358: 1429-1435.

Alexander, R. M. and Bennet-Clark, H. C. (1977). Storage of elastic strain energy in muscle and other tissues. Nature 265: 114-117.

Alexander, R. M. and Vernon, A. (1975). The Mechanics of Hopping by Kangaroos (Macropodidae). Journal Zool Lond 177: 265-303.

Amadio, A. C. and Baumann, W. (2000). Aspects of the methodology to determine the internal forces of the locomotor system. Revista Brasileira de Biomecânica Ano 1: 7-14.

Amarantini, D. and Martin, L. (2004). A method to combine numerical optimization and EMG data for the estimation of joint moments under dynamic conditions. J Biomech 37: 1393-1404.

An, K. N.; Hui, F. C.; Morrey, B. F.; Linscheid, R. L. and Chao, E. Y. (1981). Muscles across the elbow joint: a biomechanical analysis. J Biomech 14: 659-669.

Anderson, F. C. and Pandy, M. G. (1993). Storage and utilization of elastic strain energy during jumping. J Biomech 26: 1413-1427.

Anderson, F. C. and Pandy, M. G. (2001). Dynamic optimization of human walking. J Biomech Eng 123: 381-390.

Arndt, A. N.; Komi, P. V.; Bruggemann, G. P. and Lukkariniemi, J. (1998). Individual muscle contributions to the *in vivo* achilles tendon force. Clin Biomech 13: 532-541.

Arnold, A. S.; Salinas, S.; Asakawa, D. J. and Delp, S. L. (2000). Accuracy of muscle moment arms estimated from MRI-based musculoskeletal models of the lower extremity. Comput Aided Surg 5: 108-119.

Asmussen, E. and Bonde-Petersen, F. (1974). Storage of elastic energy in skeletal muscles in man. Acta Physiol Scand 91: 385-392.

Basmajian, J. V. and De Luca, C. J. (1985). Muscles Alive. Their Funtions Revealed by Electromiography. Williams & Wilkins, Baltimore.

Bennet, M. B.; Ker, R. F.; Dimery, N. J. and Alexander, R. M. (1986). Mechanical properties of various mammalian tendons. Journal of Zoology 290A: 537-548.

Bennett, D. J.; De Serres, S. J. and Stein, R. B. (1996). Gain of the triceps surae stretch reflex in decerebrate and spinal cats during postural and locomotor activities. J Physiol 496 (Pt 3): 837-850.

Biewener, A. A.; Konieczynski, D. D. and Baudinette, R. V. (1998). In vivo muscle force-length behavior during steady-speed hopping in tammar wallabies. J Exp Biol 201: 1681-1694.

Biewener, A. A. and Roberts, T. J. (2000). Muscle and tendon contributions to force, work, and elastic energy savings: a comparative perspective. Exerc Sport Sci Rev 28: 99-107.

Bobbert, M. F. (2001). Dependence of human squat jump performance on the series elastic compliance of the triceps surae: a simulation study. J Exp Biol 204: 533-542.

Bobbert, M. F.; Gerritsen, K. G.; Litjens, M. C. and Van Soest, A. J. (1996). Why is countermovement jump height greater than squat jump height? Med Sci Sports Exerc 28: 1402-1412.

Bobbert, M. F.; Huijing, P. A. and van Ingen Schenau, G. J. (1986a). An estimation of power output and work done by the human triceps surae muscle-tendon complex in jumping. J Biomech 19: 899-906.

Bobbert, M. F.; Huijing, P. A. and van Ingen Schenau, G. J. (1986b). A model of the human triceps surae muscle-tendon complex applied to jumping. J Biomech 19: 887-898.

Bobbert, M. F. and van Ingen Schenau, G. J. (1988). Coordination in vertical jumping. J Biomech 21: 249-262.

Bocquet, J.-C. and Noel, J. (1987). Sensitive skin-pressure and strain sensor with optical fibres. 2nd Congress on Strutural Mechanics of Optical Systems, Los Angeles, California, USA

Bogey, R. A.; Perry, J. and Gitter, A. J. (2005). An EMG-to-force processing approach for determining ankle muscle forces during normal human gait. IEEE Trans Neural Syst Rehabil Eng 13: 302-310.

Bosco, C.; Komi, P. V. and Ito, A. (1981). Prestretch potentiation of human skeletal muscle during ballistic movement. Acta Physiol Scand 111: 135-140.

Bosco, C.; Tarkka, I. and Komi, P. V. (1982a). Effect of elastic energy and myoelectrical potentiation of triceps surae during stretch-shortening cycle exercise. Int J Sports Med 3: 137-140.

Bosco, C.; Viitasalo, J. T.; Komi, P. V. and Luhtanen, P. (1982b). Combined effect of elastic energy and myoelectrical potentiation during stretch-shortening cycle exercise. Acta Physiol Scand 114: 557-565.

Brand, R. A.; Crowninshield, R. D.; Wittstock, C. E.; Pedersen, D. R.; Clark, C. R. and van Krieken, F. M. (1982). A model of lower extremity muscular anatomy. J Biomech Eng 104: 304-310.

Braune, W.; Fischer, O.; Maquet, P. and Furlong, R. (1987). The human gait. Springer Verlag, Berlin.

Buchanan, T. S.; lloyd, D. G.; Manal, K. and Besier, T. F. (2004). Neuromusculoskeletal Modeling: Estimation of Muscle Forces and Joint Moments and Movements drom Measurements of Neural Command. Journal of Applied Biomechanics 20: 367-395.

Buchanan, T. S.; Lloyd, D. G.; Manal, K. and Besier, T. F. (2005). Estimation of muscle forces and joint moments using a forward-inverse dynamics model. Med Sci Sports Exerc 37: 1911-1916.

Butler, D. L.; Grood, E. S.; Noyes, F. R. and Zernicke, R. F. (1978). Biomechanics of ligaments and tendons. Exerc Sport Sci Rev 6: 125-181.

Candau, R.; Belli, A.; Chatard, J. C.; Carrez, J.-P. and Lacour, J.-R. (1993). Stretching shortening cycle in the skating technique of cross-country skiing. Sci Motricité 22: 252-256.

Cavagna, G. A. (1971). Power Output of the Previously Stretched Muscle. Medicine and Sport 6: Biomechanics II: 159-167.

Cavagna, G. A. (1977). Storage and utilization of elastic energy in skeletal muscle. Exerc Sport Sci Rev 5: 89-129.

Cavagna, G. A.; Dusman, B. and Margaria, R. (1968). Positive work done by a previously stretched muscle. J Appl Physiol 24: 21-32.

Cavagna, G. A.; Saibene, F. P. and Margaria, R. (1965). Effect of Negative Work on the Amount of Positive Work Performed by an Isolated Muscle. J Appl Physiol 20: 157-158.

Challis, J. H. and Kerwin, D. G. (1993). An analytical examination of muscle force estimations using optimization techniques. Proc Inst Mech Eng [H] 207: 139-148.

Chapman, A. E. (1985). The mechanical properties of human muscle. Exerc Sport Sci Rev 13: 443-501.
Cholewicki, J. and McGill, S. M. (1994). EMG assisted optimization: a hybrid approach for estimating muscle forces in an indeterminate biomechanical model. J Biomech 27: 1287-1289.
Cholewicki, J.; McGill, S. M. and Norman, R. W. (1995). Comparison of muscle forces and joint load from an optimization and EMG assisted lumbar spine model: towards development of a hybrid approach. J Biomech 28: 321-331.
Clarys, J. P. (2000). Electromyography in sports and occupational settings: an update of its limits and possibilities. Ergonomics 43: 1750-1762.
Collins, J. J. (1995). The redundant nature of locomotor optimization laws. J Biomech 28: 251-267.
Conceição, F. (2004). Estudo Biomecânico do Salto em Comprimento. Modelação, simulação e optimização da chamada. Biomechanics. University of Porto, Porto
Cook, C. S. and McDonagh, M. J. (1995). Force responses to controlled stretches of electrically stimulated human muscle-tendon complex. Exp Physiol 80: 477-490.
Crago, P. E. (2000). Creating Neuromusculoskeletal Models. In: Winters, J. M., Crago, P. E. (eds) Biomechanics and Neural Control of Posture and Movement. Springer, New-York, pp. 119-133.
Crowninshield, R. D. and Brand, R. A. (1981a). A physiologically based criterion of muscle force prediction in locomotion. J Biomech 14: 793-801.
Crowninshield, R. D. and Brand, R. A. (1981b). The prediction of forces in joint structures; distribution of intersegmental resultants. Exerc Sport Sci Rev 9: 159-181.
Dietz, V.; Schmidtbleicher, D. and Noth, J. (1979). Neuronal mechanisms of human locomotion. J Neurophysiol 42: 1212-1222.
Ebashi, S. and Endo, M. (1968). Calcium ion and muscle contraction. Prog Biophys Mol Biol 18: 123-183.
Edman, K. A. (1996). Fatigue vs. shortening-induced deactivation in striated muscle. Acta Physiol Scand 156: 183-192.
Edman, K. A. (1999). The force bearing capacity of frog muscle fibres during stretch: its relation to sarcomere length and fibre width. J Physiol 519 Pt 2: 515-526.
Edman, K. A.; Caputo, C. and Lou, F. (1993). Depression of tetanic force induced by loaded shortening of frog muscle fibres. J Physiol 466: 535-552.
Edman, K. A.; Elzinga, G. and Noble, M. I. (1978). Enhancement of mechanical performance by stretch during tetanic contractions of vertebrate skeletal muscle fibres. J Physiol 281: 139-155.
Elftman, H. (1939). The function of muscles in locomotion. Am J Physiol 125: 339-356.
Enoka, R. M. (2002). Neuromechanics of Human Movement. Human Kinetics, USA.
Erdemir, A.; Hamel, A. J.; Piazza, S. J. and Sharkey, N. A. (2003). Fiberoptic measurement of tendon forces is influenced by skin movement artifact. J Biomech 36: 449-455.
Erdemir, A.; Piazza, S. J. and Sharkey, N. A. (2002). Influence of loading rate and cable migration on fiberoptic measurement of tendon force. J Biomech 35: 857-862.
Esformes, J. I.; Narici, M. V. and Maganaris, C. N. (2002). Measurement of human muscle volume using ultrasonography. Eur J Appl Physiol 87: 90-92.
Ettema, G. J.; Huijing, P. A. and de Haan, A. (1992). The potentiating effect of prestretch on the contractile performance of rat gastrocnemius medialis muscle during subsequent shortening and isometric contractions. J Exp Biol 165: 121-136.
Ettema, G. J.; Huijing, P. A.; van Ingen Schenau, G. J. and de Haan, A. (1990a). Effects of prestretch at the onset of stimulation on mechanical work output of rat medial gastrocnemius muscle-tendon complex. J Exp Biol 152: 333-351.

Ettema, G. J.; van Soest, A. J. and Huijing, P. A. (1990b). The role of series elastic structures in prestretch-induced work enhancement during isotonic and isokinetic contractions. J Exp Biol 154: 121-136.
Finni, T.; Hodgson, J. A.; Lai, A. M.; Edgerton, V. R. and Sinha, S. (2003). Nonuniform strain of human soleus aponeurosis-tendon complex during submaximal voluntary contractions in vivo. J Appl Physiol 95: 829-837.
Finni, T.; Ikegawa, S.; Lepola, V. and Komi, P. (2001a). *In vivo* Behaviour of Vastus Lateralis Muscle During Dynamic Performance. *Eur J Sports Sci* (Online) 1.http://www.humankinetics.com/ejss
Finni, T. and Komi, P. (2002). Two Methods for Estimating Tendinous Tissue Elongation During Human Movement. Journal of Applied Biomechanics 18: 180-188.
Finni, T.; Komi, P. V. and Lepola, V. (2000). In vivo human triceps surae and quadriceps femoris muscle function in a squat jump and counter movement jump. Eur J Appl Physiol 83: 416-426.
Finni, T.; Komi, P. V. and Lepola, V. (2001b). In vivo muscle mechanics during locomotion depend on movement amplitude and contraction intensity. Eur J Appl Physiol 85: 170-176.
Finni, T.; Komi, P. V. and Lukkariniemi, J. (1998). Achilles tendon loading during walking: application of a novel optic fiber technique. Eur J Appl Physiol Occup Physiol 77: 289-291.
Fukashiro, S.; Itoh, M.; Ichinose, Y.; Kawakami, Y. and Fukunaga, T. (1995a). Ultrasonography gives directly but noninvasively elastic characteristic of human tendon in vivo. Eur J Appl Physiol Occup Physiol 71: 555-557.
Fukashiro, S.; Komi, P. V.; Jarvinen, M. and Miyashita, M. (1995b). In vivo Achilles tendon loading during jumping in humans. Eur J Appl Physiol Occup Physiol 71: 453-458.
Fukunaga, T.; Ichinose, Y.; Ito, M.; Kawakami, Y. and Fukashiro, S. (1997a). Determination of fascicle length and pennation in a contracting human muscle in vivo. J Appl Physiol 82: 354-358.
Fukunaga, T.; Ito, M.; Ichinose, Y.; Kuno, S.; Kawakami, Y. and Fukashiro, S. (1996a). Tendinous movement of a human muscle during voluntary contractions determined by real-time ultrasonography. J Appl Physiol 81: 1430-1433.
Fukunaga, T.; Kawakami, Y.; Kuno, S.; Funato, K. and Fukashiro, S. (1997b). Muscle architecture and function in humans. J Biomech 30: 457-463.
Fukunaga, T.; Kubo, K.; Kawakami, Y.; Fukashiro, S.; Kanehisa, H. and Maganaris, C. N. (2001). *In vivo* behaviour of human muscle tendon during walking. Proc R Soc Lond B Biol Sci 268: 229-233.
Fukunaga, T.; Kubo, K.; Kawakami, Y. and Kanehisa, H. (2000). Effect of elastic tendon properties on the performance of stretch-shortening cycles. In: Herzog, W. (ed) Skeletal Muscle Mechanics. Wiley and Sons, Ltd, Chichester, pp. 289-303.
Fukunaga, T.; Roy, R. R.; Shellock, F. G.; Hodgson, J. A.; Day, M. K.; Lee, P. L.; Kwong-Fu, H. and Edgerton, V. R. (1992). Physiological cross-sectional area of human leg muscles based on magnetic resonance imaging. J Orthop Res 10: 928-934.
Fukunaga, T.; Roy, R. R.; Shellock, F. G.; Hodgson, J. A. and Edgerton, V. R. (1996b). Specific tension of human plantar flexors and dorsiflexors. J Appl Physiol 80: 158-165.
Gielen, S.; Van Ingen Schenau, G. J.; Tax, T. and Theeuwen, M. (1990). The activation of mono- and bi-articular muscles in multi-joint movements. In: Winters, J. M., Woo, S. L. (eds) Multiple Muscle System. Springer, New York, pp. 302-311.
Glitsch, U. and Baumann, W. (1997). The three-dimensional determination of internal loads in the lower extremity. J Biomech 30: 1123-1131.

Gollhofer, A.; Strojnik, V.; Rapp, W. and Schweizer, L. (1992). Behaviour of triceps surae muscle-tendon complex in different jump conditions. Eur J Appl Physiol Occup Physiol 64: 283-291.

Gordon, A. M.; Huxley, A. F. and Julian, F. J. (1966). The variation in isometric tension with sarcomere length in vertebrate muscle fibres. J Physiol 184: 170-192.

Gregoire, L.; Veeger, H. E.; Huijing, P. A. and van Ingen Schenau, G. J. (1984). Role of mono- and biarticular muscles in explosive movements. Int J Sports Med 5: 301-305.

Gregor, R. J.; Roy, R. R.; Whiting, W. C.; Lovely, R. G.; Hodgson, J. A. and Edgerton, V. R. (1988). Mechanical output of the cat soleus during treadmill locomotion: in vivo vs in situ characteristics. J Biomech 21: 721-732.

Griffiths, R. I. (1991). Shortening of muscle fibres during stretch of the active cat medial gastrocnemius muscle: the role of tendon compliance. J Physiol 436: 219-236.

Guimaraes, A. C.; Herzog, W.; Allinger, T. L. and Zhang, Y. T. (1995). The EMG-force relationship of the cat soleus muscle and its association with contractile conditions during locomotion. J Exp Biol 198: 975-987.

Guimaraes, A. C.; Herzog, W.; Hulliger, M.; Zhang, Y. T. and Day, S. (1994). EMG-force relationship of the cat soleus muscle studied with distributed and non-periodic stimulation of ventral root filaments. J Exp Biol 186: 75-93.

Happee, R. (1994). Inverse dynamic optimization including muscular dynamics, a new simulation method applied to goal directed movements. J Biomech 27: 953-960.

Hatze, H. (1977). A myocybernetic control model of skeletal muscle. Biol Cybern 25: 103-119.

Hatze, H. (1978). A general myocybernetic control model of skeletal muscle. Biol Cybern 28: 143-157.

Hatze, H. (1990). The charge-transfer model of myofilamentary interaction: prediction of force enhancement and related myodynamic phenomena. In: Winters, J. M., Woo, S. L.-Y. (eds) Multiple Muscle SystemsBiomechanics and Movement Organization. Springer-Verlag, New York, pp. 24-45.

Hatze, H. (2000). The inverse dynamics problem of neuromuscular control. Biol Cybern 82: 133-141.

Hawkins, D. (2000). A non-invasive approach for studying human muscle-tendon units *in vivo*. In: Herzog, W. (ed) Skeletal Muscle Mechanics. Wiley and Sons, Ltd, Chichester, pp. 305-326.

Henchoz, Y.; Malatesta, D.; Gremion, G. and Belli, A. (2006). Effects of the transition time between muscle-tendon stretch and shortening on mechanical efficiency. Eur J Appl Physiol 96: 665-671.

Henriksson-Larsen, K.; Wretling, M. L.; Lorentzon, R. and Oberg, L. (1992). Do muscle fibre size and fibre angulation correlate in pennated human muscles? Eur J Appl Physiol Occup Physiol 64: 68-72.

Herzog, W. (1987). Individual muscle force estimations using a non-linear optimal design. J Neurosci Methods 21: 167-179.

Herzog, W. (2000a). Muscle Activation and Motor Control. In: Nigg, B. M., Brian R., M., Mester, J. (eds) Biomechanics and Biology of Movement. Human Kinetics, Champaign, pp. 179-192.

Herzog, W. (2000b). Skeletal Muscle Mechanics. From Mechanisms to Function. John Wiley & Sons, Chichester.

Herzog, W.; Guimaraes, A. C. and Zhang, Y. T. (1994a). EMG. In: Nigg, B. M., Herzog, W. (eds) Biomechanics of the Musculo-Skeletal System. John Wiley & Sons, Chichester

Herzog, W. and Leonard, T. R. (1991). Validation of optimization models that estimate the forces exerted by synergistic muscles. J Biomech 24 Suppl 1: 31-39.

Herzog, W. and Leonard, T. R. (1997). Depression of cat soleus-forces following isokinetic shortening. J Biomech 30: 865-872.
Herzog, W. and Leonard, T. R. (2002). Force enhancement following stretching of skeletal muscle: a new mechanism. J Exp Biol 205: 1275-1283.
Herzog, W.; Zatsiorsky, V.; Prilutsky, B. I. and Leonard, T. R. (1994b). Variations in force-time histories of cat gastrocnemius, soleus and plantaris muscles for consecutive walking steps. J Exp Biol 191: 19-36.
Hijikata, T.; Wakisaka, H. and Niida, S. (1993). Functional combination of tapering profiles and overlapping arrangements in nonspanning skeletal muscle fibers terminating intrafascicularly. Anat Rec 236: 602-610.
Hill, A. V. (1938). The heat of shortening and the dynamic constants of muscle. Proc Roy Soc B: 136-195.
Hof, A. L. (1998). In vivo measurement of the series elasticity release curve of human triceps surae muscle. J Biomech 31: 793-800.
Hof, A. L. (2003). Muscle mechanics and neuromuscular control. J Biomech 36: 1031-1038.
Hof, A. L.; Geelen, B. A. and Van den Berg, J. (1983). Calf muscle moment, work and efficiency in level walking; role of series elasticity. J Biomech 16: 523-537.
Hoffer, J. A. and Andreassen, S. (1981). Regulation of soleus muscle stiffness in premammillary cats: intrinsic and reflex components. J Neurophysiol 45: 267-285.
Huijing, P. A. (1992). Elastic Potenciation of Muscle. In: Komi, P. V. (ed) Strenght and Power in Sport. Blackwell Scientific Publications, Oxford, pp. 151-168.
Huijing, P. A. (1999). Muscle as a collagen fiber reinforced composite: a review of force transmission in muscle and whole limb. J Biomech 32: 329-345.
Huijing, P. A. (2000). Length, shortening velocity, activation, and fatigue are not independent factors determining muscle force exerted. In: Winters, J. M., Crago, P. E. (eds) Biomechanics and Neural Control of Posture and Movement. Springer, New York, pp. 83-91.
Huxley, A. F. (1957). Muscle structure and theories of contraction. Prog Biophys Biophys Chem 7: 255-318.
Huxley, A. F. (2000a). Cross-bridge action: present views, prospects, and unknowns. J Biomech 33: 1189-1195.
Huxley, A. F. (2000b). Mechanics and models of the myosin motor. Philos Trans R Soc 355: 433-440.
Huxley, A. F. and Simmons, R. M. (1971). Proposed mechanism of force generation in striated muscle. Nature 233: 533-538.
Huxley, H. and Hanson, J. (1954). Changes in the cross-striations of muscle during contraction and stretch and their structural interpretation. Nature 173: 973-976.
Ishikawa, M.; Finni, T. and Komi, P. V. (2003). Behaviour of vastus lateralis muscle-tendon during high intensity SSC exercises *in vivo*. Acta Physiol Scand 178: 205-213.
Ishikawa, M.; Komi, P. V.; Grey, M. J.; Lepola, V. and Bruggemann, G. P. (2005a). Muscle-tendon interaction and elastic energy usage in human walking. J Appl Physiol 99: 603-608.
Ishikawa, M.; Niemela, E. and Komi, P. V. (2005b). Interaction between fascicle and tendinous tissues in short-contact stretch-shortening cycle exercise with varying eccentric intensities. J Appl Physiol 99: 217-223.
Ito, M.; Kawakami, Y.; Ichinose, Y.; Fukashiro, S. and Fukunaga, T. (1998). Nonisometric behavior of fascicles during isometric contractions of a human muscle. J Appl Physiol 85: 1230-1235.
Jacobs, R.; Bobbert, M. F. and van Ingen Schenau, G. J. (1993). Function of mono- and biarticular muscles in running. Med Sci Sports Exerc 25: 1163-1173.

Jacobs, R.; Bobbert, M. F. and van Ingen Schenau, G. J. (1996). Mechanical output from individual muscles during explosive leg extensions: the role of biarticular muscles. J Biomech 29: 513-523.
Jacobs, R. and van Ingen Schenau, G. J. (1992). Intermuscular coordination in a sprint push-off. J Biomech 25: 953-965.
Joyce, G. C.; Rack, P. M. and Westbury, D. R. (1969). The mechanical properties of cat soleus muscle during controlled lengthening and shortening movements. J Physiol 204: 461-474.
Jozsa, L.; Kvist, M.; Balint, B. J.; Reffy, A.; Jarvinen, M.; Lehto, M. and Barzo, M. (1989). The role of recreational sport activity in Achilles tendon rupture. A clinical, pathoanatomical, and sociological study of 292 cases. Am J Sports Med 17: 338-343.
Kannus, P. and Jozsa, L. (1991). Histopathological changes preceding spontaneous rupture of a tendon. A controlled study of 891 patients. J Bone Joint Surg Am 73: 1507-1525.
Kannus, P.; Jozsa, L.; Natri, A. and Jarvinen, M. (1997). Effects of training, immobilization and remobilization on tendons. Scand J Med Sci Sports 7: 67-71.
Katz, B. (1939). The Relation Between Force and Speed in Muscular Contraction. Journal of Physiology 96: 45-64.
Kawakami, Y.; Abe, T. and Fukunaga, T. (1993). Muscle-fiber pennation angles are greater in hypertrophied than in normal muscles. J Appl Physiol 74: 2740-2744.
Kawakami, Y.; Ichinose, Y. and Fukunaga, T. (1998). Architectural and functional features of human triceps surae muscles during contraction. J Appl Physiol 85: 398-404.
Kawakami, Y.; Ichinose, Y.; Kubo, K.; Ito, M.; Imai, M. and Fukunaga, T. (2000). Architecture of Contracting Human Muscles and Its Funtional Significance. Journal of Applied Biomechanics 16: 88-98.
Kawakami, Y.; Muraoka, T.; Ito, S.; Kanehisa, H. and Fukunaga, T. (2002). In vivo muscle fibre behaviour during counter-movement exercise in humans reveals a significant role for tendon elasticity. J Physiol 540: 635-646.
Ker, R. F. (1981). Dynamic tensile properties of the plantaris tendon of sheep (Ovis aries). J Exp Biol 93: 283-302.
Ker, R. F.; Alexander, R. M. and Bennet, M. B. (1988). Why are Mammalian Tendons so Thick. Journal of Zoology 216: 309-324.
Ker, R. F.; Alexander, R. M. and Bennet, M. B. (1998). Why are Mammalian Tendons so Thick. Journal of Zoology 216: 309-324.
Ker, R. F.; Wang, X. T. and Pike, A. V. (2000). Fatigue quality of mammalian tendons. J Exp Biol 203 Pt 8: 1317-1327.
Kilani, H. A.; Palmer, S. S.; Adrian, M. J. and Gapsis, J. J. (1989). Block of the Stretch Reflex of Vastus Lateralis During Vertical Jumps. Human Movement Science 8: 247-269.
Koehl, M. A. (2003). Physical modelling in biomechanics. Philos Trans R Soc Lond B Biol Sci 358: 1589-1596.
Komi, P. and Ishikawa, M. (2003). In Vivo function of human Achilles and Patella tendons during normal locomotion. ICO Workshop on Tendinopathy
Athens
Komi, P. V. (1973). Relationship between muscle tension, EMG and velocity of contraction under concentric and eccentric work. In: JE, D. (ed) New Developments in Electromiography and Clinical Neurophysiology. Kargel, Basel, pp. 596-606.
Komi, P. V. (1984). Physiological and biomechanical correlates of muscle function: effects of muscle structure and stretch-shortening cycle on force and speed. Exerc Sport Sci Rev 12: 81-121.

Komi, P. V. (1987). Neuromuscular Factors Related to Physical Performance. Med Sport Sci 26: 48-66.
Komi, P. V. (1990). Relevance of in vivo force measurements to human biomechanics. J Biomech 23 Suppl 1: 23-34.
Komi, P. V.; Belli, A.; Huttunen, V.; Bonnefoy, R.; Geyssant, A. and Lacour, J. R. (1996). Optic fibre as a transducer of tendomuscular forces. Eur J Appl Physiol Occup Physiol 72: 278-280.
Komi, P. V.; Belli, A.; Huttunen, V. and Partio, E. (1995). Optic fiber as a transducer for direct *in- vivo* measurements of human tendomuscular forces. In: Häkkinen, K., Keskinen, K. L., Komi, P. V., Mero, A. (eds) XVth ISB Jyväskylä, Finland, pp. 494-495.
Komi, P. V. and Bosco, C. (1978). Utilization of stored elastic energy in leg extensor muscles by men and women. Med Sci Sports 10: 261-265.
Komi, P. V.; Fukashiro, S. and Järvinen, M. (1992). Biomechanical Loading of Achilles Tendon During Normal Locomotion. Clinics in Sports Medicine 11: 521-531.
Komi, P. V. and Gollhofer, A. (1997). Stretch reflexes can have an important role in force enhancement during SSC exercise. j Appl Biomech 13: 451-460.
Komi, P. V. and Nicol, C. (2000). Stretch-Shortening Cycle Fatigue. In: Nigg, B. M., MacIntosh, B. R., Mester, J. (eds) Biomechanics and Biology of Movement. Human Kinetics, Champaign, pp. 385-408.
Komi, P. V.; Salomen, M. and Järvinen, M. (1984). *In vivo* measurements of Achilles tendon forces in man. Americam College of Sports Medicine, Annual Meeting, San Diego, USA
Komi, P. V.; Salomen, M. and Järvinen, M. (1985). Measurement of *in vivo* Achilles tendon forces in man and their calibration. Americam College of Sports Medicine, Annual Meeting, Nashville, USA
Komi, P. V.; Salonen, M.; Jarvinen, M. and Kokko, O. (1987). In vivo registration of Achilles tendon forces in man. I. Methodological development. Int J Sports Med 8 Suppl 1: 3-8.
Koo, T. K. and Mak, A. F. (2005). Feasibility of using EMG driven neuromusculoskeletal model for prediction of dynamic movement of the elbow. J Electromyogr Kinesiol 15: 12-26.
Kubo, K.; Kanehisa, H.; Takeshita, D.; Kawakami, Y.; Fukashiro, S. and Fukunaga, T. (2000). In vivo dynamics of human medial gastrocnemius muscle-tendon complex during stretch-shortening cycle exercise. Acta Physiol Scand 170: 127-135.
Kubo, K.; Kawakami, Y. and Fukunaga, T. (1999). Influence of elastic properties of tendon structures on jump performance in humans. J Appl Physiol 87: 2090-2096.
Kurokawa, S.; Fukunaga, T. and Fukashiro, S. (2001). Behavior of fascicles and tendinous structures of human gastrocnemius during vertical jumping. J Appl Physiol 90: 1349-1358.
Lieber, R. L. and Friden, J. (2000). Functional and clinical significance of skeletal muscle architecture. Muscle Nerve 23: 1647-1666.
Lieber, R. L. and Friden, J. (2001). Clinical significance of skeletal muscle architecture. Clin Orthop: 140-151.
Lieber, R. L.; Jacobson, M. D.; Fazeli, B. M.; Abrams, R. A. and Botte, M. J. (1992). Architecture of selected muscles of the arm and forearm: anatomy and implications for tendon transfer. J Hand Surg [Am] 17: 787-798.
Lieber, R. L.; Leonard, M. E. and Brown-Maupin, C. G. (2000). Effects of muscle contraction on the load-strain properties of frog aponeurosis and tendon. Cells Tissues Organs 166: 48-54.

Lloyd, D. G. and Besier, T. F. (2003). An EMG-driven musculoskeletal model to estimate muscle forces and knee joint moments in vivo. J Biomech 36: 765-776.
Lloyd, D. G. and Buchanan, T. S. (1996). A model of load sharing between muscles and soft tissues at the human knee during static tasks. J Biomech Eng 118: 367-376.
Loocke, M. V.; Lyons, C. G. and Simms, C. (2004). The three-dimensional mechanical properties of skeletal muscle: experiments and modelling In: McHugh, P. J. P. P. E. (ed) Topics in bio-medical engineering Trinity Centre for Bio-Engineering, Dublin, pp. 216-234.
Loren, G. J. and Lieber, R. L. (1995). Tendon biomechanical properties enhance human wrist muscle specialization. J Biomech 28: 791-799.
Maas, H.; Yucesoy, C. A.; Baan, G. C. and Huijing, P. A. (2003). Implications of Muscle Relative Position as a Co-Determinant of Isometric Muscle Force: A Review and Some Experimental Results. Journal of Mechanics in Medicine and Biology 3: 145-168.
Maganaris, C. N.; Baltzopoulos, V.; Ball, D. and Sargeant, A. J. (2001). In vivo specific tension of human skeletal muscle. J Appl Physiol 90: 865-872.
Maganaris, C. N. and Paul, J. P. (1999). In vivo human tendon mechanical properties. J Physiol 521 Pt 1: 307-313.
Magnusson, S. P.; Aagaard, P.; Dyhre-Poulsen, P. and Kjaer, M. (2001). Load-displacement properties of the human triceps surae aponeurosis in vivo. J Physiol 531: 277-288.
Malamud, J. G.; Godt, R. E. and Nichols, T. R. (1996). Relationship between short-range stiffness and yielding in type-identified, chemically skinned muscle fibers from the cat triceps surae muscles. J Neurophysiol 76: 2280-2289.
Manal, K. and Buchanan, T. S. (2003). A one-parameter neural activation to muscle activation model: estimating isometric joint moments from electromyograms. J Biomech 36: 1197-1202.
Marsh, E.; Sale, D.; McComas, A. J. and Quinlan, J. (1981). Influence of joint position on ankle dorsiflexion in humans. J Appl Physiol 51: 160-167.
Matthews, P. B. (1981). Evolving views on the internal operation and functional role of the muscle spindle. J Physiol 320: 1-30.
Mazzone, M. F. and McCue, T. (2002). Common conditions of the achilles tendon. Am Fam Physician 65: 1805-1810.
McCully, K. K. and Faulkner, J. A. (1986). Characteristics of lengthening contractions associated with injury to skeletal muscle fibers. J Appl Physiol 61: 293-299.
McGill, S. M. (1992). A myoelectrically based dynamic three-dimensional model to predict loads on lumbar spine tissues during lateral bending. J Biomech 25: 395-414.
Mitsiopoulos, N.; Baumgartner, R. N.; Heymsfield, S. B.; Lyons, W.; Gallagher, D. and Ross, R. (1998). Cadaver validation of skeletal muscle measurement by magnetic resonance imaging and computerized tomography. J Appl Physiol 85: 115-122.
Miyatani, M.; Kanehisa, H. and Fukunaga, T. (2000). Validity of bioelectrical impedance and ultrasonographic methods for estimating the muscle volume of the upper arm. Eur J Appl Physiol 82: 391-396.
Monti, R. J.; Roy, R. R.; Hodgson, J. A. and Edgerton, V. R. (1999). Transmission of forces within mammalian skeletal muscles. J Biomech 32: 371-380.
Morgan, D. L. (1990). New insights into the behavior of muscle during active lengthening. Biophys J 57: 209-221.
Morse, C. I.; Thom, J. M.; Birch, K. M. and Narici, M. V. (2005). Changes in triceps surae muscle architecture with sarcopenia. Acta Physiol Scand 183: 291-298.

Muramatsu, T.; Muraoka, T.; Takeshita, D.; Kawakami, Y.; Hirano, Y. and Fukunaga, T. (2001). Mechanical properties of tendon and aponeurosis of human gastrocnemius muscle in vivo. J Appl Physiol 90: 1671-1678.

Muraoka, T.; Kawakami, Y.; Tachi, M. and Fukunaga, T. (2001). Muscle fiber and tendon length changes in the human vastus lateralis during slow pedaling. J Appl Physiol 91: 2035-2040.

Nagano, A.; Komura, T.; Fukashiro, S. and Himeno, R. (2005). Force, work and power output of lower limb muscles during human maximal-effort countermovement jumping. J Electromyogr Kinesiol 15: 367-376.

Nakagawa, Y.; Hayashi, K.; Yamamoto, N. and Nagashima, K. (1996). Age-related changes in biomechanical properties of the Achilles tendon in rabbits. Eur J Appl Physiol Occup Physiol 73: 7-10.

Narici, M. V.; Binzoni, T.; Hiltbrand, E.; Fasel, J.; Terrier, F. and Cerretelli, P. (1996). In vivo human gastrocnemius architecture with changing joint angle at rest and during graded isometric contraction. J Physiol 496 (Pt 1): 287-297.

Narici, M. V.; Landoni, L. and Minetti, A. E. (1992). Assessment of human knee extensor muscles stress from in vivo physiological cross-sectional area and strength measurements. Eur J Appl Physiol Occup Physiol 65: 438-444.

Narici, M. V.; Maganaris, C. N.; Reeves, N. D. and Capodaglio, P. (2003). Effect of aging on human muscle architecture. J Appl Physiol 95: 2229-2234.

Nicol, C. and Komi, P. V. (1999). Quantification of Achilles Tendon Force Enhancement by Passively Induced Dorsiflexion Stretches. Journal of Applied Biomechanics 15: 221-232.

Nicol, C.; Komi, P. V.; Horita, T.; Kyrolainen, H. and Takala, T. E. (1996). Reduced stretch-reflex sensitivity after exhausting stretch-shortening cycle exercise. Eur J Appl Physiol Occup Physiol 72: 401-409.

Nigg, B. M. (1994). Modelling. In: Nigg, B. M., Herzog, W. (eds) Biomechanics of the Musculo-Skeletal System. John Wiley & Sons, Chichester, pp. 365-566.

Nigg, B. M. and Herzog, W. (1994). Biomechanics of the Musculo-Skeletal System. John Wiley & Sons, Chichester.

Norman, R. W. and Komi, P. V. (1979). Electromechanical delay in skeletal muscle under normal movement conditions. Acta Physiol Scand 106: 241-248.

O'Brien, M. (1992). Functional Anatomy and Physiology of Tendons. Clinics in Sports Medicine 11: 505-520.

Ounjian, M.; Roy, R. R.; Eldred, E.; Garfinkel, A.; Payne, J. R.; Armstrong, A.; Toga, A. W. and Edgerton, V. R. (1991). Physiological and developmental implications of motor unit anatomy. J Neurobiol 22: 547-559.

Pandy, M. G. (1990). An Analytical Framework for Quantifying Muscular Action During Human Movement. In: Woo, J. M. W. a. S. L.-Y. (ed) Multiple Muscle SystemsBiomechanics and Movement Organization. Springer-Verlag, New York, pp. 653-662.

Pandy, M. G. (2001). Computer modeling and simulation of human movement. Annu Rev Biomed Eng 3: 245-273.

Pandy, M. G. and Zajac, F. E. (1991). Optimal muscular coordination strategies for jumping. J Biomech 24: 1-10.

Pandy, M. G.; Zajac, F. E.; Sim, E. and Levine, W. S. (1990). An optimal control model for maximum-height human jumping. J Biomech 23: 1185-1198.

Prilutsky, B. I.; Herzog, W. and Leonard, T. (1996). Tranfer of mechanical energy between ankle and knee joints by gastrocnemius and plantaris muscles during cat locomotion. Journal of Biomechanics 29: 391-403.

Prilutsky, B. I. and Zatsiorsky, V. M. (1994). Tendon action of two-joint muscles: transfer of mechanical energy betwee joints during jumping, landing and running. Journal of Biomechanics 27: 25-34.
Proske, U. and Morgan, D. L. (1987). Tendon stiffness: methods of measurement and significance for the control of movement. A review. J Biomech 20: 75-82.
Rack, P. M. and Westbury, D. R. (1974). The short range stiffness of active mammalian muscle and its effect on mechanical properties. J Physiol 240: 331-350.
Rack, P. M. and Westbury, D. R. (1984). Elastic properties of the cat soleus tendon and their functional importance. J Physiol 347: 479-495.
Rainoldi, A.; Nazzaro, M.; Merletti, R.; Farina, D.; Caruso, I. and Gaudenti, S. (2000). Geometrical factors in surface EMG of the vastus medialis and lateralis muscles. J Electromyogr Kinesiol 10: 327-336.
Rassier, D. E.; MacIntosh, B. R. and Herzog, W. (1999). Length dependence of active force production in skeletal muscle. J Appl Physiol 86: 1445-1457.
Reeves, N. D.; Maganaris, C. N. and Narici, M. V. (2004). Ultrasonographic assessment of human skeletal muscle size. Eur J Appl Physiol 91: 116-118.
Reeves, N. D.; Narici, M. V. and Maganaris, C. N. (2003). Strength training alters the viscoelastic properties of tendons in elderly humans. Muscle Nerve 28: 74-81.
Roberts, T. J. (2002). The integrated function of muscles and tendons during locomotion. Comp Biochem Physiol A Mol Integr Physiol 133: 1087-1099.
Roberts, T. J.; Marsh, R. L.; Weyand, P. G. and Taylor, C. R. (1997). Muscular force in running turkeys: the economy of minimizing work. Science 275: 1113-1115.
Salmons, S. (1969). The 8th International Conference on Medical and Biomechanical Engineering - meeting report. Bio Med Eng. pp. 467-474.
Scott, S. H. and Loeb, G. E. (1995). Mechanical properties of aponeurosis and tendon of the cat soleus muscle during whole-muscle isometric contractions. J Morphol 224: 73-86.
Shorten, M. R. (1987). Muscle Elasticity and Human Performance. Med Sport Sci 25: 1-18.
Sidles, J. A.; Clark, J. M. and Garbini, J. L. (1991). A geometric theory of the equilibrium mechanics of fibers in ligaments and tendons. J Biomech 24: 943-949.
Sinkjaer, T. (1997). Muscle, reflex and central components in the control of the ankle joint in healthy and spastic man. Acta Neurol Scand Suppl 170: 1-28.
Soma, C. A. and Mandelbaum, B. R. (1994). Achilles tendon disorders. Clin Sports Med 13: 811-823.
Stefanyshyn, D. J. and Nigg, B. M. (1998). Contribution of the lower extremity joints to mechanical energy in running vertical jumps and running long jumps. J Sports Sci 16: 177-186.
Stein, R.; Zehr, P. E. and Bobet, J. (2000). Basic Concepts of Movement Control. In: Nigg, B., Macintosh, B., Mester, J. (eds) Biomechanics and Biology of Movement. Human -Kinetics, pp. 163-178.
van Ingen Schenau, G. J. (1989). From rotation to translation: constraints on multi-joint movements and the unique action of bi-articular muscles. Human Movement Science 8: 301-337.
van Ingen Schenau, G. J.; Bobbert, M. F. and Haan, A. (1997). Does elastic energy enhance work and efficiency in the stretch-shortening cycle? Journal of Applied Biomechanics 13: 389-415.
van Ingen Schenau, G. J.; Bobbert, M. F.; Huijing, P. A. and Woittiez, R. D. (1985). The instantaneous torque-angular velocity relation in plantar flexion during jumping. Med Sci Sports Exerc 17: 422-426.
van Ingen Schenau, G. J.; Bobbert, M. F. and Rozendal, R. H. (1987). The unique action of bi-articular muscles in complex movements. J Anat 155: 1-5.

van Ingen Schenau, G. J.; Bobbert, M. F. and van Soest, A. J. (1990). The unique action of bi-articular muscles in leg extensions In: Winters, J. M., Woo, S. L. (eds) Multiple Muscle System. Springer, New York, pp. 639-352.

van Ingen Schenau, G. J. and Cavanagh, P. R. (1990). Power equations in endurance sports. J Biomech 23: 865-881.

van Soest, A. J.; Schwab, A. L.; Bobbert, M. F. and van Ingen Schenau, G. J. (1993). The influence of the biarticularity of the gastrocnemius muscle on vertical-jumping achievement. J Biomech 26: 1-8.

Veloso, A. P. and Abrantes, J. (1991). Concepção Geral de Um Modelo Biomecânico e Sua Aplicação Específica a Duas Situações de Corrida. Motricidade Humana 6: 179-189.

Voigt, M.; Dyhre-Poulsen, P. and Simonsen, E. B. (1998). Modulation of short latency stretch reflexes during human hopping. Acta Physiol Scand 163: 181-194.

Walmsley, B.; Hodgson, J. A. and Burke, R. E. (1978). Forces produced by medial gastrocnemius and soleus muscles during locomotion in freely moving cats. J Neurophysiol 41: 1203-1216.

Walshe, A. D. and Wilson, G. J. (1997). The influence of musculotendinous stiffness on drop jump performance. Can J Appl Physiol 22: 117-132.

Walshe, A. D.; Wilson, G. J. and Ettema, G. J. (1998). Stretch-shorten cycle compared with isometric preload: contributions to enhanced muscular performance. J Appl Physiol 84: 97-106.

Wang, K.; McClure, J. and Tu, A. (1979). Titin: major myofibrillar components of striated muscle. Proc Natl Acad Sci U S A 76: 3698-3702.

Wells, R. P. (1981). The projection of the ground reaction force as a predictor of internal joint moments. Bull Prosthet Res 10-35: 15-19.

Wickiewicz, T. L.; Roy, R. R.; Powel, P. L.; Perrine, J. J. and Edgerton, V. R. (1984). Muscle Architecture and Force-Velocity Relationships in Humans. Journal of Applied Physiol 57: 435-443.

Winter, D. A. (1990). Biomechanics and motor control of human movement. Jonh Willey & Sons, New York.

Winter, D. A. (1991). The biomechanics and motor control of human gait: normal, elderly and pathological. Waterloo Biomechanics, Waterloo.

Winters, J. M. (1990). Hill-Based Muscle Models: A Systems Enginnering Perspective. In: Winters, J. M., Woo, S. L.-Y. (eds) Multiple Muscle SystemsBiomechanics and Movement Organization. Springer-Verlag, New York, pp. 69-93.

Woods, J. J. and Bigland-Ritchie, B. (1983). Linear and non-linear surface EMG/force relationships in human muscles. An anatomical/functional argument for the existence of both. Am J Phys Med 62: 287-299.

Yamaguchi, G. T.; Sawa, A. G. U.; Morgan, D. W.; Fessler, M. J. and Winters, M. (1990). A survey of human musculotendon actuator parameters. In: Woo, J. M. W. a. S. L.-Y. (ed) Multiple Muscle Systems: Biomechanics and Movement Organization. Springer-Verlag, New York, pp. 717-773.

Yang, J. F.; Stein, R. B. and James, K. B. (1991). Contribution of peripheral afferents to the activation of the soleus muscle during walking in humans. Exp Brain Res 87: 679-687.

Yeadon, M. R.; Atha, J. and Hales, F. D. (1990). The simulation of aerial movement--IV. A computer simulation model. J Biomech 23: 85-89.

Young, M.; Paul, A.; Rodda, J.; Duxson, M. and Sheard, P. (2000). Examination of intrafascicular muscle fiber terminations: implications for tension delivery in series-fibered muscles. J Morphol 245: 130-145.

Zahalak, G. I. (1990). Modeling Muscle Mechanics (and Energetics). In: Woo, J. M. W. a. S. L.-Y. (ed) Multiple Muscle SystemsBiomechanics and Movement Organization. Springer-Verlag, New York, pp. 1-23.

Zahalak, G. I. and Ma, S. P. (1990). Muscle activation and contraction: constitutive relations based directly on cross-bridge kinetics. J Biomech Eng 112: 52-62.

Zajac, F. E. (1989). Muscle and tendon: properties, models, scaling, and application to biomechanics and motor control. Crit Rev Biomed Eng 17: 359-411.

Zajac, F. E. (1993). Muscle coordination of movement: a perspective. J Biomech 26 Suppl 1: 109-124.

Chapter 3

Force, Articular Moment and Mechanical Power in Elementary Ballet Jumps

3.1 Introduction

The purpose of this first study was to access the internal dynamics of some balletic movements, e.g. the internal knee and ankle loads and their potential for injury.

The most attractive tool for accessing internal loads is the inverse dynamics technique (Cluss et al., 2006; Simpson and Kanter, 1997; Simpson and Pettit, 1997). It is a non-invasive technique, and in this kind of population, can even be used in a live performance if the stage or the shoes are well instrumented.

Unfortunately with this technique it's difficult to include the cocontraction effects. In this first study we try to evaluate its importance and introduce the effects of cocontractions in the inverse dynamics algorithm.

In biomechanics it's usually assumed the human body as a chain of a few rigid bodies (Winter, 1980). It is possible to videograph the body and acquires the spatial coordinates of the articular points (r_i) by offline digitalisation (manual or automated). Simultaneously the external forces (F_{ext}) and moments (M_{ext}) acting on the body must be measured. Then, the successive solution of the Newton-Euler equations gives us the net forces acting in each segment or rigid body. For the k segment, with mass m_k, moment of inertia I_k, location of centre of mass r_k, and angular position θ_k, the relevant equations are:

$$\sum_j \vec{F}_j = m_k \ddot{\vec{r}}_k \tag{3.1}$$

$$\sum_j \vec{M}_j = I_k \ddot{\vec{\theta}}_k \tag{3.2}$$

The main problems using the inverse dynamics approach are:

- the numerical derivatives of kinematical data can be a source of error much larger than all the others.
- the usual filtering or smoothing schemes distort real short-timed events as the ground contact in a drop jump.

3.2. The Study

An initial study, to access the applicability of this tool to classical ballet was executed and firstly published as:

"Force, Articular Moment and Mechanical Power in Elementary Ballet Jumps"

Sousa F[1], Loss J[2], Soares D[2], Scarrone F[2], Carvalho JM[3], Vilas-Boas JP[1] (2001). Force, Articular Moment and Mechanical Power in Elementary Ballet Jumps. In*:* Proceedings of *IX Brazilian Congress of Biomechanics*, pp.143-148. Brazilian Society of Biomechanics, Federal University of Rio Grande do Sul, Gramado, Brazil.

[1] Laboratory of Biomechanics, Faculty of Sports, University of Porto, Portugal.

[2] Laboratory of Research on Exercise, Physical Education School, Federal University of Rio Grande do Sul, Brazil.

[3] Department of Physic, Faculty of Engineering, University of Porto, Portugal.

Abstract

The purpose of the present study was to present a methodology to assess the dynamical study of the lower limb in different elementary ballet jumps using an inverse dynamics method. Muscle mechanical power, joint forces and moments were computed. Two ballet dancers with more than ten years of experience performed 3 trials of 3 different jumps. Performances were videotaped for 2D analysis (Peak 5 System) and reaction forces data were recorded using a force plate. The intra-coherence of the results showed that the methodology seems appropriated for the biomechanical analysis of ballet jumps, and allow to differentiate techniques.

Key Words: biomechanics, inverse dynamics, joint force, joint moment, muscle mechanical power, ballet jumps.

Introduction

Injuries of the lower extremities are very frequent among dancers (classical ballet, modern dance, jazz, etc.) (Grego et al., 1999; Hardaker et al., 1985; Schneider et al., 1974). Approximately 86% of these injuries are reported to ballet dancers and have especial incidence in the lower limb. According to some authors, the majority of these injuries are

chronic (Hardaker and Erickson, 1987; Hardaker et al., 1985; Simpson and Kanter, 1997; Simpson and Pettit, 1997), being 64% of these injuries induced from microtraumatic overuse injuries, determining the typical stress at which the anatomical structures (especially the foot and ankle) are submitted in classical ballet.

In classical ballet, the jumps are one of the most important and usual elements that compose each training practice and each custom performance, being repeated constantly during the whole life of a dancer. In sport science it is well demonstrated that the magnitude of forces produced during some jump performances can exceed largely the subject's body mass (Amadio and Duarte, 1996). On the other hand, in dance, some studies confirm a relationship between the amplitude and the magnitude of articular forces during jumps, as well as recognize the potential damage consequences to the tissues involved in its dissipation (Simpson and Kanter, 1997; Simpson and Pettit, 1997).

In classical ballet, due to the nature of movements, which involves in its majority great unusual amplitudes of movement, articular positions, and muscular efforts with excessive impact forces, it's understandable to recognize a significant degeneration of the anatomical structures, like bone tissue, tendons, ligaments, and others (Amadio et al., 2000; Simpson and Kanter, 1997; Simpson and Pettit, 1997). The amount of articular moment produced and the reduced contact area of the patella-femoral joint, induces substantial gradients of force, and at the same time, the weakness and exposure of the structures to injuries (Clippinger-Robertson et al., 1986). According to Simpson and Pettit (1997), the repetitive axial and shear forces, in combination with the rapidly of applied loading, that occurs especially during dance movements, is involved in the etiology of injuries, namely the osteoarthritis, very characteristic and common in dancers. According to Hardaker et al. (1985), the deficient technique of dancers can also influence resulting injury potential. Chronic dance injuries have been, although, associated to improper landing techniques (Gans, 1985).

The knowledge of the magnitude and rate of forces application involved in dance movements is determinant not only in the prevention of injuries, but also in the optimization of technique, in order to create more safely, graceful and imposing movements (Picon et al., 2000).

The assessment of *in vivo* internal forces is especially difficult in biomechanics. The direct measurement of forces is virtually impossible without invasive methods. In this way, the availability of non invasive techniques, even being indirect, can represent a significant contribution to the progress of knowledge in the scientific domain in question. The inverse dynamics is a promising tool that provides the quantification of internal forces, through the knowledge of the remaining involved forces, as well as the acceleration of the body.

The purpose of the present study was to explore a methodology to assess the dynamical of the lower limb in different elementary ballet jumps using an inverse dynamics approach. Muscle mechanical power, joint forces and moments were computed.

Methods

The inverse dynamics approach was used to estimate the joint force, moments and mechanical power of the right lower limb, assuming a bidimensional model with tree rigid segments representing the thigh, shank and foot (Loss, 2001). The forces and internal moments acting on distal part of the segment S_i will be obtained following the equations:

$$F_{Pix} + F_{Dix} = m_i a_x \tag{3.3}$$

$$F_{Piy} + F_{Diy} - m_i g = m_i a_y \tag{3.4}$$

$$M_{Piz} + M_{Diz} + \left(L_D \times F_D\right) + \left(L_P \times F_P\right) = I\ddot{\theta}_i \tag{3.5}$$

where, L_D and L_P represent the lever arms vectors of the intersegmental forces (distal and proximal respectively), and F_{Pix},F_{Piy},F_{Dix}, and F_{Diy} are the x and y components of the resulting forces acting in the proximal and distal extremities, respectively. This last forces are contact forces acting in the extremities of S_i, and due to the presence of adjacent body segments, include the compressive effects of neighbouring structures, such articular and bone tissues, as well as the tensions developed by muscles and ligaments.

Reducing the movement and considering it as occurring in only one plane, besides the kinematics, anthropometric data and ground reaction forces at the distal end of the distal segment, it is known:

$a_x, a_y =$ acceleration of the segment centre of mass

$\ddot{\theta}_i$ = angular acceleration of the segment in the plane of movement α=

R_{xd}, R_{yd} = reaction forces acting at the distal end of the segment

M_{Diz} = net muscle moment acting at the distal joint

It is unknown:

R_{xp}, R_{yp} = reaction forces acting at the proximal joint

M_{Piz} = net muscle moment acting on the segment at the proximal joint

Experimental Protocol

The jumps were recorded in videotape, at 120 images per second, and later digitized with the Peak-5 analysis system (Peak Performance Technologies, Inc.). The video camera optical axis was perpendicular to the plane of movement analysis. The body segments (thigh, shank and foot) were delimited through the anatomical articular surfaces: (a) *trochanter* major, (b) lateral *epicondile* of the *femur*, (c) lateral *maleolus* and (d) fifth *metatarsus* head. The ground reaction forces were measured with an AMTI force plate, with a sample frequency of 500 Hz. The anthropometric variables mass, centre of mass and moment of inertia of each segment, were obtained from the table of Clauser et al. (1969). An electronic pulse from Peak Performance System was used to synchronize all the acquisition systems.

To illustrate the application of the proposed method, two ballet dancers with more than ten years of practice were selected (one with 25 years old, 54 kg of body mass and 1.58 m height, and the other with 24 years old, 43 kg of body mass and 1.54 m height).

Three basic typical jumps from classical ballet were selected:
Jump1 - *sauté* in first position; Jump 2 - *sauté* in fifth position; and Jump 3 - *sauté en cou-de-pied*,

After the warm-up exercises, selected individually by each dancer, a session of familiarization with the procedures for the data collection started. The jumps were

performed in a way so that the analyzed limb moved predominantly in the perpendicular plane of a video camera optical axis.

The first tree jumps (Jump1 - *sauté* in first position -, Jump 2 - *sauté* in fifth position - and Jump 3 - *sauté en cou-de-pied*) were executed individually by each dancer, in tree blocks of five successive repetitions, always with the landing and take-off phases of the jumps above the force plate. The jumps were executed in a random order.

Results and Discussion

In figure 3.1, it's possible to observe a representative example of estimated values of articular force (a), net moment (b), and mechanical power (c), in the knee joint, during the execution of a block of five consecutive *sautés* in first position (jump 1).

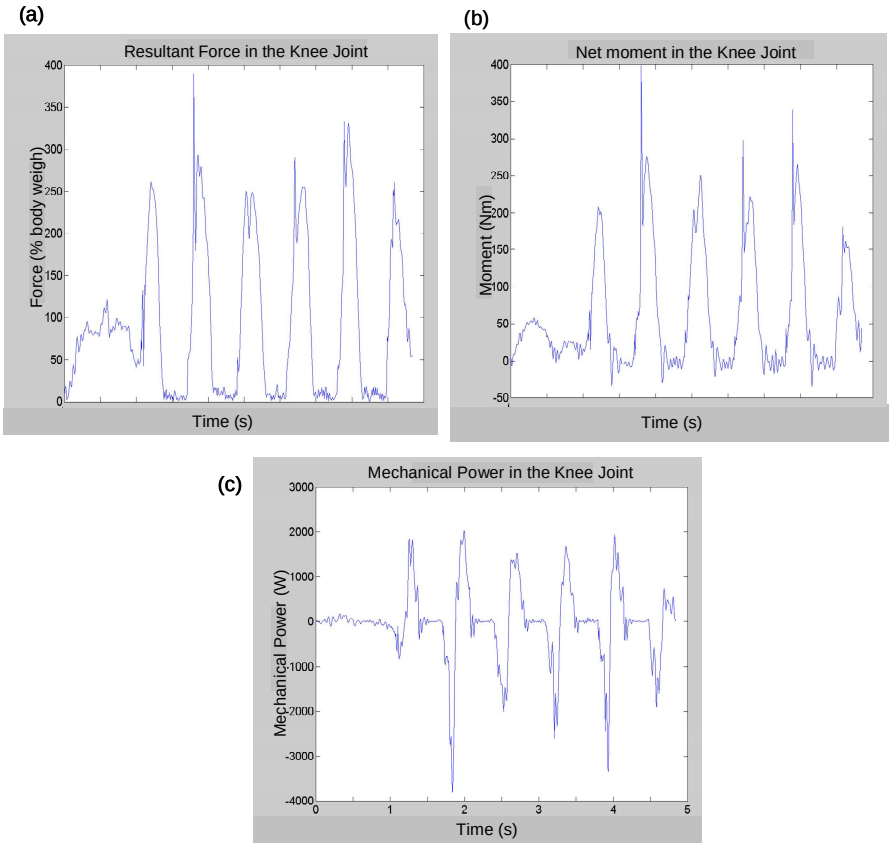

Figure 3.1. Estimated values of articular force (a), moment (b) and mechanical power (c), in the knee joint, during five consecutive *sautés* in first position (Jump 1).

Based on the articular force peak values and time duration of the jumps (figure 3.1(a)), it is possible to observe a similar execution pattern during the successive five repetitions of the jump. Although this is only a representative example, the same pattern was observed in all attempts from all jumps, and in both subjects, demonstrating a high consistence of the averaged results obtained to the peak values of articular force. This force is the intra-articular contact force between segments, which is the result of the ground reaction force applied to the lower limb and is propagated throughout the body segment.

In this example, the instant in time in which a maximum flexion of the lower limb was assumed, correspond to the landing phase after the jump, instant at which the articular moment is maximum, and the mechanical power is null (angular velocity is zero) .

When we develop in the analysis from proximal to more distal articular joints, it is possible to observe an increase in the noise associated to the results. This is due to an increase dependency, from forces and moments, in the precise calculation of acceleration. Besides, eventual non intentional movements out of the plane, ignored in the bidimensional analysis, can also contribute to this effect.

Figure 3.2 presents the peak average values from articular force, in relation to body weight, from each subject (A and B), in ankle, knee and hip joints, during the execution of the three jumps selected. As expected, the peak of articular force decrease, comparing the ankle with the knee joint, and the knee with the hip joint, in every the three jumps of both ballerinas. This decrease of force from one joint to another joint is imputable to the occurrence of absorption phenomenons induced by the body tissues.

In relation to the magnitude of peak values from of articular force, it is possible to observe that in the Jump 3, the values obtained are in order of 3 times the body weight. Because during each training practice and each custom performance, the dancers constantly repeat these jumps, the incidence of overload injuries becomes more pronounced (Amadio and Duarte, 1996; Simpson and Kanter, 1997; Simpson and Pettit, 1997).

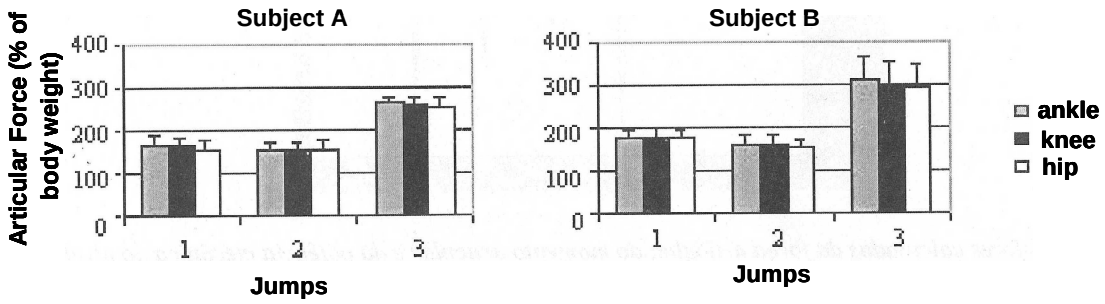

Figure 3.2. Mean and standard deviation values from peak articular force estimated in the ankle, knee and hip joints from each subject (A and B), during the three different jumps.

Figure 3.3 presents the values of the integral average of articular force, in relation to the body weight from each of the two subjects, in the ankle, knee and hip joints, during the execution of the five jumps selected.

As it's possible to observe in figure 3.3, the integral average values of articular force, as expected, decreases from the ankle to the knee joint, and from the knee to the hip joint, in the five jumps selected, and in both subjects. This decrease in the force values from one joint to another is due to the fact that a small quantity of mass acting in each joint is more and more smaller as proximal is the segment.

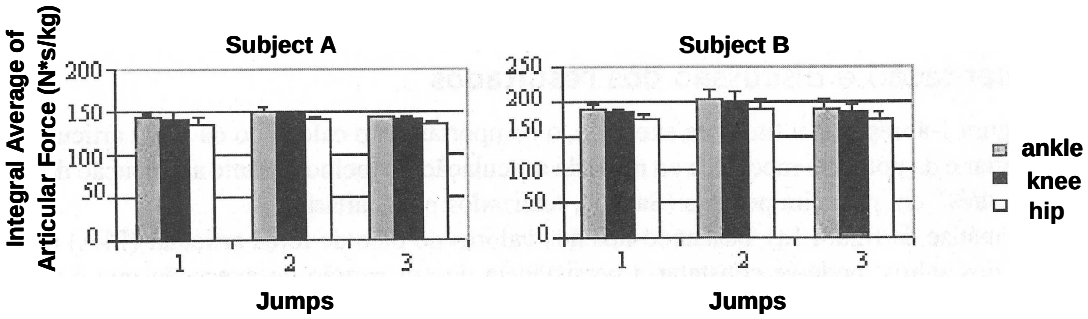

Figure 3.3. Mean and standard deviation values from integral articular force estimated in the ankle, knee and hip joints from each subject (A and B).

Figure 3.4 presents the values of the integral average of articular moment, in relation to the body weight, from each of the two subjects, in the ankle, knee and hip joints, during the execution of the three jumps selected.

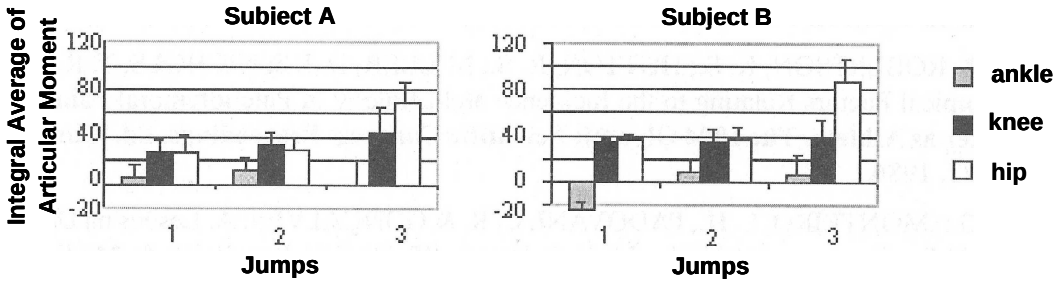

Figure 3.4. Mean and standard deviation values from integral articular moment estimated in the ankle, knee and hip joints from each subject (A and B).

Taking into account that articular moments are related with muscular activity from agonist and antagonist muscles, it is possible to observe, in the last figure, that both subjects used different strategies in the performance of the jumps. For example in the jump 1, the subject A uses in the performance of the jump, extensor musculature in the ankle, knee and hip joints. Nevertheless, the subject B, in the same jump, uses flexor musculature in the ankle joint, and for this reason, need more activity from extensor musculature in the knee and hip, to perform the same jump.

Figure 3.5 presents the peak average values from muscular mechanical work in the knee joint, from each of the two subjects, during the execution of the three jumps selected. The muscular mechanical work was not calculated in the hip joint, because the trunk was not included in the initial model. The amplitude of ankle flexions was so small, very susceptible to digitizing errors, that the muscular mechanical work was also not calculated.

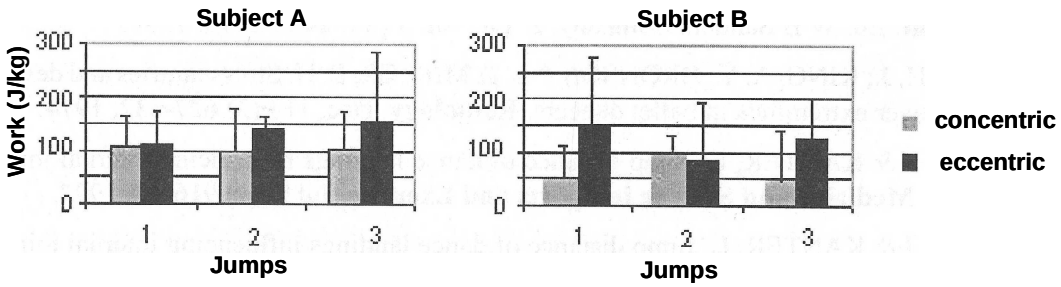

Figure 3.5. Mean and standard deviation values from muscular mechanical work (concentric and eccentric), estimated in the ankle and knee joints from each subject (A and B).

Figure 3.5 shows, almost in a systematic way that the eccentric work is higher than the concentric work. This difference is only possible due to the balance movements from other body segments that for several reasons were more intense in the take off phase of the jump than in the landing.

Conclusions

The estimated results obtained in this study, using the inverse dynamics approach to calculate the forces and articular moments, as well as the muscular mechanical power, showed a high internal coherence, and an individual persistence to point out.

Complementarily, the results obtained are according to theoretical expectations, suggesting that this methodology is adequate to the problem approached.

Through the analysis of the magnitude of the peak values from articular force estimated, it is possible to observe that, in some jumps, the values of forces are of the order of three times the body weight, showing the high injury potential that the anatomical structures of ballet dancers are exposed to.

The evaluation of movement in terms of moments and power, allow a better and new comprehension about the individual strategies of movement performance, occasionally allowing a technical intervention, helping in the improvement of the performance.

The knowledge of intra articular forces, particularly in this activity and also in many others, is very important to the understanding of the risks of injury associated to repetitive efforts and his eventual prevention.

3.3. Next Goals

Improve the precision of the kinematical data by the simultaneous use of video redundancy and accelerometers.

Wavelet denoising techniques support short and long timed events properly, so it is a promising tool. Also Splines and Padè approximants are able to describe both smooth and non-differentiable curves, and we are testing their applicability.

3.4. References:

Amadio, A. C. and Duarte, M. (1996). Fundamentos biomecanicos para a analise do movimento. EEF-USP, Laboratório de Biomecânica, Sao Paulo.

Amadio, A. C.; Sacco, I. C.; Lobo da Costa, P. H.; Picon, A. P. and Sousa, F. (2000). Peak plantar pressure during ballet movements: a preliminary study. Emed Scientific Millennium Meeting, Münich, Germany, p. 27.

Clauser, C. E.; Mcconville, J. T. and Young, J. W. (1969). Weight, volume and center of mass of segments of the human body. AMRL Technical Report, Wright-Patterson Air Force Base, Ohio.

Clippinger-Robertson, K. S.; Hutton, R. S.; Miller, D. I. and Nichols, T. R. (1986). Mechanical and Anatomical Factors Relating to the Incidence and Etiology of Patellofemoral Pain in Dancers. In: Shell, C. G. (ed) The Dancer as Athlete - The 1984 Olympic Scientific Congress Proceedings. Human Kinetics Publishers, Champaing, Illinois, pp. 53-72.

Cluss, M.; Laws, K.; Martin, N. and nNowicki, S. (2006). The indirect measurement of biomechanical forces in the moving human body. Am J Phys 74: 102-108.

Gans, A. (1985). The relationship of heel contact in ascent and descent from jumps to the incidence of shin splints in ballet dancers. Phys Ther 65: 1192-1196.

Grego, L. G.; Monteiro, H. L.; Padovani, C. R. and Gonçalves, A. (1999). Lesões na dança: estrudo transversal híbrido em academias da cidade de Bauru-SP. Revista Brasileira de medicina do Esporte 5: 47-54.

Hardaker, W. T., Jr. and Erickson, L. C. (1987). Medical considerations in dance training for children. Am Fam Physician 35: 93-99.

Hardaker, W. T., Jr.; Margello, S. and Goldner, J. L. (1985). Foot and ankle injuries in theatrical dancers. Foot Ankle 6: 59-69.

Loss, J. F. (2001). Efeitos de Parâmetros Inerciais Obtidos Através de Diferentes Procedimentos na Determinação de Forças e Torques Articulares Resultantes. Engenharia Mecânica. Universidade Federal do Rio Grande do Sul, Porto Alegre

Picon, A. P.; Lobo da Costa, P. H.; Sousa, F.; Sacco, I. C. N. and Amadio, A. C. (2000). Biomechanical approach to ballet movements: a preliminary study. XVIII International Symposium on Biomechanics in Sports, Hong Kong, pp. 472-475.

Schneider, H. J.; King, A. Y.; Bronson, J. L. and Miller, E. H. (1974). Stress injuries and developmental change of lower extremities in ballet dancers. Radiology 113: 627-632.

Simpson, K. J. and Kanter, L. (1997). Jump distance of dance landings influencing internal joint forces: I. Axial forces. Med Sci Sports Exerc 29: 916-927.

Simpson, K. J. and Pettit, M. (1997). Jump distance of dance landings influencing internal joint forces: II. Shear forces. Med Sci Sports Exerc 29: 928-936.

Winter, D. A. (1980). Biomechanics of Human Movements. Wiley, New York.

Chapter 4

Biomechanical Analysis of Elementary Ballet Jumps: Integration of Force Plate Data and EMG Records

4.1. Introduction

Even if an inverse dynamics scheme could provide exact net torques, these are needed to be decomposed in the various muscular contributions. There is the necessity to consider co-contractions in mono and bi-articular muscles, etc. This can't be done easily as there are more variables than equations (Collins, 1995). There are two main possible approaches facing this indeterminacy problem:

a) Optimization of some function as energy, stress, or some other performance indicator (Herzog and Binding, 1993). Optimization techniques are comparatively easy to use but the optimization function is not known and probably it's not unique. For ballet movements this function probably it's not energy or stress minimization. Also there is no way of roughly accessing the "quality" of the results.

b) Use of electromyography (EMG) data to estimate muscle contribution (Lloyd and Besier, 2003; Lloyd and Buchanan, 2001; McGill, 1992). EMG driven muscular force prediction is not very precise as it depends on the physiological model (Hill, activation, etc.). This direct dynamic tool must be combined with the inverse dynamics to estimate the muscular loads. The process of fitting both approaches involves a previous step of optimization to obtain the individual activation parameters.

4.2. The Study

In a second exploratory analysis, using EMG data, we tried to access the importance of co-contractions in our ballet movements. This second study was firstly published as:

"Biomechanical Analysis of Elementary Ballet Jumps: Integration of Force Plate Data and EMG Records"

Sousa F[1], Conceição F[1], Gonçalves P[1], Carvalho JM[3], Soares D[2], Scarrone F[2], Loss J[2], Vilas-Boas JP[1] (2002). Biomechanical analysis of elementary ballet jumps: integration of force plate and EMG records. In: Gianilelis, K. E. (ed.), Proceedings of XX *International Symposium on Biomechanics in Sports*, pp, 175-178. Faculty of Sport Sciences, Universidad de Extremadura, Cáceres.

[1] Laboratory of Biomechanics, Faculty of Sports, University of Porto, Portugal.

[2] Laboratory of Research on Exercise, Physical Education School, Federal University of Rio Grande do Sul, Brazil.

[3] Department of Physic, Faculty of Engineering, University of Porto, Portugal.

Abstract

The purpose of this research was to analyse the electromyographic (EMG) activity, ground reaction force and muscular behaviour (concentric, isometric or eccentric) of the lower limb during elementary ballet jumps: *sauté* in first position, *sauté* in fifth position, and *sauté en cou de pié*. The present study evaluated one experienced female *ballet* dancer with no relevant clinical history. She performed three trials, of each three different jumps. Results were considered as mean values of the three trials for each jump. Kinematical and dynamical data were obtained from video and a force plate in the usual setup. Electromyographic data were collected using active surface electrodes, placed over eight muscles on the right side of the lower limb: *adductors*, *gluteus maximus*, *rectus femoris*, hamstrings, *tibialis anterior*, *peronaeus*, medial *gastrocnemius* and *soleus*. Electromyographic records were smoothed (RMS envelope) and presented as a percentage of the maximum voluntary isometric contraction (%MVC). Muscular contraction velocities were calculated by deriving the relative muscular length, obtained from kinematical data using the expressions from Hawkins and Hull (1990). Results pointed out the existence of important pre-activation and co-contractions that needs to be taken into account in future inverse dynamic studies of ballet movements.

Key Words: EMG, Dynamometry, Ballet

Introduction

The assessment of internal forces in general Biomechanics, as well as in sport Biomechanics, remains a very difficult task, and a main topic of interest. The evaluation of internal forces, meanwhile, is determinant for the understanding of mechanical stress of biomaterials and injuries (Simpson and Kanter, 1997; Simpson and Pettit, 1997). Equally important for this purpose is the knowledge of muscular activity (Trepman et al., 1998; Trepman et al., 1994), specially if related with internal and/or external forces. The purpose of this research was to analyze the electromyographic (EMG) activity, ground reaction force and muscular behaviour (concentric, isometric or eccentric) of the lower limb during elementary ballet jumps.

Methods

The present study evaluated one experienced female *ballet* dancer (25 years old, 54 kg, 158 cm) with no relevant clinical history. She performed three trials, of three different *ballet* jumps referred as 1, 2 and 3: *sauté* in first position, *sauté* in fifth position, and *sauté en cou de pié*. Results were considered as mean values of the three trials for each jump.

Vertical ground reaction force was recorded using an AMTI force plate sampled at 500Hz. The forces were presented in percentage of body weight.

Electromyographic data were collected using active surface electrodes, placed over eight muscles on the right side of the lower limb: *adductors*, *gluteus maximus*, *rectus femoris*, hamstrings, *tibialis* anterior, *peronaeus*, medial *gastrocnemius* and *soleus*. Electromyographic records were smoothed (RMS envelope) and presented as a percentage of the EMG obtained during a maximum voluntary isometric contraction (%MVC). The isometric condition was ensured by constraining the relevant joint movements.

The jumps were recorded in videotape, at 120 images per second, and later digitized in the APAS Ariel system (Ariel Performance Analysis System, USA). Muscular contraction velocities were calculated by differentiation the relative muscular length, obtained from kinematical data using the expressions from the model of Hawkins and Hull (1990):

$$L = C0 + C1\alpha + C2\beta + C3\beta^2 + C4\phi \qquad (4.1)$$

where, L represents the normalized muscle length, $C0$ to $C4$ the regression coefficients, and $\alpha, \beta,$ and ϕ, the hip, knee and ankle angles respectively, measured in degrees, and obtained from kinematical data. The normalized muscle length and regression coefficients were obtained in the table 1 and table 2 of the study of Hawkins and Hull (1990), only possible to *rectus femoris*, hamstrings, *tibialis* anterior, medial *gastrocnemius* and *soleus* muscles. No data from adductors, *gluteos maximum* and *peroneaus* muscles are available in the model.

Results and Discussion

The main results of the study are summarized in Tables 4.1 to 4.4. They exhibit the maximum relative ground reaction force on the landing [Fz(land)] and take off phases [Fz(to)] and the maximum EMG records on the landing [%mvc(land)] and take-off phases [%mvc(to)]. As these maximums don't occur simultaneously, we also report the difference between those two instants [dt(land)] and [dt(to)], where a positive value means that the maximum EMG activity occurs before the maximum ground reaction force. Note that the maximum voluntary isometric contraction for the *soleus* was, most probably, incorrectly executed, because the values are very different with comparison from the other muscles. Additionally we report the relative muscle contraction velocity at the same time that the maximum EMG record occurs. This allows the identification of the contraction regime (eccentric, isometric or concentric).

Table 4.1. Results on the time duration (dt), EMG records as percentage of maximal voluntary contraction (%MVC), and estimations of relative muscular contraction velocity (Veloc) of the landing phase (land) and the take-off (to) phase obtained during the *sauté* in first position (jump 1).

	dt(land) s	dt(to) s	MVC (land) %	MVC (to) %	Veloc (land) m/s	Veloc (to) m/s
Adductors	0.02	-0.02	0.94	0.95	---	---
Gluteos Maximus	0.01	0.04	0.29	0.36	---	---
Rectus Femoris	0.02	0.01	1.13	1.12	0.29	0.11
Hamstrings	0.00	0.01	0.40	0.59	-0.25	-0.05
Tibialis Anterior	-0.05	-0.01	0.51	0.42	0.12	-0.06
Peroneaus	0.05	0.05	0.67	0.91	---	---
Medial Gastrocnémius	0.03	0.04	0.81	0.80	-0.16	0.08
Soleus	0.04	0.03	3.82	4.11	-0.06	0.06

Table 4.2. Results on the time duration (dt), EMG records as percentage of maximal voluntary contraction (%MVC), and estimations of relative muscular contraction velocity (Veloc) of the landing phase (land) and the take-off (to) phase obtained during the *sauté* in fifth position (jump 2).

	dt(land) s	dt(to) s	MVC (land) %	MVC (to) %	Veloc (land) m/s	Veloc (to) m/s
Adductors	0.00	-0.01	1.03	0.94	---	---
Gluteos Maximus	-0.02	0.02	0.35	0.40	---	---
Rectus Femoris	0.00	0.02	0.97	0.94	-0.04	0.05
Hamstrings	-0.04	0.04	0.55	0.49	-0.03	-0.09
Tibialis Anterior	-0.07	0.04	0.43	0.29	-0.06	0.07
Peroneaus	0.02	0.08	0.81	0.85	---	---
Medial Gastrocnémius	0.02	0.09	0.82	1.18	0.00	-0.01
Soleus	0.01	0.03	3.64	4.22	0.03	-0.04

Table 4.3. Results on the time duration (dt), EMG records as percentage of maximal voluntary contraction (%MVC), and estimations of relative muscular contraction velocity (Veloc) of the landing phase (land) and the take-off (to) phase obtained during the *sauté en cou de pié* (jump 3).

	dt(land) s	dt(to) s	MVC (land) %	MVC (to) %	Veloc (land) m/s	Veloc (to) m/s
Adductors	0.00	0.01	0.89	0.90	---	---
Gluteos Maximus	-0.04	0.01	0.66	0.79	---	---
Rectus Femoris	0.00	0.01	1.05	1.28	0.01	-0.03
Hamstrings	-0.06	-0.04	0.40	0.40	0.12	0.21
Tibialis Anterior	-0.06	0.03	0.53	0.27	0.00	0.06
Peroneaus	0.02	0.05	0.50	0.71	---	---
Medial Gastrocnémius	0.01	0.03	0.86	1.05	0.04	-0.18
Soleus	0.03	0.04	3.31	4.13	-0.01	-0.10

Table 4.4. Relative ground reaction force on the landing [Fz(land)] and take off phases [Fz(to)].

	Jump 1	Jump 2	Jump 3
Fz (land)	3.54	3.11	2.63
Fz (to)	3.04	3.00	2.58

Although the EMG activation sequence varies from jump to jump (it is very dependent on the technique), a pre-activation or increased activity just before ground contact is visible (Figure 4.1).

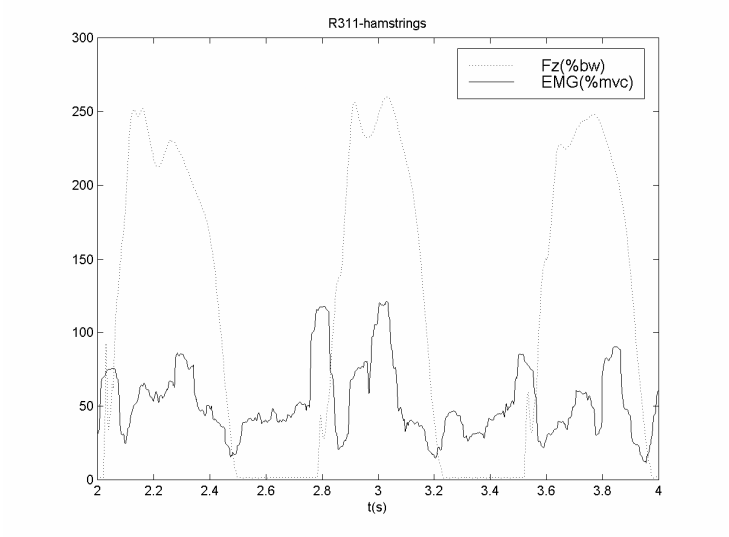

Figure 4.1. Example of synchronized records of ground reaction forces (Fz), presented in percentage of body weight, and EMG activity, as a percentage of maximal voluntary contraction, of the hamstrings during the first trial of the third jump (*sauté en cou de pié*).

The main EMG activity occurs in the *adductors*, *rectus femoris* and medial *gastrocnemius*. From the delay analysis, it is apparent the co-activation of the *adductors* and *rectus femoris*. A cross-correlation of the EMG records of these muscles is summarized on table 4.5.

Table 4.5. Cross-correlation between EMG records from *adductors* and *rectus femoris*

	Jump 1/ exec.1	Jump 1/ exec 2	Jump 2/ exec.1	Jump 2/ exec.2	Jump 2/ exec.3	Jump 3/ exec 1	Jump 3/ exec 2
Correlation	0.671	0.493	0.358	0.677	0.673	0.662	0.366
Delay (s)	0.07	0.10	0.08	0.10	0.08	0.07	0.10

Although there is a large variability, some jumps show a high correlation between the EMG activity of *adductors* and *rectus femoris*. There is also a large correlation between the *rectus femoris* EMG and the ground reaction force, as can be seen in table 4.6.

Table 4.6. Cross-correlation between EMG from *rectus femoris* and vertical ground reaction force

	Jump 1/ exec.1	Jump 1/ exec 2	Jump 2/ exec.1	Jump 2/ exec.2	Jump 2/ exec.3	Jump 3/ exec 1	Jump 3/ exec 2
Correlation	0.716	0.753	0.801	0.649	0.750	0.863	0.806
Delay (s)	0.20	0.14	0.16	0.14	0.12	0.19	0.18

Also from the delay analysis, it is apparent that the medial *gastrocnemius* and *soleus*, in jumps 1 and 3, work closely. Table 4.7 summarizes the cross-correlation between the EMG records of these two muscles.

Table4.7. Cross-correlation between EMG records from medial *gastrocnemius* and *soleus*

	Jump 1/ exec.1	Jump 1/ exec 2	Jump 2/ exec.1	Jump 2/ exec.2	Jump 2/ exec.3	Jump 3/ exec 1	Jump 3/ exec 2
Correlation	0.802	0.704	0.735	0.694	0.754	0.705	0.694
Delay (s)	0.10	0.12	0.18	0.29	0.21	0.07	0.06

The correlations show that medial *gastrocnemius* and *soleus* have indeed a high correlation in their activity, although with lags varying with the type of jump.

Finally, we noted a negative correlation within the agonist-antagonist pair of muscles, medial *gastrocnemius* and *tibialis anterior* (table 4.8).

Table 4.8. Cross-correlation between EMG records from medial *gastrocnemius* and *tibialis anterior*

	Jump 1/ exec.1	Jump 1/ exec 2	Jump 2/ exec.1	Jump 2/ exec.2	Jump 2/ exec.3	Jump 3/ exec 1	Jump 3/ exec 2
Correlation	-0.466	-0.590	-0.560	-0.503	-0.549	-0.453	-0.224
Delay (s)	0.19	0.18	0.23	0.25	0.28	0.21	0.21

Other correlations have been tried but were found too weak or with lags longer than the contact phase (about 0.3 s).

The above relationship between the medial *gastrocnemius* and *soleus* (*tricepts surae*) and the *tibialis anterior* are also present in the relative contraction velocities (tables 4.1 to 4.3). Whenever the *tricepts surae* is working eccentrically, the *tibialis anterior* is working concentrically, and *vice-versa*. This is not always observed for the pair *rectus femoris/* hamstrings (although it is in co-contraction almost all the time) as they are both multi-joint muscles.

Finally, as it is apparent from the results presented above, there are large variations in all the parameters from execution to execution, as they are very dependent on the technique. However this does not change the qualitative aspects stated above.

Conclusions

Results pointed out the existence of a pre-activation effect before landing in almost all cases.

It can also be concluded from the correlations obtained that co-contractions are intense and should be taken into account during biomechanical analysis of Ballet jumps, namely in an inverse dynamics approach.

We also observed large changes in the recorded parameters from execution to execution, and with simple changes in the jumps performed, making it problematic to generalize the quantitative results. The qualitative conclusions – the existence of important pre-activation and co-contractions -, however, will need to be taken into account in the inverse dynamic studies that will follow.

4.3. Next Goals

Test the applicability of unusual filtering techniques to smooth the kinematical data.

Test either approaches (optimization and EMG) in the context of ballet jumps.
Explore the coordinative and inter-segmentar energy transfer ideas.

4.4. References:

Collins, J. J. (1995). The redundant nature of locomotor optimization laws. J Biomech 28: 251-267.

Hawkins, D. and Hull, M. L. (1990). A method for determining lower extremity muscle-tendon lengths during flexion/extension movements. J Biomech 23: 487-494.

Herzog, W. and Binding, P. (1993). Cocontraction of pairs of antagonistic muscles: analytical solution for planar static nonlinear optimization approaches. Math Biosci 118: 83-95.

Lloyd, D. G. and Besier, T. F. (2003). An EMG-driven musculoskeletal model to estimate muscle forces and knee joint moments in vivo. J Biomech 36: 765-776.

Lloyd, D. G. and Buchanan, T. S. (2001). Strategies of muscular support of varus and valgus isometric loads at the human knee. J Biomech 34: 1257-1267.

McGill, S. M. (1992). A myoelectrically based dynamic three-dimensional model to predict loads on lumbar spine tissues during lateral bending. J Biomech 25: 395-414.

Simpson, K. J. and Kanter, L. (1997). Jump distance of dance landings influencing internal joint forces: I. Axial forces. Med Sci Sports Exerc 29: 916-927.

Simpson, K. J. and Pettit, M. (1997). Jump distance of dance landings influencing internal joint forces: II. Shear forces. Med Sci Sports Exerc 29: 928-936.

Trepman, E.; Gellman, R. E.; Micheli, L. J. and De Luca, C. J. (1998). Electromyographic analysis of grand-plie in ballet and modern dancers. Med Sci Sports Exerc 30: 1708-1720.

Trepman, E.; Gellman, R. E.; Solomon, R.; Murthy, K. R.; Micheli, L. J. and De Luca, C. J. (1994). Electromyographic analysis of standing posture and demi-plie in ballet and modern dancers. Med Sci Sports Exerc 26: 771-782.

Chapter 5

Data Processing and Filtering of Kinematical Signals

5.1. Introduction

All position measurements of a given movement always contain some errors originated by limitations in the technology used and inaccurate measurements due to the subject that collects the data. The systems motion capture currently used in biomechanical analysis introduce measurement errors, that appear in the form of noise in the recorded displacement signals (Alonso et al., 2005; Georgakis et al., 2002). The small measurement errors originated by a motion analysis system are amplified when the derivatives, velocity and acceleration, are calculated.

To minimize such propagating errors, since they may lead to large errors, for example in an inverse dynamics approach, it is necessary to filtering and smoothing the displacement signal prior to differentiation.

A filter is a mathematical tool (or a physical device) which perform signal processing functions, specifically intended to remove unwanted signal components and/ or enhance wanted ones. The aim of a filter is to decompose a signal, identifying the real signal and remove the contaminating part, the noise. (Figure 5.1)

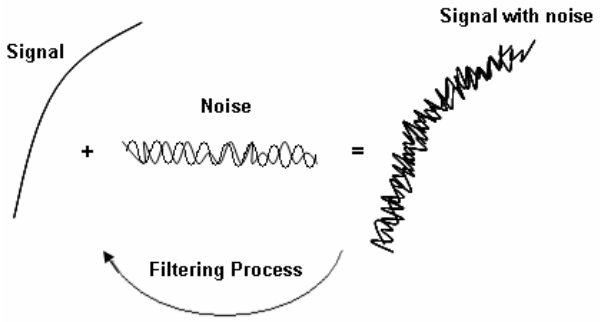

Figure 5.1. The filtering process.

At first instance, it is important to recognize that a filter always change the original signal. So, in order to choose an appropriate filter, it is fundamental to know as much as possible about the signal, like its origin and the movement that represents, and/or to recognize the origin of the noise.

Common filtering and smoothing techniques involve computing a mathematical function to represent the data, by using polynomial functions, cubic spline functions, Fourier series, etc., or techniques that use averaging procedures to reduce the irregularities in the data, like for

example, the digital filters (Butterworth) (Boor, 2001; Cadzow, 1987; Giakas and Baltzopoulos, 1997; Giakas et al., 1998). The details are available in Appendix I.

5.2. The Study

A third study (a technical note), to access the applicability of alternative filtering and smoothing schemes to process signals obtained from kinematics, was executed, and firstly presented as:

"Data Processing and Filtering of Kinematical Signals"

Sousa F[1], Carvalho, J[2] Machado L[1], Vilas-Boas JP[1] (2006). Data Processing and Filtering of Kinematical Signals.

[1] Laboratory of Biomechanics, Faculty of Sports, University of Porto, Portugal.

[2] Physics Department, Faculty of Engineering, University of Porto, Portugal.

Abstract

The aim of the present study was to present some filtering and smoothing schemes to process signals obtained from kinematics, in order to increase the accuracy of the inverse dynamic approach in the calculations of intra articular moments and forces. We test the applicability of these new approximants, by comparing both usual and alternative filtering and smoothing techniques, in 2D kinematical signals collected with a high-speed video camera, during the performance of very demanding jumps from classical ballet. Three professional high level ballet dancers from "The National Ballet Company", of Portugal, participated voluntarily in the study. The results show that the uniform treatment of the kinematical signal is not a reasonable strategy. The data must be cut in several phases, according to the movement, and the signal should be filtered individually in each phase.

Key Words: filtering techniques, kinematics, inverse dynamics, ballet jumps.

Introduction

The numerical derivative of kinematical data can be a source of error much larger than the noise of the signal given rise by the digitizing errors, or the movements out of the plane of motion.

According to Hatze (2000; 2002), the principal disadvantage of using inverse dynamics is that errors embedded in the position-time data are greatly magnified when the data is processed to yield acceleration.

Therefore, the importance of good data filtering to the accuracy of inverse dynamics is decisive. The usual filtering or smoothing schemes distort real short-timed events as the ground contact in a drop jump, transforming a sharp contact into a smooth one. Although the frequency content of the aerial phases of the motion generally consist of low frequency components, the impact phases of motion exhibit a range of higher frequencies depending on the type and intensity of the impact involved.

According to Georgakis et al. (2002), the non-stationary nature of biomechanical signals, especially when the motion involves impacts, yields Fourier transform-based techniques inefficient for the analysis and filtering of such signals. The authors suggest alternative filter techniques which can represent the signal both in the time and in the frequency domain, identifying areas of higher and lower frequencies (impact and aerial phases, respectively), and filtering the signals applying different cut-off thresholds at different times.

Wavelet denoising techniques support short and long timed events properly, so it is a promising tool (Giakas et al., 2000; Mallat, 1998). Also Splines are able to describe both smooth and non-differentiable curves (Boor, 2001; Giakas and Baltzopoulos, 1997; Giakas et al., 1998), and we have testing their applicability.

Methods

A Matlab software routine was created to filter the transformed coordinates obtained after manual digitalisation of the jumps. After an exhaustive evaluation of the horizontal and vertical original displacement data, from the three articular joints considered in the model (ankle, knee and hip), the Matlab routine allows the identification of particular points in the trajectory that should be minutely and individually observed. They are the real short-timed sequence of events, as the ground contact in drop jumps.

Figure 5.2 shows a representative example of the vertical displacement of the fifth metatarsus, during the performance of a highly technical demand ballet jump. As it is

possible to observe, the Matlab routine allows the identification of the instant of time in which the fifth metatarsus touch the ground (vertical line). This real short-timed event (the ground contact), is determinant in the performance of the jumps. Extremely high impact loads are applied to the body structures, in these brief instants of time.

The knowledge of the internal loading experienced by the body segments during dynamic activities is extremely important. The assessment of biomechanical loading and a better understanding of how the body transmit and attenuate the impact forces through the muscles, bones and joint tissues is an extremely important topic of interest for exercise prescription and injury prevention.

The usual filtering routines usually distort the signal, smoothing the real important events, like the corner trajectory of the original signal obtained in impetuous ballet jumps (short ground contact time).

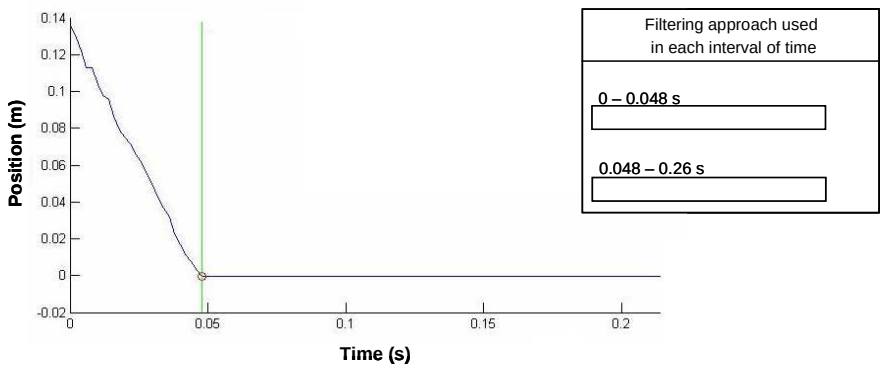

Figure 5.2. Representative example of the vertical displacement from fifth metatarsus joint, during the performance of a high technically demand ballet jump.

After the clear identification of notable points, with the reconnaissance of the different phases of each jump (aerial and touch down), subsequently, the Matlab routine allows the selection of a filter, or different filters, in each interval of time selected in each identified phase of the event. The selected filters are now applicable to the relevant part of the original signal.

Experimental Protocol

To illustrate the application of the proposed method, three professional ballet dancers from "The National Ballet Company", of Portugal, participated voluntarily in the study (two male

subjects and one female). The physical characteristics of subjects are presented in table 5.1. The subjects were informed about the purpose of the study and risks associated, and signed an informed and free consent agreeing with their participation. None of the dancers presented at that moment any kind of injury that could influence the performance of the jumps.

Table 5.1. Physical characteristics of subjects

Subject	Gender	Age (yrs)	Height (cm)	Body mass (kg)
1	Male	25	180	74
2	Male	31	177	63
3	Female	30	158	51

The jumps selected to the this study were: 1*. Sissonnes ouverte*; 2. *Jeté temps levé battu;* 3. *Ballonnés*; 4. *Ballottés*; 5. *Cabriole*; 6. *Grand Jeté*; 7. *Grand Jeté en Attitude*; 8. *Grand Jeté Entrelacé*.

The experimental protocol took place in the Laboratory of Biomechanics of the Faculty of Human Movement, from Lisbon Technical University. After the warm-up exercises, selected individually by each dancer, a session of familiarization with the procedures for the data collection started. The jumps were performed in a way so that the analyzed limb moved predominantly in the perpendicular plane of the video camera optical axis. Following a random order, every jump was repeated three times, and the best of the three repetitions was selected by an expertise person from classical ballet, for posterior treatment.

The reaction forces (in the two axis where motion of the kinematics chain occurs) were measured using a Kistler force plate (9281b) with a sample frequency of 1000 Hz. The dancers perform the selected jumps always with take-off out of the force plate and landing on the force plate. During the jump performances, the subjects were video-recorded with a high speed video camera with a sample frequency of 500 Hz. The optical axis of the camera was placed normal to the plane of motion of the preferred limb. The analyzed segments (thigh, shank and foot) were delimited with reflective markers placed on the centre of rotation of the *trochanter major*, lateral femoral epicondyle, lateral *malleolus*, *calcaneous* and fifth metatarsal head, and then manually digitized using the APAS software (Ariel Performance Analysis System, USA, Ariel Dynamics).

As linear and angular displacement data (500 Hz) and force plate curves (1000 Hz) were obtained at different acquisition frequencies, in order to synchronise them, the force curves were downsample from 1000 Hz to 500 Hz using the *resample* routine of Matlab program, witch implements a polyphase filter. The transformed coordinates were than filtered according to the routines previously described.

The anthropometrical variables mass, centre of mass and moment of inertia of each segment were obtained from the database proposed by National Aeronautics and Space Administration (NASA, 1978).

Results and Discussion

Figure 5.3 shows a representative example of the original displacement data (horizontal and vertical) of the hip, knee, ankle and fifth metatarsus joints obtained from the kinematics. As it is possible to observe, the original displacement of the different articular joints studied, in both vertical and horizontal axis of movement, exhibit small ripples in its trajectory which we do know, are not true displacements, but rather, have their origin during the digitizing process and should be minimized with an accurate treatment of the signal. It is also possible to observe, especially in the trajectory of the vertical displacement of the ankle and fifth metatarsus (in the bottom-right panel), the presence of a corner (sharp) trajectory of the signal that should be especially treated with adequate filters.

Figure 5.4 shows a representative example of the original displacement data of the hip, knee, ankle and fifth metatarsus joints obtained from the kinematics, and a new trajectory of the signal obtained after a low-pass Butterworth filter with cut frequency of 8 Hz.

As we may observe, the trajectory of the subject during the aerial phase preparing the approach to the landing, is seemingly smooth and harmonious until the contact time with the ground. At this instant, due to the extremely high impact load originated and the technical complexity of the movements studied (ballet jumps), the trajectory at the impact looks like a corner (fifth metatarsus, both horizontal and vertical displacement). In this example, and especially in the horizontal and vertical displacement of fifth metatarsus, the cut frequency of this filter (8Hz) was not appropriated. The filter failed because it can not follow the corner trajectory of the original signal.

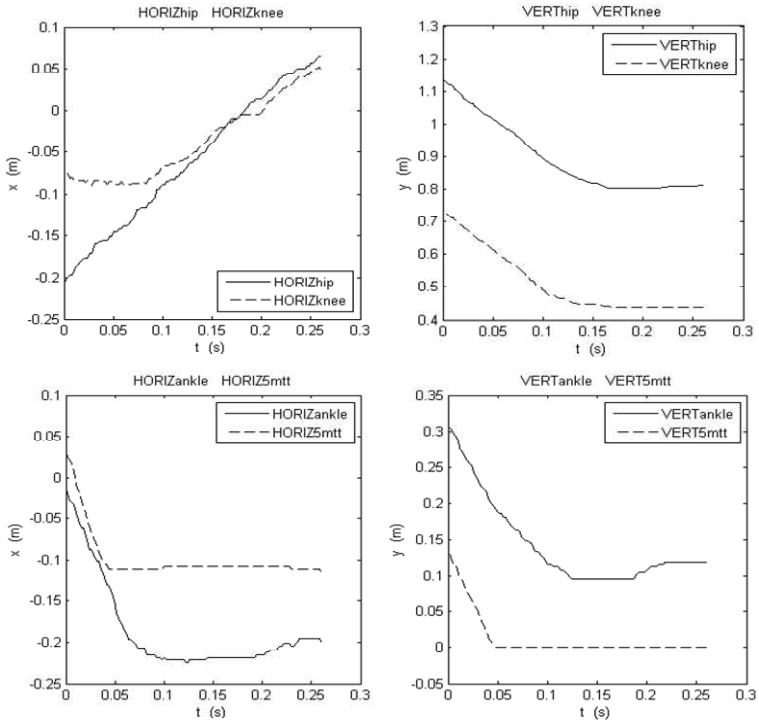

Figure 5.3. Representative example of original displacement data of the hip, knee, ankle and fifth metatarsus joints obtained from the kinematics, during the performance of a ballet jump.

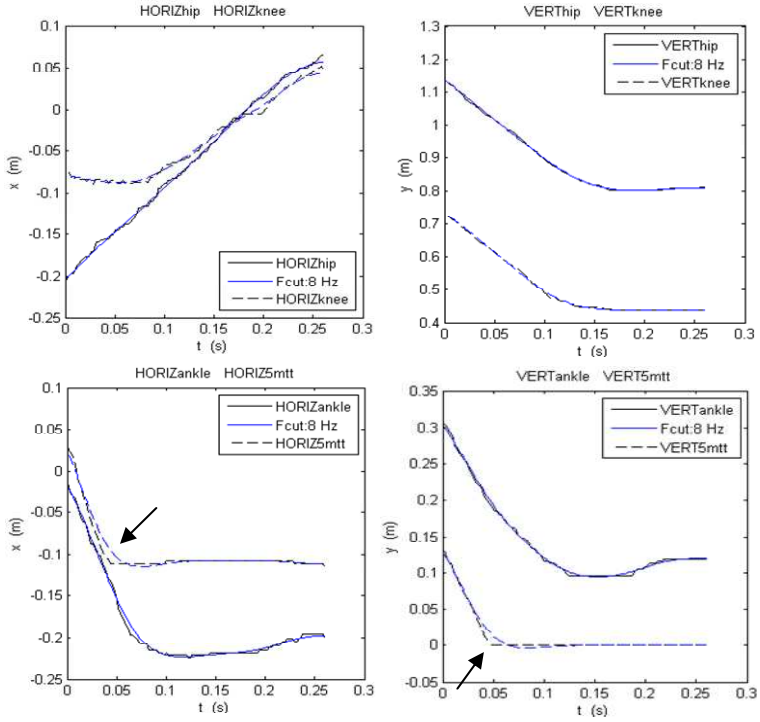

Figure 5.4. Representative example of original displacement data of the hip, knee, ankle and fifth metatarsus joints obtained from the kinematics during the performance of a ballet jump and the Butterworth filtered signal. The arrows indicate the sharp trajectory of the original data.

Figure 5.5 shows a representative example of the original displacement data of the hip, knee, ankle and fifth metatarsus joints obtained from the kinematics and a new trajectory of the signal obtained after a low-pass Butterworth filter of 15 Hz.

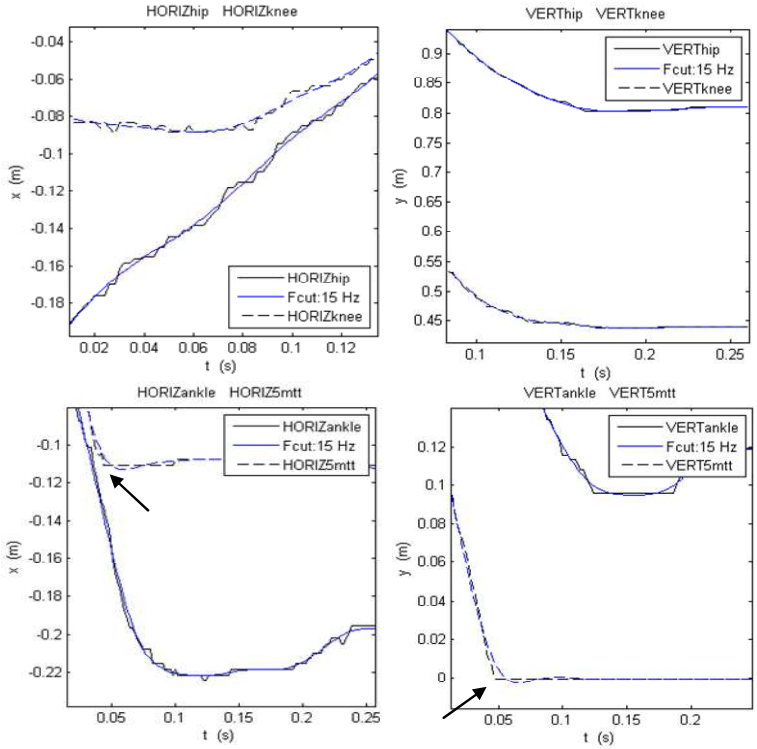

Figure 5.5. Representative example of original displacement data of the hip, knee, ankle and fifth metatarsus joints obtained from the kinematics during the performance of a ballet jump and the Butterworth filtered signal. The arrows indicate the sharp trajectory of the original data.

As it is possible to observe in this example and especially in the horizontal and vertical displacement of the fifth metatarsus, the cut- off frequency of this filter (15Hz) continues not to be the most appropriated, because, like in the previous example (8 Hz), the new filter can't follow the corner trajectory of the original signal.

Figure 5.6 shows at the same time a representative example of the original displacement data of the hip, knee, ankle and fifth metatarsus joints obtained from the kinematics and a new trajectory of the signal obtained after a Butterworth low-pass filter of 20 Hz.

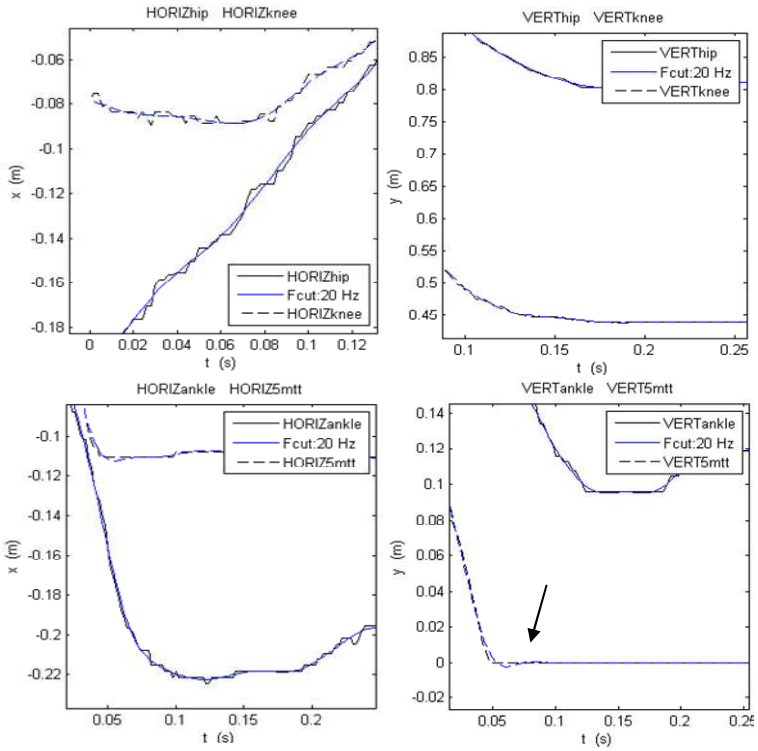

Figure 5.6. Representative example of original displacement data of the hip, knee, ankle and fifth metatarsus joints obtained from the kinematics during the performance of a ballet jump and the Butterworth filtered signal. The arrow indicates the ripples (Gibbs phenomenon) of the filtered signal.

The cut-off frequency of this filter (20Hz), contrary to the previously used frequencies, is the most appropriated in the sense of better following the corner trajectory of the signal. Nevertheless, as it is possible to observed in figure 5.6, after the impact instant (the corner) the filter demonstrate to be inappropriate because the “Gibbs phenomenon” (small ripples about the original signal), is now more intense, and is evident that the filter can not follow the trajectory of the original data.

Figure 5.7 shows a representative example of the original displacement data of the hip, knee, ankle and fifth metatarsus joints obtained from the kinematics and a new trajectory of the signal obtained after a cubic Hermit spline smoothing.

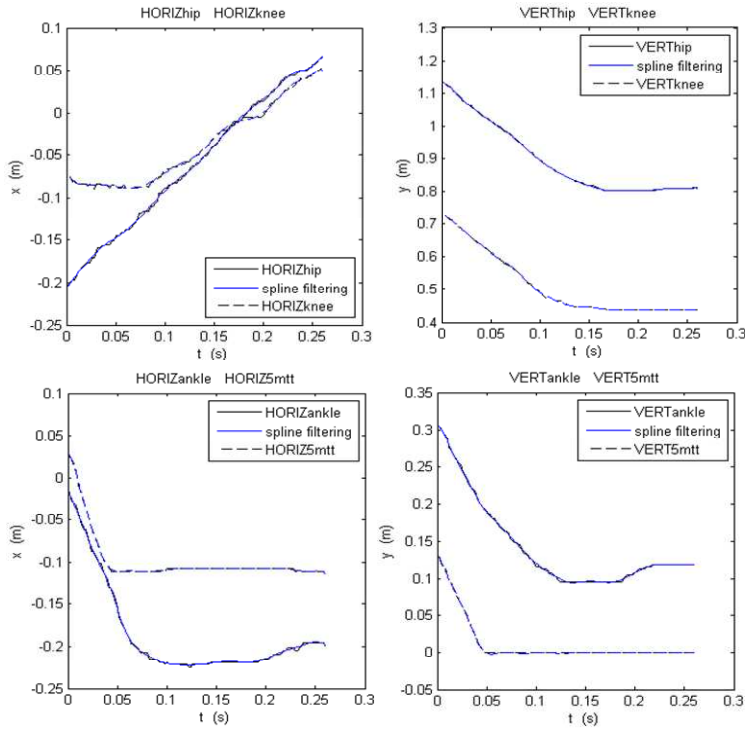

Figure 5.7. Representative example of original displacement data of the hip, knee, ankle and fifth metatarsus joints obtained from the kinematics during the performance of a ballet jump and a spline filtered signal.

As it is possible to observe in detail in the figure 5.8, especially in the horizontal and vertical displacement of the fifth metatarsus, the spline is now closer to the signal, nevertheless continues not to follow the corner trajectory of the original signal and presents some ripples.

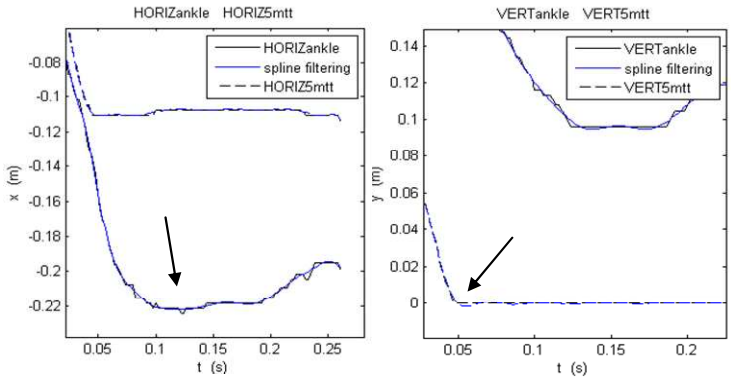

Figure 5.8. Representative example of original displacement data of the hip, knee, ankle and fifth metatarsus joints obtained from the kinematics during the performance of a ballet jump and a spline filtered signal. The arrows indicate the ripples of the filtered signal.

Figure 5.9 shows a representative example of the original displacement data of the hip, knee, ankle and fifth metatarsus joints obtained from the kinematics and a new trajectory of the signal obtained after discrete wavelet filtering (threshold 100). As it is possible to observe in the figure, the wavelet filter threshold 100 follows the signal, but with some ripples. The threshold level is not appropriated.

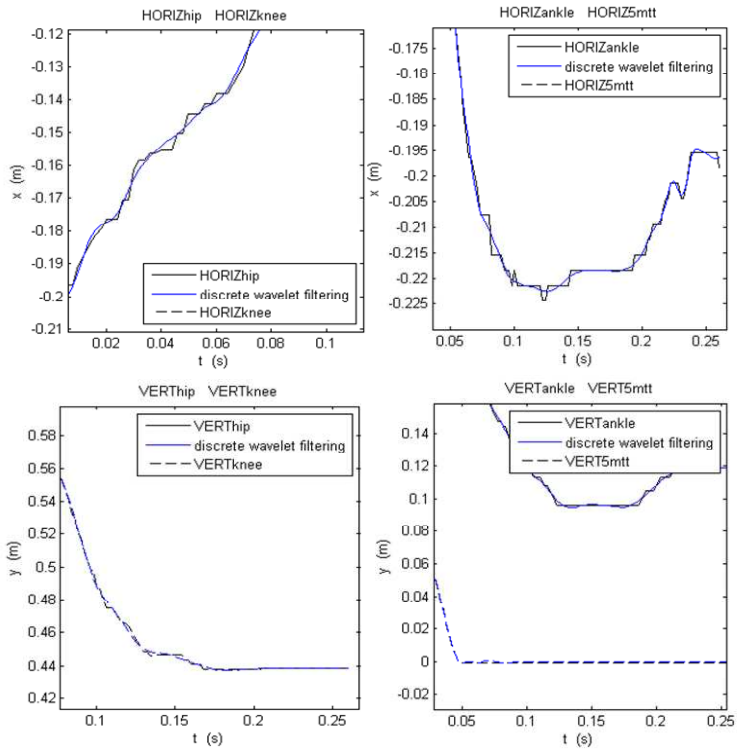

Figure 5.9. Representative example of original displacement data of the hip, knee, ankle and fifth metatarsus joints obtained from the kinematics during the performance of a ballet jump and a wavelet threshold 100 filtered signal.

Figure 5.10 shows a representative example of the original displacement data of the hip, knee, ankle and fifth metatarsus joints obtained from the kinematics and a new trajectory of the signal obtained after discrete wavelet filtering (threshold 500). As it is possible to observe in the figure, the wavelet filter threshold 500 follows the signal excessively. It is almost not possible to observe the filtering approach with this filter.

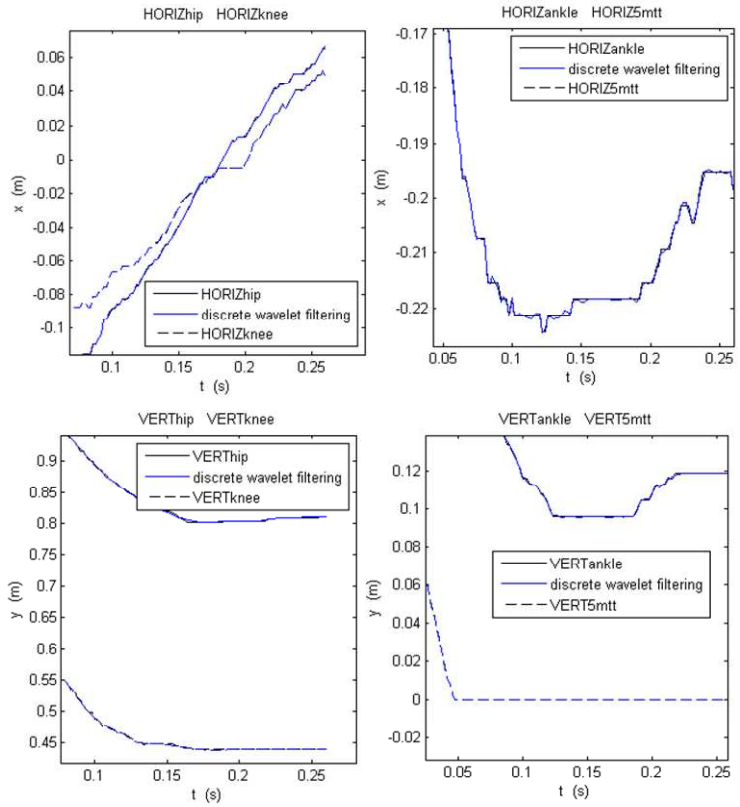

Figure 5.10. Representative example of original displacement data of the hip, knee, ankle and fifth metatarsus joints obtained from the kinematics during the performance of a ballet jump and a wavelet threshold 500 filtered signal.

From figures 5.4 to 5.10 it was possible to observe the application of different filters in the original displacement data of the hip, knee, ankle and fifth metatarsus joints obtained from the kinematics. In all cases a given filter was applied throughout the time lapse of the movement's performance. None of the filters appears to be particularly interesting and suitable for represent the characteristics of the underlay signal, namely the short-time event of the ground contact and the subsequent sharp trajectory of the signal (especially the fifth metatarsus joint). These results suggest that is necessary to identify notable points, namely the sharp corners corresponding to the first contact with the ground, and to split the signal into two, or more, pieces and apply different filters to each phase. Although the filters applied to each section are different, they may be of the same nature, i.e., one may apply a spline filter to each section.

Figure 5.11 shows a representative example of the original displacement data of the hip, knee, ankle and fifth metatarsus joints (A) and in detail for the fifth metatarsus (B), obtained from the kinematics and a new trajectory of the signal obtained after a cubic Hermit spline filter, where the fifth metatarsus trajectories were filtered with two splines, before and after the contact time (vertical line).

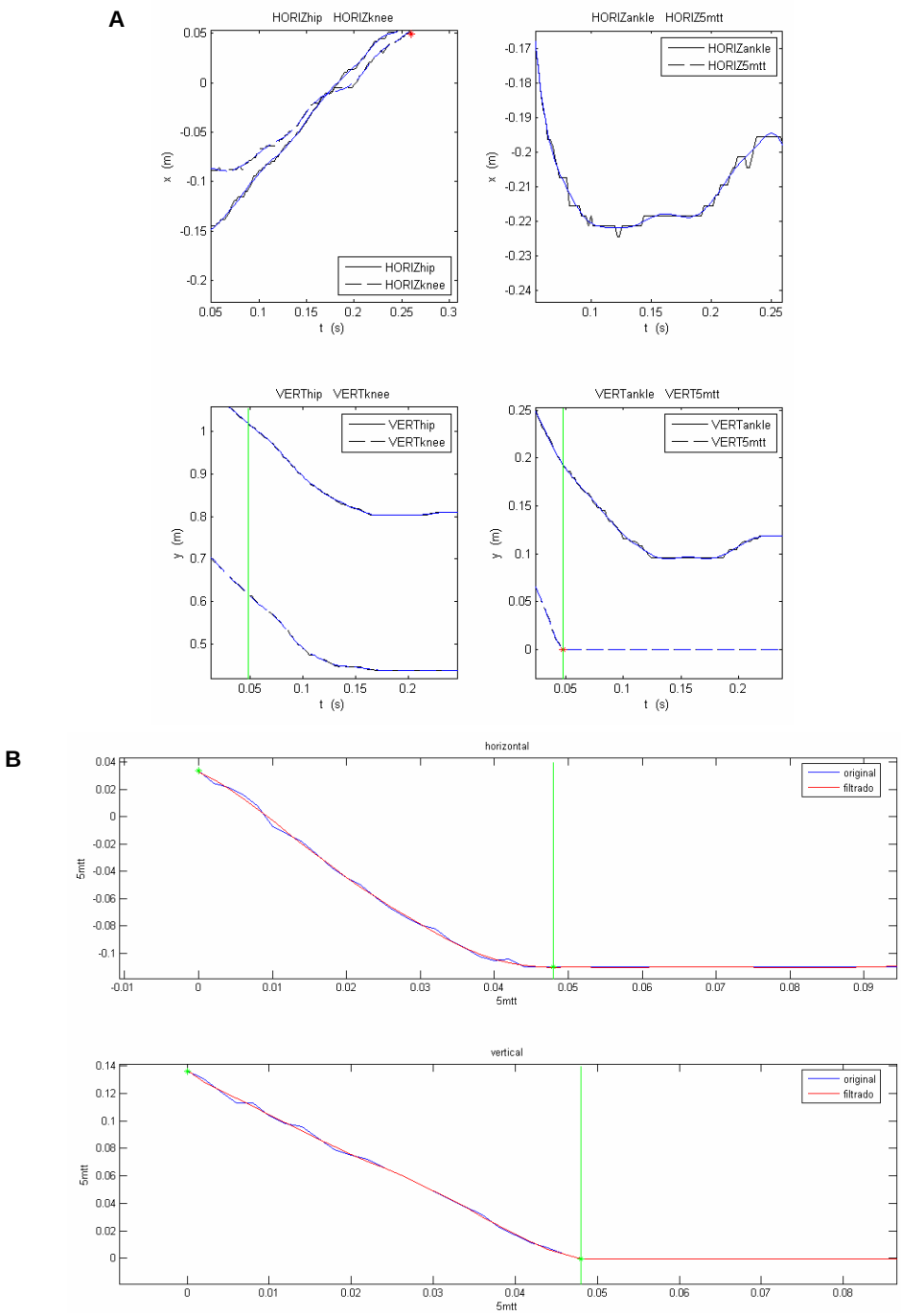

Figure 5.11. Representative example of original displacement data of the hip, knee, ankle and fifth metatarsus joints (A) and in detail the fifth metatarsus (B) obtained from the kinematics during the performance of a ballet jump and a cubic Hermit spline filtered signal.

As it is possible to observe, this filtering technique demonstrates to be very effective as it followed, in a continuous way, the sharp trajectory of the fifth metatarsus in the first ground contact, without any ripples, and it also allowed a smooth filtering of the other trajectories (aerial phase).

We found in the literature a few studies dedicated to explore alternative filtering methods in contrast to the current methods used in biomechanics to filter displacement signals, in order to obtain accurate higher derivatives (Alonso et al., 2005; Georgakis et al., 2002; Giakas et al., 2000). According to these authors, the alternative filtering methods proposed, demonstrate to be more accurate than the usual methods used in the estimation of the second derivatives of kinematic signal with impacts. In movements that involve impacts, there are dramatic changes in the frequency content of the overall kinematic signal obtained, and a significantly transition from low (aerial phase) to high (impact phase) frequency components. In this way, the conventional filters used in biomechanics, that view the signal as stationary and are applied to the whole signal, are not a proper choice. The time-frequency domain filters were found to be superior to conventional filters. The main reason for this is that different filters (cut-off) can be applied at different time intervals.

Conclusions

Different kind of filters must be selected in each phase of the selected movements. In the present study, the usual filtering techniques, such as the Butterworth technique, seems to be appropriated to apply in the aerial phase of the jumps. In the brief impact phases of these jumps, the signal must be treated in a different way. The filter should be less severe than Butterworth (for example splines), so that the corner trajectory of the signal, i.e., the most important phase when studying impacts, doesn't disappear.

When we cut the signal in several pieces, and apply the selected filter, or different filters, it is necessary to ensure the continuity of the trajectory of the signal, that is, it is necessary to "glue" appropriately all the pieces obtained.

In sum, we believe that the biomechanics community will benefit from this alternative filtering technique, which has proven its effectiveness with complex signals, as an alternative or complement to usual smoothing techniques.

Nevertheless, future studies need to be done in order to produce more accurate filtering algorithms.

5.3. Next Goals

Apply other alternative filtering techniques to smooth the kinematical data and test their applicability in the inverse dynamics approach.

Improve the precision of the kinematical data by the simultaneous use of video redundancy and accelerometers.

5.4. References:

Alonso, F. J.; Pintado, P. and Del Castillo, J. M. (2005). Filtering of kinematic signals using the Hodrick-Prescott filter. J Appl Biomech 21: 271-285.

Boor, C. d. (2001). A Pratical Guide to Splines (Applied Mathematical Sciences). Springer-Verlag, New York.

Cadzow, J. A. (1987). Foundations of Digital Signal Processing and Data Analysis. Mcmillan Publishing Company, New York.

Georgakis, A.; Stergioulas, L. K. and Giakas, G. (2002). Automatic algorithm for filtering kinematic signals with impacts in the Wigner representation. Med Biol Eng Comput 40: 625-633.

Giakas, G. and Baltzopoulos, V. (1997). Optimal digital filtering requires a different cut-off frequency strategy for the determination of the higher derivatives. J Biomech 30: 851-855.

Giakas, G.; Baltzopoulos, V. and Bartlett, R. M. (1998). Improved extrapolation techniques in recursive digital filtering: a comparison of least squares and prediction. J Biomech 31: 87-91.

Giakas, G.; Stergioulas, L. K. and Vourdas, A. (2000). Time-frequency analysis and filtering of kinematic signals with impacts using the Wigner function: accurate estimation of the second derivative. J Biomech 33: 567-574.

Hatze, H. (2000). The inverse dynamics problem of neuromuscular control. Biol Cybern 82: 133-141.

Hatze, H. (2002). The fundamental problem of myoskeletal inverse dynamics and its implications. J Biomech 35: 109-115.

Mallat, S. (1998). A wavelet tour of signal processing. Academic Press.

NASA (1978). Anthropometric Source Book, technical report 1024. NASA Scientific and Technical Information Office, Houston.

Chapter 6

Estimation of Muscle Forces and Joint Moments using a Forward-Inverse Dynamics Model

6.1. Introduction

The determination of joint reaction forces and moments of force allows the understanding of the magnitude of internal loading experienced by the body segments during dynamic activities. The assessment of biomechanical loading, and a better understanding of how the body transmits and attenuates the impact forces through the muscles, bones and joint tissues, is an extremely important topic of interest for exercise prescription and injury prevention.

6.2. The Study

A fourth study, to estimate forces and moments of individual muscles around the ankle, knee and hip joints, and the energy transfer between bi-articular muscles, was not yet submitted for publication and is firstly presented as:

"Estimation of Muscle Forces and Joint Moments using a Forward-Inverse Dynamic Model"

Sousa F[1], Carvalho J[2], Machado L[1], Vilas-Boas JP[1] (2006). Estimation of Muscle Forces and Joint Moments using a Forward-Inverse Dynamics Model.

[1] Laboratory of Biomechanics, Faculty of Sports, University of Porto, Portugal.

[2] Physics Department, Faculty of Engineering, University of Porto, Portugal.

Abstract

The main purposes of this study were:

1) to calculate the joint reaction forces and moments of forces in the ankle, knee, and hip joints, during very demanding ballet jumps, using the inverse dynamics approach;

2) to present a forward-inverse dynamics model to estimate muscle forces. A forward dynamics model was used, with neural inputs optimized, to match the moments obtained in (1). From the moments of forces determined by the forward model we extracted the individual muscle forces around the ankle, knee and hip joints (Figure 6.4).

3) to present an electromyographic (EMG) driven forward-inverse dynamics model to estimate muscle forces and joint moments. From the same core ideas as in (2), but using the available EMG records as indicators of muscle activation, an optimization in the remaining muscles was performed, with increased efficiency.

The results from the classical inverse dynamics approach are very sensitive to the input data precision (video, GRF). The efforts to refine the filtering and differentiation of these reveal no significant improvement in desensitising these results, and a greater effort has to be done at the acquisition level, including the usage of redundant sources, e.g., video cameras, accelerometers, etc. The usage of a hybrid forward-inverse dynamical model seems to desensitise it from the objective function. This is beneficial as these functions are not physically or physiologically founded. These hybrid models can be seen as the result of an exchange of the importance of the ad-hoc objective functions to the importance of the muscle model, more easy to found in the physiology (Hill's or Huxley's models, etc). It is possible to conclude that the results obtained from the extended inverse dynamics approach (muscular decomposition) with and without EMG, are not radically different. The biggest differences are particularly observed in the role of mono and bi-articular muscles. We think it is necessary much more research around this theme. Another kind of results should be expected if we have EMG from all the superficial muscles (mono and bi-articular) from the lower limb, and if possible, combined with direct measurements from muscular force. Without direct measures one can not make a definite case in favour of any of the strategies. Nevertheless, the ecological tool would avoid the usage of intrusive techniques like EMG and internal force sensors.

Key Words: forward-inverse dynamics, EMG, ballet jumps.

Introduction

Biomechanical modelling of the lower extremity provides additional and alternative information about the mechanical loading over a large range of performance conditions. Parameters such as the kinematics, ground reaction forces, and activation, are included in the mechanical loading assessment (Enoka, 2002; Nigg, 1999).

Inverse dynamics and forward dynamics are the two traditional modelling approaches used to study the biomechanics of human movement. Nevertheless, both have known limitations (Bogey et al., 2005; Buchanan et al., 2004; Buchanan et al., 2005). A better tool seems to arise from the combined use of the two approaches (Buchanan et al., 2004). The muscle decomposition of the joints moments in the classical inverse dynamics is dependent exclusively of the *Ad-Hoc* objective function. The inclusion of a (direct) muscle model reduces this dependence and makes the result more stable in the numerical sense. This

was the final strategy we followed, including a complex and recent muscle model (Arampatzis et al., 2001; Conceição, 2004).

The inverse dynamics provides the joint torques and forces that the forward dynamics has to match by appropriate choice of neural inputs. In this way, the muscular dynamics is much more physiological and realistic, although the relative muscle contributions may still not be accurate as they depend on an *Ad-Hoc* objective function.

The main purposes of this study were:
1) to calculate the joint reaction forces and moments of forces in the ankle, knee, and hip joints, during very demanding ballet jumps, using the inverse dynamics approach;
2) to present a forward-inverse dynamics model to estimate muscle forces. A forward dynamics model was used, with neural inputs optimized, to match the moments obtained in (1). From the forward model we extract the individual muscle forces around the ankle, knee and hip joints (Figure 6.4).
3) to present an electromyographic (EMG) driven forward-inverse dynamics model to estimate muscle forces and joint moments. From the same core ideas as in (2), but using the available EMG records as indicators of muscle activation, an optimization in the remaining muscles was performed, with increased efficiency.

Methods

In this section, the theoretical background of the model will be firstly presented, followed by the description of the data acquisition procedures.

Classical Inverse Dynamics

The classical inverse dynamics approach was used to estimate the intersegmentar forces and torques, assuming a bidimensional model of the lower limb. In our model, the lower limb was considered to consist of tree rigid segments: the thigh, the shank, and the foot (figure 6.1). The joints were assumed to be point like (hinge joints).

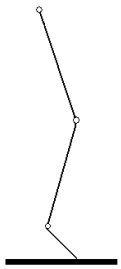

Figure 6.1. Bidimensional model of the lower limb, with tree rigid segments representing the thigh, shank and foot.

In the inverse dynamics approach, the main idea is to solve Newton's second law equations, knowing the kinematics and some forces (GRF) and obtaining the unknown forces and torques, usually starting from the single contact point and moving upwards into the model.

Starting from the bottom, the foot, we use the GRF data and the foot's kinematics to obtain the reaction forces and moments applied at the ankle.

According to Newton's third law (the action-reaction principle) there is an equal and opposite force acting at each hinge joint in the model. So, in the inverse dynamics approach, the reaction forces at each joint are calculated starting at the ankle and continuing up to the knee and hip, obtaining the forces and moments. The same principle can be applied to all other segments of the body, if one wishes.

The forces and internal moments acting on the distal part of the segment S_i will be obtained following the equations:

$$F_{Pix} + F_{Dix} = m_i a_x \tag{6.1}$$

$$F_{Piy} + F_{Diy} - m_i g = m_i a_y \tag{6.2}$$

$$M_{Piz} + M_{Diz} + \left(L_D \times F_D\right) + \left(L_P \times F_P\right) = I\ddot{\theta}_i \tag{6.3}$$

where, L_D and L_P represent the lever arms vectors of the intersegmental forces (distal and proximal respectively), and $F_{Pix}, F_{Piy}, F_{Dix}$, and F_{Diy} are the x and y components of the resulting forces acting in the proximal and distal extremities, respectively. This last forces

are contact forces acting in the extremities of S_i, and due to the presence of adjacent body segments, include the compressive effects of neighbouring structures, such as articular and bone tissues, as well as the tensions developed by muscles and ligaments.

Reducing the movement and considering it as occurring in only one plane, besides the kinematics, anthropometric data and ground reaction forces at the distal end of the distal segment, are known (figure 6.2):

a_x, a_y - acceleration of the segment centre of mass

$\ddot{\theta}_i$ - angular acceleration of the segment in the plane of movement (α_i)

R_{xd}, R_{yd} - reaction forces acting at the distal end of the segment

M_{Diz} - net muscle moment acting at the distal joint

I - tensor of inertia

Are unknown:

R_{xp}, R_{yp} - reaction forces acting at the proximal joint

M_{Piz} - net muscle moment acting on the segment at the proximal joint

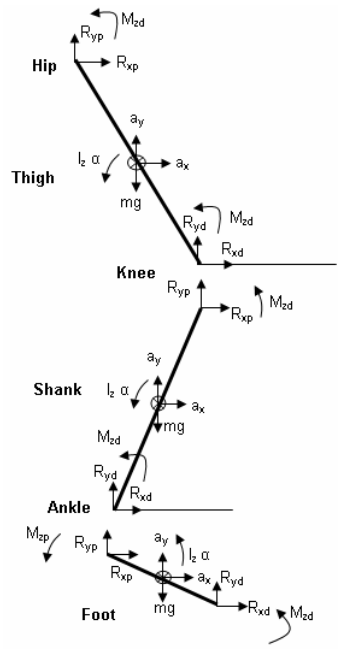

Figure 6.2. Free-body diagram of the tree body segments composing the lower limb, showing the reaction and gravitational forces, moments of forces, linear and angular accelerations.

Two small problems must be referred when the inverse dynamics is used:

1. We measure the spatial coordinates and numerically estimate the accelerations. This is very error prone and relies heavily on filtering techniques. We have made some effort on this area, and we have described these in chapter 5. An alternative approach would be to measure the accelerations directly. The main problem here is how to obtain a proper coupling of the accelerometer with the segment centre of mass.
2. The exact inertial and geometrical properties of the subjects are usually unknown, and can have a significative effect on the calculations. We have address these by using a sophisticated anthropometric model from NASA (NASA, 1978).

Forward-inverse Dynamics Model (muscular decomposition)

The classical inverse dynamics gives us the joint restriction forces. These are the forces that act between the segments, i.e., avoiding that the segments become separated or interpenetrate. They are a good tool to estimate bone or ligamentar injury potential. From these we can also evaluate the adequacy of prosthetics, as in Loss (2001).

From the classical inverse dynamics we also obtain the net joint moments. These can be used to estimate the muscular forces applied to that joint. This is no easy task as we only know the sum of the applied moments, and we are interested to know each of the parcels. Usually this is addressed postulating an economy function (something like energy expenditure) that has to be minimized. This *Ad-Hoc* hypothesis is the most fragile construction of these models. We have chosen to use the sum of the squared forces, according to several authors (Böhm, 2002; Buchanan et al., 2004; Koo and Mak, 2005; Lloyd and Besier, 2003; Manal and Buchanan, 2003). We can however desensitize the model from this choice, coupling a forward-dynamics model and using EMG data. The EMG data gives a rough description of the muscle activity and the forward dynamics model tries to estimate the muscular force corresponding to that EMG. We can now optimise some parameters of the model or obtain, by optimization, the activation functions of the muscles for which we don't have EMG records.

Other problems arise from the need to know a lot more physiological and anthropometric parameters. We have tried to address these by considering lengthy joints, the angular

dependence of muscular moment arms, and a set of musculotendinous parameters already tested (Böhm, 2002; Winters and Woo, 1990; Yamaguchi et al., 1990).

Our muscular model included 8 muscle groups: (1) the *gluteus*, (2) the *iliopsoas*, (3) the hamstrings, (4) the *rectus femoris*, (5) the *vastus*, (6) the *gastrocnemius*, (7) the *tibialis*, and (8) the *soleus* (figure 6.3).

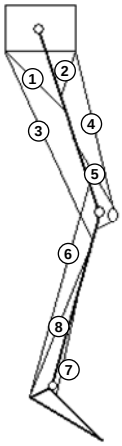

Figure 6.3. Model of the lower limb of the human body with the string model of (1) *gluteus*, (2) *iliopsoas*, (3) hamstrings, (4) *rectus femoris*, (5) *vastus*, (6) *gastrocnemius*, (7) *tibialis*, and (8) *soleus* muscle groups.

Figure 6.4 presents our hybrid forward-inverse dynamics model to estimate joint moments.

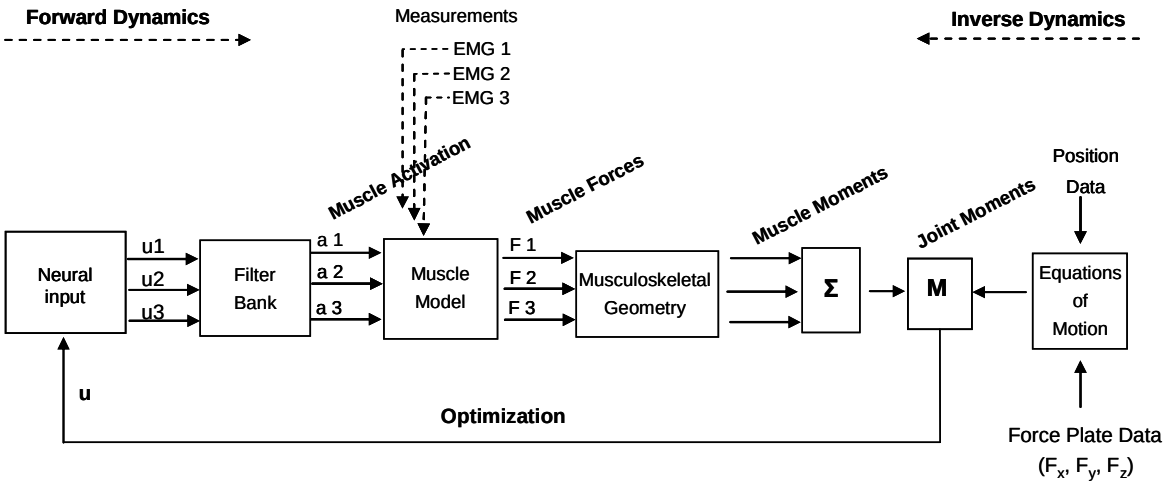

Figure 6.4. Schematic forward-inverse dynamics model used to estimate muscle forces around the ankle, knee, and hip joints, where u are the neural input, a the muscle activation and F the muscle forces.

From the left to the right -hand side (figure 6.4):

- The forward approach begins with the neural input. For the muscles that have no EMG records, we obtain the activation function from the neural input. These are just obtained by optimization;

- The filter banks, as in Hapee (1994), are just a set of first order low-pass filters that mimic the neuromuscular delay and the physiologically smooth changes in the activation parameters;

$$\begin{cases} \dfrac{da}{dt} = \dfrac{E-a}{\tau_A} \\ \dfrac{dE}{dt} = \dfrac{u-E}{\tau_E} \end{cases} \tag{6.4}$$

where *a* is the activation function, E is an intermediate variable (excitation) and u is the neural input. τ_E = 40ms and $\tau_A = \begin{cases} 50ms \Leftarrow E > a \\ 10ms \Leftarrow else \end{cases}$

- The muscle model, as in Conceição (2004), is an Hill-type model with two main changes: the activation function is included in the force-velocity function, as in Chow and Darling (1999), making the maximum contraction velocity depend on the activation; the second change is the potentiation function that is an attempt to include some impulsive dynamics relevant to the SSC, that is partially described by the Huxley model (1957) and other sources (Bobbert et al., 1986b; Cavagna et al., 1968; Dietz et al., 1979; Enoka, 2002; Ettema et al., 1990; Gollhofer et al., 1992; Hatze, 1990; Herzog and Leonard, 2002; Huxley and Simmons, 1971; Komi, 1987; Komi and Bosco, 1978; Morgan, 1990; Nicol and Komi, 1999; Rack and Westbury, 1974; Wang et al., 1979). The global equation is:

$$F_{CE} = F_{\max} * \left[\; F_L(L_{CE}) * F_V(\dot{L}_{CE}, a) * \left(\; 1 + pot(\dot{L}_{CE}, a, t) \; \right) \right] + F_{PEE}(L_{CE}) \tag{6.5}$$

where, for each muscle, F_{CE} is the contractile element force, $F_{\max}$ the maximum isometric force, F_L the force-length relationship, L_{CE} the length of the contractile

element, F_v the force-velocity relationship, a the activation function, pot the potentiation, t the time, and F_{PEE} the parallel elastic element force.

The force-length relationship (Hill type) is parabolic:

$$F_L = c\left(\frac{L_{CE}}{L_{CEopt}}\right)^2 - 2c\left(\frac{L_{CE}}{L_{CEopt}}\right) + c + 1 \tag{6.6}$$

where, F_L is the force-length relationship, $c = \frac{1}{width^2}$, L_{CE} the length of the contractile element, and L_{CEopt} the optimal length of the contractile element (figure 6.5).

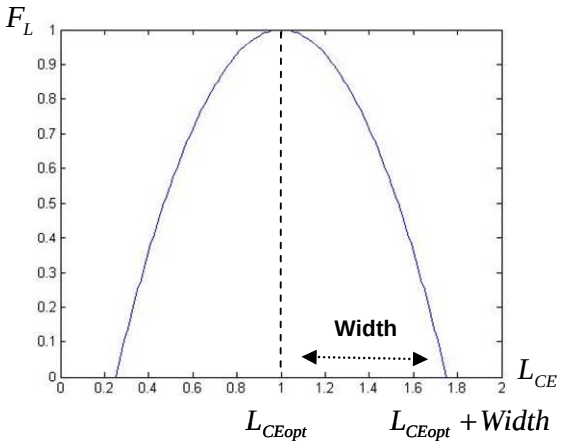

Figure 6.5.Force-length relationship.

The force-velocity relationship is a double hyperbole (Hill type), not differentiable at the origin, and with the concentric branch depending on the activation (figure 6.6):

$$F_v = \frac{f_1(a) + f_2(a)V_r}{f_3(a) - V_r} \tag{6.7}$$

where, F_v is the force-velocity relationship, a is the active state, $V_r = \frac{V_{CE}}{V_{\max}}$ is the CE normalized velocity, $V_{\max}$ is the maximal CE concentric velocity (when a =1) and the auxiliary functions $f_1(a),\ f_2(a),\ f_3(a)$ are:

$$f_2(a) = \begin{cases} -0.89(a-0.942)^2 + 0.593 & \Leftarrow \quad V_r \le 0 \\ -a_f \cdot a & \Leftarrow \quad V_r > 0 \end{cases} \tag{6.8}$$

$$f_3(a) = \begin{cases} -1.47(a-0.700)^2 + 0.720 & \Leftarrow \quad V_r \le 0 \\ a \cdot (1-a_f) \cdot \left(-1.47(a-0.700)^2 + 0.720\right) / \left(s_f \cdot \left(a - 0.89(a-0.942)^2 + 0.593\right)\right) & \Leftarrow \quad V_r > 0 \end{cases} \tag{6.9}$$

$$f_1(a) = a \cdot f_3(a) \tag{6.10}$$

and $a_f = 1.6$ is the asymptotic eccentric force (when a=1) and $s_f = 2$ is the slope discontinuity at the origin (when a=1).

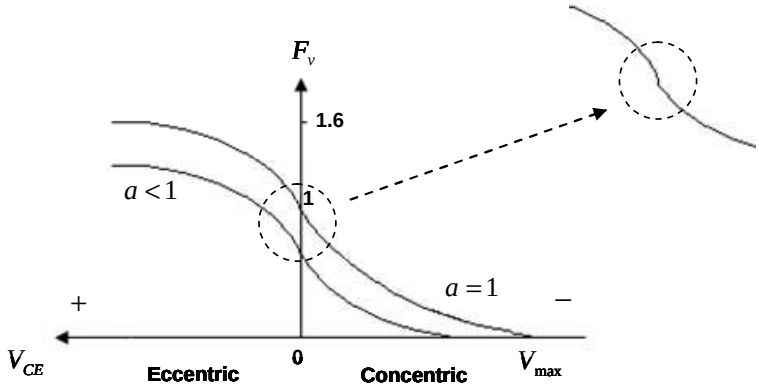

Figure 6.6.Force-velocity relationship.

The model for the force enhancement (potentiation) has four assumptions:

1. An increase of the force enhancement with the activation and the lengthening velocity until a maximum of 1.6 (Cook and McDonagh, 1995):

$$\frac{dpot_1}{dt} = \alpha \cdot a \cdot V_r \quad \alpha \approx 10 \tag{6.11}$$

where,

α is a gain factor , whose empirical value is approximately 10 (Conceição, 2004; Cook and McDonagh, 1995).

a is the activation

$V_r = \frac{V_{CE}}{V_{\max}}$ is the CE normalized velocity

pot_1 is the eccentric component of the force enhancement function

2. An exponential decay of the force enhancement in time:

$$\frac{dopt_2}{dt} = -\delta \cdot pot_2 \quad \delta \approx 1.9 \tag{6.12}$$

where,

δ is a decay factor, whose empirical value is approximately 1.9 (Conceição, 2004; Cook and McDonagh, 1995)

pot_2 is the time component of the force enhancement function

3. The concentric actions promote a decay of the force enhancement capability (Epstein and Herzog, 1998):

$$\frac{dpot_3}{dt} = -\beta \cdot V_r \quad \beta \approx 4 \tag{6.13}$$

where,

β is the decay factor, whose empirical value is approximately 4 (Conceição, 2004; Cook and McDonagh, 1995)

$V_r = \frac{V_{CE}}{V_{\max}}$ is the CE normalized velocity

pot_3 is the concentric component of the force enhancement function

4. The force enhancement is related to the number of cross-bridges, so it is proportional to the muscular PCSA or to $F_{\max}$ (Epstein and Herzog, 1998).

Globally, the force enhancement function is given by the sum of these four assumptions:

$$\frac{dpot}{dt} = \begin{cases} -\delta \cdot pot + \alpha \cdot a \cdot V_r & \Leftarrow \quad V_r > 0 \\ -\delta \cdot pot - \beta \cdot V_r & \Leftarrow \quad V_r \le 0 \end{cases} \tag{6.14}$$

The parallel elastic element force is defined as:

$$F_{PEE} = K_{PEE}\left(\max\left(L_{PEE} - L_{PEEslack}, 0\right)\right)^2 \tag{6.15}$$

where,

F_{PEE} is the force of the parallel elastic elements, $\max$ the maximum function, L_{PEE} the length of the parallel elastic elements, $L_{PEEslack}$ the minimum parallel elastic element's length to have elastic characteristics, and K_{PEE} it's stiffness.

The series elastic element force is defined as:

$$F_{SEE} = K_{SEE} \max^2 \left(L_{SEE} - L_{SEEslack}, 0\right) \tag{6.16}$$

where,

F_{SEE} is the force of the series elastic elements, $\max$ the maximum function, L_{SEE} the length of the series elastic elements, $L_{SEEslack}$ the minimum series elastic element's length to have elastic characteristics and K_{SEE} it's stiffness.

- The activation *a* is obtained as above (filter banks), or from the EMG data, if available. The EMG raw data is transformed in order to obtain its *envelope* by digitally filtering the squared raw data with a 4th order Butterworth bandpass filter with cutting frequencies of 1Hz and 8Hz. This *envelope* is used directly as the activation *a*, as we have found no need for the Manal and Buchanan (2003) techniques. According to the authors, at high levels of activation, there are a linear relationship between activation and the EMG *envelope*. The comparison of muscle forces produced by optimization-only and by EMG-and-optimization (see ahead) are similar enough not to justify those added hypothesis.

- The musculoskeletal geometry determines three aspects of the MTU: the MTU length dependence on the joint angles (cubic); the moment arms of the muscles (just the derivative of the previous length); the series elastic elements and the contractile element have a length distribution that is not fixed in time and attempt to simulate the muscle-tendon energy transfer. We also added a restriction function to avoid non-anatomical joint angles, besides the parallel elastic elements mechanism:

$$M_j = -400 \cdot \Delta\varphi_j{}^2 - 40 \cdot \Delta\varphi_j \dot{\varphi}_j \tag{6.17}$$

where,

M_j represents the moment, j the articular joint, and $\Delta\varphi_j$ the articular angle.

From the right to the left-hand side (figure 6.4):

- The joint moments estimated from classical inverse dynamics. By comparison the unknown neural inputs are estimated and the direct and inverse approaches must obtain the same moments. There are, however, several possibilities for this to happen. The selection of those minimizing the sum of the squared forces is made, transforming the procedure in an optimization scheme (Böhm, 2002; Buchanan et al., 2004; Koo and Mak, 2005; Lloyd and Besier, 2003; Manal and Buchanan, 2003).

All the routines of the proposed hybrid forward-inverse dynamics model were created in the Matlab software.

Subjects and Tasks

To illustrate the application of the proposed method, three professional ballet dancers from "The National Ballet Company of Portugal", participated voluntarily in the study (two male subjects and one female). The physical characteristics of subjects are presented in table 6.1. The subjects were informed about the purpose of the study and risks associated, and signed an informed consent agreeing with their participation. None of the dancers presented at that moment any kind of injury that could influence the performance of the jumps.

Table 6.1. Physical characteristics of subjects

Subject	Gender	Age (yrs)	Height (cm)	Body mass (kg)
1	Male	25	180	74
2	Male	31	177	63
3	Female	30	158	51

Classical ballet's technique and terminology are reasonably standard. There are only a few differences of interpretation between schools and teachers. Thanks to its original development in France during the 1600's, the French terminology is used. The jumps selected to the this study were: 1*. Sissonnes ouverte*; 2. *Jeté temps levé battu;* 3. *Ballonnés*; 4. *Ballottés*; 5. *Cabriole*; 6. *Grand Jeté*; 7. *Grand Jeté en Attitude*; 8. *Grand Jeté Entrelacé*.

Experimental protocol

The experimental protocol took place in the Laboratory of Biomechanics of the Faculty of Human Movement, at the Lisbon Technical University. After the warm-up exercises, selected individually by each dancer, a session of familiarization with the procedures for the data collection started. The jumps were performed in a way so that the analyzed limb moved predominantly in the perpendicular plane of a video camera optical axis. Following a random order, every jump was repeated three times, and the best of the three repetitions was selected by an expertise person from classical ballet, for posterior treatment.

The reaction forces were measured using a Kistler force plate (9281b) with a sampling frequency of 1000 Hz. The dancers performed the selected jumps always with take-off out of the force plate and the landing on the force plate.

Electromyographic activity from the *adductor*, *vastus lateralis*, *vastus medialis*, *hamstrings*, *medial gastrocnemius, tibialis* anterior, and *soleus*, from the preferred limb were collected to a personal computer through an AD BIOPAC converter at a sampling rate of 1000 samples per second. Surface bipolar EMG electrodes were used to record the muscle activity from the different muscles. Bipolar EMG electrodes with an interelectrode distance of 20 mm (Beckman miniature skin electrode 650437, USA) were placed on the bellies at locations chosen according to the SENIAM (1999) recommendations. The skin was lightly treated with sandpaper, and care was taken so that the interelectrode resistance was below 5 kΩ. EMG activities were bandpass filtered (5-500 Hz) and amplified (input impedance 25MΩ, common mode rejection ratio >90dB), and then sent telemetrically to the recording AD converter.

During the jump performances, the subjects were video-recorded with a high speed video camera with a sampling frequency of 500 Hz. The optical axis of the camera was placed normal to the plane of motion of the preferred limb. The analyzed segments (thigh, shank and foot) were delimited with reflective markers placed on the centre of rotation of the *trochanter* major, lateral *femoral epicondyle*, lateral *malleolus*, *calcaneous* and fifth metatarsal head, and then manually digitized using the APAS software (Ariel Performance Analysis System, USA). The use of a redundant space calibration object (figure 6.5) helped to obtain a precise coordinate transformation (Direct Linear Transformation – DLT) (Abdel-Aziz and Karara, 1971). Raw (unfiltered) data was used for further processing – chapter 5.

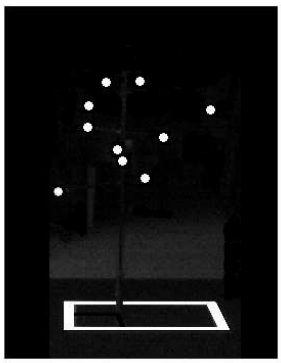

Figure 6.7. The redundant calibration object used to obtain precise coordinate transformation.

In order to synchronise as the linear and angular displacement data (500 Hz), force plate curves (1000 Hz), and EMG records (1000 Hz), which were obtained at different acquisition frequencies, the trajectory curves were downsampled from 1000 Hz to 500 Hz using the *resample* routine of Matlab program, which implements a polyphase filter.

The transformed coordinates were than filtered according to the routines previously described in the chapter 5 (Data Processing and Filtering of Kinematical Signals).

The anthropometrical variables mass, centre of mass and moment of inertia of each segment were obtained from the database proposed by the National Aeronautics and Space Administration (NASA, 1978).

The study evolves around the basic mechanical variables in a two-dimension analysis: forces, moments of force, impulses, power and energy.

The only statistical results presented are descriptive ones (central tendency and dispersion), as there are only two or three subjects available.

Results and Discussion

Classical Inverse Dynamics

Figure 6.8 shows a representative example of a time course data from the vertical component (Fz) of the ground reaction force (GRF), as a function of the body weight (BW), during the performance of one of the selected jumps.

In classical ballet, according to very precise and restricted technical recommendations, all the landing phases of jumps must be performed softly, following the demand: the first contact should be done by the point of the toe, followed by the *metatarsus* joint, and finally the heel contact (Clarkon and Skrinar, 1988). In figure 6.8., the dotted circles indicate the force peaks respectively created by the end of the toe, the *metatarsus* joint, and the heel. The second dotted circle indicates the GRF passive peak.

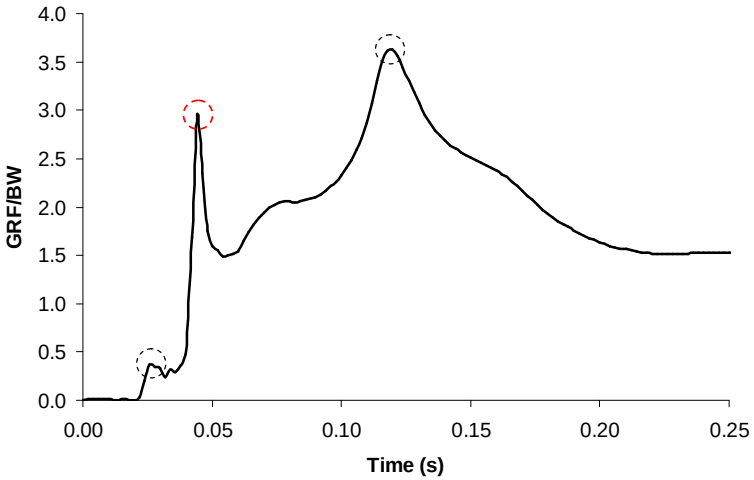

Figure 6.8. Representative example of a time course data from GRF as a function of the BW, during the performance of a selected jump. The dotted circles indicate the force peaks created respectively by the end of the toe, the *metatarsus* joint and the heel. The second dotted circle indicates the passive peak of GRF.

Based on the literature (Witzke and Snow, 2000) and our previous studies (Sousa et al. 2001, Sousa et al. 2002), high skeletal loading intensity has been defined as GRF of greater than four times the BW, moderate intensity as two to four times the BW, and low intensity as less than two times the BW.

In human locomotion, the impact forces results from the landing of the foot on the ground with a force maximum (passive peak) earlier than 50 ms (Nigg, 2000) after the first contact. In the present study, and in each subject (A, B, and C), the jumps were separated and grouped in moderate and high impact jumps, according to the peak values registered in the passive peak of the GRF curve (second dotted circle). Although in ballet technique terms, all the selected jumps were physically very demanding, it was possible to observe different impact loadings during their performance. All of the selected jumps reached values above two times the BW. The jumps that reached GRF passive peak values between two and four times the body weight were included in the moderate impact jumps group. All the other

jumps, were the GRF passive peak value surpasses four times the body weight were included in the group of high impact jumps (figure 6.9). The moderate or the high impact jumps groups include the same kind of jumps in each subject.

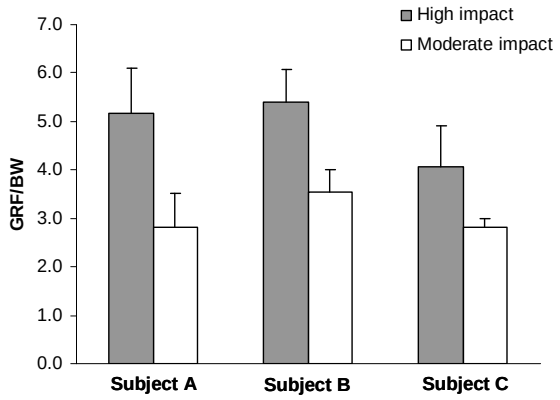

Figure 6.9. Average and SD peak ground reaction forces values from subject A, B, and C, during the moderate impact jumps and high impact jumps.

Figure 6.10, presents the average values of the time integrated GRF (impulse normalized to BW) in moderate and high impact jumps, for each subject. As expected, the impulse values in all subjects were always higher in high impact jumps than in moderate ones. As larger the impulse value is, the more energy will be dissipated and more effort will be necessary to perform the jump.

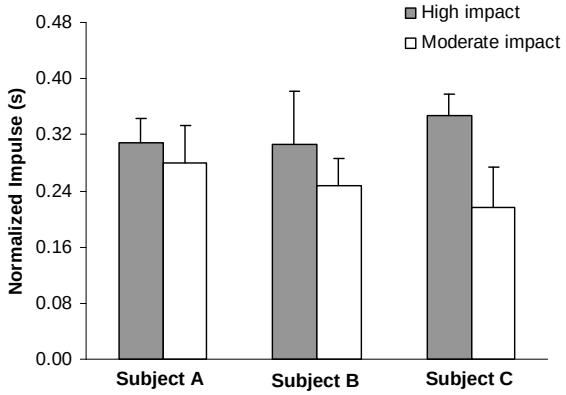

Figure 6.10. Average and SD normalized values of impulse of force from subject A, B, and C, during the moderate impact jumps and high impact jumps.

Figure 6.11 presents the normalized mean loading rate (force gradient) and standard deviation values to moderate and high impact jumps, for subject A, B, and C. In all subjects,

the mean loading rate values are higher in high impact jumps than in moderate impact jumps. According to Nigg et al. (2000) the loading rate of a force acting on the locomotor system is associated with the development of movement-related injuries. The results suggest that the loading rate in subject A in high impact jumps (much higher than in subjects B and C) may approach this injure regime.

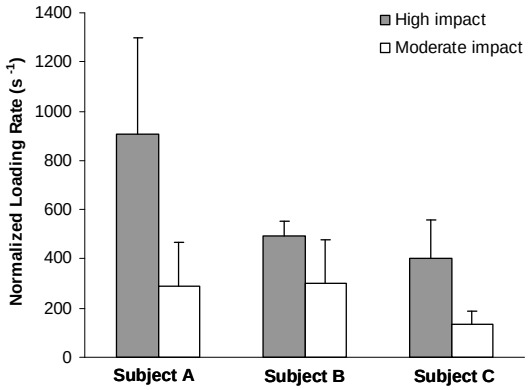

Figure 6.11. Normalized loading rate and SD values to moderate and high impact jumps, from subject A, B, and C.

The peak articular forces estimated by inverse dynamic (normalized to BW), in subject A, B, and C, in the ankle, knee and hip joints, during the performance of moderate and high impact jumps are presented in figure 6.12. The peak values of articular force decrease as we move upwards into the body, i.e., the ankle peak contact force is larger than the knee peak contact force, which in turn, is larger than the peak contact force in the hip joint, in every jump, and in each subject. This decrease of force from one joint to another is probably related to the dissipation of energy by the muscles.

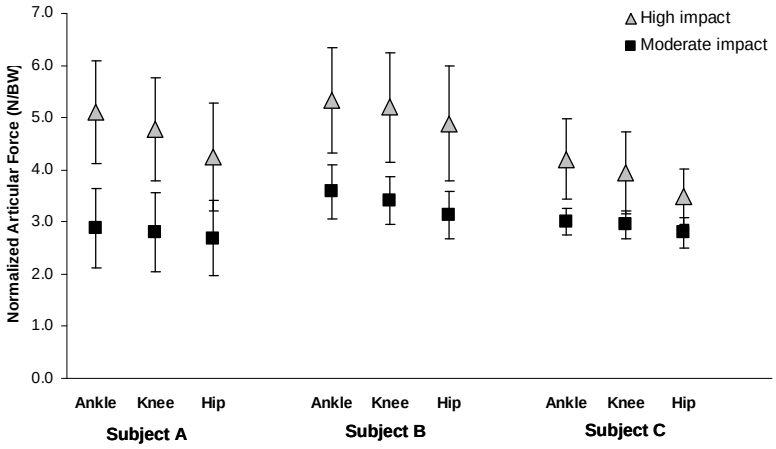

Figure 6.12. Average and SD values from peak articular force estimated in the ankle, knee and hip joints, from subject A, B, and C, during moderate and high impact jumps.

As observed, the peak articular force values obtained, during the moderate impact jumps are 3 to 4 times the body weight. For high impact jumps the values of peak articular force obtained, are 4 to 5 times the body weight, with exception of subject C, in the hip joint. The intra-subject variability observed in subject C, during the performance of both moderate and high impact jumps is smaller than in the other subjects, especially in moderate impact group, demonstrating more consistency in technical execution.

Figure 6.13 presents the integral average values of articular forces, normalized to the body weight from subjects A, B, and C in the ankle, knee and hip joints, during the execution of the moderate and high impact selected jumps. As we may observe, and in accordance with the previous chart, the integral average values of articular forces decrease from the ankle to the knee joint, and from the knee to the hip joint, in both moderate and high impact jumps, and in all subjects. This is just the same effect as in figure 6.12, but in the impulse space (variation of momentum).

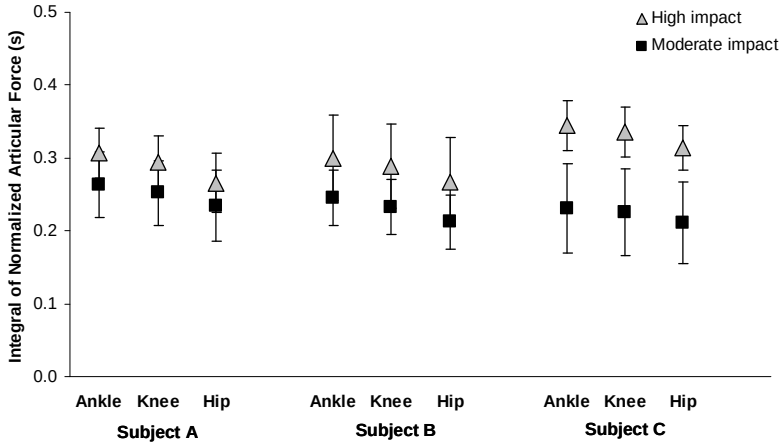

Figure 6.13. Average and SD values from normalized integral of articular force, estimated in the ankle, knee and hip joints, from subjects A, B, and C, during moderate and high impact jumps.

Figure 6.14 presents mean values of the articular moment, normalized to the body weight, in subjects A, B, and C in the ankle, knee and hip joints, during the execution of moderate and high impact selected jumps. The peak values of the articular moment decrease, comparing the ankle with the knee joint, and the knee with the hip joint, in every jump and in each subject, just like with the articular force peak values. However, note that the hip moments in subject B and C are flexor (negative), probably due to technical peculiarities and energy transfer mechanisms. Also the error bars are increasingly bigger (form ankle to hip), due to cumulative round off errors.

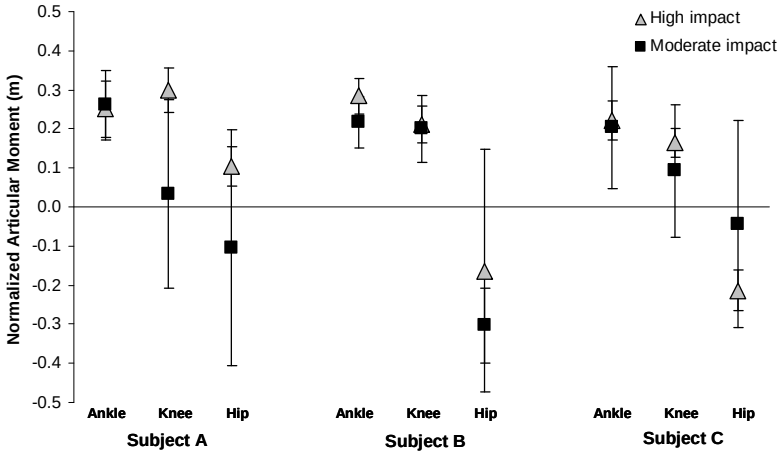

Figure 6.14. Average and SD values from normalized peak articular moment estimated in the ankle, knee and hip joints, from subject A, B, and C, during moderate and high impact jumps.

Figure 6.15 presents the mean values of the integral of the articular moment, normalized to the body weight and estimated in subjects A, B, and C in the ankle, knee and hip joints, during the execution of moderate and high impact selected jumps. The quantity decay from the ankle to the knee and then to the hip, is expected from the consecutive mass reduction. The ankle has to support all the body weight. The knee has to support all the weight, but the shanks, and the hip has to support all the weight but the shanks and the thighs. One other mechanism that complement this mass decay between adjacent segments and contributes to the reduction in articular moment is energy transfer between adjacent joints by the bi-articular muscles. The above charts (6.12 to 6.15) reflect this balance between the two effects (mass decay and energy transfer). At this point of analysis one cannot quantify each of the effects. However we emphasise the negative moment at the hip.

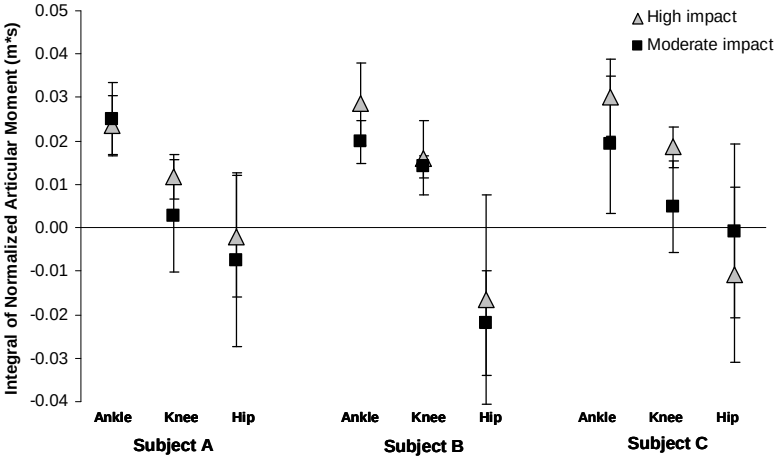

Figure 6.15. Average and SD values from the integral of normalized articular moment estimated in the ankle, knee and hip joints, from subject A, B, and C, during moderate and high impact jumps.

The normalized integral values of ankle and knee power (mechanical work) are presented in the figure 6.16.

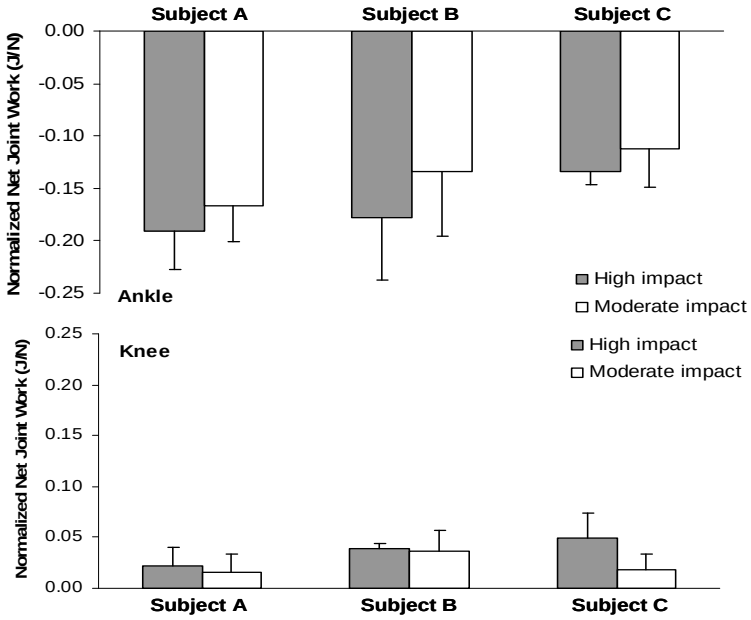

Figure 6.16. Average and SD values of the normalized net joint work, in the ankle and knee joints, from subject A, B, and C, during moderate and high impact jumps.

The mechanical power in the ankle joint was predominantly eccentric, as one would expect from a simple analysis. On the contrary, the mechanical power in the knee joint was predominantly concentric, nevertheless, with much smaller values. This is a consequence of the small knee excursion, with a small flexion (negative work), followed by an isometric phase (null work) and, finally, by a small extension (positive work). This is in clear contradiction with a bioenergetic approach, where all the terms are positive and additive (there is no such thing as negative energy expenditure or null expenditure at an isometric effort).

Due to the cumulative round off errors of the inverse dynamics algorithm (Hatze, 2000; Hatze, 2002), the hip joint values are not reliable enough to display. We will ignore them from know on.

This type of inverse dynamic analysis is especially important for the study of the contact forces and consequent articular tissue injury. The moments *per se* are difficult to analyse and less relevant from an injury perspective, unless a muscular decomposition is

performed. At this point a biomechanical analysis based on the net joints moments cannot elucidate the potentially different mechanical contributions of individual muscles to the overall movement performance. The muscular decomposition, nevertheless, is a very arguably technique as it needs some *Ad-Hoc* hypothesis, not even physiologically founded. Nonetheless, it is the most promising way of obtaining a muscular injury figure and energy transfer insight from the articular moments just obtained (Neptune et al., 2001).

Extended Inverse Dynamics (muscular decomposition) – no EMG data

Figure 6.17 presents the peak values from muscular force estimated in the eight muscle groups (mono and bi-articular) that compose our model: the *gluteus,* the *iliopsoas*, the hamstrings, the *rectus femoris*, the *vastus*, the *gastrocnemius*, the *tibialis*, and the *soleus*. The figure shows the data from subject A, B, and C in moderate and high impact jumps.

With few exceptions, the peak muscular forces in the high impact jumps are greater than the ones for the moderate impact jumps, but in all cases the differences have no statistically relevance.

In all subjects the peak muscular forces in *tibialis* and hamstrings muscles were smaller than the peak muscular forces obtained in the other muscles. The *iliopsoas*, *vastus* and *soleus* muscles showed a larger peak muscular force than the other muscles. There is an apparent consistency in the peak muscular force distribution across the three subjects.

The selected jumps of our study have different kinds of technical executions and have different muscular solicitations. For this reason, trying to better understand the performance of the different muscles, the jumps were divided in four groups, according to their characteristics.

In the figure 6.18 it is possible to observe the peak values from muscular force estimated in the eight muscle groups (mono and bi-articular) that compose our model, in the four groups of jumps selected: *sissounnes ouverte*, *jeté temps levé battu*, *ballonnés/ballottés/cabriole* and *grand jetés*.

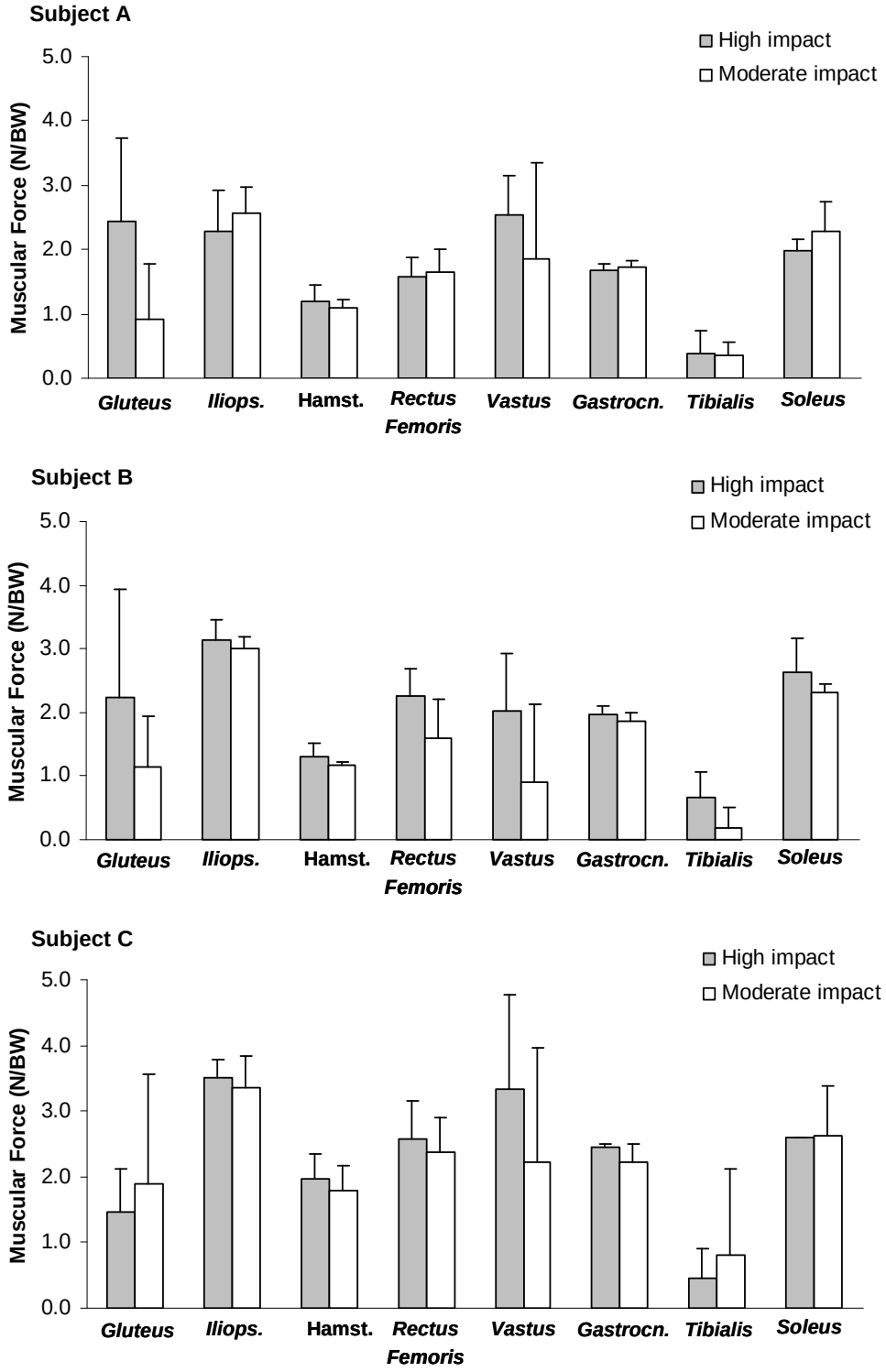

Figure 6.17. Average and SD values of the peak muscular force normalized to BW, in the *gluteus, iliopsoas*, hamstrings, *rectus femoris*, *vastus*, *gastrocnemius*, *tibialis*, and *soleus* muscle groups, in subject A, B, and C, during moderate and high impact jumps.

On the ankle joint, the *soleus* (mono-articular) has larger peak forces than the *gastrocnemius* (bi-articular agonist) and both are larger that the antagonist *tibialis*. On the knee joint things are not so regular with a distribution depending slightly on the jump type and subject. Contrary to an elementary reasoning, the *hamstrings* play a significant role in all jumps and subjects.

There is a variation between subjects probably related to technical execution (e.g. *gluteus* on the *sissounnes ouverte*) and there is also a variation between jumps (e.g. *vastus* between the *jeté temps levé battu* and the *grand jetés*). These variations make it difficult to extract global conclusions about the population or the jumps. In fact these types of analysis should ideally be case specific.

A similar analysis can be done over the integrated forces (impulse) shown in figures 6.19 and 6.20.

In the *per subject* analysis (figure 6.19), the role of the *tibialis* muscle is even less relevant, comparatively with its antagonists *soleus* and *gastrocnemius*. In the knee joint, the *gastrocnemius* is also the most relevant muscle, with all the other with similar values. In the hip joint the *iliopsoas* has much higher values than the gluteus.

In the *per jump* analysis (figure 6.20) we can draw the same conclusions. The *gastrocnemius* and the *soleus* have more or less the same impulse, and the *tibialis* is, with the exception of subject C on the j*eté temps levé battu*, almost zero. This is consistent with what we would expect from landing movements. At the knee joint, the role of the various muscles is more balanced, but is subject and movement dependent. At the hip joint one would expect the gluteus to have the most relevant role, but this is not the case as the *iliopsoas* is the one with greater impulse.

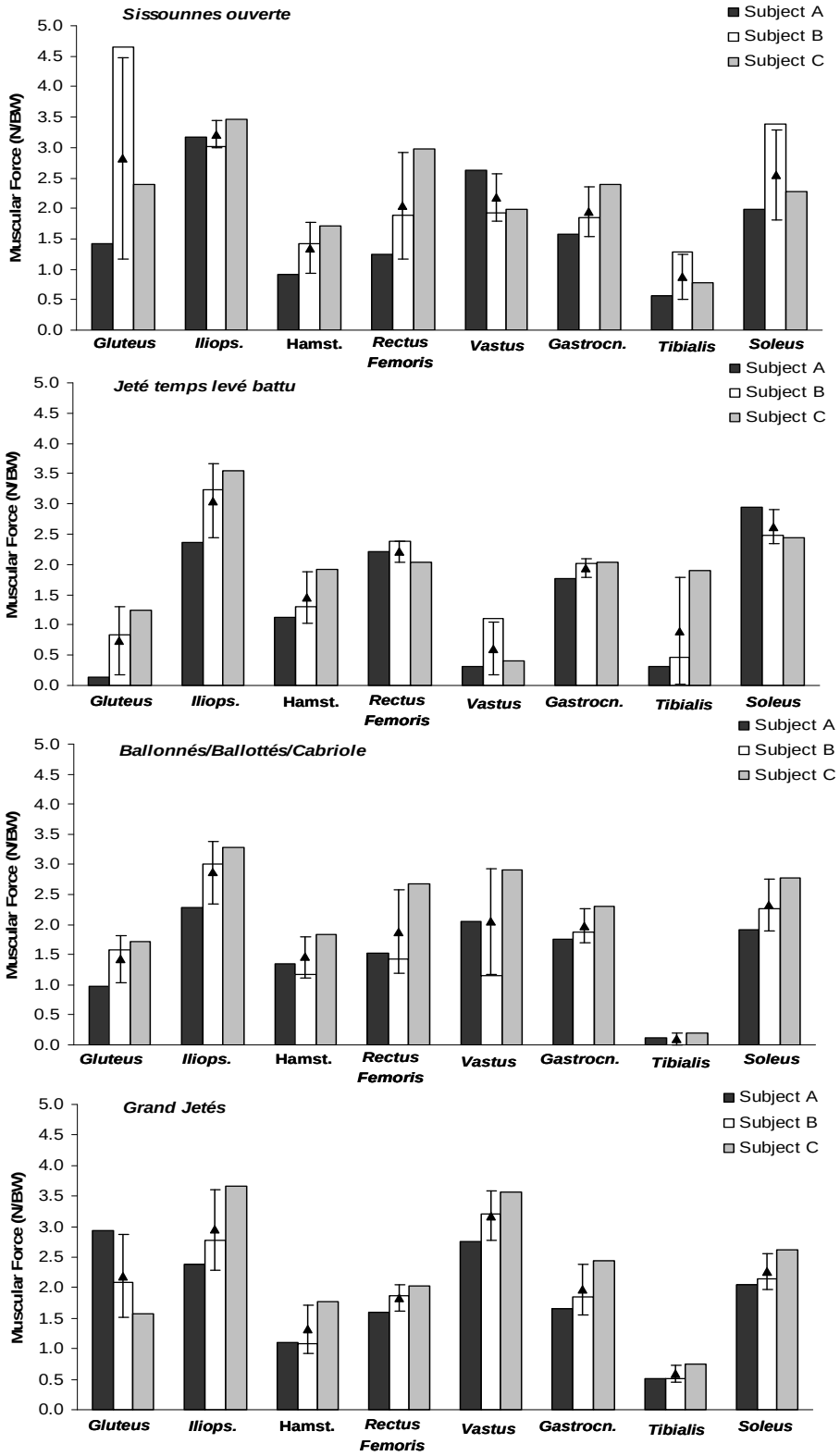

Figure 6.18. Average values of the peak muscular force normalized to BW, in the *gluteus, iliopsoas*, hamstrings, *rectus femoris*, *vastus*, *gastrocnemius*, *tibialis*, and *soleus* muscle groups, in subject A, B, and C, during *Sissounnes ouverte*, *Jeté temps levé battu*, *Ballonnés/Ballottés/Cabriole* and *Grand Jetés* jumps. The small triangles with error bars indicate the normalized mean and SD values for the three subjects.

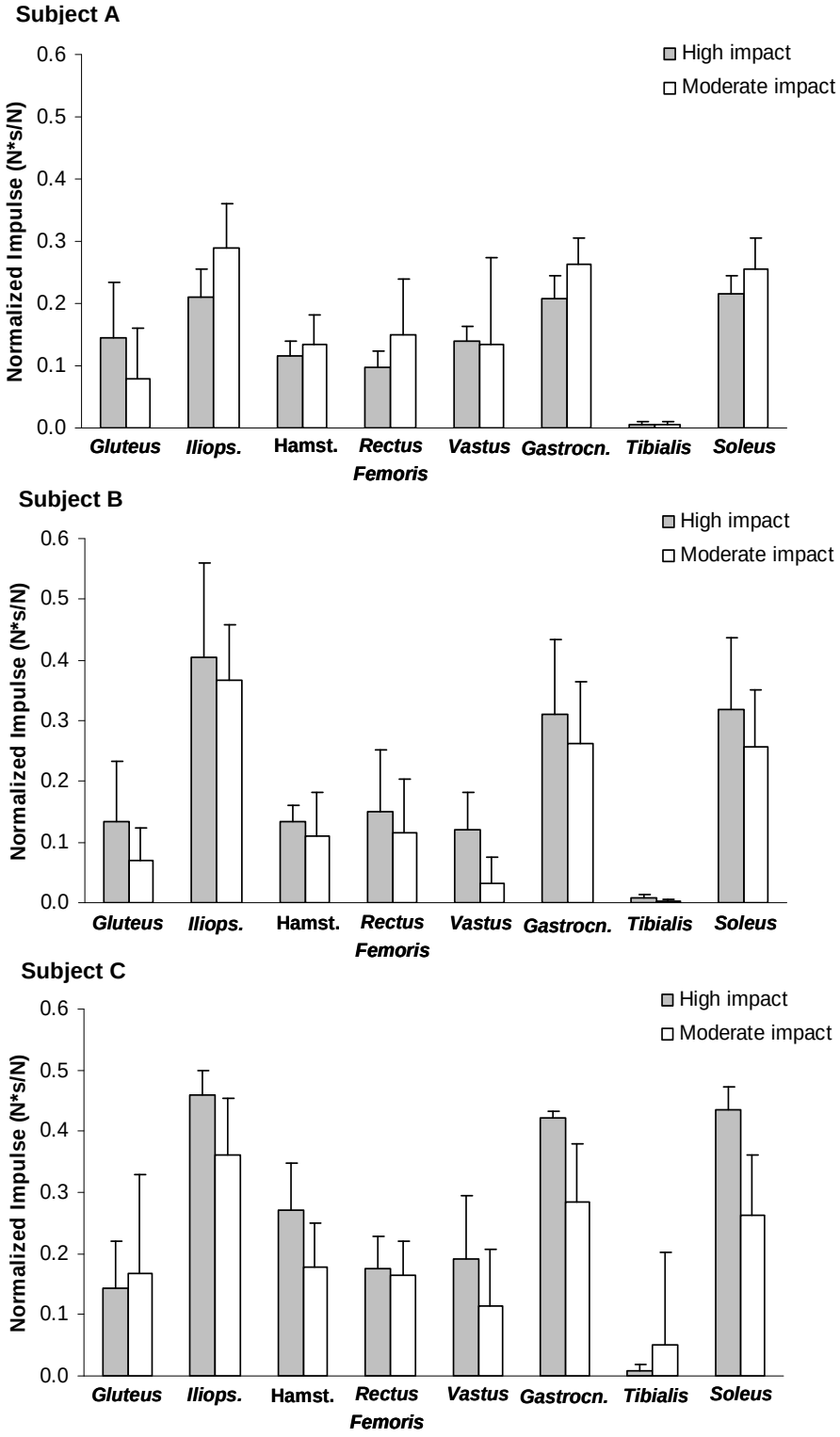

Figure 6.19. Average and SD values of the normalized impulse, in the *gluteus, iliopsoas*, hamstrings, *rectus femoris*, *vastus*, *gastrocnemius*, *tibialis*, and *soleus* muscle groups, in subject A, B, and C, during moderate and high impact jumps.

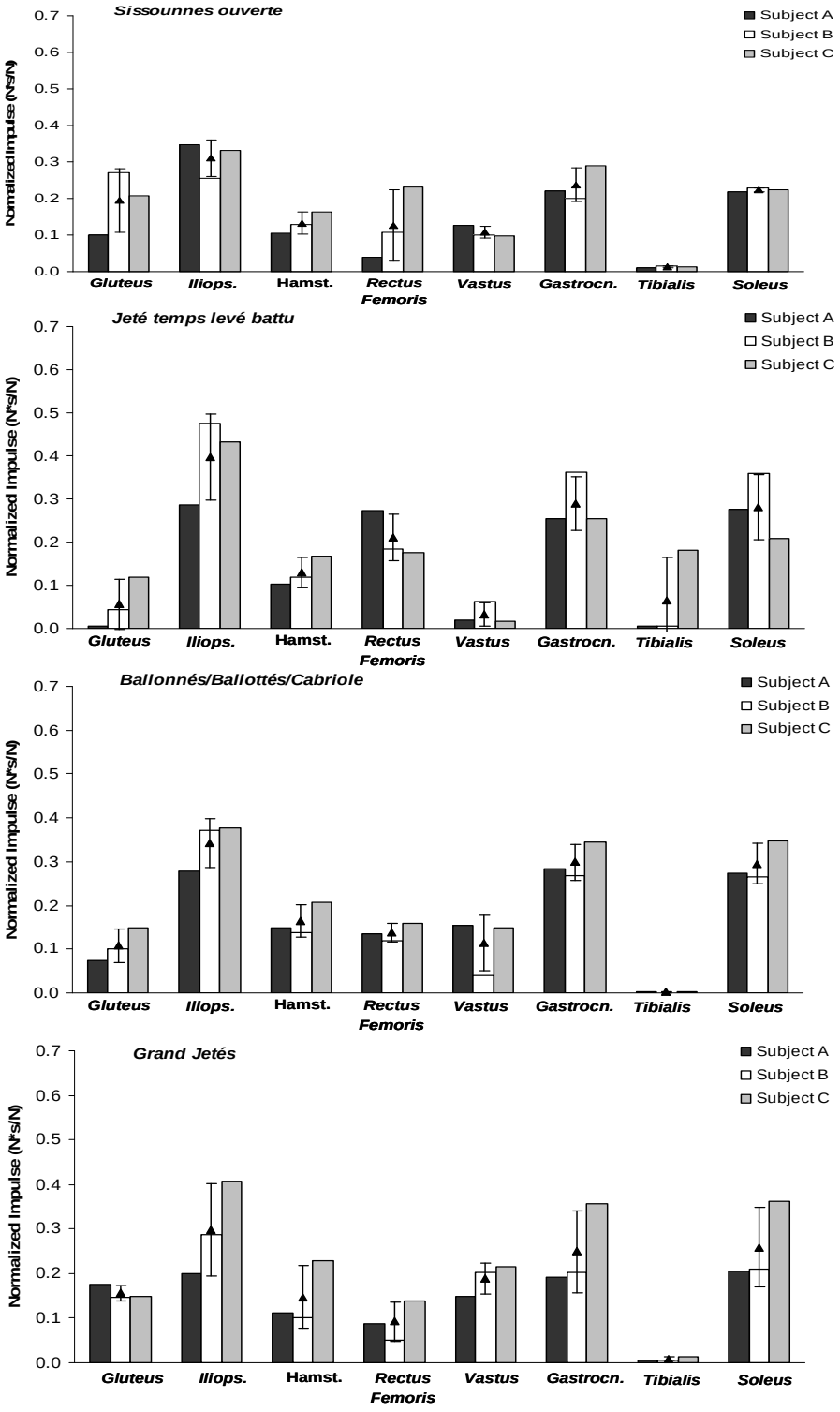

Figure 6.20. Average values of the normalized impulse, in the *gluteus, iliopsoas*, hamstrings, *rectus femoris*, *vastus*, *gastrocnemius*, *tibialis*, and *soleus* muscle groups, in subject A, B, and C, during *Sissounnes ouverte*, *Jeté temps levé battu*, *Ballonnés/Ballottés/Cabriole* and *Grand Jetés* jumps. The small triangles with error bars indicate the normalized mean and SD values for the three subjects.

The contribution of a muscle to external work depends on the amount of power a muscle can generate. Figure 6.21 presents the peak values of mechanical power normalized to BW estimated in the eight muscle groups (mono and bi-articular) that compose our model: the *gluteus,* the *iliopsoas*, the hamstrings (proximal and distal ends), the *rectus femoris* (proximal and distal ends), the *vastus*, the *gastrocnemius* (proximal and distal ends), the *tibialis*, and the *soleus*. The figure shows the data from subjects A, B, and C, in moderate and high impact jumps.

Being the receptions from vigorous jumps the movements selected in this study, we expect the *rectus femoris*, *vastus*, *gastrocnemius* and *soleus* to be the most solicited muscles, in eccentric regime (negative power). As it is possible to observe in all subjects, the peak values of mechanical power were especially high and eccentric in the distal portion of the *gastrocnemius* and in the *soleus* muscles. Around the knee joint the *vastus* and the distal end of the *rectus femoris* are the most significant muscles, working concentrically. At the hip joint there is no defined pattern. Relevant is the fact that the higher in the body the lower are the muscle powers produced, as expected (mass reduction).

The tendency of the muscular power produced in the several muscles studied and both groups of high or moderate impact jumps is similar in all subjects.

This figure (6.21) shows that the bi-articular muscles, although crossing two joints, have a joint where the majority of its power is developed - usually the distal one. Comparing the mono-articular with the bi-articular muscles, we see no defined preference on either of them, with subjects with a bigger role in the *vastus* and *soleus* (subject A) and others with a bigger role on the distal portions of the *rectus femoris* and *gastrocnemius* muscles. This shows that the optimisation criteria do not *prefer* the mono or the bi-articular muscles and so does not introduce a significant bias in this matter.

In figure 6.22 it is possible to observe the peak values of mechanical power normalized to BW, in the eight muscle groups (mono and bi-articular) that compose our model (proximal and distal ends), in the four groups of jumps selected: *sissounnes ouverte*, *jeté temps levé battu*, *ballonnés/ballottés/cabriole*, and *grand jetés*.

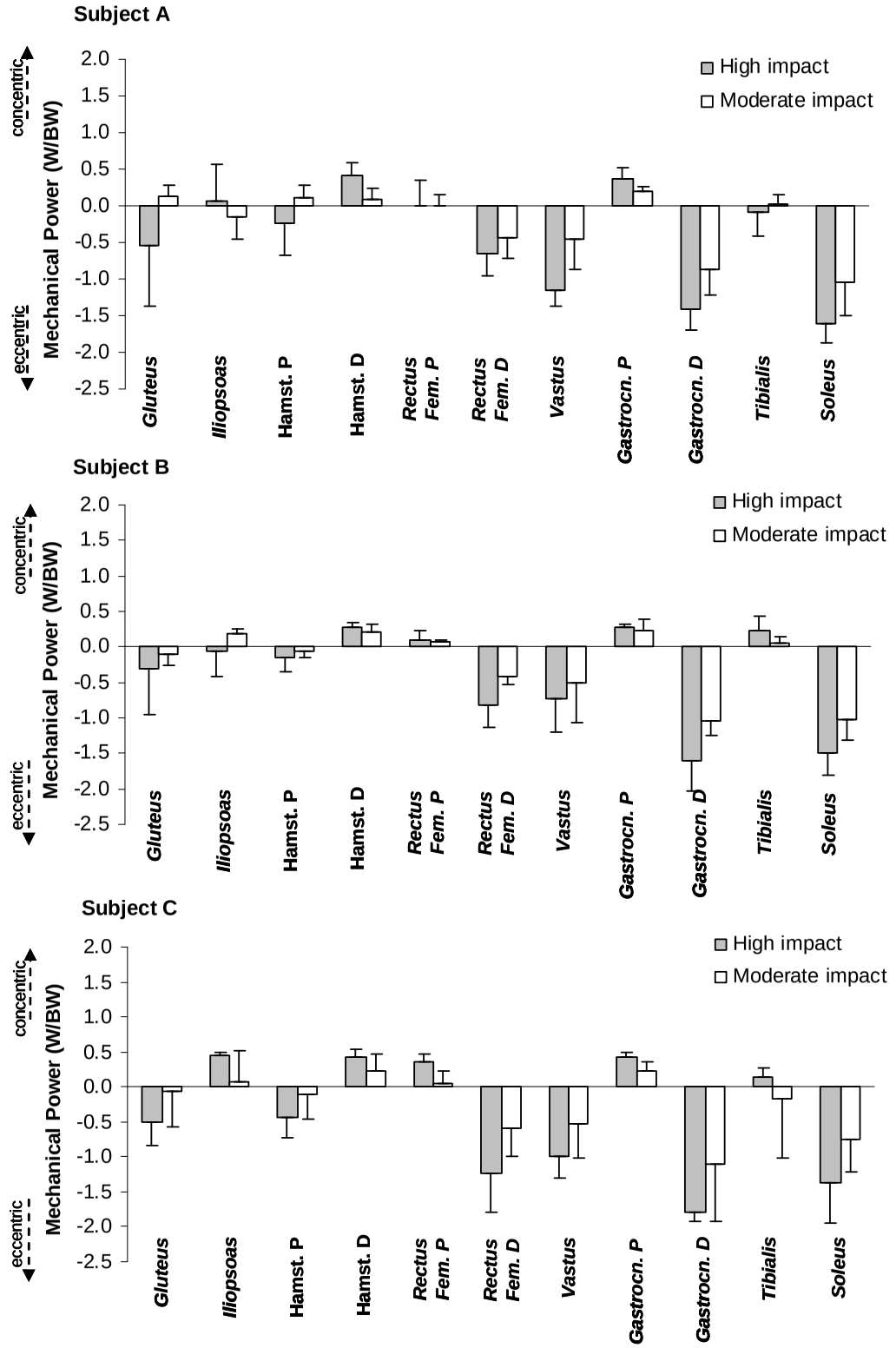

Figure 6.21. Average and SD values from peak mechanical power normalized to BW in the *gluteus, iliopsoas*, hamstrings (proximal (P) and distal (D) ends), *rectus femoris* (proximal (P) and distal (D) ends), *vastus*, *gastrocnemius* (proximal (P) and distal (D) ends), *tibialis*, and *soleus* muscle group, in subject A, B, and C, and in moderate and high impact jumps.

As it is possible to observe in figure 6.22, there are no new observations as the *soleus*, *gastrocnemius*, *vastus* and *rectus* muscles behave generically in the same way and the other muscles have a much less significant role. The most notable fact is that in the *jeté temps levé battu* the *vastus* (mono-articular) is working less than the distal portion of the *rectus femoris* and in the *grand jetés* the situation is reversed. This is probably technical related as is consistent over all subjects.

Muscle mechanical energy expenditure (or power) is an important quantity to analyse in human locomotion, since it reflects the neuromuscular strategies used by the nervous system and is directly related to the efficiency of the movement (Sasaki and Neptune, 2006; Zajac et al., 2002). The performance of different motor tasks requires the coordination of the many involved muscles. An accurate determination of muscle function requires the quantification of the contributions of individual muscles to the energetics of individual body segments (Neptune et al., 2001). The energetics of walking, running, and other movements has been very difficult to explain, because the distribution of energy used among individual muscles has not yet been determined.

Figure 6.23 presents the mean values of mechanical energy estimated in the eight muscle groups (mono and bi-articular) that compose our model: the *gluteus*, the *iliopsoas*, the hamstrings (proximal and distal ends), the *rectus femoris* (proximal and distal ends), the *vastus*, the *gastrocnemius* (proximal and distal ends), the *tibial*, and the *soleus*. The figure shows the data from subject A, B, and C in moderate and high impact jumps.

The tendency of the mechanical energy produced in the several muscles studied in both groups of high or moderate impact jumps is similar to the observed for the peak power (figure 6.21). As it is possible to observe in all subjects, mechanical energy values are especially higher in the *rectus femoris* (distal end), *vastus*, *gastrocnemius* (distal end) and *soleus* muscles, in moderate and high impact jumps, around the knee and ankle joints. The ankle and knee are flexing in the landing phase and so, as expected, all these muscles work eccentrically.

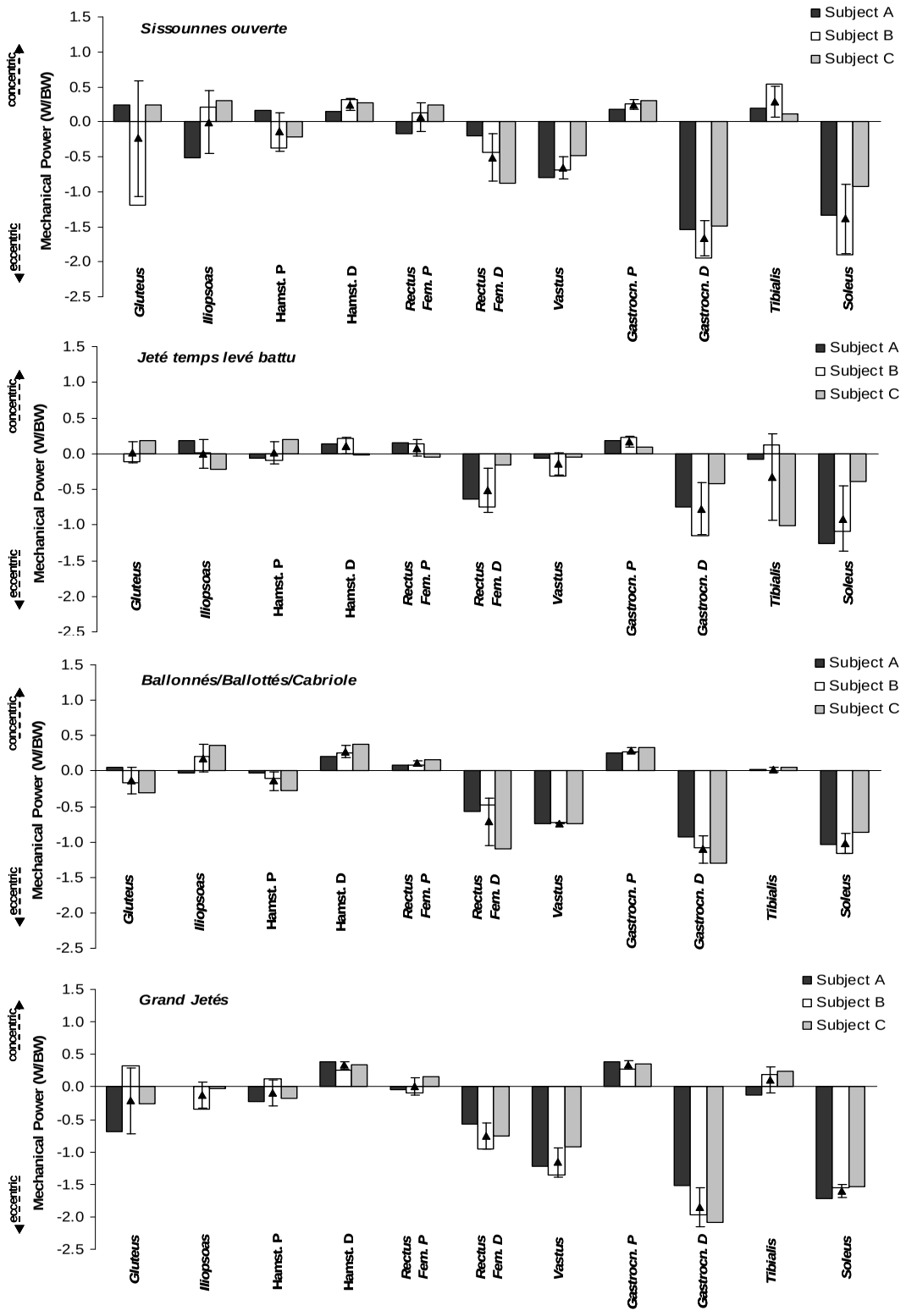

Figure 6.22. Average values from peak mechanical power normalized to BW in the *gluteus, iliopsoas*, hamstrings (proximal (P) and distal (D) ends), *rectus femoris* (proximal (P) and distal (D) ends), *vastus*, *gastrocnemius* (proximal (P) and distal (D) ends), *tibialis*, and *soleus* muscle groups, in subject A, B, and C, during *Sissounnes ouverte*, *Jeté temps levé battu*, *Ballonnés/Ballottés/Cabriole* and *Grand Jetés* jumps. The small triangles with error bars indicate the normalized mean and SD values for the three subjects.

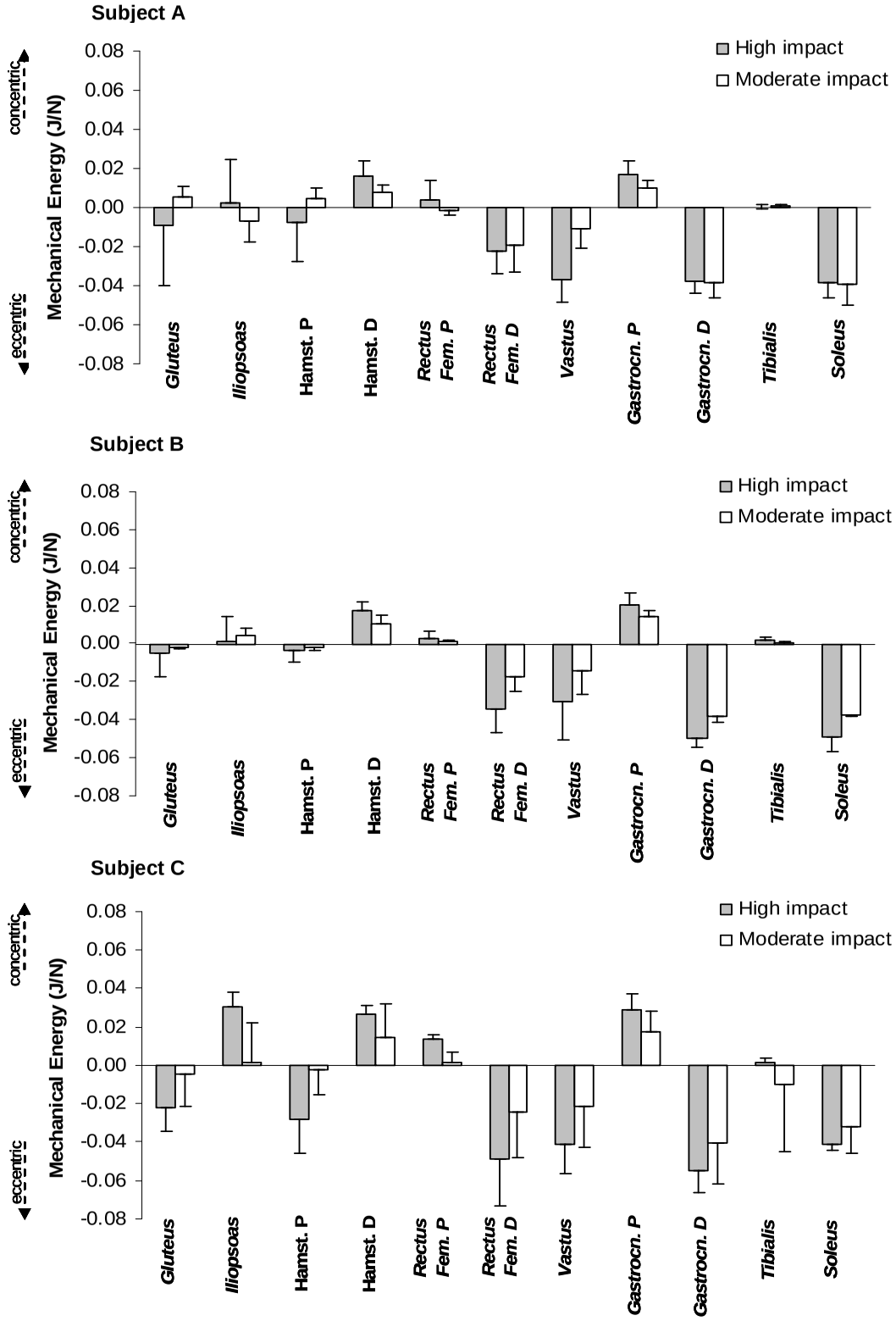

Figure 6.23. Average and SD values from mechanical energy normalized to BW estimated in the *gluteus, iliopsoas*, hamstrings (proximal (P) and distal (D) ends), *rectus femoris* (proximal (P) and distal (D) ends), *vastus*, *gastrocnemius* (proximal (P) and distal (D) ends), *tibialis*, and *soleus* muscle groups, in subject A, B, and C, and in moderate and high impact jumps.

A decomposition by jump type is presented in figure 6.24, where we report the mean values of mechanical energy normalized to BW, in the eight muscle groups (mono and bi-articular) that compose our model (proximal and distal ends), in the four groups of jumps selected: *sissounnes ouverte*, *jeté temps levé battu*, *ballonnés/ballottés/cabriole* and g*rand jetés*. Similarly to the previous case and to the peak power analysis, the *vastus* and the *rectus femoris* (distal end), have a similar participation at the knee at all jumps. The same happens with the *soleus* and the *gastrocnemius* (distal end) at the ankle joint. The only remarkable note is the intense eccentric participation of the *tibialis* in subject C during the *jeté temps levé battu*, in what is most probably an error from unknown provenience or an unexpected cocontraction.

Figure 6.25 shows a representative example of how the mechanical energy flows between segments, for the three bi-articular muscles included in our model. The example shows the mechanical energy transfer estimated in the proximal and distal joints, for the *gastrocnemius* muscle group (1), *rectus femoris* muscle (2), and in the hamstrings muscle group (3), during the performance of a moderate impact jump.

It is known from literature, that the *gastrocnemius* muscle plays an unique role in power transfer from knee to ankle joint in jumping exercises (Bobbert et al., 1986a; Bobbert et al., 1986b; Gregoire et al., 1984; van Ingen Schenau et al., 1987; van Zandwijk et al., 1998), and nearly 50% of the total mechanical energy of the body is stored in the AT and arch of the foot during movements such as walking, running or jumping (Alexander and Bennet-Clark, 1977; Ker et al., 1987).

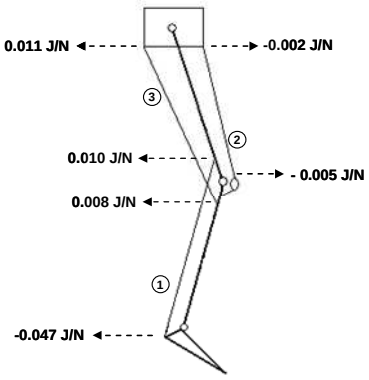

Figure 6.25. Representative example of the mechanical energy transfer estimated in the proximal and distal joints, during the performance of a ballet jump (moderate impact), in the *gastrocnemius* (1), *rectus femoris* (2) and hamstrings (3) muscle groups.

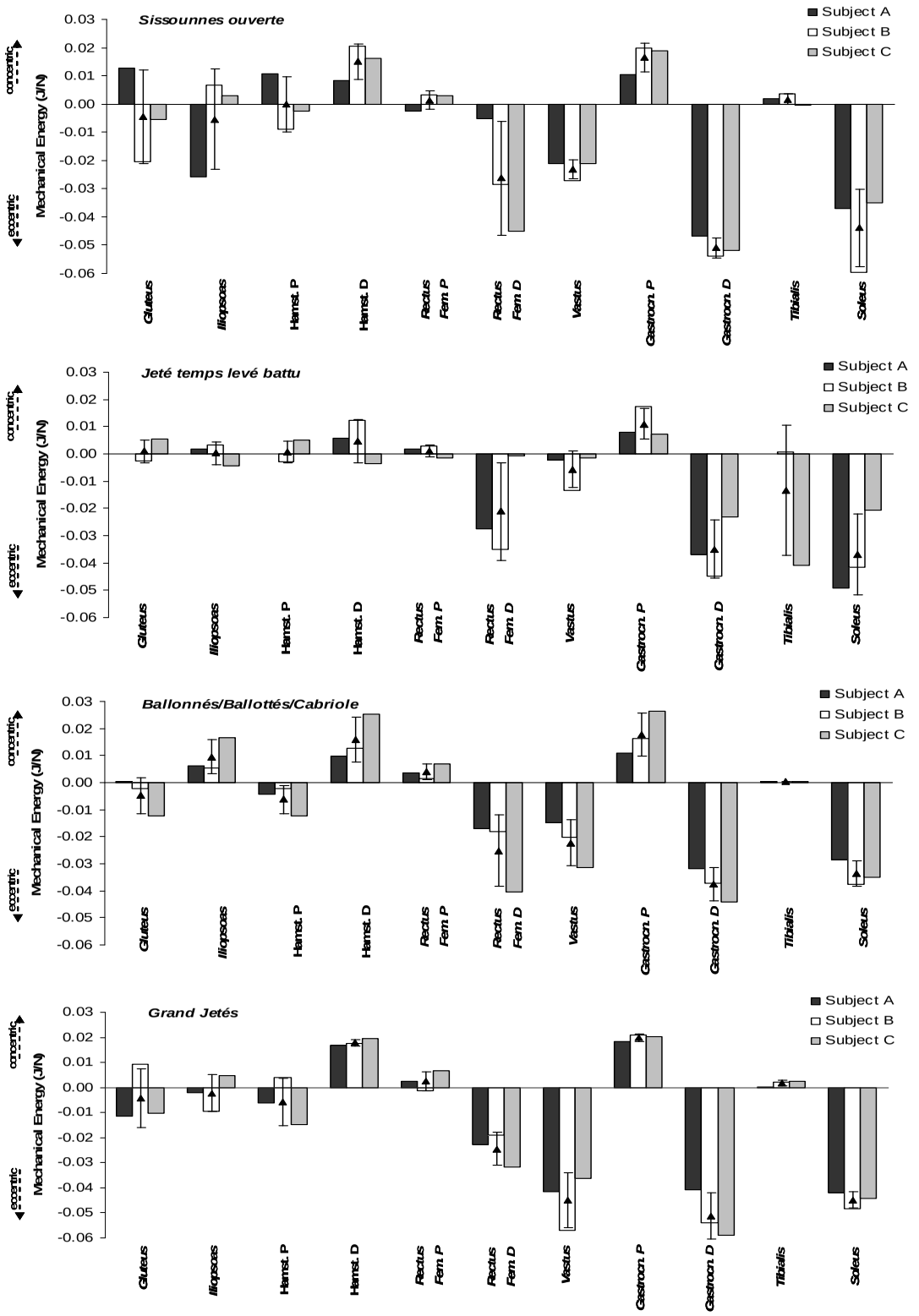

Figure 6.24. Average values from mechanical energy normalized to BW estimated in the *gluteus, iliopsoas*, hamstrings (proximal (P) and distal (D) ends), *rectus femoris* (proximal (P) and distal (D) ends), *vastus*, *gastrocnemius* (proximal (P) and distal (D) ends), *tibialis*, and *soleus* muscle groups, in subject A, B, and C, during *Sissounnes ouverte*, *Jeté temps levé battu*, *Ballonnés/Ballottés/ Cabriole* and *Grand Jetés* jumps. The small triangles with error bars indicate the normalized mean and SD values for the three subjects.

In the figure 6.25, in the *gastrocnemius* muscle (1), the total mechanical energy estimated was about 57 mJ/N, distributed to the distal (ankle) and proximal (knee) joints, respectively, 47 mJ/N and 10 mJ/N. Effectively, from the 47 mJ/N that the muscle must absorbed, only about 37 mJ/N will be really absorb by the ankle joint, since about 10 mJ/N will be transferred upward to the knee joint. In this example, the concentric movement of the *gastrocnemius* muscle around the knee joint (10 mJ/N) will reduce the angle between the thigh and the shank. On the other hand, the eccentric movement of the *gastrocnemius* muscle around the ankle joint (47 mJ/N) will reduce the angle between the shank and the foot. In the *rectus femoris* muscle (2), the mechanical energy estimated was 2 mJ/N to the proximal joint (hip) and 5 mJ/N to the distal joint (knee). The eccentric movement of the *rectus femoris* muscle (2m J/N), around the hip joint will tend to straighten the trunk. On the other hand, the eccentric movement of the *rectus femoris* muscle (5 mJ/N), around the knee joint will reduce the angle between the thigh and the shank. In this example, effectively, in both proximal and distal ends, there's no energy transfer between muscular groups. The muscular group dissipate all the energy supplied by both extremities. In relation to the hamstrings muscle (3), the mechanical energy estimated was 11 mJ/N to the proximal joint (hip) and 8 mJ/N to the distal joint (knee).The concentric movement of the hamstrings muscle (11 mJ/N), around the hip joint will tend to straighten the trunk, increasing the angle between the trunk and the thigh. On the other hand, the concentric movement of the hamstrings muscle (8 mJ/N), around the knee joint will reduce the angle between the thigh and the shank.

Table 6.2 presents the energy transfer estimated for subject A, B, and C, in the proximal and distal ends, of the *gastrocnemius*, *rectus femoris*, and in the hamstrings muscles, during the performance of high and moderate impact jumps.

Values of energy transfer near 100% means an almost total energy transfer. Values above 100% means the energy transfer is in direction from proximal to distal joints. And finally, a negative value of energy transfer refers to the simultaneous concentric or simultaneous eccentric works. In these cases there are no energy transfers and the bi-articular muscle is not taking advantage over the mono-articular muscles.

Table 6.2. Energy transfer (mJ/N) estimated in the proximal and distal joints (P and D), of the hamstrings, *rectus femoris,* and *gastrocnemius* muscles during the performance of high and moderate impact jumps, in subject A, B, and C.

Jump/Muscle	Hamst. P	Hamst. D	*Rectus* P	*Rectus* D	*Gastroc.* P	*Gastroc.* D
Subject A						
High Impact (mJ/N)	-8.00	-16.00	4.00	23.00	-17.00	-38.00
% energy transfer	50%		17%		45%	
Moderate Impact (mJ/N)	5.00	-8.00	-1.00	19.00	-10.00	-39.00
% energy transfer	-63%		-6%		26%	
Subject B						
High Impact (mJ/N)	-3.00	-17.00	2.00	34.00	-21.00	-50.00
% energy transfer	19%		7%		41%	
Moderate Impact (mJ/N)	-2.00	-10.00	1.00	18.00	-14.00	-39.00
% energy transfer	16%		7%		37%	
Subject C						
High Impact (mJ/N)	-28.00	-27.00	14.00	49.00	-29.00	-55.00
% energy transfer	104%		28%		53%	
Moderate Impact (mJ/N)	-3.00	-14.00	2.00	24.00	-17.00	-40.00
% energy transfer	18%		7%		43%	

When there is a distal eccentric work and a proximal concentric one, the bi-articular muscle is minimizing its length changes (its mechanical work) and transferring some load to the next joint, resulting in an effective work lower than the one needed by a pair of mono-articular muscles on the same joints. If, as usual in landing tasks, the eccentric work is higher (in absolute value) than the proximal one, the muscle is transferring energy from the distal to the proximal end – positive transfer. If the proximal work is higher (in absolute value) than the distal one, as is usual in take-off tasks, the energy transfer is from the proximal to the distal joints – negative transfer. Other situations are possible, as a simultaneous concentric or simultaneous eccentric works. In these cases there is no energy transfer and the bi-articular muscle is not taking advantage over the mono-articular muscles.

In table 6.2 it is apparent the usage of energy transfer mechanism in subject A, at least in the high intensity jumps. In the low intensity ones, the *hamstrings* and *rectus* have no energy transfer as the former is working concentrically in both joints and the later is working eccentrically. In subject B the energy transfer is used in all jumps (curiously is technically the best performer). In subject C all except the hamstrings in the high impact jumps are transferring energy. However the hamstrings are working almost isometrically (a very small negative energy transfer) and this small difference to the full energy transfer case (100%), may be due to computation errors.

Table 6.3 presents the energy transfer estimated for subject A, B, and C, in the proximal and distal joints, of the *gastrocnemius*, *rectus femoris*, and in the hamstrings muscle groups, during the performance of *Sissounnes ouvert*, *Jeté temps levé battu*, *Ballonés/ Ballottés/Cabriole* and *Grand Jetés* jumps.

Table 6.3. Energy transfer (mJ/N) estimated in the proximal and distal joints (P and D) of the hamstrings, *rectus femoris,* and *gastrocnemius* muscle groups during the performance of *Sissounnes ouverte*, *Jeté temps levé battu*, *Ballonnés/ballottés/cabriole* and *Grand Jetés* jumps.

Jumps/Muscle	Hamst. P	Hamst. D	*Rectus* P	*Rectus* D	*Gastroc.* P	*Gastroc.* D
Sissounnes (mJ/N)	-0.14	-15.00	1.00	26.00	-16.00	-51.00
% energy transfer	1%		5%		32%	
Jeté Tenleve Battu (mJ/N)	0.69	-5.00	1.00	21.00	-11.00	-35.00
% energy transfer	-15%		5%		31%	
Ballonnés/ballottés/cabriole (mJ/N)	-6.00	-16.00	4.00	25.00	-18.00	-38.00
% energy transfer	40%		16%		47%	
Grand Jetés (mJ/N)	-6.00	-18.00	3.00	24.00	-20.00	-51.00
% energy transfer	32%		11%		39%	

It is apparent a systematic and efficient usage of energy transfer mechanism in all the jumps selected except in hamstrings muscles in the *jeté temps levé battu*. In classical ballet the turnout of the lower limbs at the hip joint makes the hamstrings play the role of the *adductors*. In the *jeté temps levé battu* the adductors/abductors are highly solicited, and so the hamstrings role has to be understood in this context.

The results suggest that the forces of bi-articular muscles are organized in order to provide efficient performance of jumps (Prilutsky et al., 1996; Prilutsky and Zatsiorsky, 1994). According to the author's the design of the *gastrocnemius* muscle (high percentage of fast-twitch muscle fibres, large pennation angles, short fibre lengths, and long tendons) seems to be well suited for transferring mechanical energy between the ankle and the knee, due to the favourable contractile abilities of this muscle at high speeds of locomotion, trotting, etc. In this way, the *gastrocnemius* muscle might be useful in distributing mechanical energy between the ankle and the knee when there is an increase demand for mechanical energy to be absorbed or generated at the ankle joint.

Extended Inverse Dynamics (muscular decomposition) – with EMG data

A hybrid scheme that combines forward and inverse dynamics methods was presented by Lloyd and Buchanan (2003) to examine the loads experienced by muscles and ligaments in the knee during walking, running and cutting manoeuvres. They colleted EMG from ten

muscles and, muscle forces and ligaments were estimated. According to Buchanan et al. (2004), the calibration of this EMG-driven model was done by comparing the joint flexion-extension moments obtained from the forward solution with those obtained from the inverse dynamics solution. The squared differences between the two solutions were used to adjust the model parameters. The authors suggest that the model is able to predict joint moments very well, as well as muscle forces. The same procedures for calibration identical models were used for several other authors (Bogey et al., 2005)

Figure 6.26 presents the peak values from muscular force estimated in the eight muscle groups (mono and bi-articular) that compose our model: the *gluteus,* the *iliopsoas*, the hamstrings, the *rectus femoris*, the *vastus*, the *gastrocnemius*, the *tibialis*, and the *soleus*. The activation values for the hamstrings (*biceps femoris)*, *vastus* (lateralis and medialis), *gastrocnemius* (medialis), *tibialis*, and the *soleus* muscles, were obtained from the EMG records. As the EMG records for the *gluteus, iliopsoas*, and the *rectus femoris* muscles could not be obtained, the activation values for these muscles were estimated by optimization (minimizing the sum of the squared forces produced). The figure shows the data from subject A and B in moderate and high impact jumps. Due to technical problems, the EMG data from subject C could not be considered.

With few exceptions, the peak muscular forces in the high impact jumps are greater than the ones for the moderate impact jumps, but with no statistical significance.

In all subjects the peak muscular forces in *tibialis* and hamstrings muscles were smaller than the peak muscular forces obtained in the other muscles. The *vastus* and *soleus* muscles showed a larger peak muscular force that the other muscles. There is an apparent consistency in the peak muscular force distribution across the two subjects.

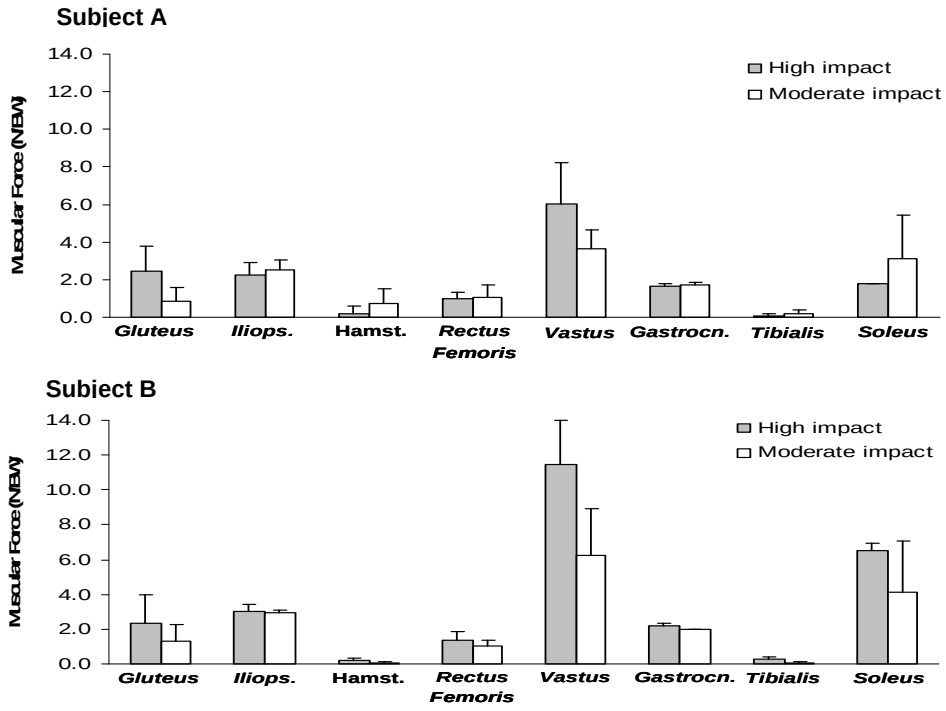

Figure 6.26. Average and SD values of the peak muscular force normalized to BW, in the *gluteus, iliopsoas*, hamstrings, *rectus femoris*, *vastus*, *gastrocnemius*, *tibialis*, and *soleus* muscle groups, in subject A, and B, during moderate and high impact jumps.

Comparing these results with the ones from a pure optimization (figure 6.17) it is possible to note an increased role of the mono-articular muscles *vastus* and *soleus* over the bi-articular agonist's *rectus* and *gastrocnemius*, respectively.

The selected jumps of our study have different kinds of technical executions and have different muscular solicitations. For this reason, trying to better understand the performance of the different muscles, the jumps were divided in four groups, according to their characteristics. In the figure 6.27 it is possible to observe the peak values from muscular force estimated in the eight muscle groups (mono and bi-articular) that compose our model in: *sissounnes ouverte*, *jeté temps levé battu*, *ballonnés/ballottés/cabriole* and *grand jetés*.

On the ankle joint, the *soleus* (mono-articular) has larger peak forces than the *gastrocnemius* (bi-articular agonist) and both are larger that the antagonist *tibialis*. On the knee joint the prevalence of the *vastus* over the bi-articular agonist *rectus* and the almost complete absence of the hamstrings (antagonists), is the observable pattern in all jumps. Contrary to the results obtained previously from a pure optimization, we see an increased

role of the mono-articular muscles and a decrease of the antagonists' role, i.e. reduced cocontractions.

There is a large variation between subjects, e.g. *vastus* in all jumps and *soleus* in *sissounnes ouverte* and *grand jetés*, but there are no significative variations between jumps. This is probably related to differences in technical execution.

Similar analysis can be done over the integrated forces (impulse) in figures 6.29 and 6.30.

Figure 6.28 (A and B) shows a representative example of estimated values from muscular force in the *gluteus, iliopsoas*, hamstrings, *rectus femoris*, *vastus*, *gastrocnemius*, *tibialis*, and *soleus* muscle groups, in subject A during a moderate impact jump. In figure 6.28 (A) the activation values for the several muscles were obtained by pure optimization procedure. In figure 6.28 (B) the activation values for the hamstrings (*biceps femoris)*, *vastus* (*lateralis* and *medialis*), *gastrocnemius* (*medialis*), *tibialis*, and the *soleus* muscles, were obtained from the EMG records. The activation values for the other muscles were optimized.

Comparing the two plots (A and B) of the figure 6.28, we can see an increased role of the mono-articular muscle *vastus* in the case were the EMG record is used for generating the activation function over the case were the activation is exclusively obtained by optimization. This trend is generally observed in this study and is the major difference between the two cases. The other curves from muscular force do change from case to the other but only slightly and without significantly changing the statistics of figures 6.26, 6.27, 6.29 to 6.34 when compared with figures 6.17 to 6.24.

In a study from Cholewicki et al. (1995), the authors present a complex model to estimate joint compressive forces in L4/L5 lumbar joints, using a pure optimization approach and an EMG assisted approach, in order to determine if the distribution of the forces and possible injury mechanisms were the same. They found significant differences between the two methods in the estimation of compressive forces and the injury risk of the exerted loads. The authors suggest that, in spite of the both methods need further improvements, the EMG assisted approach, due to its biological content, has a considerable potential and confidence in estimation individual muscle forces.

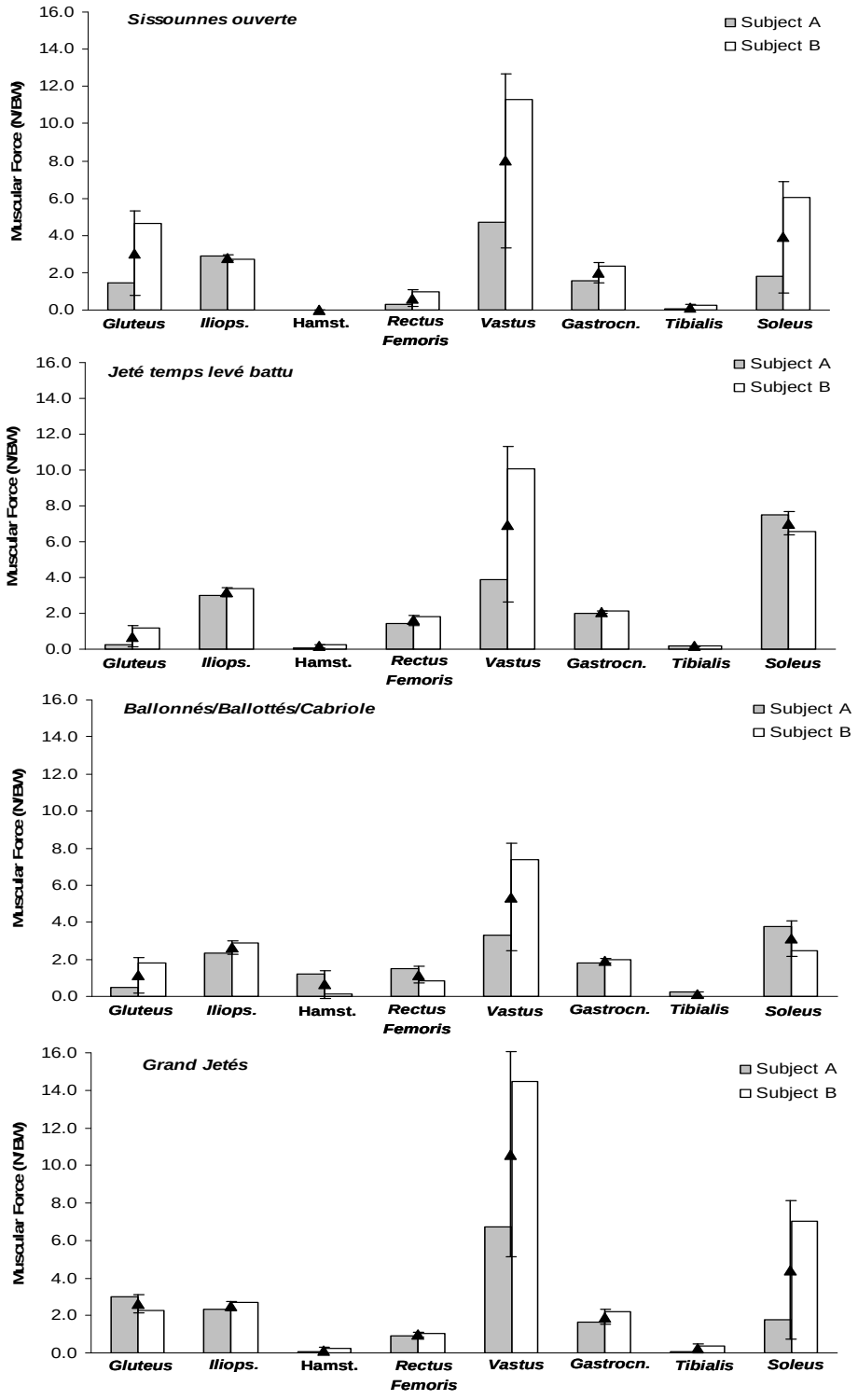

Figure 6.27. Average values of the peak muscular force normalized to BW, in the *gluteus, iliopsoas*, hamstrings, *rectus femoris*, *vastus*, *gastrocnemius*, *tibialis*, and *soleus* muscle groups, in subject A, and B, during *Sissounnes ouverte*, *Jeté temps levé battu*, *Ballonnés/Ballottés/Cabriole* and *Grand Jetés* jumps. The small triangles with error bars indicate the normalized mean and SD values for the two subjects.

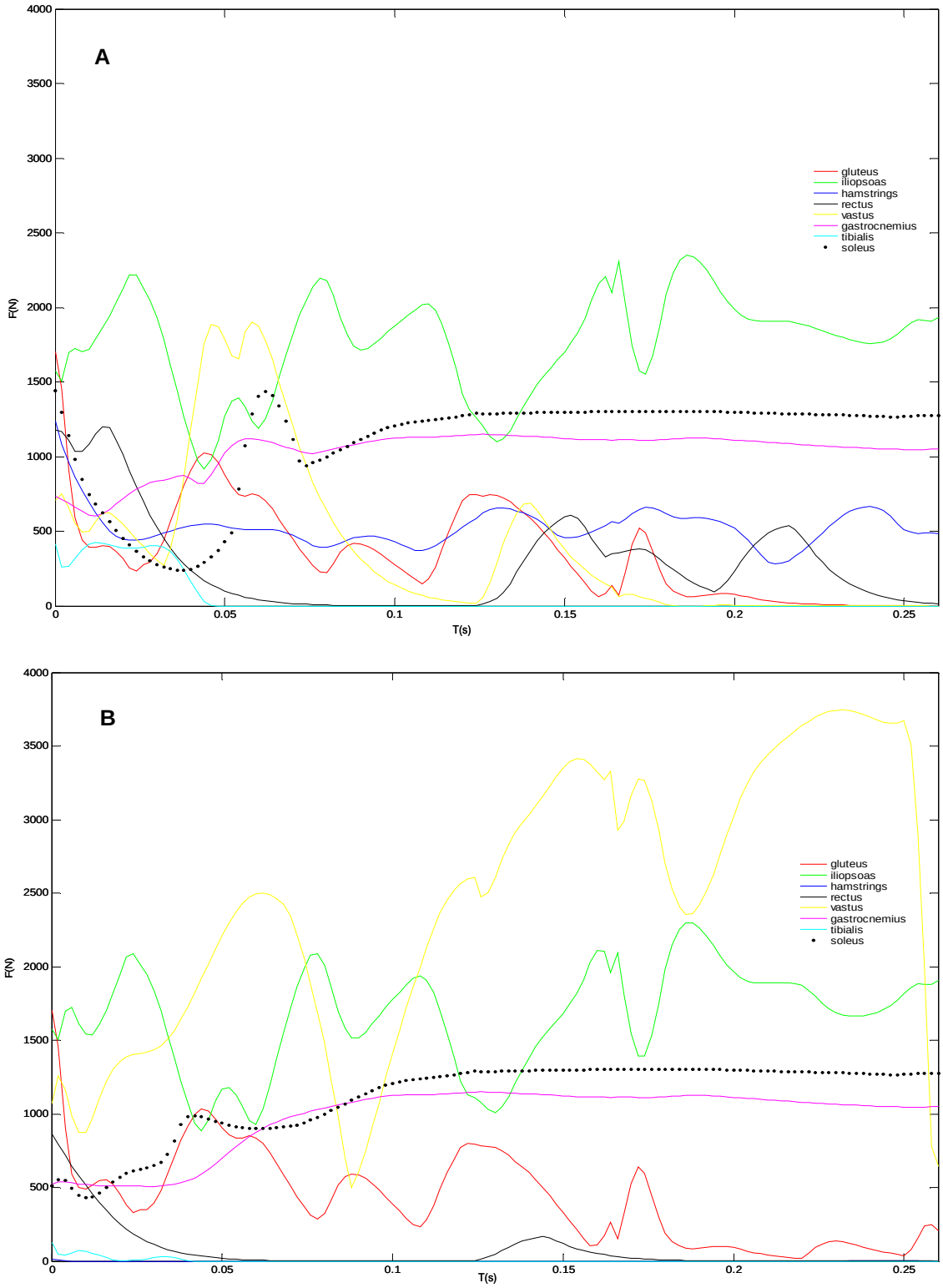

Figure 6.28. Representative example of muscular force normalized to BW, estimated in the *gluteus, iliopsoas*, hamstrings, *rectus femoris*, *vastus*, *gastrocnemius*, *tibialis*, and *soleus* muscle groups, in subject A, during a moderate impact jump, using in (A) the pure optimization technique and (B) using the activation values for some muscles from EMG records.

In the *per subject* analysis (figure 6.29), the *soleus* and *gastrocnemius* have a similar role (the *soleus* slightly larger in subject B), and the antagonist (*tibialis*) is almost irrelevant, comparatively. In the knee joint, the *vastus* is the most relevant muscle, followed by the *gastrocnemius.* The *rectus femoris* has a very discreet participation. In the hip joint the *iliopsoas* has higher values than the gluteus.

In the *per jump* analysis (figure 6.30) we can draw the same conclusions. The *vastus* is the most relevant muscle, especially in subject B, followed by the *soleus* and the *gastrocnemius* with more or less the same impulse. The participation of the *tibialis* is almost zero. This is consistent with what we would expect from landing movements. At the knee joint, the role of the various muscles is more balanced, but is subject and movement dependent. At the hip joint one would expect the *gluteus* to have the most relevant role but this is not the case as the *iliopsoas* is the one with greater impulse. Again a comparison with the full optimization procedure (figure 6.18) reveals a weaker participation of the bi-articular and antagonist muscles than in the full optimization case.

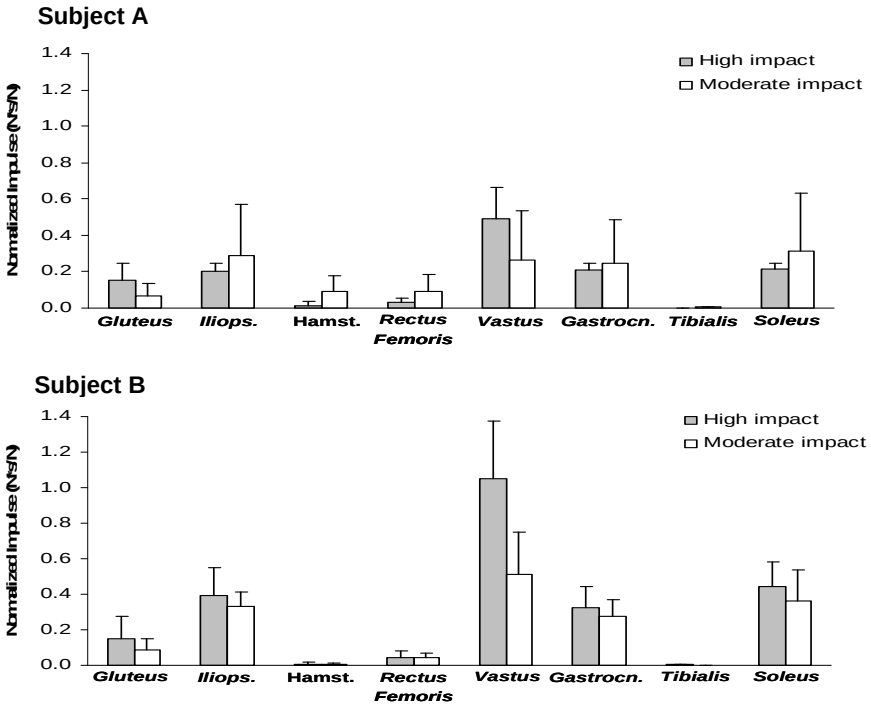

Figure 6.29. Average and SD values of the normalized impulse, in the *gluteus, iliopsoas*, hamstrings, *rectus femoris*, *vastus*, *gastrocnemius*, *tibialis*, and *soleus* muscle groups, in subject A, and B, during moderate and high impact jumps.

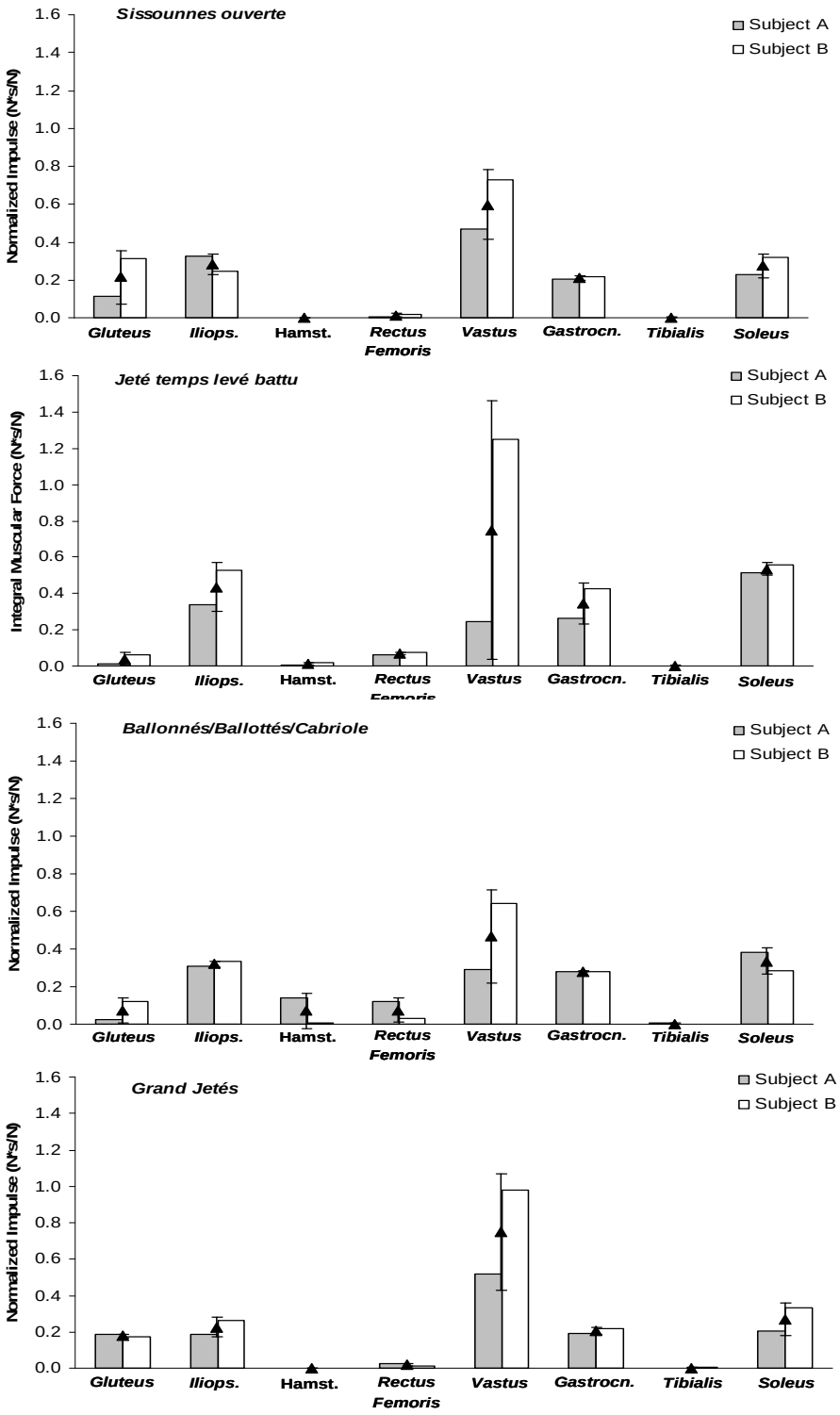

Figure 6.30. Average values of the normalized impulse, in the *gluteus, iliopsoas*, hamstrings, *rectus femoris*, *vastus*, *gastrocnemius*, *tibialis*, and *soleus* muscle groups, in subject A, and B, during *Sissounnes ouverte*, *Jeté temps levé battu*, *Ballonnés/Ballottés/Cabriole* and *Grand Jetés* jumps. The small triangles with error bars indicate the normalized mean and SD values for the two subjects.

Figure 6.31 presents the peak values of mechanical power normalized to BW estimated for the eight muscle groups (mono and bi-articular) that compose our model: the *gluteus,* the *iliopsoas*, the hamstrings (proximal and distal ends), the *rectus femoris* (proximal and distal ends), the *vastus*, the *gastrocnemius* (proximal and distal ends), the *tibialis*, and the *soleus* muscle. The figure shows the data from subject A and B in moderate and high impact jumps.

The first observation is that the peak power on the high impact jumps is always greater than in the low impact ones. The second one is that the pattern seen before can be seen here again but with a more emphatic role of the *vastus* and *soleus* over its agonist and antagonist muscles.

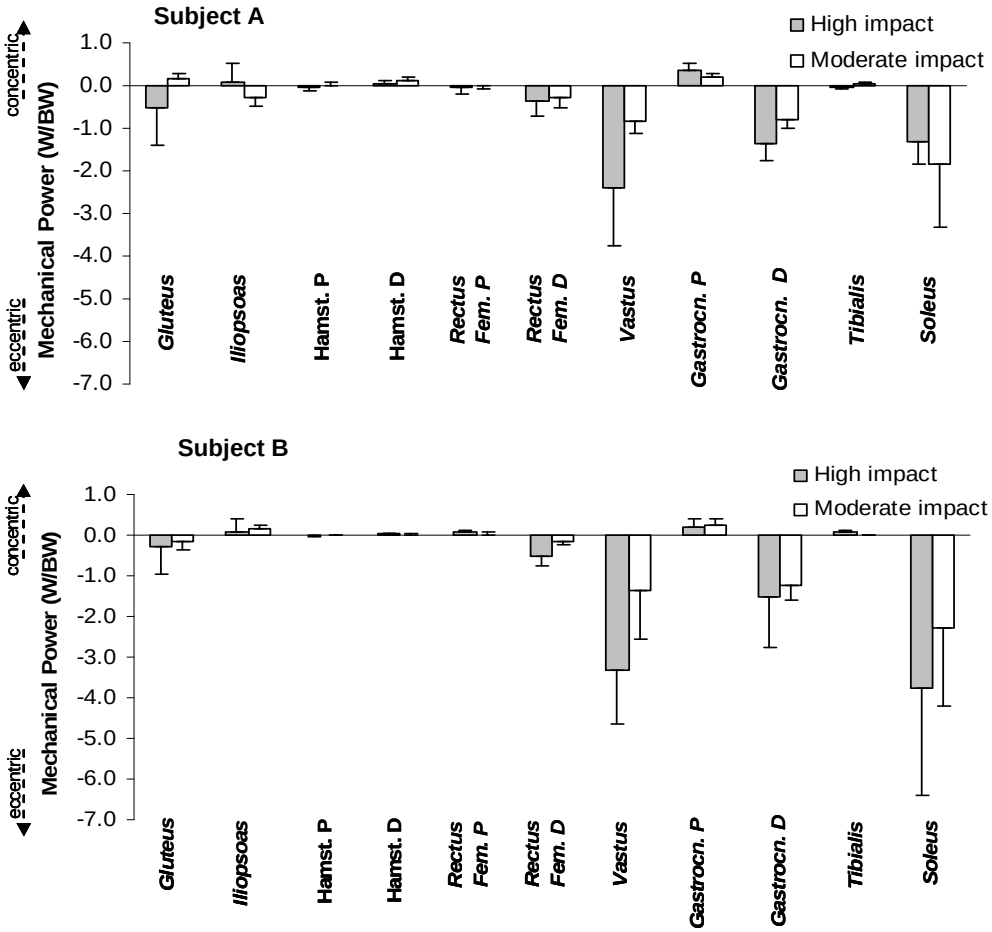

Figure 6.31. Average and SD values from peak mechanical power normalized to BW in the *gluteus, iliopsoas*, hamstrings (proximal (P) and distal (D) ends), *rectus femoris* (proximal (P) and distal (D) ends), *vastus*, *gastrocnemius* (proximal (P) and distal (D) ends), *tibialis*, and *soleus* muscle groups, in subject A and B, and in moderate and high impact jumps.

In the figure 6.32 it is possible to observe the peak values of mechanical power normalized to BW, in the eight muscle groups (mono and bi-articular) that compose our model (proximal and distal ends), in the four groups of jumps selected: *sissounnes ouverte*, *jeté temps levé battu*, *ballonnés/ballottés/cabriole* and *grand jetés*.

The highest values of the *soleus* peak power occur in both subjects in the unsuspected *jeté temps levé battu*. The optimization only results (figure 6.22) do not reveal this feature. As before, we can see an increased role of all mono-articular muscles over the bi-articular ones, and a decrease of the antagonists' role, i.e. reduced cocontractions.

Figure 6.33 presents the mean values of mechanical energy estimated in the eight muscle groups (mono and bi-articular) that compose our model: the *gluteus* muscle, the *iliopsoas* muscle, the hamstrings muscle (proximal and distal ends), the *rectus femoris* muscle (proximal and distal ends), the *vastus* muscle, the *gastrocnemius* muscle (proximal and distal ends), the *tibial* muscle, and the *soleus* muscle. The figure shows the data from subject A and B in moderate and high impact jumps. Once again we see an increased role of all mono-articular muscles, particularly the *vastus*, over the bi-articular ones, and a decrease of the antagonists' role.

In figure 6.34 it is possible to observe the mean values of mechanical energy normalized to BW, in the eight muscle groups (mono and bi-articular) that compose our model (proximal and distal ends), in the four groups of jumps selected: *sissounnes ouverte*, *jeté temps levé battu*, *ballonnés/ballottés/cabriole* and *grand jetés*. Here we can see the same result of an inflated mono-articular role and a degradation of the antagonists' role. There is also a pair of dissimilar results for *gastrocnemius* and the *soleus* in the *jeté temps levé battu*, with subject A having concentric contractions and subject B having eccentric ones. This, if true, can only be explained by technical or anatomical differences.

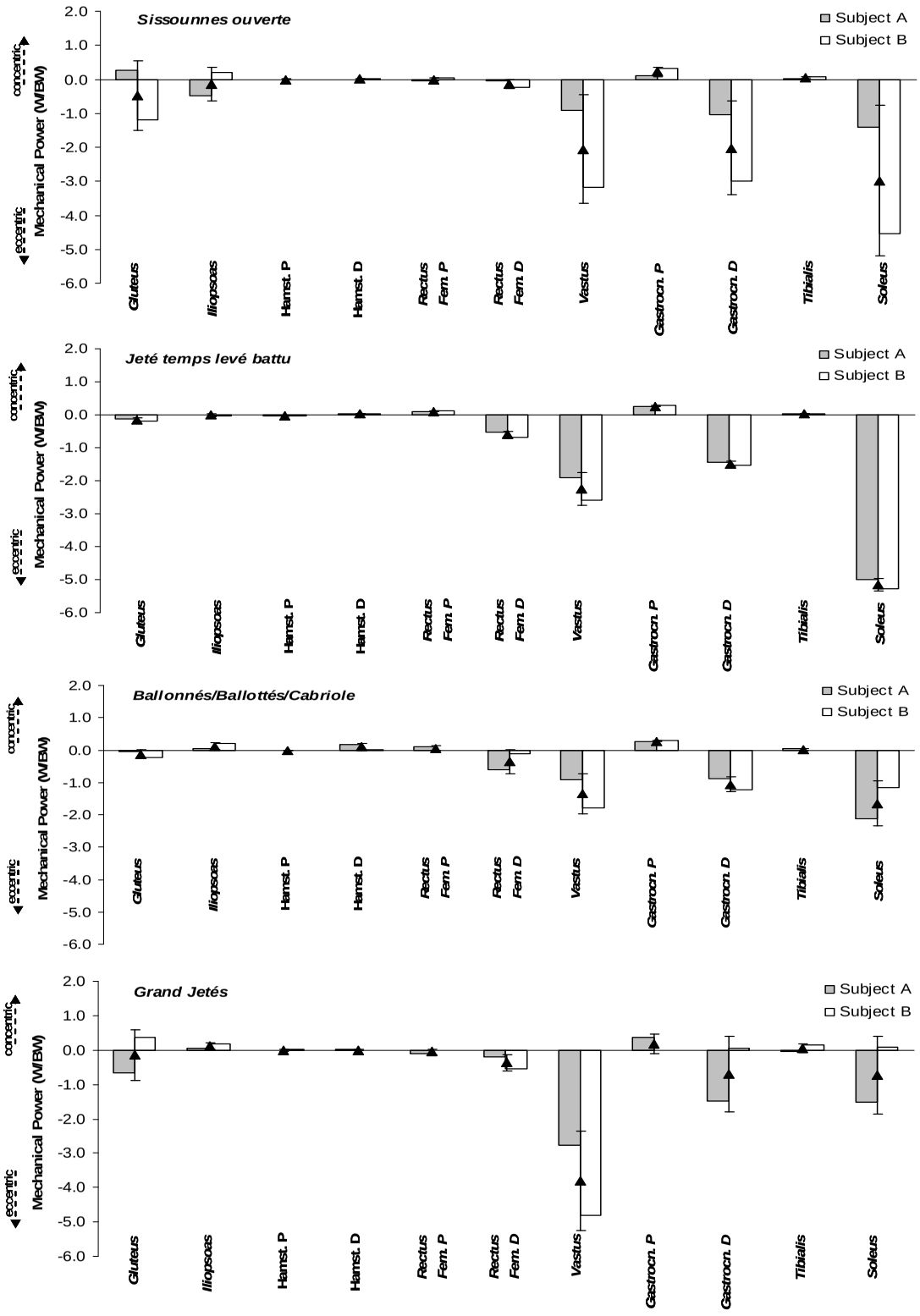

Figure 6.32. Average values from peak mechanical power normalized to BW in the *gluteus, iliopsoas*, hamstrings (proximal (P) and distal (D) ends), *rectus femoris* (proximal (P) and distal (D) ends), *vastus*, *gastrocnemius* (proximal (P) and distal (D) ends), *tibialis*, and *soleus* muscle groups, in subject A, and B, during *Sissounnes ouverte*, *Jeté temps levé battu*, *Ballonnés/Ballottés/Cabriole* and *Grand Jetés* jumps. The small triangles with error bars indicate the normalized mean and SD values for the two subjects.

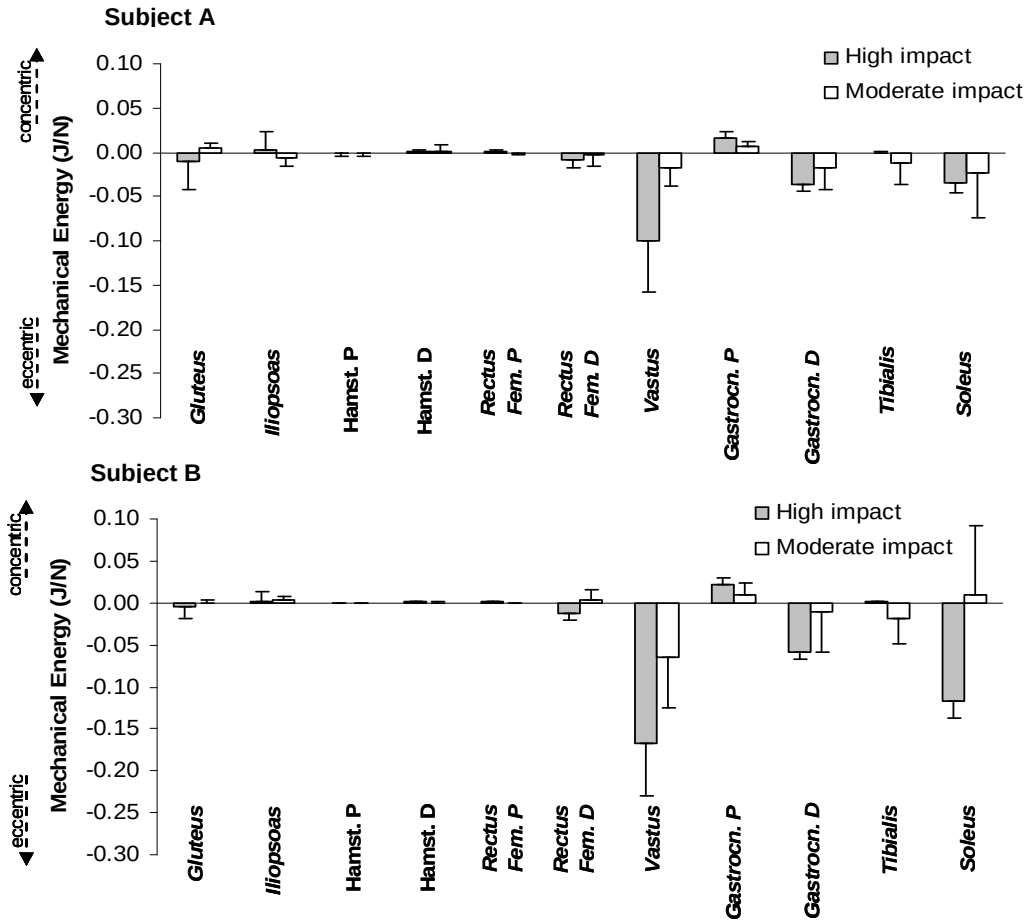

Figure 6.33. Average and SD values from mechanical energy normalized to BW estimated in the *gluteus, iliopsoas*, hamstrings (proximal (P) and distal (D) ends), *rectus femoris* (proximal (P) and distal (D) ends), *vastus*, *gastrocnemius* (proximal (P) and distal (D) ends), *tibialis*, and *soleus* muscle groups, in subject A and B, and in moderate and high impact jumps.

Table 6.4 presents the energy transfer estimated for subject A and B, in the proximal and distal joints, of the *gastrocnemius*, *rectus femoris*, and in the hamstrings muscle groups, during the performance of high and moderate impact jumps.

Table 6.4. Energy transfer (mJ/N) estimated in the proximal and distal joints (P and D), of the hamstrings, *rectus femoris,* and *gastrocnemius* muscle groups during the performance of high and moderate impact jumps, in subject A and B.

Jump/Muscle	Hamst. P	Hamst. D	*Rectus* P	*Rectus* D	*Gastroc.* P	*Gastroc.* D
Subject A						
High Impact (mJ/N)	-2.00	-1.00	0.40	9.00	-17.00	-37.00
% energy transfer	141%		5%		46%	
Moderate Impact (mJ/N)	-0.9	-2.00	-0.50	3.70	-6.00	-17.00
% energy transfer	50%		-14%		34%	
Subject B						
High mpact (mJ/N)	-0.38	-1.00	0.70	13.00	-22.00	-58.00
% energy transfer	38%		5%		39%	
Moderate Impact (mJ/N)	-0.009	0.11	-0.14	-4.00	-9.00	-12.00
% energy transfer	-9%		4%		77%	

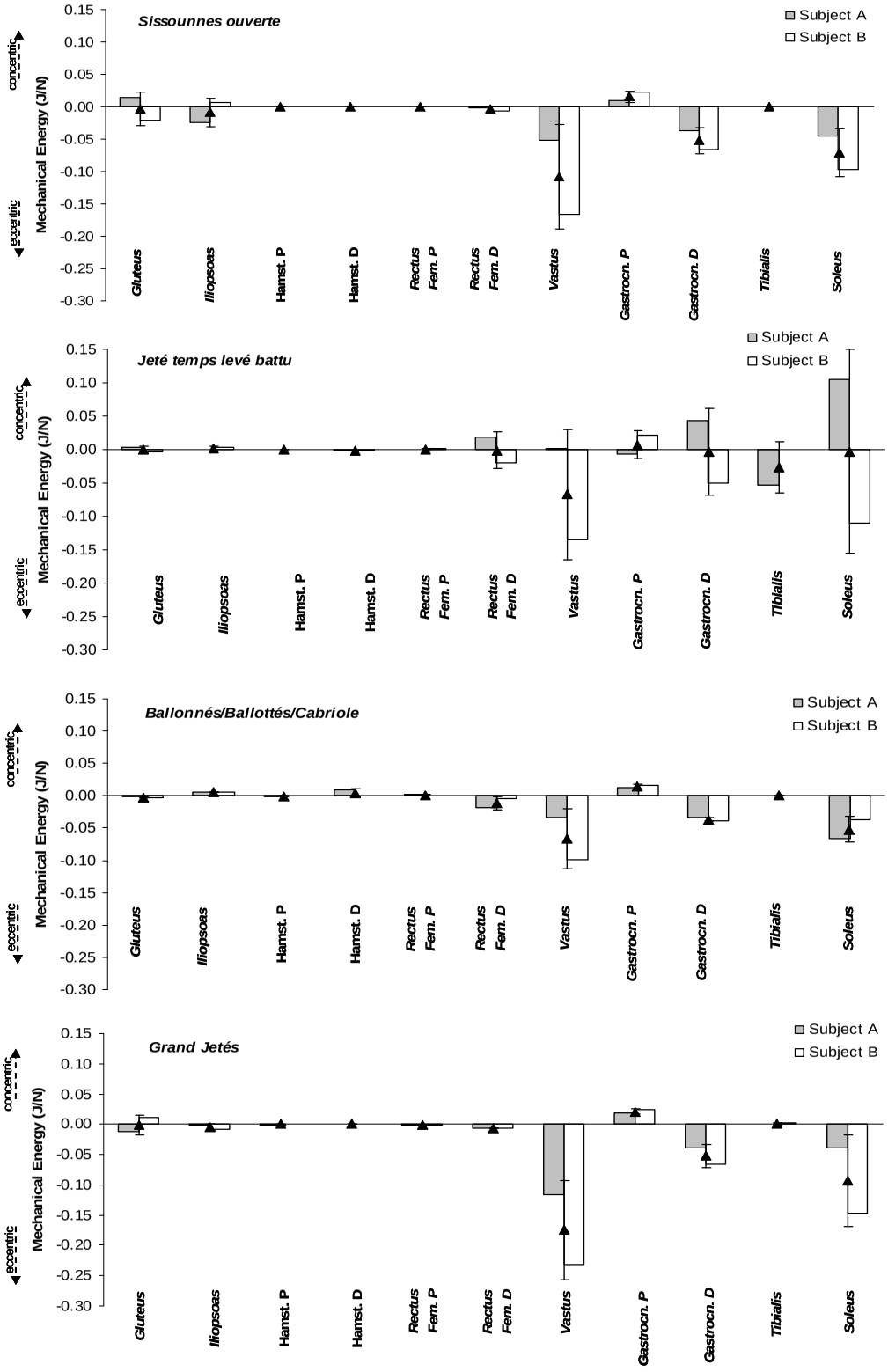

Figure 6.34. Average values from mechanical energy normalized to BW estimated in the *gluteus, iliopsoas*, hamstrings (proximal (P) and distal (D) ends), *rectus femoris* (proximal (P) and distal (D) ends), *vastus*, *gastrocnemius* (proximal (P) and distal (D) ends), *tibialis*, and *soleus* muscle groups, in subject A and B, during *Sissounnes ouverte*, *Jeté temps levé battu*, *Ballonnés/Ballottés/Cabriole* and *Grand Jetés* jumps. The small triangles with error bars indicate the normalized mean and SD values for the two subjects.

In table 6.4 it is apparent the usage of the energy transfer mechanisms in almost all cases. The three exceptions are the hamstrings of subject B in moderate impact jumps and of subject A in high impact jumps and also the *rectus* in moderate impact jumps of the same subject. This is somehow a similar result to the obtained from the optimization only strategy (table 6.2).

Table 6.5 presents the energy transfer estimated for subject A and B, in the proximal and distal joints, of the *gastrocnemius*, *rectus femoris*, and in the hamstrings muscle groups, during the performance of *Sissounnes ouvert*, *Jeté temps levé battu*, *Ballonnés/Ballottés/ Cabriole* and *Grand Jetés* jumps.

Table 6.5. Energy transfer (mJ/N) estimated in the proximal and distal joints (P and D) of the hamstrings, *rectus femoris,* and *gastrocnemius* muscle groups during the performance of *Sissounnes ouverte*, *Jeté temps levé battu*, *Ballonnés/ballottés/cabriole* and *Grand Jetés* jumps.

Jumps/Muscle	Hamst. P	Hamst. D	*Rectus* P	*Rectus* D	*Gastroc*. P	*Gastroc.* D
Sissounnes (mJ/N)	-0.008	0.012	-0.033	3.50	-16.00	-52.00
% energy transfer	-65%		-1%		30%	
Jeté Tenleve Batttu (mJ/N)	-0.26	1.90	0.42	0.89	-73.00	-4.00
% energy transfer	-14%		48%		201%	
Ballonnés/ballottés/cabriole (mJ/N)	-0.62	-5.00	0.92	11.20	-14.30	-37.00
% energy transfer	13%		8%		39%	
Grand Jetés (mJ/N)	-0.30	-0.48	-0.80	7.00	-21.00	-52.00
% energy transfer	60%		-11%		40%	

Table 6.5 is in contrast with table 6.3. In all *Ballonnés/Ballottés/ Cabriole* there is energy transfer. Besides that, there are four more cases of positive energy transfer, but with no defined pattern.

According to some authors, an EMG-to-force processing model, very similar to the model presented here, appears to be a very practical instrument to determine individual muscle forces. Our overall impression is in complete agreement with Hof (1990), that gracefully stated: …"what makes this line of work so interesting is that one can in fact *see* into the muscle itself and, in that way gain insights about, not only movements are performed, but also why they are performed in the way they are"…

Conclusions

Classical Inverse Dynamics

The results from the classical inverse dynamics approach are very sensitive to the input data precision (video, GRF). The efforts to refine the filtering and differentiation of these reveal no significant improvement in desensitising these results. This is the weak point of this phase and we think that a greater effort has to be done at the acquisition level, including the usage of redundant sources, e.g., video cameras, accelerometers, etc.

Through the analysis of the magnitude of the peak values from articular forces estimated in the ankle, knee and hip joints, it was possible to observe that, in some jumps, the values registered are of the order of three times the body weight, showing the injury potential that the anatomical structures of ballet dancers are exposed to.

The peak values of articular force estimated in every jump and subject, decrease, comparing the ankle with the knee joint, and the knee with the hip joint. As expected, this decrease of force from one joint to another joint is possibly due to the occurrence of absorption phenomenons induced by the body tissues. This occurrence will put in perspective the energy transfer phenomena processed by the bi-articular muscles, subsequently calculated in second part of this study (the hybrid forward-inverse dynamic model).

When the focus of the analysis is the injury potential of forces what is happening externally (GRF) is not a direct indicator of internal loads. A simple thought about forces produced doesn't include the time duration of the impact forces, therefore, is not a reasonable indicator about their injury potential. The injury potential is probably related with energy dissipation.

Extended Inverse Dynamics (muscular decomposition)

The usage of a hybrid forward-inverse dynamical model seems to desensitise it from the objective function. This is beneficial as these functions are not physically or physiologically founded. These hybrid models can be seen as the result of an exchange of the importance of the ad-hoc objective functions to the importance of the muscle model, more easy to found in the physiology (Hill's or Huxley's models, etc).

After the analysis of the forces and energies produced by each muscle included in our model, and in each jump, it was possible to observe that the behaviour of the musculature involved, is somehow dependent on the technique used in the performance. Small external changes, i.e., small technical changes, can result in significant internal changes. The technique can modify the internal distribution of forces.

Initially the jumps were separated and grouped in moderate and high impact jumps, according to the peak values registered in the GRF passive peak curve. Nevertheless, the moderate and high impact groups don't reflect what is internally happening. The moderate and high impact does not mean the same for all the muscle groups. Muscles do not work more or less due to the fact of the jump classification.

The model is very dependent on its assumptions and parameters, like anatomical and physiological. The final accuracy of our model is greatly influenced by the accuracy of the anatomical data, which must include a full rigorous model of the musculoskeletal geometry.

It is possible to conclude that the results obtained from the extended inverse dynamics approach (muscular decomposition) with and without EMG, are not radically different. The biggest differences are particularly observed in the role of mono and bi-articular muscles.

What should be the way to follow? With or without EMG?
Our results suggest that the extended inverse dynamics approach with some activation values obtained from the EMG records were more incoherent, in the sense that there is an excessive role attributed to the mono-articular muscles in detriment of the bi-articular ones. One can not say if the problem is related to the combination of the two sources of activation information (or the missing EMG records from other muscles) or if it is related to the unsubstantiated usage of EMG data to estimate activation in impulsive movements. Nevertheless, it is known from literature the important role of bi-articular muscles, specially the mechanism of energy transfer.

In our study, the results obtained from pure optimization procedures, which are highly dependent on pure conjectures, were more according to expectations. We can observe the important role of bi-articular muscles and the mechanism of energy transfer, between adjacent muscles and segments.

We think it is necessary more research around this theme. Another kind of results should be expected if we have EMG from all the superficial muscles (mono and bi-articular) from the lower limb, and if possible, combined with direct measurements from muscular force.

Without direct measures one can not make a definite case in favour of any of the strategies. Nevertheless, the ecological tool would avoid the usage of intrusive techniques like EMG and internal force sensors.

6.3 . Next Goals

Direct measures (with ultrasonography) of the behaviour of the two compartments (contractile and elastic components), of the muscle-tendon complex of the synergistic pair of muscles, medial gastrocnemius and soleus, during high intensity drop jumps (SSC movements). Examine the contribution of the contractile and the elastic components to the potentiation of the muscle-tendon complex.

Combine the *in vivo* (direct measurements of the Achilles tendon) muscular force measurements with fascicle length measurements, during high intensity drop jumps, to better understand the muscle mechanics in SSC movements.

Compare the inverse dynamics solutions with the *in vivo* direct measurements.

6.4. References:

Abdel-Aziz, Y. I. and Karara, H. M. (1971). Direct Linear Transformation from Comparator Coordinates into Object Space Coordinates in Close-Range Photogrammetry. American Society for Photogrammetry Symposium on Close-Range Photogrammetry. Falls Church, VA: American Society for Photogrammetry, Urbana, IL, pp. 1-18.

Alexander, R. M. and Bennet-Clark, H. C. (1977). Storage of elastic strain energy in muscle and other tissues. Nature 265: 114-117.

Arampatzis, A.; Schade, F.; Walsh, M. and Bruggemann, G. P. (2001). Influence of leg stiffness and its effect on myodynamic jumping performance. J Electromyogr Kinesiol 11: 355-364.

Bobbert, M. F.; Huijing, P. A. and van Ingen Schenau, G. J. (1986a). An estimation of power output and work done by the human triceps surae muscle-tendon complex in jumping. J Biomech 19: 899-906.

Bobbert, M. F.; Huijing, P. A. and van Ingen Schenau, G. J. (1986b). A model of the human triceps surae muscle-tendon complex applied to jumping. J Biomech 19: 887-898.

Bogey, R. A.; Perry, J. and Gitter, A. J. (2005). An EMG-to-force processing approach for determining ankle muscle forces during normal human gait. IEEE Trans Neural Syst Rehabil Eng 13: 302-310.

Böhm, H. (2002). Computer Simulation of Muscle Series Elastic Element Function in Drop Jumping. Biomechanics. German Sport University Cologne, Cologne

Buchanan, T. S.; lloyd, D. G.; Manal, K. and Besier, T. F. (2004). Neuromusculoskeletal Modeling: Estimation of Muscle Forces and Joint Moments and Movements drom Measurements of Neural Command. Journal of Applied Biomechanics 20: 367-395.

Buchanan, T. S.; Lloyd, D. G.; Manal, K. and Besier, T. F. (2005). Estimation of muscle forces and joint moments using a forward-inverse dynamics model. Med Sci Sports Exerc 37: 1911-1916.

Cavagna, G. A.; Dusman, B. and Margaria, R. (1968). Positive work done by a previously stretched muscle. J Appl Physiol 24: 21-32.

Cholewicki, J.; McGill, S. M. and Norman, R. W. (1995). Comparison of muscle forces and joint load from an optimization and EMG assisted lumbar spine model: towards development of a hybrid approach. J Biomech 28: 321-331.

Chow, J. W. and Darling, W. G. (1999). The maximum shortening velocity of muscle should be scaled with activation. J Appl Physiol 86: 1025-1031.

Clarkon, P. M. and Skrinar, M. (1988). Science of Dance Training. Human Kinetics, Champaign.

Conceição, F. (2004). Estudo Biomecânico do Salto em Comprimento. Modelação, simulação e optimização da chamada. Biomechanics. University of Porto, Porto

Cook, C. S. and McDonagh, M. J. (1995). Force responses to controlled stretches of electrically stimulated human muscle-tendon complex. Exp Physiol 80: 477-490.

Dietz, V.; Schmidtbleicher, D. and Noth, J. (1979). Neuronal mechanisms of human locomotion. J Neurophysiol 42: 1212-1222.

Enoka, R. M. (2002). Neuromechanics of Human Movement. Human Kinetics, USA.

Epstein, M. and Herzog, W. (1998). Theoretical Models of Skeletal Muscle:Biological and Mathematical Considerations. John Wiley and Sons, New York.

Ettema, G. J.; Huijing, P. A.; van Ingen Schenau, G. J. and de Haan, A. (1990). Effects of prestretch at the onset of stimulation on mechanical work output of rat medial gastrocnemius muscle-tendon complex. J Exp Biol 152: 333-351.

Gollhofer, A.; Strojnik, V.; Rapp, W. and Schweizer, L. (1992). Behaviour of triceps surae muscle-tendon complex in different jump conditions. Eur J Appl Physiol Occup Physiol 64: 283-291.

Gregoire, L.; Veeger, H. E.; Huijing, P. A. and van Ingen Schenau, G. J. (1984). Role of mono- and biarticular muscles in explosive movements. Int J Sports Med 5: 301-305.

Happee, R. (1994). Inverse dynamic optimization including muscular dynamics, a new simulation method applied to goal directed movements. J Biomech 27: 953-960.

Hatze, H. (1990). The charge-transfer model of myofilamentary interaction: prediction of force enhancement and related myodynamic phenomena. In: Winters, J. M., Woo, S. L.-Y. (eds) Multiple Muscle SystemsBiomechanics and Movement Organization. Springer-Verlag, New York, pp. 24-45.

Hatze, H. (2000). The inverse dynamics problem of neuromuscular control. Biol Cybern 82: 133-141.

Hatze, H. (2002). The fundamental problem of myoskeletal inverse dynamics and its implications. J Biomech 35: 109-115.

Herzog, W. and Leonard, T. R. (2002). Force enhancement following stretching of skeletal muscle: a new mechanism. J Exp Biol 205: 1275-1283.

Hof, A. (1990). Assessment of muscle force in complex movements by EMG. In: deGroot, G., Hollander, A., Huijing, P., Shenau, G. I. (eds) Biomechanics XI-A. The Netherlands: University Park Press, Amsterdam, pp. 111-117.

Huxley, A. F. (1957). Muscle structure and theories of contraction. Prog Biophys Biophys Chem 7: 255-318.

Huxley, A. F. and Simmons, R. M. (1971). Proposed mechanism of force generation in striated muscle. Nature 233: 533-538.

Ker, R. F.; Bennett, M. B.; Bibby, S. R.; Kester, R. C. and Alexander, R. M. (1987). The spring in the arch of the human foot. Nature 325: 147-149.

Komi, P. V. (1987). Neuromuscular Factors Related to Physical Performance. Med Sport Sci 26: 48-66.

Komi, P. V. and Bosco, C. (1978). Utilization of stored elastic energy in leg extensor muscles by men and women. Med Sci Sports 10: 261-265.

Koo, T. K. and Mak, A. F. (2005). Feasibility of using EMG driven neuromusculoskeletal model for prediction of dynamic movement of the elbow. J Electromyogr Kinesiol 15: 12-26.

Lloyd, D. G. and Besier, T. F. (2003). An EMG-driven musculoskeletal model to estimate muscle forces and knee joint moments in vivo. J Biomech 36: 765-776.

Loss, J. F. (2001). Efeitos de Parâmetros Inerciais Obtidos Através de Diferentes Procedimentos na Determinação de Forças e Torques Articulares Resultantes. Engenharia Mecânica. Universidade Federal do Rio Grande do Sul, Porto Alegre

Manal, K. and Buchanan, T. S. (2003). A one-parameter neural activation to muscle activation model: estimating isometric joint moments from electromyograms. J Biomech 36: 1197-1202.

Morgan, D. L. (1990). New insights into the behavior of muscle during active lengthening. Biophys J 57: 209-221.

NASA (1978). Anthropometric Source Book, technical report 1024. NASA Scientific and Technical Information Office, Houston.

Neptune, R. R.; Kautz, S. A. and Zajac, F. E. (2001). Contributions of the individual ankle plantar flexors to support, forward progression and swing initiation during walking. J Biomech 34: 1387-1398.

Nicol, C. and Komi, P. V. (1999). Quantification of Achilles Tendon Force Enhancement by Passively Induced Dorsiflexion Stretches. Journal of Applied Biomechanics 15: 221-232.

Nigg, B. M. (2000). Forces Acting on and in the Human Body. In: Nigg, B. M., MacIntosh, B. R., Mester, J. (eds) Biomechanics an Biology of Movement. Human Kinetics, Champaign, pp. 253-268.

Nigg, B. M.; Macintosh, B. R. and Mester, J. (2000). Biomechanics and biology of movement. Human Kinetics, Champaign.

Nigg, B. M. H., W. (1999). Biomechanics of the Musculo-Skeletal System. John Wiley & Sons, Chichester.

Prilutsky, B. I.; Herzog, W. and Leonard, T. (1996). Tranfer of mechanical energy between ankle and knee joints by gastrocnemius and plantaris muscles during cat locomotion. Journal of Biomechanics 29: 391-403.

Prilutsky, B. I. and Zatsiorsky, V. M. (1994). Tendon action of two-joint muscles: transfer of mechanical energy betwee joints during jumping, landing and running. Journal of Biomechanics 27: 25-34.

Rack, P. M. and Westbury, D. R. (1974). The short range stiffness of active mammalian muscle and its effect on mechanical properties. J Physiol 240: 331-350.

Sasaki, K. and Neptune, R. R. (2006). Muscle mechanical work and elastic energy utilization during walking and running near the preferred gait transition speed. Gait Posture 23: 383-390.

van Ingen Schenau, G. J.; Bobbert, M. F. and Rozendal, R. H. (1987). The unique action of bi-articular muscles in complex movements. J Anat 155: 1-5.

van Zandwijk, J. P.; Bobbert, M. F.; Harlaar, J. and Hof, A. L. (1998). From twitch to tetanus for human muscle: experimental data and model predictions for m. triceps surae. Biol Cybern 79: 121-130.

Wang, K.; McClure, J. and Tu, A. (1979). Titin: major myofibrillar components of striated muscle. Proc Natl Acad Sci U S A 76: 3698-3702.

Winters, J. M. and Woo, S. L.-Y. (1990). Multiple Muscle Systems: Biomechanics and Movement Organization. Springer- Verlag, New York.

Witzke, K. A. and Snow, C. M. (2000). Effects of plyometric jump training on bone mass in adolescent girls. Med Sci Sports Exerc 32: 1051-1057.

Yamaguchi, G. T.; Sawa, A. G. U.; Morgan, D. W.; Fessler, M. J. and Winters, M. (1990). A survey of human musculotendon actuator parameters. In: Woo, J. M. W. a. S. L.-Y. (ed) Multiple Muscle Systems: Biomechanics and Movement Organization. Springer-Verlag, New York, pp. 717-773.

Zajac, F. E.; Neptune, R. R. and Kautz, S. A. (2002). Biomechanics and muscle coordination of human walking. Part I: Introduction to concepts, power transfer, dynamics and simulations. Gait Posture 16: 215-232.

Chapter 7

Intensity and Muscle Specific Fascicle Behaviour during Human Drop Jumps

7.1. Introduction

The assessment of biomechanical loading and a better understanding of how the body transmit and attenuate the impact forces through the muscles, bones and joint tissues is an extremely important topic of. The direct assessment (with ultrasonography) of the behaviour of the two compartments (contractile and elastic components), of the muscle-tendon complex of the synergistic pair of muscles, medial *gastrocnemius* and *soleus*, during high intensity drop jumps, will be interesting to internally better understand the potentiation phenomenon in SSC movements.

7.2. The Study

A fifth study, to examine the behaviour of fascicle and tendon of the synergistic medial *gastrocnemius* and *soleus* muscles during the performance of human drop jumps, was executed and firstly published as:

"Intensity and Muscle Specific Fascicle Behaviour during Human Drop Jumps"

Sousa F[1,2], Ishikawa M[1],Vilas-Boas JP [2], Komi PV[1] (2006). Intensity and Muscle Specific Fascicle Behaviour during Human Drop Jumps. *J. Appl. Physiol*. (JAP-00274-2006.R2).

[1] Neuromuscular Research Center, Department of Biology of Physical Activity, University of Jyväskylä, 40014 Jyväskylä, Finland.

[2] Laboratory of Biomechanics, Faculty of Sports, University of Porto, Portugal.

Abstract

The present study was designed to examine how fascicle-tendon interaction takes place in the synergistic medial *gastrocnemius* (MG) and *soleus* (SOL) muscles during drop jumps (DJ) performed from different drop heights (DH). Eight subjects performed unilateral DJ on a sledge apparatus from different DH with maximal rebounds. During the exercises, fascicle length (using ultrasonography) and electromyographic activities were measured. The results showed that the fascicles of the MG and SOL muscles behaved differently during the contact phase, while the whole muscle-tendon unit (MTU) and its tendinous tissue (TT) lengthened prior to shortening in both muscles. The SOL fascicles lengthened prior to shortening during the ground contact in all conditions. During the braking phase, the SOL activation increased with increasing DH. However, the lengthening amplitudes of the SOL

fascicles during braking phase did not show clear dependence on the DH. On the other hand, the MG fascicles primarily shortened during the braking phase in the lower DH condition. Thereafter, in the higher DH conditions, the MG fascicles did not shorten, but behaved isometrically or were lengthened during the braking phase. These results suggest that the fascicles of synergistic muscles (MG and SOL) can behave differently during DJ, and that there may be specific length change patterns of the MG fascicles with increasing DH, but not that of the SOL fascicles.

Keywords:
Stretch-shortening cycle, ultrasound, bi-articular muscle, elasticity, inhibition,

Introduction

Fascicles of skeletal muscle consist of bundles of muscle fibres usually arranged in parallel. Ultrasonography (ULS) is increasingly used in the assessment of superficially located soft-tissue structures (fascicle and tendon) during movements of major leg extensor muscles. In this regard, the function of the fascicles in the *triceps surae* muscle has received special attention during human locomotion from both neurophysiological and biomechanical points of view. These muscles are known to have either mono- (*soleus* muscle) or bi-articular (*gastrocnemius* muscle) function and they may consequently show different functional behaviour. For example, in H-reflex modulation, the medial *gastrocnemius* (MG) and *soleus* (SOL) muscles show similar patterns during the ground contact of human hopping, but the amplitudes of the modulation were different between these muscles (Moritani et al., 1990; Voigt et al., 1998). Consequently, it has been suggested that there are differences between the two muscles in the distribution of peripheral afferent feedback to their respective motor neuron pools (van Ingen Schenau et al., 1994). In line with this suggestion, Kokkorogiannis (2004) reported that the SOL has 3 times more spindles than *gastrocnemius* muscle. In human movements, Voigt et al. (1998) reported that the movement-induced short latency stretch reflex (SLR) during hopping was consistently observed in the electromyogram (EMG) of SOL, but not always in MG. However, Moritani et al. (1990) reported that the amplitude of H-reflex modulation was higher in MG than in SOL during maximal effort hopping and suggested that there is a preferential and movement phase-dependent neuromuscular activation within the human ankle extensor synergistic muscles. Consequently, these modulations of muscle activation in MG and SOL may depend not only

on the difference distribution of muscle spindles but also on the mechanical effects, such as intensity of the movements. This is because the fascicle behaviour is depending on the muscle (Ishikawa et al., 2005a; Ishikawa et al., 2005b) and intensity (Ishikawa et al., 2003; Ishikawa and Komi, 2004; Ishikawa et al., 2005b) during the high intensity human stretch-shortening cycle (SSC) movements. One may question whether the fascicles of the MG and SOL muscles can behave differently during different intensity SSC movements. This question can be answered by performing real-time ultrasonographic scanning of the fascicle and tendon behaviour during human movements (Fukunaga et al., 1997; Fukunaga et al., 2001), provided that the ultrasound scanning frequency is high enough to capture the fast movement (Ishikawa et al., 2005a; Ishikawa et al., 2005b).

Repeated DJ can be used to study fascicle behaviour, especially when investigating the utilization of TT elasticity (Ishikawa et al., 2003; Ishikawa et al., 2005b). It has been suggested (Ishikawa et al., 2005b) that the fascicles of a bi-articular muscle may not behave in the same way as the fascicles of a mono-articular muscle. However, this suggestion was based on a comparison between the MG and *vastus lateralis* (VL) muscles. During DJ, the MTU lengthening of MG (5.2%) was less than that of VL muscle (11%).

In the *triceps surae* muscle group, only one study has shown that fascicles of the synergistic MG and SOL behaved differently during human walking (Ishikawa et al., 2005a). The MG fascicles were stretched during the early single-stance phase and then remained isometric during the late-single stance phase. In contrast, the SOL fascicles were lengthened during the single-stance phase. During this long contact phase of slow walking, the peak Achilles tendon load was quite low (-1600N). It is believed that this low impact condition cannot be used to generalize the fascicle behaviour of these muscles, as slow speed walking clearly differs from other forms of movement. Consequently, there is a need for a more detailed understanding of the muscle specific fascicle behaviour during higher Achilles tendon loading conditions of human SSC movements.

The objectives of the present study were to investigate fascicle-TT interaction in a synergistic pair of muscles (MG and SOL) during DJs of different impact loading conditions. We hypothesized that during the braking phase, the MG fascicles would shorten, when the impact loads were low. However, with increasing impact loads (higher drop heights in DJ), the MG fascicles would gradually less shorten during the braking phase due to the

increasing the impact load and then lengthen when the impact load is extremely high. In the SOL muscle, on the other hand, the fascicles were always expected to lengthen regardless of the stretch (impact) condition. Both of these hypotheses suggest that the MG muscle is much more sensitive to variation in the impact loads as compared to the SOL muscle during the high impact SSC movements. It must be emphasized that, to the best of our knowledge with except of the human walking (Ishikawa et al., 2005a), the SOL fascicle-TT interaction has not been studied previously under natural stretch (impact) conditions and simultaneously with MG muscles.

Methods

Subjects and experimental procedure

Eight physically active subjects: age 26.6 (SD 2.8) yr, height 170.1 (6.8) cm and body mass 61.9 (9.9) kg, who were familiarized with the sledge DJ exercises, participated in this study after giving informed consent of the procedures and risks. The study was approved by the Ethics Committee of the University of Jyväskylä.

After determining the lowest position of the sledge seat at rest with knee and ankle angles of 50 and 85 degrees, respectively (0 degree is extended position), the subjects performed several unilateral maximum DJs from different DH on the sledge apparatus (Horita et al., 2003; Ishikawa et al., 2003; Ishikawa and Komi, 2004; Kyrolainen and Komi, 1995) in order to decide the individual optimal DH for each subject. This was determined by dropping the subject from different heights to find the greatest rebound height of the center of gravity (Komi and Bosco, 1978). Thereafter, subjects performed the DJ with maximal rebounds from the four individually predetermined DHs: 50, 75, 100, and 120% of the optimal DH (DJ1, DJ2, DJ3 and DJ4, respectively), in a random order (Figure 7.1). Unilateral jump was chosen for the experimental condition for secure relatively higher impact load as compared to bilateral jump. To obtain the same condition bilaterally would not have been possible in our sledge apparatus. In the present study, the inclination was set 43 degrees from the horizontal position. During the jumping tasks, the lowest sledge seat position (see above) and maximal jumping height were confirmed by monitoring signals of the position sensor attached to the sledge seat during trials. Three successful trials were required for each task.

Figure 7.1. Schematic presentation of the experimental protocol.

Reaction forces (F_z; parallel to the movement plane of the sledge seat), sledge displacement, velocity of sledge displacement and EMG activity of the MG and SOL muscles of the right leg were stored simultaneously on a personal computer via an AD converter (Sampling rate 2 kHz; Power 1401, Cambridge Electronics Design Ltd, England). Surface bipolar EMG electrodes were used to record the MG and SOL muscle activities (Ag/AgCL miniature surface bipolar electrodes, inter-electrode distance of 20 mm; Beckman skin electrode 650437, USA). To place the EMG electrodes on the muscle belly, the B-mode ultrasound images were used to locate the midbellies of the muscle exactly and individually.

The midbellies of the muscles were confirmed from the B-mode ultrasonographic images. EMG signals were amplified (input impedance 25MΩ, common mode rejection ratio >90dB) and then sent telemetrically to the AD converter. The skin was lightly treated with sandpaper to secure an inter-electrode resistance value below 5 kΩ.

In all DJs, the subjects were video-recorded with a high speed video camera (200 fps; Peak Performance Inc, USA) from the right side, perpendicular to the plane of motion, to calculate the joint angles of the lower limb (knee and ankle). Reflective markers were placed on the centre of rotation of the shoulder, *trochanter major*, centre of rotation of the knee, lateral *malleolus*, heel and fifth metatarsal head, and then digitized automatically using Peak Motus software (Peak Performance Inc, USA). The transformed coordinates were digitally filtered with a Butterworth fourth-order zero–lag low-pass filter (cut-off frequency: 8Hz).

Longitudinal images of the MG and SOL muscles of the right leg were obtained during movement using a real-time B-mode ultrasound apparatus (SSD-5500, Aloka, Japan). An adhesive silicon pad was placed between the skin and the ultrasound probe to avoid

movement of the ultrasound transducer. The probe was fixed securely with a special support device made of polystyrene. The ultrasonographic apparatus was used to measure two-dimensional fascicle length in the MG and SOL muscles during the DJ (96 images·s^{-1}, 6 cm linear array probes with scanning frequency 10MHz, Aloka, JAPAN) (Ishikawa et al., 2005a; Ishikawa et al., 2005b). The width and depth (thickness) of the scanning images were 5.91 (330 pixels) and 5.38 (248 pixels) cm, respectively. The superior and inferior *aponeurosis* and the MG and SOL fascicles were identified and digitized in each image (Fukunaga et al., 2001; Ishikawa et al., 2005a; Ishikawa et al., 2005b; Kawakami et al., 2002) (Figure 7.2).

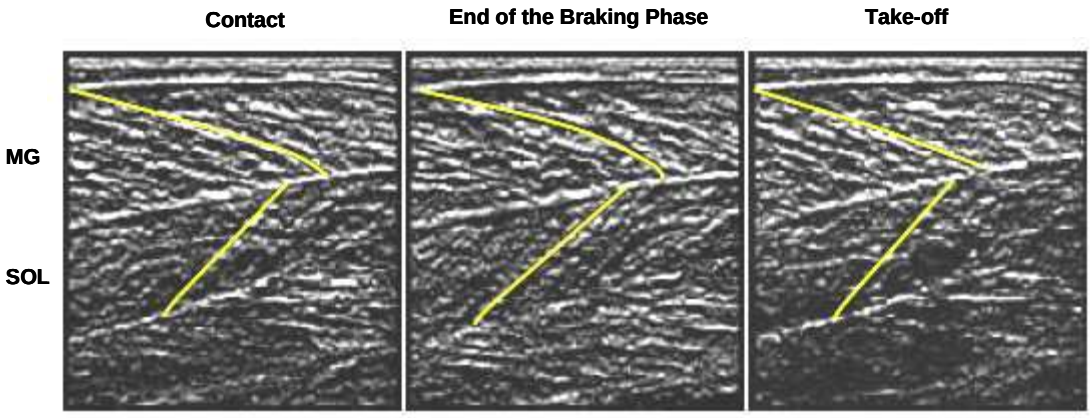

Figure 7.2. A typical example of the sequence of longitudinal ultrasonic images of the MG and SOL muscles during the drop jumps. Each longitudinal ultrasonic images was recorded at 96 Hz.

The reliability of the ultrasound method of the fascicle length has been established elsewhere with the coefficient of variation between 0-6 % (Fukunaga et al., 1997; Ishikawa et al., 2006; Kawakami et al., 1998; Kawakami et al., 2002; Kurokawa et al., 2001). An electronic pulse was used to synchronize the EMG, kinetic, kinematic and ultrasonographic data.

Analyses

The model of Hawkins & Hull (Hawkins and Hull, 1990) was used to estimate MTU length (L_{MTU}) changes in MG and SOL muscles from the joint angular data. The fascicle length data acquired at 96 Hz were interpolated to 100 Hz. After the L_{MTU} of MG and SOL data were re-sampled at 100 Hz, the length changes in TT were calculated by subtracting the

horizontal length component of the identified MG and SOL fascicle from the L_{MTU} (Fukunaga et al., 2001; Ishikawa et al., 2005a; Ishikawa et al., 2005b; Kurokawa et al., 2001).

$$L_{TT} = L_{MTU} - L_{fa} \cdot \cos \alpha,$$

where L_{TT} is the TT length, L_{MTU} is the muscle-tendon unit length, L_{fa} is the fascicle length and α is the angle between the fascicle line and the *aponeurosis* (pennation angle) (Figure 7.3). The estimated TT strain was calculated from the length changes of TT from the point of contact to the point of the peak TT length divided by the TT length at the contact moment.

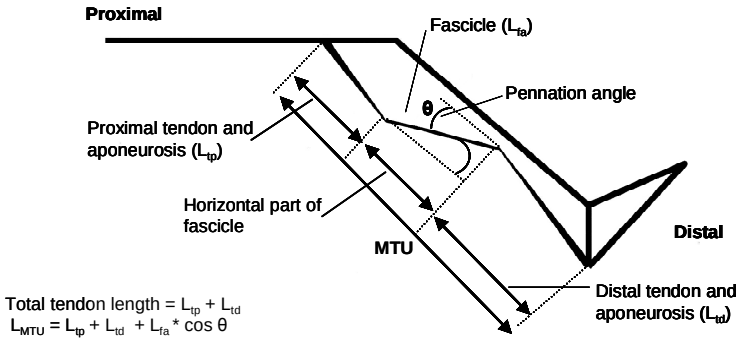

Figure 7.3. Schematic model of the triceps surae muscle group. The method requires that the total MTU length is kinematically continuously recorded, during the drop jumps.

EMG signals were full-wave rectified and low-pass filtered at 75Hz (Butterworth type fourth-order low-pass digital filter). The EMG signals were integrated and then averaged (aEMG) individually and separately for the following three phases during the ground contact of DJ: pre-activation, braking and push-off phases. The pre-activation phase was defined as the 100ms period preceding the ground contact. The transition from the braking phase to the push-off phase was determined while the sledge was at its lowest position.

Statistics

Values are presented as means and standard deviations (SD) unless stated otherwise. For the sledge speed and Fz, a one way Analysis Of Variance (ANOVA) with repeated measures with post hoc least significant difference multiple comparison was used to analyze the differences between the different DH conditions. A multivariable ANOVA was used to access the difference in the EMG and length data as well as interactions of the DH intensity with each muscle, and of the DH intensity with each phase. If interactions were

present, a post hoc Tukey test was used to test the difference between them. The Spearman's rank correlation coefficient for polynomial regression analysis of variables was used to calculate the statistical significance of the relationship between the dropping sledge speed and the fascicle stretch length. The probability level accepted for statistical significance was $P < 0.05$.

Results

Changes in mechanical parameters

As shown in Table 7.1, the sledge jump performances were in accordance with our hypotheses: the peak Fz and the peak dropping speed increased significantly from DJ1 to DJ4 and the corresponding peak rebound speeds increased until DJ3 (optimal DH).

Table 7.1. Average and SD values for drop speed, rebound speed, peak reaction force, and contact times for all subjects (n=8) and all dropping conditions (DJ1, DJ2, DJ3 and DJ4).

	DJ1	DJ2	DJ3	DJ4
Drop Speed (m/s)	0.48 (0.15)	0.76 (0.05) **	0.94 (0.07) **, ##	1.15 (0.12) **, ##, ¶¶
Rebound speed (m/s)	0.95 (0.17)	1.07 (0.16)	1.20 (0.11) **	1.13 (0.09) *
Peak Fz (N)	786.1 (101.5)	854.9 (137.6)	918.9 (129.6)	1060.1 (242.3) **, #
Contact time (ms)	453 (56)	432 (51)	420 (43)	410 (49)
Braking phase	237 (36)	215 (27)	207 (24) *	195 (27) **
Push-off phase	217 (28)	217 (27)	213 (25)	215 (27)

Values are expressed as means (S.D.)
*, ** Significantly different from DJ1 at P<0.05 and P<0.01 respectively
#, ## Significantly different from DJ2 at P<0.05 and P<0.01 respectively
¶¶ Significantly different from DJ3 at P<0.01

DJ4 was intended to represent an excessive DH (prestretch speed), and the resulting peak rebound speed of 1.13±0.09m·s^{-1} did not show any significant increase as compared to DJ3 (1.20±0.11m·s^{-1}). Although the total contact time did not show any significant change, the duration of the braking phase decreased in DJ3 and DJ4 as compared to DJ1 (Table 7.1).

Changes in EMG activity

As SSC of muscle function can be divided into three important parts: the preactivation, braking and push-off phases (Komi, 2000); the recorded EMG signals were consequently analysed for these phases during the four DH conditions (DJ1, DJ2, DJ3 and DJ4) performed with maximal rebounds. These results are shown in Figure 7.4. When a

significant interaction between a muscle and a particular phase (P<0.01) was found, the difference of the DH intensity was examined for each muscle. The most obvious finding was the significant increase of preactivation of MG and SOL muscles as a function of the DH. In addition, in the braking phase, the DJ3 condition showed higher aEMG values of both muscles as compared to DJ1 (Figure 7.4). When DJ3 was compared with DJ4, the SOL aEMG continued to increase in the braking phase.

This was not the case for the MG muscle, although its aEMG at DJ4 was still higher than at DJ1 (P<0.05). In the inter-muscular comparison, significant differences were observed between MG and SOL muscles from DJ1 to DJ3, but this significance disappeared at DJ4. The push-off phase EMG activities showed similar amplitudes, independent of the DH conditions in the evaluated muscles.

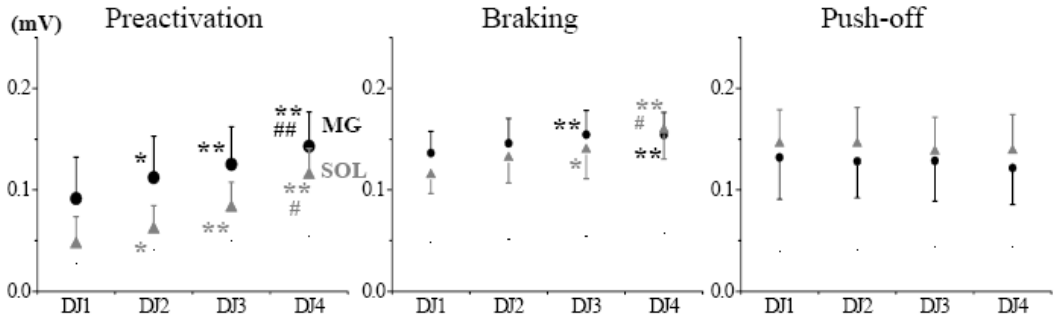

Figure 7.4. Average EMG values (+/-SD) for Medial *Gastrocnemius* (MG) and *Soleus* (SOL) muscles, in preactivation, braking and push-off phases for all dropping conditions (DJ1, DJ2, DJ3 and DJ4).
*, ** Significantly different from DJ1 at P<0.05 and P<0.01, respectively
#, ## Significantly different from DJ2 at P<0.05 and P<0.01, respectively

Changes in fascicle-TT

As the major purpose of the present study was to compare the fascicle behaviour between the two muscles (MG and SOL), Figure 7.5 was constructed to give a representative example of the changes in the examined parameters during the contact phase (DJ1, DJ2, DJ3 and DJ4). The curves were obtained from three repetitions, with the first contact on the force plate used as a trigger point for averaging. As shown in figure 7.5, and also verified for the entire sample group, the MG and SOL muscles both exhibited similar MTU behaviour across all jumping conditions. In all DJs, the MTU of the two muscles demonstrated a

typical SSC behaviour: stretch prior to shortening during contact with the force plate. The same was also observed for the behaviour of the TT in both muscles.

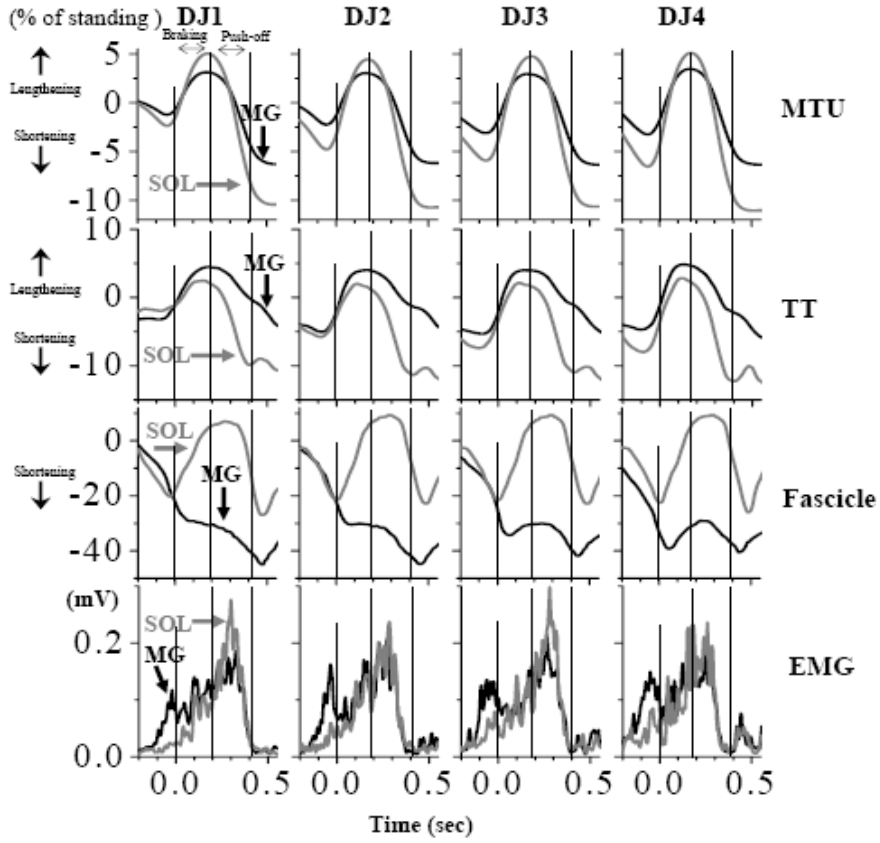

Figure 7.5. Representative example of the time course data of the lengths of the medial *gastrocnemius* (MG) and *soleus* (SOL) muscle-tendon units (MTU), tendinous tissue (TT) and fascicle, together with the EMG activity of the MG and SOL muscles. 0.0 in the x-axis shows the contact moment of the DJ. "% of standing" in the y-axis for the first 3 rows show the relative changes from the length in the upright position. Vertical dotted lines show the points of the contact, end of the braking phase and take-off.

The amplitudes of the respective stretch and shortening of the MTU and TT, in the braking and push-off phases, are shown in Figure 7.6. The stretch amplitudes of the two muscles increased as a function of DH intensity, and the amplitudes of shortening remained constant within each muscle, across conditions.

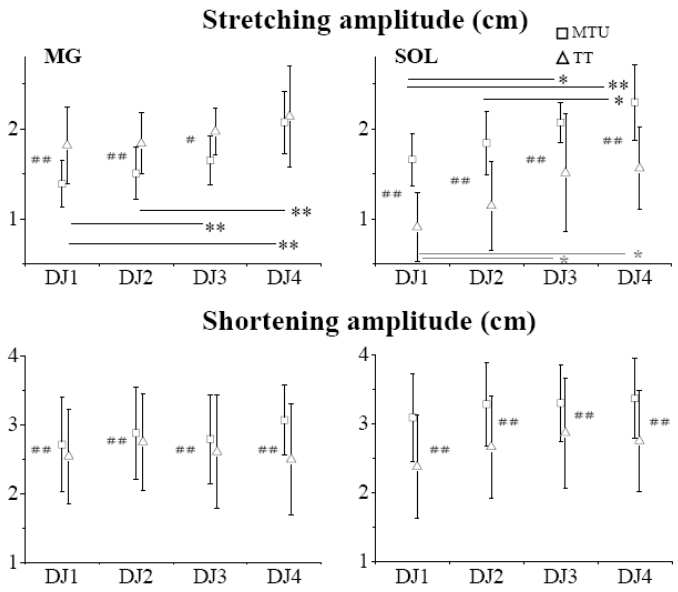

Figure 7.6. Amplitudes of stretch (upper) and shortening (lower) in the braking phase and push-off phases for muscle-tendon unit (MTU) and tendinous tissue (TT) of the Medial *Gastrocnemius* (MG) and *Soleus* (SOL) muscles for all dropping conditions (DJ1, DJ2, DJ3 and DJ4).
*, ** Significantly different between conditions at P<0.05 and P<0.01, respectively
#, ## Significantly different between MTU and TT at P<0.05 and P<0.01, respectively

The effects of DH on TT strain are displayed for both muscles in Fig 7.7. There was a significant interaction between the factors of DH and the muscle that was investigated (P<0.05), and the subsequent analysis of the effects of DH showed that the TT strain of SOL increased with increasing DH (P<0.05). This was not the case for MG (Figure7.7).

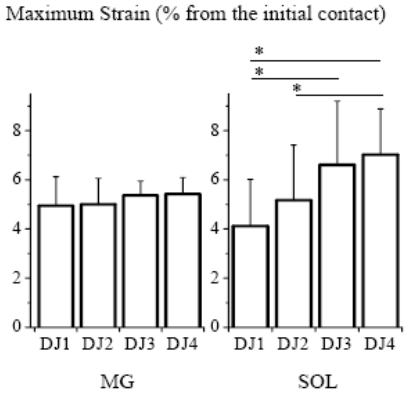

Figure 7.7. Calculated Peak TT strains of the MG and SOL during DJs under the different DH conditions. The bars show group means+SD. The strain was calculated from the length at the initial contact to the length at the peak TT stretch during contact divided by the TT length at the initial contact. There was a significant increase in the TT strain of SOL when the DH increased (* P<0.05).

The situation became more complicated, however, when fascicle length changes were compared. As already shown in Figure 7.5, different fascicle length behaviour was observed between the two muscles when the DH was increased. Until the point of contact, the fascicles of both muscles shortened, but thereafter the patterns became different. After the initial contact, the SOL fascicles began lengthening before shortening in all subjects (Table 7.2), thus following the SSC concept. The MG fascicles, however, continued shortening during the early braking phase in all DH conditions in all subjects (Figure 7.5 and Table 7.2). Thereafter, the MG fascicles behaved differently during the late braking phase depending on DH condition. In DJ1 and DJ2, the MG fascicles further shorten or remained the same length during the late braking phase. In DJ4, which represents very high stretch loads upon impact, a sudden stretch of the MG fascicles after 30-60 ms of the contact were observed in all subjects (also in DJ3 in some subjects). In the subsequent push-off phase, the MG fascicles shortened again in all subjects (Figure 7.5 and Table 7.2).

Table 7.2. The fascicle length (cm) at the contact, end of the braking phase and take-off moments during the contact of drop jumps.

	Contact		End of Braking Phase		Take-off	
MG						
DJ1	3.76 (0.39)	#	3.54 (0.27)	*	3.27 (0.60)	**, $
DJ2	3.62 (0.40)		3.51 (0.27)	*	3.17 (0.40)	**, $
DJ3	3.57 (0.41)		3.48 (0.27)		3.21 (0.42)	*, $
DJ4	3.25 (0.31)		3.38 (0.27)	*	3.17 (0.26)	$
SOL						
DJ1	4.41 (0.99)		5.04 (0.96)	*	4.29 (0.96)	$
DJ2	4.35 (1.05)		5.05 (0.96)	*	4.44 (0.95)	$
DJ3	4.35 (1.06)		5.02 (0.94)	* #	4.43 (1.01)	$
DJ4	4.34 (1.04)		4.97 (0.92)	*	4.52 (0.84)	$

Values are expressed as means (S.D.)
Significantly different from DJ1 to other DJs at P<0.05
*, ** Significantly different from the contact at P<0.05, and P<0.01, respectively
$ Significantly different from end of the braking phase to the take-off at P<0.05

Discussion

Previous investigations have suggested that the patterns of fascicle length changes during SSC exercises are muscle and intensity (DH and rebound effort) specific (Ishikawa and Komi, 2004; Ishikawa et al., 2005b). The present work represents the first attempt to compare the fascicle behaviour in synergistic muscles (MG and SOL) during different SSC exercises, including very high impact load (DH) conditions. In the present DJ movements, different patterns of fascicle length changes were observed between the MG and SOL

muscles. The SOL fascicles demonstrated lengthening prior to shortening during the contact phases of all DJ conditions. Moreover, with increasing DH, in which the peak Fz increased and the contact time during the braking phase decreased, the stretch amplitudes of the SOL fascicles did not show any clear difference whilst EMG activation increased. On the other hand, the MG fascicles behaved differently from those of the SOL muscle during the DJs (Figure 7.5), especially during the late braking phase. With increasing DH, which represent much higher impact loads than those measured during walking (Ishikawa et al., 2005a), the MG fascicles shortened less during the late braking phase and then they were sudden stretched in DJ4 (also DJ3 in some subjects) (Figure 7.5, Table 7.2). The present results thus emphasize that the MG fascicle behaviour were varied during the braking phase of DJ depending on DH and the fascicles of MG and SOL muscles do not show the same behaviour during the braking phase of DJ. This was in spite of the fact that the EMG activation of both muscles trended to increase similarly from DJ1 to DJ3 (Fig 7.4). These results thus clearly indicate the existence of muscle specific fascicle behaviour (MG and SOL) that is also dependent on the DH.

In order to compare the influence of the DH on fascicle length changes during the braking phase, Figure 7.8 plots these attributes against each other for this particular phase. The length change patterns tend to have an opposite quadratic relationship relative to the prestretch intensity (dropping speed). In the MG muscles, there is perhaps a critical level of the stretch load (DH), beyond which the MG fascicles lose their ability to tolerate the imposed load (Figure 7.8A). It is interesting to observe that the result shown in Figure 7.8A is almost identical to the one presented in a previous report (Ishikawa et al., 2005b), which used a different SSC exercise to the present study. These results also suggest that the MG and SOL fascicles can behave differently during DJ, as well as that there may be specific length change patterns of the MG and SOL fascicles depending on the DH intensity.

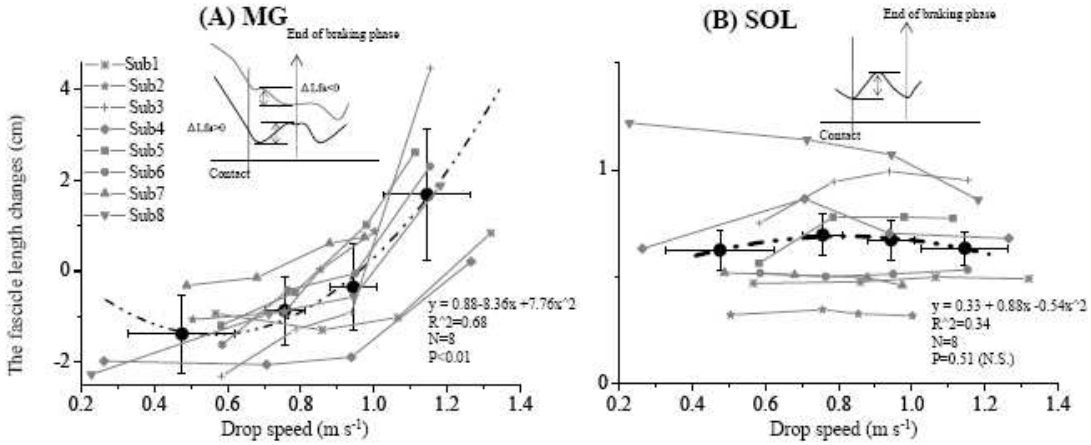

Figure 7.8. The slope of MG (A) and SOL (B) fascicle length changes versus the peak dropping speed of the sledge displacements in the braking phase (n=8). The filled circles and bars show the averaged data and standard errors. The inset shows how the fascicle length changes were calculated (see also Ishikawa et al. 2005).

The observed difference in the fascicle behaviour between the two muscles is interesting from several points of view. One may first think that the result can be explained from the pure anatomical differences between the muscles. The MG muscle is clearly a bi-articular muscle and has unique functions in saving energy and power flow from one joint to another during human locomotion (Elftman, 1939; van Ingen Schenau et al., 1987; van Ingen Schenau et al., 1990). The results presented in Figure 7.5 and 7.6 also highlight the differences between mono- and bi-articular muscles, in which the stretched MTU length was significantly shorter in MG than in SOL muscle for all DH conditions (Figure 7.5, 7.6). At the fascicle level, the stretched fascicle length was smaller in MG than in SOL (Figure 7.5, Table 7.2). Figure 7.9 shows the relation between the absolute/relative MTU and fascicle stretch amplitudes from contact to the end of the braking phase in both muscles. If the MTU stretch is measured in absolute terms, then the fascicles are less stretched in MG than in SOL (Figure 7.9). However, it may be possible that the fascicles behave in a similar way, if the relative values are considered (Figure 7.9B). Consequently, these results cannot clarify that the smaller MTU stretch in the bi-articular MG muscle is a factor that is specific to MG fascicle behaviour during DJs.

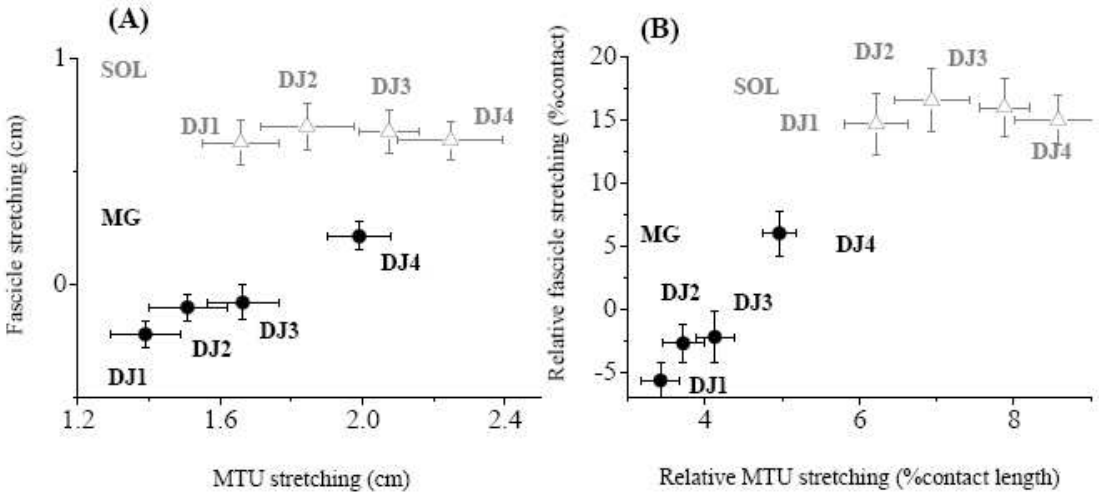

Figure 7.9. The fascicle-MTU stretch relationship during the different DH conditions between MG and SOL muscles (circle: MG, triangle: SOL). (A) shows the absolute stretch length from the contact to the end of the braking phase. (B) shows the relative stretch from the length at contact.

The functional difference between the MG and Sol muscles warrants further attention from the present results. In the comparison between MG and SOL muscles of the present study, the TT stretch amplitudes were greater in MG than in SOL. In addition, in SOL the TT stretch amplitudes were significantly smaller than the MTU stretch amplitudes in all DJ conditions. The MG muscle showed the opposite result in this regard (Figure 7.6). This is in line with the previous study that compared MG and VL muscles (Ishikawa et al., 2005b). Furthermore, the present study showed that the difference of the TT and MTU stretch amplitudes in MG became smaller with higher DH conditions, but this was not the case in SOL (Figure 7.6). In terms of the calculated TT strain during the contact of DJs, MG did not show any significant variation between the conditions, although SOL showed significantly higher strain values with increasing DH (Figure 7.7). These results could also imply different roles that the MG and SOL muscles play during locomotion. They may be related to the idea of the bi-articular muscle function proposed by van Ingen Schenau et al. (1987), in which a bi-articular muscle may be involved in the fine regulation of the distribution of net torques over two joints, whereas the mono-articular muscles act mainly as force or work generators.

When a similar exercise protocol using different contact times (bilateral DJs) was used to observe MG fascicle (Ishikawa et al., 2005b), the results were identical to those observed

in the present study. However, the SOL muscle was not investigated in the previous study (Ishikawa et al., 2005b). In the present study, the SOL muscle behaved differently from MG in several ways. The SOL muscle activity in the preactivation and braking phases trended to be higher in DJ4 than DJ3, but not in MG (Figure 7.4). Correspondingly, the SOL fascicle length at the end of the braking phase is shorter in DJ4 than in DJ3 (only significant difference between DJ2 and DJ4, Table 7.2). This suggests that the SOL muscle is still able to function “normally” without any additional rapid fascicle length changes (MG).

It would be beneficial to also discuss the results from the point of view of neural influences. The results presented in Figure 7.5 and Table 7.2 clarify the findings obtained in studies where running and various intensity hopping exercises were used. Voigt et al. (1998) reported that in the SOL muscle, the SLR in SSC is very apparent and easier to record than in the MG muscle during submaximal hopping. In contrast, Dietz et al. (1979) observed the SLR responses in MG during running and Moritani et al. (1990) reported that the amplitude of H-reflex modulation was higher in MG than in SOL during maximal effort hopping.

According to the present study, it seems evident that the fascicles of MG shortened during the braking phase of the DJ1 and DJ2 conditions, while those of SOL were stretched (Figure 7.5). On the other hand, with higher impact loads (DH) the MG fascicle stretching were observed during the late braking phase (in DJ4) (Figure 7.5), while the SOL fascicles remained the similar behaviour (stretching-shortening) in all DH conditions (Table 7.2). These results can partially explain the different results of Voigt et al. (1998), and Dietz et al. (1979) and Moritani et al. (1990; 1991). Consequently, the DH intensity and muscle specific fascicle length changes during the braking phase of DJs may influence the stretch-induced muscle activation.

Furthermore, it has been suggested that in extreme high DJ exercises, inhibitory effects from the Golgi tendon organ (GTO) may be operative. It would be useful to know if there are any differences in inhibitory inputs to the two muscles in DJs. In the present results, the MG aEMG during the braking phase did not increase from DJ3 to DJ4 (Figure 7.4), while the MG fascicles were stretched during the braking phase in DJ4 (Figure 7.5, 7.8, and 7.9). In the SOL muscle however, the aEMG increased and the stretch amplitudes of the SOL fascicles did not show any difference between DJ3 and DJ4 or were lower in DJ4 (Figure 7.8 , 7.9, and Table 7.2). One may speculate that while the MG muscle receives less

facilitatory Ia afferent input (the muscle spindle content is greater in SOL than MG (Kokkorogiannis, 2004)), the same amount of Ib input would have greater inhibitory influences on the MG as compared to the SOL muscle. This different muscle fibre composition of respective muscles may influence the observed different fascicle behaviour to the DH intensity. This assumption also depends upon additional unknown factors, such as the possibility that the induced stretch loads have equal excitatory effects on the activation of Ib afferents in both muscles. However, it is still not easy to see how the possible inhibitory influences, for example from the GTO, would operate differently between the two synergistic muscles.

In the previous study (Ishikawa et al., 2005b), our major argument was that the “yielding” that occurred simultaneously with fascicle lengthening was due to sudden cross-bridge detachment in high DH conditions. The present results showed that the MG fascicles were stretched during the braking phase of DJ4 (Figure 7.5). The contact times of the braking phase are twice as long in the present study (approximately 200ms) as compared to the previous one (Ishikawa et al., 2005b) (<100ms). Therefore, the sudden cross-bridge detachment may not occur at the same magnitude as in the DJ condition of the previous study (Ishikawa et al., 2005b). This is seen from the slopes of the fascicle stretch that were approximately twice as steep in the previous study (Ishikawa et al., 2005b). It has been suggested that DJ performance reduction during the extreme high DH condition can be affected by neural inhibition, as well as by mechanical cross-bridge slipping (or detachment) (Ishikawa et al., 2005b). In the present study, the inhibitory effects from the GTO, if present, may be mainly operative in the performance reduction of the long contact and extreme high DJ condition (the present DJ4).

Whatever the possible mechanism is, the observed intermuscular differences in fascicle behaviour are very important findings of the present study. They certainly mean that the whole concept of the SSC of muscle function needs to be assessed very critically, especially regarding the way in which fascicles interact with TT during normal locomotion. An equally important consideration is that the fascicle behaviour is task dependent, at least in some muscles. For example, there is a preferential and movement phase-dependent neuromuscular activation within the human ankle extensor synergistic muscles (Moritani et al., 1991). In addition, and as shown in the present study, the preactivation may be DH dependent (see also Ishikawa and Komi 2004 and Ishikawa et al. 2005). There are,

however, reports in the literature that question the inter-dependence of DH and EMG preactivation (Arampatzis et al., 2001). Dietz (1992), while supporting the intensity dependent preactivation, suggested that the foot position and expectancy of the moment of ground contact may be critical factors for preactivation.

Conclusions

In summary, the results of the present study highlight different fascicle behaviour in synergistic muscles (MG and SOL) during DJ exercises. In addition, both muscles did not show DH dependent fascicle behaviour in a similar manner, although the EMG activities of these muscles were dependent on DH. Although some of these aspects had been previously observed to a certain degree (Ishikawa et al., 2003; Ishikawa et al., 2005b), the present comparison with simultaneous recording of two synergist muscles emphasizes the above mentioned differences even more strongly.

7.3. Next Goals

Combine the *in vivo* (direct measurements of the Achilles tendon) muscular force measurements with fascicle length measurements, during high intensity drop jumps, to better understand the muscle mechanics in SSC movements.

Compare the inverse dynamics solutions with the direct comparison of the *in vivo* direct measurements.

7.4. References:

Arampatzis, A.; Schade, F.; Walsh, M. and Bruggemann, G. P. (2001). Influence of leg stiffness and its effect on myodynamic jumping performance. J Electromyogr Kinesiol 11: 355-364.

Dietz, V. (1992). Human neuronal control of automatic functional movements: interaction between central programs and afferent input. Physiol Rev 72: 33-69.

Dietz, V.; Schmidtbleicher, D. and Noth, J. (1979). Neuronal mechanisms of human locomotion. J Neurophysiol 42: 1212-1222.

Elftman, H. (1939). The function of muscles in locomotion. Am J Physiol 125: 339-356.

Fukunaga, T.; Ichinose, Y.; Ito, M.; Kawakami, Y. and Fukashiro, S. (1997). Determination of fascicle length and pennation in a contracting human muscle in vivo. J Appl Physiol 82: 354-358.

Fukunaga, T.; Kubo, K.; Kawakami, Y.; Fukashiro, S.; Kanehisa, H. and Maganaris, C. N. (2001). *In vivo* behaviour of human muscle tendon during walking. Proc R Soc Lond B Biol Sci 268: 229-233.

Hawkins, D. and Hull, M. L. (1990). A method for determining lower extremity muscle-tendon lengths during flexion/extension movements. J Biomech 23: 487-494.

Horita, T.; Komi, V.; Hamalainen, I. and Avela, J. (2003). Exhausting stretch-shortening cycle (SSC) exercise causes greater impairment in SSC performance than in pure concentric performance. Eur J Appl Physiol 88: 527-534.

Ishikawa, M.; Finni, T. and Komi, P. V. (2003). Behaviour of vastus lateralis muscle-tendon during high intensity SSC exercises *in vivo*. Acta Physiol Scand 178: 205-213.

Ishikawa, M. and Komi, P. V. (2004). Effects of different dropping intensities on fascicle and tendinous tissue behavior during stretch-shortening cycle exercise. J Appl Physiol 96: 848-852.

Ishikawa, M.; Komi, P. V.; Grey, M. J.; Lepola, V. and Bruggemann, G. P. (2005a). Muscle-tendon interaction and elastic energy usage in human walking. J Appl Physiol 99: 603-608.

Ishikawa, M.; Niemela, E. and Komi, P. V. (2005b). Interaction between fascicle and tendinous tissues in short-contact stretch-shortening cycle exercise with varying eccentric intensities. J Appl Physiol 99: 217-223.

Ishikawa, M.; Pakaslahti, J. and Komi, P. V. (2006). Medial gastrocnemius muscle behavior during human running and walking. Gait Posture (in press)

Kawakami, Y.; Ichinose, Y. and Fukunaga, T. (1998). Architectural and functional features of human triceps surae muscles during contraction. J Appl Physiol 85: 398-404.

Kawakami, Y.; Muraoka, T.; Ito, S.; Kanehisa, H. and Fukunaga, T. (2002). In vivo muscle fibre behaviour during counter-movement exercise in humans reveals a significant role for tendon elasticity. J Physiol 540: 635-646.

Kokkorogiannis, T. (2004). Somatic and intramuscular distribution of muscle spindles and their relation to muscular angiotypes. J Theor Biol 229: 263-280.

Komi, P. V. (2000). Stretch-shortening cycle: a powerful model to study normal and fatigued muscle. J Biomech 33: 1197-1206.

Komi, P. V. and Bosco, C. (1978). Utilization of stored elastic energy in leg extensor muscles by men and women. Med Sci Sports 10: 261-265.

Kurokawa, S.; Fukunaga, T. and Fukashiro, S. (2001). Behavior of fascicles and tendinous structures of human gastrocnemius during vertical jumping. J Appl Physiol 90: 1349-1358.

Kyrolainen, H. and Komi, P. V. (1995). Differences in mechanical efficiency between power- and endurance-trained athletes while jumping. Eur J Appl Physiol Occup Physiol 70: 36-44.

Moritani, T.; Oddsson, L. and Thorstensson, A. (1990). Differences in modulation of the gastrocnemius and soleus H-reflexes during hopping in man. Acta Physiol Scand 138: 575-576.

Moritani, T.; Oddsson, L. and Thorstensson, A. (1991). Phase-dependent preferencial activation of the soleus and gastrocnemius muscle during hopping in humans. J Electromyogr Kinesiol 1: 33-40.

van Ingen Schenau, G. J.; Bobbert, M. F. and Rozendal, R. H. (1987). The unique action of bi-articular muscles in complex movements. J Anat 155: 1-5.

van Ingen Schenau, G. J.; Bobbert, M. F. and van Soest, A. J. (1990). The unique action of bi-articular muscles in leg extensions In: Winters, J. M., Woo, S. L. (eds) Multiple Muscle System. Springer, New York, pp. 639-352.

van Ingen Schenau, G. J.; de Koning, J. J. and de Groot, G. (1994). Optimization of Sprinting Performance in Running, Cycling and Speed Skating. Sports Med 17: 259-275.

Voigt, M.; Dyhre-Poulsen, P. and Simonsen, E. B. (1998). Modulation of short latency stretch reflexes during human hopping. Acta Physiol Scand 163: 181-194.

Chapter 8

Conclusions

8.1. Main Findings

The main conclusions from the first study (chapter 3) were:

- The estimated results obtained in this study, using the inverse dynamics approach to calculate the forces and articular moments, as well as the muscular mechanical power, showed a high internal coherence, and an individual persistence to point out.

- Complementarily, the results obtained are according to theoretical expectations, suggesting that this methodology is adequate to the problem approached.

- Through the analysis of the magnitude of the peak values from articular force estimated, it is possible to observe that, in some jumps, the values of forces are of the order of three times the body weight, showing the high injury potential that the anatomical structures of ballet dancers are exposed to.

- The evaluation of movement in terms of moments and power, allow a better and new comprehension about the individual strategies of movement performance, occasionally allowing a technical intervention, helping in the improvement of the performance.

- The knowledge of intra articular forces, particularly in this activity and also in many others, is very important to the understanding of the risks of injury associated to repetitive efforts and his eventual prevention.

The main conclusions from the second study (chapter 4) were:

- Results pointed out the existence of a pre-activation effect before landing in almost all cases.

- It can also be concluded from the correlations obtained that co-contractions are intense and should be taken into account during biomechanical analysis of Ballet jumps, namely in an inverse dynamics approach.

- We also observed large changes in the recorded parameters from execution to execution, and with simple changes in the jumps performed, making it problematic to

generalize the quantitative results. The qualitative conclusions – the existence of important pre-activation and co-contractions -, however, will need to be taken into account in the inverse dynamic studies that will follow.

The main conclusions from the third study, (the technical note, chapter 5) were:

- Different kind of filters must be selected in each phase of the selected movements. In the present study, the usual filtering techniques, such as the Butterworth technique, seems to be appropriated to apply in the aerial phase of the jumps. In the brief impact phases of these jumps, the signal must be treated in a different way. The filter should be less severe than Butterworth (for example splines), so that the corner trajectory of the signal, i.e., the most important phase when we studying impacts, doesn't disappear.

- The problem when the signal is cut in several pieces is that, after the selection and application of the filter, or different filters, it is necessary to ensure the continuity of the trajectory of the signal. That is, it is necessary to "glue" appropriately all the pieces obtained from the initial phase of cut and separate the signal in several parts.

- In sum, we believe that the biomechanics community will benefit from this alternative filtering technique, which has proven its effectiveness with complex signals, as an alternative or complement to usual smoothing techniques.

- Nevertheless, future studies need to be done in order to produce more accurate filtering algorithms.

The main conclusions from the fourth study, (chapter 6) were:

Classical Inverse Dynamics

- The results from the classical inverse dynamics approach are very sensitive to the input data precision (video, GRF). The efforts to refine the filtering and differentiation of these reveal no significant improvement in desensitising these results. This is the weak

point of this phase and we think that a greater effort has to be done at the acquisition level, including the usage of redundant sources, e.g., video cameras, accelerometers, etc.

- Through the analysis of the magnitude of the peak values from articular forces estimated in the ankle, knee and hip joints, it was possible to observe that, in some jumps, the values registered are of the order of three times the body weight, showing the injury potential that the anatomical structures of ballet dancers are exposed to.

- The peak values of articular force estimated in every jump and subject, decrease, comparing the ankle with the knee joint, and the knee with the hip joint. As expected, this decrease of force from one joint to another joint is possibly due to the occurrence of absorption phenomenons induced by the body tissues. This occurrence will put in perspective the energy transfer phenomena processed by the bi-articular muscles, subsequently calculated in second part of this study (the hybrid forward-inverse dynamic model).

- When the focus of the analysis is the injury potential of forces what is happening externally (GRF) is not a direct indicator of internal loads. A simple thought about forces produced doesn't include the time duration of the impact forces, therefore, is not a reasonable indicator about their injury potential. The injury potential is probably related with energy dissipation.

Extended Inverse Dynamics (muscular decomposition)

- The usage of a hybrid forward-inverse dynamical model seems to desensitise it from the objective function. This is beneficial as these functions are not physically or physiologically founded. These hybrid models can be seen as the result of an exchange of the importance of the ad-hoc objective functions to the importance of the muscle model, more easy to found in the physiology (Hill's or Huxley's models, etc).

- After the analysis of the forces and energies produced by each muscle included in our model, and in each jump, it was possible to observe that the behaviour of the musculature involved, is somehow dependent on the technique used in the

performance. Small external changes, i.e., small technical changes, can result in significant internal changes. The technique can modify the internal distribution of forces.

- Initially the jumps were separated and grouped in moderate and high impact jumps, according to the peak values registered in the GRF passive peak curve. Nevertheless, the moderate and high impact groups don't reflect what is internally happening. The moderate and high impact does not mean the same for all the muscle groups. Muscles do not work more or less due to the fact of the jump classification.

- The model is very dependent on its assumptions and parameters, like anatomical and physiological. The final accuracy of our model is greatly influenced by the accuracy of the anatomical data, which must include a full rigorous model of the musculoskeletal geometry.

- It is possible to conclude that the results obtained from the extended inverse dynamics approach (muscular decomposition) with and without EMG, are not radically different. The biggest differences are particularly observed in the role of mono and bi-articular muscles.

- What should be the way to follow? With or without EMG?
Our results suggest that the extended inverse dynamics approach with some activation values obtained from the EMG records were more incoherent, in the sense that there is an excessive role attributed to the mono-articular muscles in detriment of the bi-articular ones. One can not say if the problem is related to the combination of the two sources of activation information (or the missing EMG records from other muscles) or if it is related to the unsubstantiated usage of EMG data to estimate activation in impulsive movements. Nevertheless, it is known from literature the important role of bi-articular muscles, specially the mechanism of energy transfer.

- In our study, the results obtained from pure optimization procedures, which are highly dependent on pure conjectures, were more according to expectations. We can observe the important role of bi-articular muscles and the mechanism of energy transfer, between adjacent muscles and segments.

- We think it is necessary more research around this theme. Another kind of results should be expected if we have EMG from all the superficial muscles (mono and bi-articular) from the lower limb, and if possible, combined with direct measurements from muscular force.

- Without direct measures one can not make a definite case in favour of any of the strategies. Nevertheless, the ecological tool would avoid the usage of intrusive techniques like EMG and internal force sensors.

The main conclusions from the fifth study, (chapter 7) were:

- In summary, the results of the present study highlight different fascicle behaviour in synergistic muscles (MG and SOL) during DJ exercises. In addition, both muscles did not show DH dependent fascicle behaviour in a similar manner, although the EMG activities of these muscles were dependent on DH. Although some of these aspects had been previously observed to a certain degree (Ishikawa et al., 2003; Ishikawa et al., 2005b), the present comparison with simultaneous recording of two synergist muscles emphasizes the above mentioned differences even more strongly.

In general, two main findings should be stressed out from this thesis:

a) the complex interaction of muscles performing a simple task (landing), includes the role of the synergists, antagonists and bi-articular/energy transfer muscles;
b) each muscle undergoes a complex interaction with the tendon tissue to with it is connected, storing and recovering some energy, and make the overall movement a little more efficient.

Through the analysis of the magnitude of the peak values from articular force estimated, it is possible to observe the injury potential that the anatomical structures of ballet dancers are exposed to.

The evaluation of movement in terms of moments and power, allows a better and new comprehension about the individual strategies for movement performance, occasionally allowing a technical intervention, helping in the improvement of performance.

The knowledge of intra articular forces, particularly in this activity but also in many others, is an important tool for the understanding of the risks of injury associated to repetitive efforts, and its eventual prevention.

The recorded data from live executions confirm the existence of important pre-activation and co-contractions. These will need to be taken into account in any muscle decomposition/inverse dynamic approach. We have accomplished these to some extent.

The alternative filtering techniques used to smooth the kinematical data didn't present any significant improvement in desensitising the results from the errors from the input data.

In general, the studies of our thesis contribute to the knowledge of: the nature and attenuation of the imposed loads; the mechanism of energy transfer and conservation, and the potentiation of movement's efficiency.

The results of our studies contribute to increase the knowledge about exercise prescription and injury prevention. It will help the professors and choreographers in the organization of correct programs of training and the physiotherapists in the prescription of correct rehabilitation programs.

8.2. Future Research

From the conclusions of this thesis, we are now in conditions to suggest some directions for future research:

- Use three-dimensional kinematics.

- Improve the precision of the kinematical data by the simultaneous use of video redundancy and accelerometers.

- Apply other alternative filtering techniques to smooth the kinematical data and test their applicability in the inverse dynamics approach.

- To extend the usage of these tools to examine the mechanical loading in other movements and populations, once the balletic movements have very unusual kinematical restrictions.

- Combine the *in vivo* (direct measurements of the Achilles tendon) muscular force measurements with fascicle length measurements, during high intensity drop jumps, to better understand the muscle mechanics in SSC movements.

- Compare the inverse dynamics solutions with the direct comparison of the *in vivo* direct measurements.

- Try to understand, why the EMG records from MVC (isometric) are smaller than some EMG records for impulsive movements. This probably relates to neural control and reflex mechanisms. The understanding of these mechanisms is crucial to a proper extraction of the activation functions from the EMG records.

- Overall, to combine the various tools: theoretical modelling of muscular and tendinous forces, direct measurements of fascicle and tendinous elongation, direct force measurements at the tendon in order to get a broader picture of the dynamics of impulsive loads in the lower limb. This combination will be a driving force in selecting and improving the theoretical techniques.

Appendix I

I. Mathematical Filters

Here we present, in more detail the mathematical filters used in the chapter 5.

I.1. Butterworth

Butterworth filters are one of the most commonly used digital filters in motion analysis. As well as other filters like Chebyshev, Bessel, Elliptic, etc., the Butterworth is designed to have a certain frequency response (Cadzow, 1987).

The frequency response of the Butterworth filter is:

- near unity in the frequency range we do not want to filter (passband) and near zero in the frequency range were there is no relevant signal and most of the noise is present
- maximally flat (has no ripples) in the passband

For this type of filters it is essential that signal and noise have different frequency contents. The comparison of the Butterworth filter with other frequency-based filters, obtained with the same number of coefficients, is shown in the figure I.1.

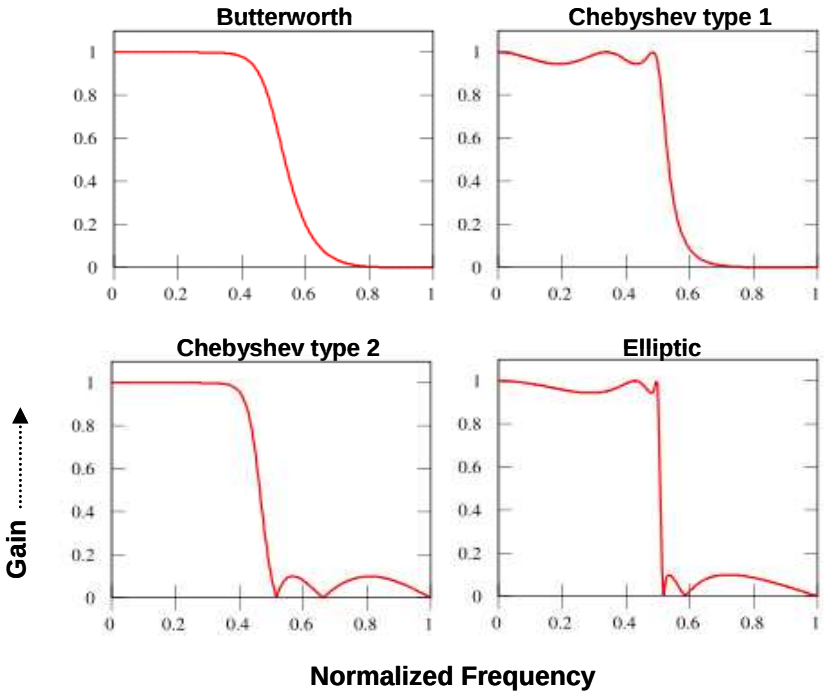

Figure I.1. Comparing the Butterworth filter with other frequency-based filters, obtained with the same number of coefficients.

It is possible to observe, that the Butterworth filter, in spite of roll off much more slowly than the others filters, don’t show any ripples in the frequency response. Because of the slower roll off, the Butterworth will require a higher order to implement a particular stopband specification. Butterworth filters have a monotonically decreasing magnitude function with ω. Comparing with other frequency-based filters, it is the only filter that maintains the same shape for higher orders (with a steeper decline in the stopband).

I.2. Spline

A spline is a special function defined by piecewise polynomials used in applications requiring data interpolation and/or smoothing. They are implemented in the time domain (Boor, 2001).

Splines are a mathematical means of representing a curve, by specifying a series of points at intervals along the curve, and defining a function that allows additional points within an interval to be calculated.

In their most general form, splines can be considered as a mathematical model that associate a continuous representation of a curve with a discrete set of points in a given space. Spline fitting is an extremely popular form of piecewise approximation using various forms of polynomials of degree “n”, on an interval in which they are fitted to the function at specified points.

In its most general form, a polynomial spline $S:[a,b]\to R$ consist of polynomial pieces $P_i:[t_i,t_{i+1}]\to R$

$$\begin{aligned} &S(t)=P_0(t), t_0\le t<t_1,\\ &S(t)=P_1(t), t_1\le t<t_2,\\ &...\\ &S(t)=P_{k-2}(t), t_{k-2}\le t_{k-1} \end{aligned} \qquad \text{(I.1)}$$

where,

$a=t_0<t_1<...<t_{k-2}<t_{k-1}=b$

The given k points (t_i) are called knots. The vector $t=(t_0,...,t_{k-1})$ is called a knot vector for the spline.

I.3. Wavelet

From Fourier theory it is well known that a signal can be expressed as the sum of a possibly infinite series of sines and cosines. The big disadvantage of a Fourier expansion however, is that it has only frequency resolution and no time resolution. This means that although we might be able to determine all the frequencies present in a signal, we do not know when they are present.

Wavelets are mathematical functions that have both frequency and time domains and that cut up data into different frequency components, and then study each component with a resolution matched to its scale. The fundamental idea behind wavelets is to analyze according to scale (Mallat, 1998).

They have advantages over traditional Fourier methods in analyzing physical situations where the signal contains discontinuities and sharp spikes. Wavelets are well suited for approximating data with sharp discontinuities.

Temporal analysis is performed with a contracted, high frequency version of the prototype wavelet, while frequency analysis is performed with a dilated, low frequency version of the same wavelet.

In wavelet analysis the use of a fully scalable modulated window solves the signal-cutting problem. The window is shifted along the signal and is calculated for every position of the spectrum. Then, this process is repeated many times with a slightly shorter (or longer) window for every new cycle. In the end the result will be a collection of time-frequency representations of the signal, all with different resolutions (Mallat, 1998).

Wavelets can be classified in to continuous (1) or discrete (2).

1. A continuous wavelet transform of a function is defined by:

$$\gamma(\tau, s) = \int_{-\infty}^{+\infty} f(t) \frac{1}{\sqrt{|s|}} \overline{\psi}\left(\frac{t-\tau}{s}\right) dt \qquad \text{(I.2)}$$

where τ represents translation, s represents the scale, ψ is the *mother wavelet*, and $\overline{z}$ is the complex conjugate of z.

The original function *f* can be reconstructed with the inverse transform

$$f(t) = \frac{1}{C_\psi} \int_{-\infty}^{+\infty} \int_{-\infty}^{+\infty} \gamma(\tau, s) \psi\left(\frac{t-\tau}{s}\right) dt \frac{ds}{|s|^2} \qquad \text{(I.3)}$$

where ,

$$C_\psi = \int_{-\infty}^{+\infty} \frac{|\hat{\psi}(\zeta)|^2}{\zeta} \, d\zeta$$

is called the admissibility constant and $\hat{\psi}$ is the Fourier transform of ψ. For a successful inverse transform, the admissibility constant has to satisfy the admissibility condition:

$$0 < C_\psi < +\infty$$

It is possible to show that the admissibility condition implies that $\hat{\psi}(0) = 0$, so that a wavelet must integrate to zero.

The function ψ is the prototype of the pattern of the signal is convolved with. It is thus called the mother wavelet. In contrast to that, the scaled and shifted variants of that function are called daughter wavelets. They are obtained as follows:

$$\psi_{s,t}(t) = \frac{1}{\sqrt{|s|}} \psi\left(\frac{t-\tau}{s}\right) \qquad \text{(I.4)}$$

2. A discrete wavelet transform of a signal x is calculated by passing it through a series of filters.

First the samples are passed through a low pass filter with impulse response g resulting in a convolution of the two:

$$y[n] = (x * g)[n] = \sum_{k=-\infty}^{\infty} x[k] \cdot g[n-k] \qquad \text{(I.5)}$$

The signal is also decomposed simultaneously using a high-pass filter h. The outputs give the detail coefficients (from the high-pass filter) and approximation coefficients (from the low-pass) (Figure I.2).

However, since half the frequencies of the signal have now been removed, half the samples can be discarding according to the Nyquist's rule. The filter outputs are then downsamples by:

$$y_{low}[n] = \sum_{k=-\infty}^{\infty} x[k] \cdot g[2 \cdot n - k]$$

$$y_{high}[n] = \sum_{k=-\infty}^{\infty} x[k] \cdot h[2 \cdot n - k] \qquad \text{(I.6)}$$

This decomposition has halved the time resolution since only half of each filter output characterises the signal. However, each output has half the frequency band of the input so the frequency resolution has been doubled.

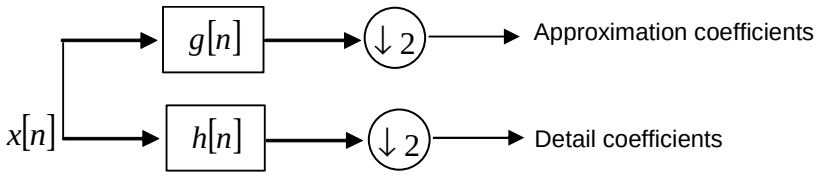

Figure I.2. Block diagram of filter analysis.

However computing a complete convolution $x * g$, with subsequent downsampling would waste computation time. The lifting scheme is an optimization where these two computations are interleaved.

Cascading and filter banks

This decomposition is repeated to further increase the frequency resolution and the approximation coefficients are decomposed with high and low pass filters and then down-sampled. This is represented as a binary tree with nodes representing a sub-space with a different time-frequency localisation (Figure I.3).

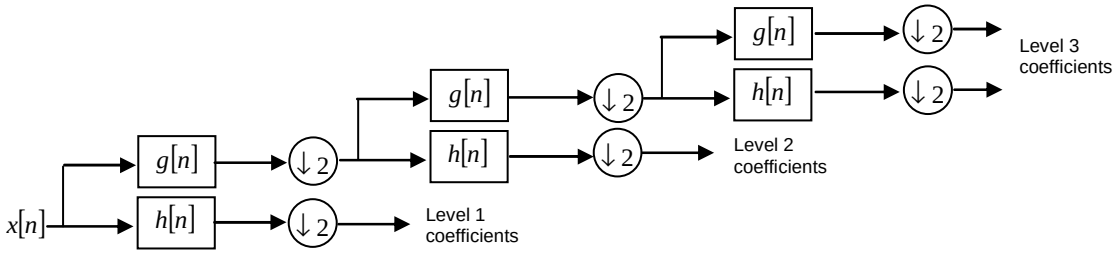

Figure I.3. A tree level filter bank.

At each level in the above diagram, the signal is decomposed into low and high frequencies. Due to the decomposition process the input signal must be a 2^n where "n" is the number of levels.

For practical applications one prefers, for efficiency reasons, continuously differentiable functions with compact support as mother (prototype) wavelet (functions). However, to satisfy analytical requirements (in the continuous Wavelets) and, in general, for theoretical reasons, one chooses the wavelet functions from a subspace of the space $L^1(R) \cap L^2(R)$. This is the space of measurable functions that are both absolutely and square integrable:

$$\int_{-\infty}^{\infty} |\psi(t)| dt < \infty \text{ and } \int_{-\infty}^{\infty} |\psi(t)|^2 dt < \infty \qquad \text{(I.7)}$$

Being in this space ensures that one can formulate the conditions of zero mean and square norm one:

$\int_{-\infty}^{\infty} \psi(t) dt = 0$ is the condition for zero mean, and

$\int_{-\infty}^{\infty} |\psi(t)|^2 dt = 1$ is the condition for square norm one

In most situations it is useful to restrict ψ to be a continuous function with a higher number, M, of vanishing moments, i.e. for all integers $n < M$.

$$\int_{-\infty}^{\infty} t^m \psi(t) dt = 0 \qquad \text{(I.8)}$$

In the next figure (Figure I.4) it is possible to observe an example of the application of an wavelet processing signal, with the decomposition at level 6:

S= a6 + d1+d2+d3+d4+d5+d6

where, a6 are the approximation coefficients, and d1 to d6 are the detail coefficients.

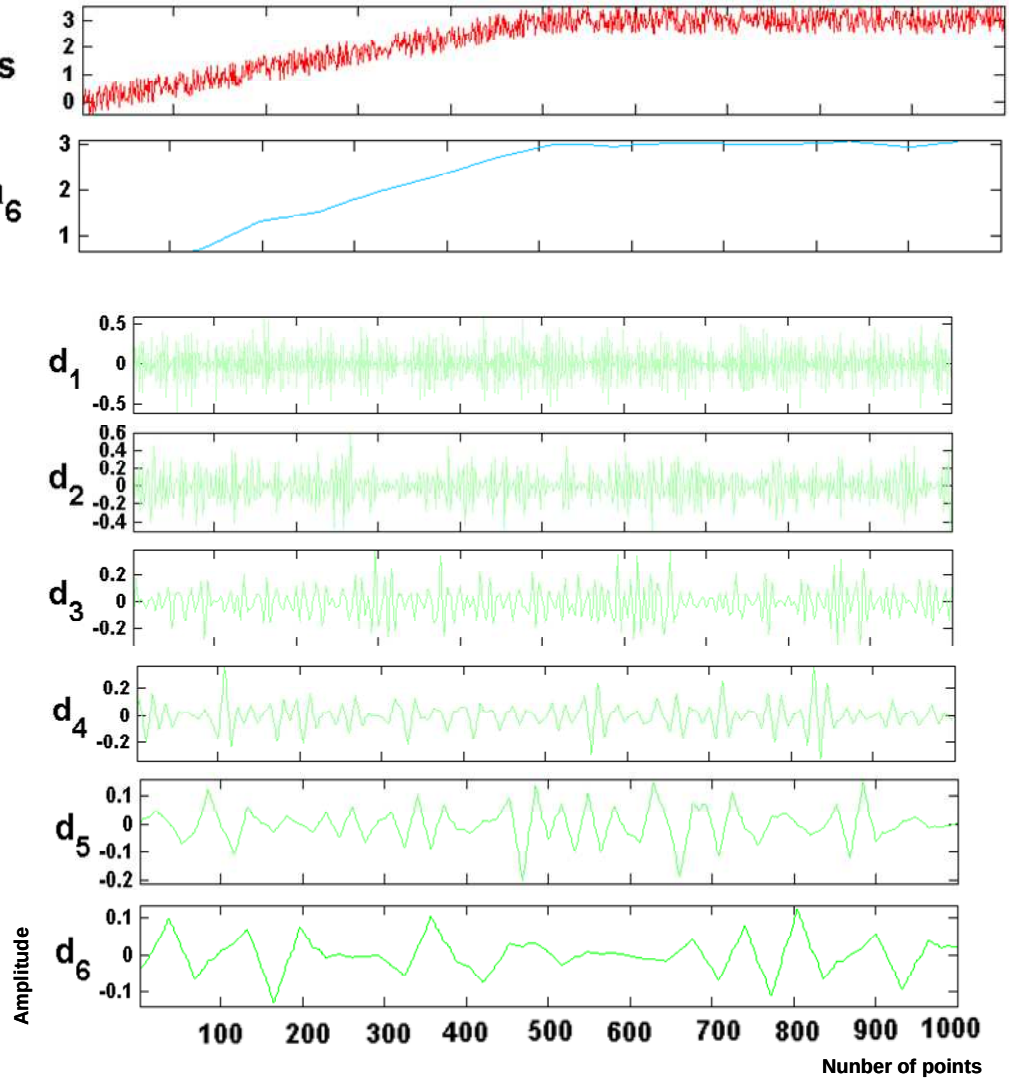

Figure I.4. Example of the application of a wavelet processing signal, with the decomposition at level 6.

The Threshold Level

As it is possible to observe, the approximation coefficients (a6), and the signal (s), must have similar amplitudes. When the detail increase to higher levels (d1 to d6), it is possible to observe that the noise is closer to zero. To a certain level of threshold, every value (in module) below the maximum value $\left(\frac{\max_{(a)}}{100} \right)$, are now zero, and this constitute a filtering procedure.

References:

Boor, C. d. (2001). A Pratical Guide to Splines (Applied Mathematical Sciences). Springer-Verlag, New York.

Cadzow, J. A. (1987). Foundations of Digital Signal Processing and Data Analysis. Mcmillan Publishing Company, New York.

Mallat, S. (1998). A wavelet tour of signal processing. Academic Press.